# FROM GENOMICS TO ANTIBIOTIC RESISTANCE IN EMERGING PATHOGENS

EDITED BY: Ravi Kant, Annamari Heikinheimo and Tarja Sironen
PUBLISHED IN: Frontiers in Microbiology

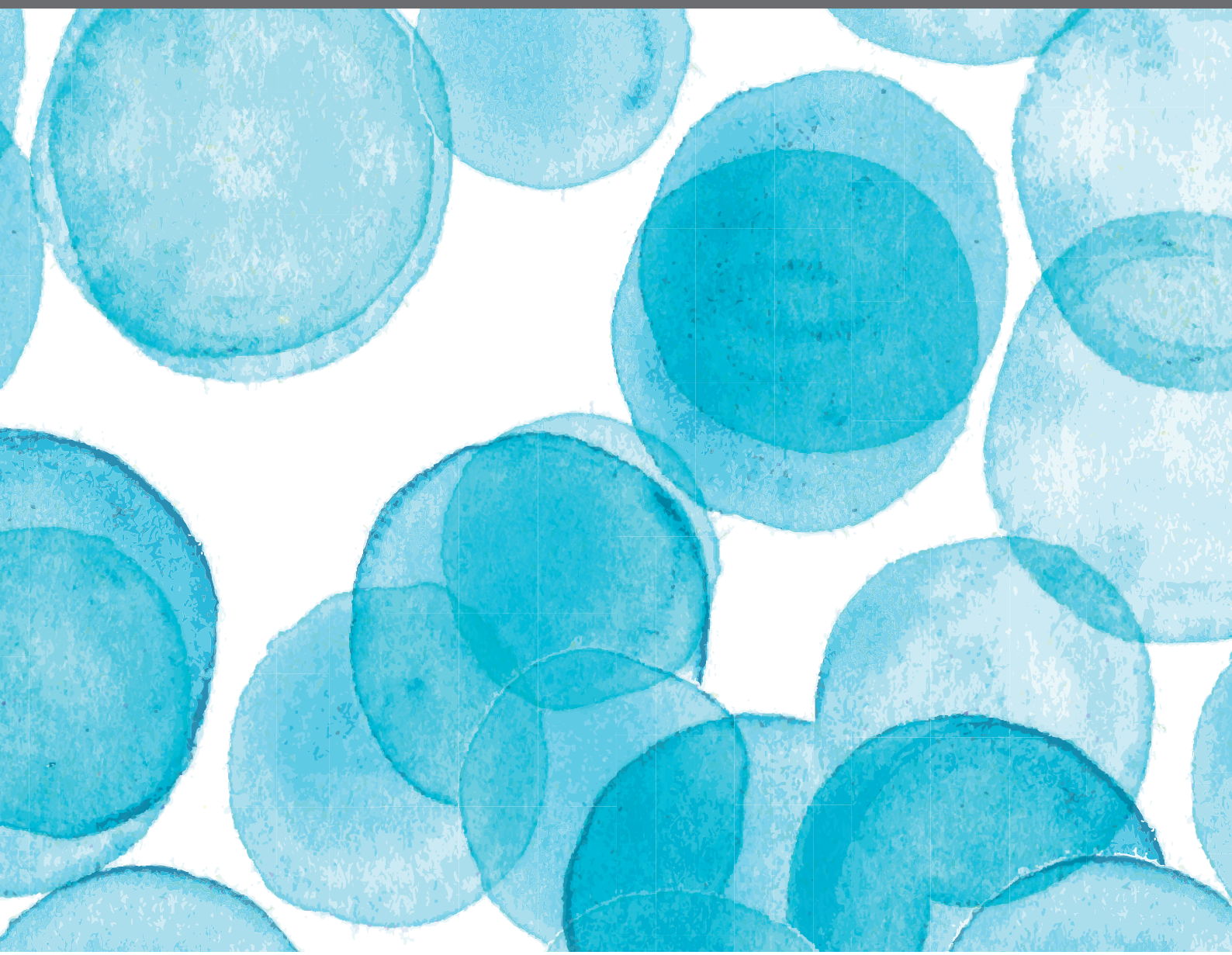

frontiers Research Topics

# frontiers



ISSN 1664-8714
ISBN 978-2-88976-871-4
DOI 10.3389/978-2-88976-871-4

## About Frontiers

Frontiers is more than just an open-access publisher of scholarly articles: it is a pioneering approach to the world of academia, radically improving the way scholarly research is managed. The grand vision of Frontiers is a world where all people have an equal opportunity to seek, share and generate knowledge. Frontiers provides immediate and permanent online open access to all its publications, but this alone is not enough to realize our grand goals.

## Frontiers Journal Series

The Frontiers Journal Series is a multi-tier and interdisciplinary set of open-access, online journals, promising a paradigm shift from the current review, selection and dissemination processes in academic publishing. All Frontiers journals are driven by researchers for researchers; therefore, they constitute a service to the scholarly community. At the same time, the Frontiers Journal Series operates on a revolutionary invention, the tiered publishing system, initially addressing specific communities of scholars, and gradually climbing up to broader public understanding, thus serving the interests of the lay society, too.

## Dedication to Quality

Each Frontiers article is a landmark of the highest quality, thanks to genuinely collaborative interactions between authors and review editors, who include some of the world's best academicians. Research must be certified by peers before entering a stream of knowledge that may eventually reach the public - and shape society; therefore, Frontiers only applies the most rigorous and unbiased reviews.
Frontiers revolutionizes research publishing by freely delivering the most outstanding research, evaluated with no bias from both the academic and social point of view. By applying the most advanced information technologies, Frontiers is catapulting scholarly publishing into a new generation.

## What are Frontiers Research Topics?

Frontiers Research Topics are very popular trademarks of the Frontiers Journals Series: they are collections of at least ten articles, all centered on a particular subject. With their unique mix of varied contributions from Original Research to Review Articles, Frontiers Research Topics unify the most influential researchers, the latest key findings and historical advances in a hot research area! Find out more on how to host your own Frontiers Research Topic or contribute to one as an author by contacting the Frontiers Editorial Office: frontiersin.org/about/contact

# FROM GENOMICS TO ANTIBIOTIC RESISTANCE IN EMERGING PATHOGENS

Topic Editors:
**Ravi Kant,** University of Helsinki, Finland
**Annamari Heikinheimo,** University of Helsinki, Finland
**Tarja Sironen,** University of Helsinki, Finland

**Citation:** Kant, R., Heikinheimo, A., Sironen, T., eds. (2022). From Genomics to Antibiotic Resistance in Emerging Pathogens. Lausanne: Frontiers Media SA. doi: 10.3389/978-2-88976-871-4

# Table of Contents

frontiers | Frontiers in Microbiology

TYPE Editorial
PUBLISHED 26 July 2022
DOI 10.3389/fmicb.2022.984301



OPEN ACCESS

EDITED AND REVIEWED BY
Rustam Aminov,
University of Aberdeen,
United Kingdom

*CORRESPONDENCE
Ravi Kant
ravi.kant@helsinki.fi

†These authors have contributed equally to this work

SPECIALTY SECTION
This article was submitted to Antimicrobials, Resistance and Chemotherapy, a section of the journal Frontiers in Microbiology

RECEIVED 01 July 2022
ACCEPTED 11 July 2022
PUBLISHED 26 July 2022

CITATION
Kant R, Heikinheimo A and Sironen T (2022) Editorial: From genomics to antibiotic resistance in emerging pathogens.
*Front. Microbiol.* 13:984301.
doi: 10.3389/fmicb.2022.984301



# Editorial: From genomics to antibiotic resistance in emerging pathogens

Ravi Kant[1,2*†], Annamari Heikinheimo[3,4†] and Tarja Sironen[1,2†]

[1]Department of Virology, Faculty of Medicine, University of Helsinki, Helsinki, Finland, [2]Department of Veterinary Biosciences, Faculty of Veterinary Medicine, University of Helsinki, Helsinki, Finland, [3]Department of Food Hygiene and Environmental Health, Faculty of Veterinary Medicine, University of Helsinki, Helsinki, Finland, [4]Unit of Microbiology, Finnish Food Authority, Seinäjoki, Finland

KEYWORDS

**antimicrobial resistance, emerging pathogens, genomics, emerging infectious disease, pathogens**

Editorial on the Research Topic
From genomics to antibiotic resistance in emerging pathogens

Antimicrobial resistance (AMR) is one of the top 10 global public health threats facing the humanity. Main drivers of pathogenic microbes becoming resistant toward antimicrobials include misuse and overuse of antimicrobials resulting in the development of drug-resistant pathogens. Lack of inadequate infection prevention, clean water and sanitation further promotes the emergence and spread of AMR pathogens. In addition to constituting a health threat, AMR has economical and social dimensions. Overall, without urgent actions, AMR threatens us from achieving the United Nations Sustainable Development Goals.

In tackling AMR, new knowledge regarding identifying, characterizing, and tracking pathogens, their virulence genes, mobile genetic elements, and antimicrobial resistance genes is crucial. In addition to traditional molecular diagnostics and genotyping methods, next generation sequencing technologies have provided strong potential in deepening our understanding of the genomes, genomic epidemiology, and transmission routes of pathogenic microbes becoming resistant toward antimicrobials (Hendriksen et al., 2019). The use of new technologies in the research and routine public health practice such as the surveillance and control of pathogens is a rapidly expanding area. Special issues on specific topics are becoming a regular feature in scientific journals based on expertise of guest editors (Kant et al., 2020). In this special Issue our focus was on genomics of pathogens, especially the emerging and re-emerging pathogens and AMR associated with them. For our special issue, we received 17 manuscripts and, through rigorous review, selected 9 for publication (8 original articles and a review).

About half of the manuscript (4) in this special issue are focused on resistance associated with various *Escherichia coli* isolates. Kurittu et al. compared Extended Spectrum Betalactamase (ESBL)-producing *E. coli* isolates in Finland from different sources. The study described clinical isolates being genetically distinct from non-human sources and gave important information on global level of the spread of ESBL-producing

*E. coli*. While, Liu et al. reported that the antibiotic resistance types of ARGs and suggested that *E. coli* is the primary antibiotic resistance reservoir of ARGs in CRC patients, providing valuable evidence for selecting appropriate antibiotics in the CRC treatment. Gonzalez et al. reported the resistance genes in 80 cefotaxime-resistant *E. coli* and 174 cefotaxime-resistant *K. pneumoniae* isolates from veal. They also followed-up the fecal carriage of ESBL-*K. pneumoniae* isolates from a subgroup of 9 animals and one animal carrying ESBL-*E. coli* to identify the clonal relatedness between the isolates. Leão et al. described the molecular epidemiology of the resistance genes and the blaCTX–M−65 genetic environment. Furthermore, they determined and described the genetic relatedness with other *E. coli* genomes for improved understandings into the public health impact of an ESBL producer seldom found in Europe.

In this special issue we also have manuscript focused on MRSA and ciprofloxacin resistant Salmonella. Sarkhoo et al. reports an upsurge in the predominance of the CC361-MRSA isolates with the dominance and transmission of a newly emerged ST672-MRSA [V/VT + fus] genotype in Kuwait hospitals. The CC361-MRSA isolates expressed resistance to different antibiotics including linezolid resistance reported for the first time in Kuwait. The discovery of the several virulence genes in these isolates and their isolation from different clinical samples signify their capacity to cause serious infections like other virulent MRSA lineages. While, Vázquez et al. characterizes ciprofloxacin resistant Salmonella Kentucky from Spanish hospitals and underlined the importance of continuous surveillance of the S. Kentucky ST198-CIPR clone.

Reslan et al. presented *Candida auris* isolates from different hospital units in Lebanon. This study disclosed the exclusivity of clade I lineage together with uniform resistance to fluconazole and amphotericin B in clinical *C. auris* isolates. Kong et al. investigated the genomic differences between a paired colistin-susceptible and -resistant *K. pneumoniae* isolates successively retrieved from a single patient, and confirmed the mechanism accountable for the emergence of high-level resistance to colistin during *in vivo* treatment and finally, McNeilly et al. highlights the antibacterial activities of NAg with its multi-targeting toxicity on *A. baumannii* and other bacteria. They also summarize the existing knowledge on the adaptive ability of *A. baumannii*, and other major bacterial species, to NAg and other silver agents. It is essential to recognize the applicability and long-term risks of the nanoparticle as a crucial alternative antimicrobial. The review also explains the emerging phenomenon of the metal-driven co-selection of antibiotic resistance to further stress the issue of overexposing bacteria to toxic heavy metals.

The articles in this special issue are focused on emerging and re-emerging pathogens and AMR associated with them. In our view, this is crucial for understanding AMR, and how this threat is currently developing. The findings in these articles could also contribute to the future development for diagnostics, therapies, and prevention tools to restrain and mitigate infectious disease threats and ensure sustainable, safe food and environment. We hope that these articles will help and stimulate readers working in the field of AMR.

## Author contributions

All authors contributed equally in writing this editorial. All authors contributed to the article and approved the submitted version.

## Acknowledgments

We thank the authors for their submission to this special issue regardless of the outcome.

## Conflict of interest

The authors declare that the research was conducted in the absence of any commercial or financial relationships that could be construed as a potential conflict of interest.

## Publisher's note

All claims expressed in this article are solely those of the authors and do not necessarily represent those of their affiliated organizations, or those of the publisher, the editors and the reviewers. Any product that may be evaluated in this article, or claim that may be made by its manufacturer, is not guaranteed or endorsed by the publisher.

## References

Hendriksen, R. S., Munk, P., Njage, P., van Bunnik, B., McNally, L., Lukjancenko, O., et al. (2019). Global monitoring of antimicrobial resistance based on metagenomics analyses of urban sewage. *Nat. Commun.* 10, 1124. doi: 10.1038/s41467-019-08853-3

Kant, R., Kumar, A., and Sironen, T. (2020). From microbial genomics to metagenomics. *Int. J. Genomics* 2020, 9357450. doi: 10.1155/2020/9357450

frontiers in Microbiology

REVIEW
published: 16 April 2021
doi: 10.3389/fmicb.2021.652863

# Emerging Concern for Silver Nanoparticle Resistance in *Acinetobacter baumannii* and Other Bacteria

*Oliver McNeilly[1], Riti Mann[1], Mohammad Hamidian[1]* and Cindy Gunawan[1,2]**

*[1]iThree Institute, University of Technology Sydney, Ultimo, NSW, Australia, [2]School of Chemical Engineering, University of New South Wales, Sydney, NSW, Australia*

The misuse of antibiotics combined with a lack of newly developed ones is the main contributors to the current antibiotic resistance crisis. There is a dire need for new and alternative antibacterial options and nanotechnology could be a solution. Metal-based nanoparticles, particularly silver nanoparticles (NAg), have garnered widespread popularity due to their unique physicochemical properties and broad-spectrum antibacterial activity. Consequently, NAg has seen extensive incorporation in many types of products across the healthcare and consumer market. Despite clear evidence of the strong antibacterial efficacy of NAg, studies have raised concerns over the development of silver-resistant bacteria. Resistance to cationic silver ($Ag^+$) has been recognised for many years, but it has recently been found that bacterial resistance to NAg is also possible. It is also understood that exposure of bacteria to toxic heavy metals like silver can induce the emergence of antibiotic resistance through the process of co-selection. *Acinetobacter baumannii* is a Gram-negative coccobacillus and opportunistic nosocomial bacterial pathogen. It was recently listed as the "number one" critical level priority pathogen because of the significant rise of antibiotic resistance in this species. NAg has proven bactericidal activity towards *A. baumannii*, even against strains that display multi-drug resistance. However, despite ample evidence of heavy metal (including silver; $Ag^+$) resistance in this bacterium, combined with reports of heavy metal-driven co-selection of antibiotic resistance, little research has been dedicated to assessing the potential for NAg resistance development in *A. baumannii*. This is worrisome, as the increasingly indiscriminate use of NAg could promote the development of silver resistance in this species, like what has occurred with antibiotics.

**Keywords: antibiotic resistance, silver nanoparticles, *Acinetobacter baumannii*, silver resistance, co-selection**

OPEN ACCESS

***Edited by:***
*Ravi Kant,*
*University of Helsinki, Finland*

***Reviewed by:***
*Dina Mosselhy,*
*University of Helsinki, Finland*
*Joseph Boll,*
*University of Texas at Arlington, United States*
*Zhi Ruan,*
*Zhejiang University, China*

****Correspondence:***
*Mohammad Hamidian*
*mohammad.hamidian@uts.edu.au*
*Cindy Gunawan*
*cindy.gunawan@uts.edu.au*

***Specialty section:***
*This article was submitted to Antimicrobials, Resistance and Chemotherapy, a section of the journal Frontiers in Microbiology*

***Received:*** *13 January 2021*
***Accepted:*** *29 March 2021*
***Published:*** *16 April 2021*

***Citation:***
*McNeilly O, Mann R, Hamidian M and Gunawan C (2021) Emerging Concern for Silver Nanoparticle Resistance in Acinetobacter baumannii and Other Bacteria. Front. Microbiol. 12:652863. doi: 10.3389/fmicb.2021.652863*

## INTRODUCTION

The WHO has acknowledged that, alongside climate change and non-communicable disease, bacterial antibiotic resistance represents one of the most important crises to human health today (Cassini et al., 2019). It is projected that over 33,000 people in Europe alone die annually from resistant bacterial-related infections, making it a near equal health burden to influenza,

HIV, and tuberculosis combined (Cassini et al., 2018, 2019). In 2014, it was estimated that infection from antibiotic-resistant bacteria in the United States resulted in a loss of over $20 billion in direct economic costs, and $35 billion through decline in societal productivity (Golkar et al., 2014; Zhen et al., 2019). The leading cause of nosocomial infections globally is due to a league of bacteria which readily develop drug resistance, collectively referred to as the ESKAPE pathogens (Rice, 2008; Santajit and Indrawattana, 2016). This group includes: *Enterococcus faecium*, *Staphylococcus aureus*, *Klebsiella pneumoniae*, *Acinetobacter baumannii*, *Pseudomonas aeruginosa*, and *Enterobacter* spp. The ESKAPE organisms represent the model archetype of virulent and adaptive bacterial organisms, as they frequently cause severe and chronic disease and 'escape' the activity of antibiotics (Santajit and Indrawattana, 2016).

Of this group, *A. baumannii* has attracted significant attention over the last two decades due to the rapid onset of antibiotic resistance and worldwide spread of this species (Howard et al., 2012). It is a Gram-negative, strictly aerobic coccobacilli and opportunistic bacterial pathogen that is generally associated with nosocomial infections, causing a range of nonspecific infections including pneumonia, soft tissue necrosis, and sepsis (Heritier et al., 2006; Alsan and Klompas, 2010; Al-Anazi and Al-Jasser, 2014; Chen et al., 2020). This bacterium became important throughout the 2001–2007 Iraqi-Afghan desert conflicts. Numerous medical and epidemiological reports documented a high incidence of multi-drug resistant *A. baumannii* infections among injured British and United States soldiers, with one report stating that 37% of the isolates was carbapenem-resistant (Alsan and Klompas, 2010; Howard et al., 2012; Hamidian and Nigro, 2019). International travel, including transportation of returning soldiers, is thought to be the main contributing factor in the global dissemination of resistance in *A. baumannii* (Peleg et al., 2008). *A. baumannii* is naturally resistant to desiccation and is primarily isolated on medical equipment in hospitals, rather than in nature, and this frequently results in the infection of patients needing treatment with invasive apparatuses (Towner, 2009). The recent COVID-19 pandemic has led to a significant surge in hospital and intensive-care unit (ICU) admissions. There have been numerous challenges in ensuring that adequate personal protective equipment (PPE) is available for medical staff and that routine sterility management practices are maintained in COVID-19 dedicated hospitals (Jain, 2020; Gottesman et al., 2021). Studies have reported increasing incidences of drug-resistant bacterial co-infections in COVID-19 patients, most often due to cross-contamination from other patients/staff and unsterile equipment (Chen et al., 2020; Sharifipour et al., 2020). Many of these incidences have included outbreaks of *A. baumannii* co-infections, particularly in ICUs, several of which have been identified as carbapenem-resistant (Perez et al., 2020; Sharifipour et al., 2020; Gottesman et al., 2021). These cases of *A. baumannii* secondary infections throughout COVID-19 dedicated hospitals has not only further burdened already pressured medical sectors around the globe, but could also inevitably accelerate the propagation and spread of antibiotic-resistant *A. baumannii* and other priority bacterial species (Clancy et al., 2020; Hsu, 2020).

The rapid emergence of drug resistance in *A. baumannii* has resulted from its ability to acquire resistance genes and adapt to environmental selective pressures (Alsan and Klompas, 2010). Consequently, this had led to the generation of multi-, extensive-, and pan-drug-resistant strains of *A. baumannii*, the bulk of which belong to two clonal lineages, namely global clone 1 (GC1) and global clone 2 (GC2; Gonzalez-Villoria and Valverde-Garduno, 2016; Hamidian and Hall, 2018; Hamidian and Nigro, 2019). Resistance development in *A. baumannii* is generally accomplished through three mechanisms: (1) acquisition of resistance genes (mainly *via* bacteria-to-bacteria horizontal gene transfer), which most often encode drug-inactivating enzymes, such as OXA-type β-lactamases (e.g., OXA-23) which hydrolyses carbapenems; (2) insertion sequence (IS)-mediated activation of resistance genes, e.g., insertion of ISAba1 upstream of the intrinsic *A. baumannii* gene *ampC* provides it with a strong promoter and results in resistance to 3rd generation cephalosporins; and (3) genetic mutation, e.g., *gyrA* and *parC* mutations alter DNA gyrase and topoisomerase IV active sites and blocks the action of quinolones (Heritier et al., 2006; Hujer et al., 2006; Asif et al., 2018). This organism was introduced as an ESKAPE member in 2009, and in 2017, the WHO and the Centers for Disease Control and Prevention (CDC) declared carbapenem-resistant *A. baumannii* as the "number one" critical priority antibiotic-resistant pathogen among a list of 12 bacteria requiring urgent antibacterial research and development (Gonzalez-Villoria and Valverde-Garduno, 2016; World Health Organization, 2017; Centers for Disease Control and Prevention, 2019). Ultimately, antibiotic resistance in *A. baumannii* and the other priority ESKAPE pathogens highlights the need for immediate action of establishing new and alternative antibacterial agents to curb the threat of infection caused by these organisms (Rice, 2008).

But, the current rate at which new drugs are being developed is very slow. Most major pharmaceutical companies have withdrawn from financially supporting the research and development of new antibiotics due to a lack of government incentives for these high risk investments (Fair and Tor, 2014; Michael et al., 2014; Ventola, 2015; Zheng et al., 2018). Naturally, the need for antibiotic substitutes is dire, and nanotechnology has proven to offer effective alternatives (Howard et al., 2012). Nanoparticles are organic (i.e., carbon-sources) or inorganic (i.e., metals) based materials, ranging in 1–100 nm in size (Silva, 2004). Silver nanoparticles (nanosilver; herein after referred to as NAg) are currently the most widely produced nanoparticle, attributed to its unique physicochemical characteristics and multifaceted antimicrobial mechanisms (Silva, 2004; Mody et al., 2010). Many studies have demonstrated the antimicrobial efficacy of NAg against many viral, fungal, parasitic, and bacterial organisms (Rai et al., 2012; Ge et al., 2014). The healthcare sector is one of the largest markets for NAg, with the nanoparticle being used as a coating agent in medical devices, such as intravenous catheters, wound dressings, and organ/dental implants to inhibit bacterial colonisation (Khan et al., 2017). Worryingly, NAg has also been incorporated into many consumer products,

and can, for example, be found in household appliances, textiles and clothing, cosmetics, childcare products, and food packaging and containers (Schäfer et al., 2011; Khan et al., 2017).

The widespread use of NAg has triggered concerns for the development of silver-resistant bacteria, diverging from the once commonly held perception that bacteria could not develop resistance to the nanoparticle (or silver in general) due to its complex antibacterial mechanisms (Rai et al., 2009; Gunawan et al., 2017). Over several years, a growing number of studies have been published describing the phenomenon of resistance in bacterial species in response to different forms of silver agents, including NAg. Silver resistance has been reported in *A. baumannii* and many other important pathogenic bacteria (Gupta et al., 1999; Gunawan et al., 2013; Muller and Merrett, 2014; Panáček et al., 2018; Hosny et al., 2019; Valentin et al., 2020).

In this paper, we highlight the antibacterial actions of NAg with its multi-targeting toxicity on *A. baumannii* and other bacteria. We also outline current knowledge on the adaptive ability of *A. baumannii*, and other significant bacterial species, to NAg and other silver agents. It is important that we understand the applicability, as well as the equally important long-term risks of the nanoparticle as a crucial alternative antimicrobial. This review also describes the emerging phenomenon of the metal-driven co-selection of antibiotic resistance, including silver, to further stress the issue of overexposing bacteria to toxic heavy metals.

## PHYSICOCHEMICAL FACTORS AND ANTIBACTERIAL PROPERTIES OF NAg

Silver nanoparticle has a number of physicochemical characteristics that affect its microbiological activity and overall stability (Rai et al., 2012). The nanoparticle exhibits distinct multi-targeting bactericidal mechanisms which are unique from common antibiotics and evidently underlines why NAg has become a popular alternative antibacterial agent (Rai et al., 2012; Yun'an Qing et al., 2018).

### Size, Shape, and Surface Properties of NAg

The physicochemical characteristics of NAg directly influence its antibacterial activity. The nanoparticles range from 1 to 100 nm size, and with their high surface-area-to-volume (SAV) ratios, each particle contains approximately 10,000–15,000 silver atoms, rendering them highly reactive (Morones et al., 2005; Zhang et al., 2016). Studies have shown that smaller particles have a higher SAV ratio and are generally associated with better physical nanoparticle-to-cell contact, and this allows for greater adherence to the bacterial surface which enhances their antibacterial activity (Morones et al., 2005; Zhang et al., 2016; Syafiuddin et al., 2017). NAg particles can be synthesised into different shapes, with the most common including spheres, truncated triangles, and rods/cylinders (Pal et al., 2007; Rai et al., 2009, 2012). A comparative study by Pal et al. (2007) found that truncated triangular shaped nanoparticles were most effective against *Escherichia coli* when compared to spherical and rod-shaped particles. The triangular shape was thought to improve reactivity of the nanoparticle due to the presence of unique active facets, which are associated with a greater concentration of silver atoms. It was also speculated that this shape enhanced particle adherence onto the bacterial surface, resulting in more extensive membrane damage and subsequent cell killing (Pal et al., 2007; Ge et al., 2014).

The size and shape of NAg determine, at least in part, the particle concentration required for effective toxicity. For example, higher concentrations of rod-shaped NAg particles at 10–100 nm (lower SAV ratio) are needed to display comparable antibacterial activity with those of truncated triangles at 1–10 nm (higher SAV ratio; Morones et al., 2005). Moreover, higher concentrations of NAg are generally required to inhibit Gram-positive bacteria in comparison to Gram-negatives (Shrivastava et al., 2007; Yun'an Qing et al., 2018). This is thought to associate with the presence of the thicker outermost peptidoglycan cell wall layer (30–100 nm) in Gram-positive bacteria, compared to those in Gram-negative bacteria (thin 2–8 nm peptidoglycan layer located between the outer and inner lipid membranes; Shrivastava et al., 2007; Silhavy et al., 2010; Yun'an Qing et al., 2018).

Another important characteristic of NAg that affects its toxicity is the presence of functional groups on the nanoparticle surface which, in many cases, act as stabilisers (to prevent aggregation) and influence the nanoparticle net surface charge (El Badawy et al., 2010; Zhang et al., 2016; Fahmy et al., 2019). Measured as zeta potential (ζ), NAg can have a positive or negative net surface charge depending on the surface functional groups (a nominally high ζ potential reflects good colloidal stability), which affects the particle electrostatic attraction with the bacterial surface (El Badawy et al., 2010). Under normal physiological conditions, the bacterial envelope has a net negative charge. The envelope itself is assembled with various biomolecules, e.g., proteins, sugars, and phospholipids, which contain many negatively charged functional groups, including carboxyl and phosphate groups (Silhavy et al., 2010). Studies have shown that nanoparticles with a highly positive ζ exhibit a greater extent of antibacterial effect than those with negative ζ, most likely due to the particle-to-bacterial envelope electrostatic interactions for the former (El Badawy et al., 2010; Rai et al., 2012; Yun'an Qing et al., 2018). This attraction allows for greater adherence and accumulation of NAg to the bacterial surface, with some studies hypothesising that this can induce neutralisation of the cell membrane and lead to the loss of its selective permeability (Morones et al., 2005; Tang and Zheng, 2018). El Badawy et al. (2010), for example, studied NAg with different coatings and observed the highest extent of bacterial surface interaction with a (branched) polyethyleneimine (BPEI)-coated nanoparticle type. This BPEI-NAg exhibited the most positive ζ [compared to negatively charged polyvinylpyrrolidone (PVP)-NAg and citrate-NAg], which was thought to interact closely with the bacterium (*Bacillus* sp.)

due to electrostatic attractions (El Badawy et al., 2010; Tang and Zheng, 2018).

## General Antibacterial Mechanisms of NAg (Cell Surface)

The antibacterial activity of NAg has been studied quite extensively (Rai et al., 2012). Four main antibacterial modes have been proposed: (A) bacterial envelope adhesion of the nanoparticle, resulting in envelope damage and cellular penetration, (B) uncoupling of the respiratory chain, (C) damage to cellular biomolecules and function, and (D) disruption of cell signalling (**Figure 1**; Dakal et al., 2016; Duval et al., 2019). As briefly discussed in "Size, Shape, and Surface Properties of NAg" section, direct physical contact of NAg with the bacterial surface is one of the initial mechanisms of its antibacterial function (Pal et al., 2007; Ge et al., 2014; Dakal et al., 2016). In Gram-negative bacteria, the 'sticking' of NAg to the outer membrane rapidly destabilises the membrane, allowing smaller-sized particles to enter the cell. This coincides with the formation of electron dense "pits" in the thin peptidoglycan layer, which enables the nanoparticle to target the inner membrane (Santajit and Indrawattana, 2016; Zhang et al., 2016; Tang and Zheng, 2018). The pitting effect is generally slower in Gram-positives, which is most likely due to the thicker outermost peptidoglycan cell wall layer (Dakal et al., 2016; Pazos-Ortiz et al., 2017; Tang and Zheng, 2018).

In an aqueous environment, NAg can interact with molecular oxygen ($O_2$), which leads to oxidative dissolution. This causes leaching of silver ions ($Ag^+$) from the nanoparticle, which are crucial to the overall antibacterial activity of NAg (Marambio-Jones and Hoek, 2010; Tang and Zheng, 2018). The morphology of NAg has been found to affect the extent and rate of $Ag^+$ release, for example, smaller sized nanoparticles (with a higher SAV ratio) have been associated with a greater rate of ion leaching compared to larger particles (Xiu et al., 2012). $Ag^+$ leached during the dissolution process are also thought to damage the bacterial membrane and membrane-bound proteins (Dakal et al., 2016; Yun'an Qing et al., 2018). $Ag^+$ acts as a soft acid and has a high affinity for electron donor groups in amino acid constituents of structural proteins and enzymes, in particular, thiol ($-S^-$) groups that are present in the amino acids cysteine and methionine, as well as amine ($NH_x$) groups in histidine ($-NH^+$), arginine ($-NH_2^+$), and lysine ($-NH_3^+$; Lara et al., 2010; Marambio-Jones and Hoek, 2010; Rai et al., 2012; Yun'an Qing et al., 2018). $Ag^+$ has been found to bind to membrane-bound transport proteins in bacteria, subsequently inhibiting the proton motive force which disrupts the in-and-out transport of protons, as well as phosphate, necessary for ATP synthesis (Lok et al., 2006). Comparable to that of NAg, studies have also reported less occurrences of $Ag^+$ penetration in Gram-positive bacteria when compared to Gram-negative bacteria. The cations are thought to be sequestrated within the thicker negatively-charged peptidoglycan layer of the former, rendering them more tolerant to $Ag^+$ (Dakal et al., 2016; Vila Domínguez et al., 2020). However, evidence suggests that $Ag^+$ is more potent than NAg against both Gram-positive and Gram-negative bacteria at equivalent silver concentrations (Li et al., 2017; Kędziora et al., 2018). In Gram-negative bacteria, this could be due to the presence of molecular transport channel proteins, e.g., outer membrane porins (OMPs), which facilitate transmembrane diffusion of ions, and in this case, $Ag^+$, into the cytoplasm (Nikaido, 1994; Lok et al., 2006; Radzig et al., 2013; Kędziora et al., 2018).

The silver-induced 'pitting' effect on the cell wall along with altered membrane permeability inevitably allows smaller NAg particles and $Ag^+$ to penetrate through the cell envelope and into the cytoplasm, while larger nanoparticles remain outside the cell (Sánchez-López et al., 2020). Studies have also hypothesised

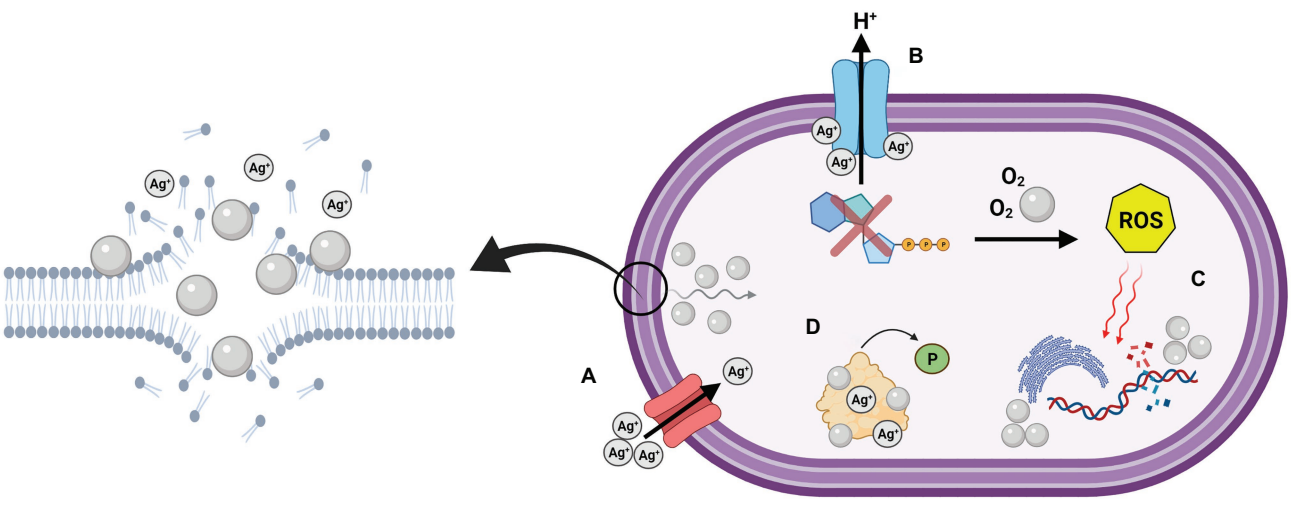


**FIGURE 1 |** Graphical depiction of the multi-target antibacterial mechanisms of silver nanoparticles (NAg) on the cell surface and cell cytoplasm. **(A)** Adhesion and "pitting" of the cell membrane, and subsequent internalisation of NAg, along with $Ag^+$ passage through outer membrane porin (OMP) channels, **(B)** uncoupling of respiratory chain by $Ag^+$, **(C)** damage to biomolecules by reactive oxygen species (ROS) and intracellular NAg, and **(D)** disruption of cell signalling through protein dephosphorylation. Created in BioRender. Adapted from Dakal et al. (2016).

a Trojan horse-type mechanism, whereby the nanoparticles are absorbed intracellularly and undergo further leaching of $Ag^+$, increasing local ion concentrations (Lemire et al., 2013; Różalska et al., 2018). Taken together, these mechanisms provide access for NAg/$Ag^+$ to target intracellular structures and biomolecules, as described in the next section (Marambio-Jones and Hoek, 2010; Dakal et al., 2016; Zhang et al., 2016).

## General Antibacterial Mechanisms of NAg (Intracellular)

As discussed in "General Antibacterial Mechanisms of NAg (Cell surface)" section, $Ag^+$ ions leached from NAg have been indicated to form complexes with electron donor groups, among these including thiol and amine groups present in structural proteins and enzymes (Lara et al., 2010). In addition to the disruption of membrane-bound transport proteins, studies have also reported inhibition of respiratory chain enzymes (e.g., NADH dehydrogenase) embedded in the inner membrane, which has been correlated to the complexing activity of $Ag^+$ (Lara et al., 2010; Marambio-Jones and Hoek, 2010; Berrisford et al., 2016). The latter is thought to result in the uncoupling of electron transport necessary for oxidative phosphorylation, and in turn, inhibits the bacteria respiration process and synthesis of ATP (Holt and Bard, 2005; Marambio-Jones and Hoek, 2010). Furthermore, the disruption of the respiratory chain has been hypothesised to cause electron leakage, which reduces the presence of molecular $O_2$ in the cytoplasm and leads to an elevated presence of NAg-induced reactive oxygen species (ROS), including superoxide ($O_2^{\bullet-}$), in bacteria (Holt and Bard, 2005; Marambio-Jones and Hoek, 2010; Dakal et al., 2016). Studies have also suggested that $Ag^+$ (and $O_2^{\bullet-}$ radicals) can target iron-sulphur (containing thiol groups) clusters in proteins, releasing Fenton-active free $Fe^{2+}$ ions which can react with cellular hydrogen peroxide ($H_2O_2$) and consequently generate highly reactive hydroxyl radicals ($OH^{\bullet}$; Xu et al., 2012; Ezraty et al., 2017). Excessively generated ROS can target cellular biomolecules and lead to oxidative stress. This can cause DNA damage and inhibition of replication, disruption of tRNA-30S ribosomal complexes involved in protein synthesis, as well as damage of proteins, e.g., *via* carbonylation, and lipids, e.g., *via* peroxidation, which has been observed for membrane phospholipids (Xiu et al., 2012; Zhao and Drlica, 2014; Kędziora et al., 2018). Interestingly, NAg has been shown to be less effective against strictly anaerobic bacteria when compared to aerobic bacteria, and this is indeed in agreement with the established role of $O_2$ in radical oxygen generation, and, as mentioned earlier, in the oxidative leaching of $Ag^+$ from the nanoparticle, both extracellularly and intracellularly (Xiu et al., 2012; Zhao and Drlica, 2014; Kędziora et al., 2018). Research inquiries have also suggested that NAg/$Ag^+$ inhibit the activity of cellular antioxidants, such as glutathione (GSH) in Gram-negative bacteria (Marambio-Jones and Hoek, 2010). Note that, under normal conditions, ROS, including $O_2^{\bullet-}$ and $H_2O_2$, are naturally generated in cells as by-products of respiration, and are neutralised by antioxidant systems when they exceed the homeostatic threshold (Ray et al., 2012; Gunawan et al., 2020). GSH neutralises ROS to non-toxic compounds, e.g., water, and in the process, GSH is oxidised to glutathione disulfide (GSSG; Marambio-Jones and Hoek, 2010; Dakal et al., 2016; Slavin et al., 2017). It is thought that NAg directly targets GSH, a glycine-cysteine-glutamic acid tripeptide (containing thiol groups), or alternatively, denatures the GSH reductase enzyme, which catalyses the GSSG-to-GSH recycling reaction (Slavin et al., 2017). For example, Singh et al. (2018) reported a decrease in the cellular presence of GSH (as well as cysteine) in *A. baumannii* with increasing NAg concentrations.

Silver nanoparticles and $Ag^+$ have been indicated to interact with nucleotides (nucleoside-phosphate groups) in DNA, intercalating between the base pairs and binding to the nucleoside structural unit (Slavin et al., 2017). Some reports have found that $Ag^+$ causes DNA condensation in both Gram-negative and Gram-positive bacteria, which is further linked to the observed inhibition of DNA replication (Feng et al., 2000; Guzman et al., 2012). Most reports have suggested that this condensation only occurs in the presence of $Ag^+$, while the nanoparticle is associated with DNA fragmentation (an outcome of hydrogen-bond disruption between nucleotides; Feng et al., 2000; Rai et al., 2012; Slavin et al., 2017). NAg and $Ag^+$ have also been found to modulate protein phosphorylation, which affects bacterial signalling pathways (Kirstein and Turgay, 2005; Shrivastava et al., 2007; Dakal et al., 2016). Protein phosphorylation acts as an essential signal relay mechanism in bacteria (and other domains of life) as it manages the "on and off" switching of proteins (Garcia-Garcia et al., 2016). Due to the high affinity of NAg/$Ag^+$ for negatively charged phosphate groups, studies have shown that phosphorylated amino acid residues (e.g., tyrosine) in proteins can be dephosphorylated by both forms of silver, which consequently changes protein conformity and disrupts cell function (Shrivastava et al., 2007; Dakal et al., 2016).

# COMBATTING ANTIBIOTIC RESISTANCE WITH NAg

A major factor to the increasing use of NAg is its proven efficacy against bacteria like *A. baumannii*, which can readily display resistance against antibiotics (Lara et al., 2010; Rai et al., 2012). The antibacterial effect of NAg is in general unaffected by antibiotic resistance mechanisms because of the nanoparticles' multi-targeting mechanisms (Rai et al., 2012). Moreover, NAg has shown promising synergy with conventional antibiotics, exhibiting enhanced toxicity when compared to NAg or antibiotics alone, even against multi-resistant bacterial species (Baptista et al., 2018). The nanoparticle could also provide a solution to the current challenge of managing chronic bacterial infections, which are often associated with the colonisation of naturally resilient biofilms (Radzig et al., 2013).

## Effect of NAg on *A. baumannii* and Other Drug-Resistant Bacteria

Several reports have described the antibacterial effects of NAg on susceptible and multi-drug-resistant (MDR) *A. baumannii* (**Table 1**) and other various Gram-negative and Gram-positive

**TABLE 1 |** Examples of several investigations on the antibacterial activity of NAg against various multi-drug-resistant (MDR) and non-MDR *Acinetobacter baumannii* strains.

| ***A. baumannii* strain** | **NAg MIC[1]** | **NAg size (nm)[2]** | **Reference** |
|---|---|---|---|
| *A. baumannii* (carbapenem- and PMB-resistant) | 3.4 μg/ml (Citrate-NAg) | 40 | Cavassin et al., 2015 |
| *A. baumannii* (carbapenem- and PMB-susceptible) | 6.7 μg/ml (Chitosan-NAg) | 25 | |
| | 13.5–≥54 μg/ml (PVA-NAg) | 10 | |
| | 1.6–3.4 μg/ml (Citrate-NAg) | | |
| | 1.6–3.4 μg/ml (Chitosan-NAg) | | |
| | 6.7–≥54 μg/ml (PVA-NAg) | | |
| *A. baumannii* (MDR) | ≤10 μg/ml | 5–10 | Chen et al., 2019a |
| *A. baumannii* ATCC 19606 | 0.78 μg/ml | 2–5 | Łysakowska et al., 2015 |
| *Acinetobacter* spp. (clinical isolates) | 0.39–0.78 μg/ml | | |
| *A. baumannii* aba1604 (carbapenem-resistant) | 2.5 μg/ml | 8.4 | Wan et al., 2016 |
| *A. baumannii* AIIMS 7 (planktonic) | 16 μg/ml | 8–12 | Singh et al., 2018 |
| *A. baumannii* AIIMS 7 (biofilm) | 2 mg/ml | | |
| *A. baumannii* SRMC 27 (biofilm) | ≤2 mg/ml | 12.05 | Gaidhani et al., 2013; Salunke et al., 2014 |
| *A. baumannii* AIIMS 7 (biofilm) | 25.6 mg/ml | 60 | |
| *A. baumannii* ATCC 19606 | 0.09 μg/ml | 8–15 | Wintachai et al., 2019 |
| *A. baumannii* NPRCOE 160575 (MDR) | 0.18 μg/ml | | |
| *A. baumannii* RS307 (carbapenem-resistant) | 30 μm[3] | ~100 | Tiwari et al., 2017 |
| *A. baumannii* NCTC 13305 | 12.5 μg/ml | 10–20 | Ebrahimi et al., 2018 |

[1]*MIC, minimum inhibitory concentration.*
[2]*Diameter of nanoparticle in nanometres (nm).*
[3]*MIC concentration was reported in μm.*

bacteria, highlighting little difference in the nanoparticle toxicity on wild-type (or non-resistant) strains when compared to resistant strains (Lara et al., 2010; Rai et al., 2012). Many researchers have compared the bactericidal activity of NAg on a variety of bacterial species, including several ESKAPE members, such as methicillin-resistant *S. aureus* (MRSA), ampicillin-resistant *E. coli*, MDR *P. aeruginosa*, ampicillin-resistant *K. pneumoniae*, and *Salmonella typhi* (Percival et al., 2007; Shrivastava et al., 2007; Lara et al., 2010; Hamida et al., 2020). Each study indicated that NAg toxicity was independent of any of the antibiotic resistance traits in these bacteria, which is thought to be due to the multi-target mechanisms of the nanoparticle. Research on the activity of NAg on *A. baumannii* has also (mostly) shown comparable efficacy of the nanoparticle against wild-type and resistant strains (Łysakowska et al., 2015; Silva Santos et al., 2016; Chen et al., 2019a; Vila Domínguez et al., 2020). In contrast, however, Łysakowska et al. (2015), when assessing NAg activity on several wild-type and MDR *A. baumannii* strains, found that on average, the resistant types were less sensitive [minimum inhibition concentration (MIC) = 0.78 μg/ml] to NAg than the wild-type strains (MIC = 0.39 μg/ml). Although a minor difference in efficacy was observed, the team hypothesised that there was caused by 'partial' NAg cross-resistance in the MDR strains due to the presence of in-built antibiotic resistance mechanisms, e.g., efflux pumps (Łysakowska et al., 2015). Cavassin et al. (2015) studied NAg with various surface coatings on carbapenem and polymyxin-B-resistant *A. baumannii*. Similar to Łysakowska et al., the work also found that the resistant *A. baumannii* were less sensitive to the nanoparticle than the wild-type strains (Cavassin et al., 2015; Łysakowska et al., 2015). Further, Cavassin et al. found little difference in the nanoparticle toxicity between the citrate- (highly negative ζ) and chitosan- (highly positive ζ) coated NAg particles (Cavassin et al., 2015; Łysakowska et al., 2015). Both types were equally more effective against resistant *A. baumannii* and other tested species when compared to the other coating type (PVA-coated; ζ potential was close to zero causing particle aggregation; El Badawy et al., 2010; Cavassin et al., 2015). This is in contrast to the observations by El Badawy et al. (2010) who noted that positively-charged nanoparticle coatings were most often correlated with a higher extent of toxicity due to closer attraction with the negatively-charged bacterial cell surface.

There has been extensive evidence highlighting the synergistic benefits of nanoparticle-antibiotic combination therapies; moreover, many studies have described an enhanced antibacterial effect compared to that of NAg or antibiotics alone (McShan et al., 2015; Baptista et al., 2018; Singh et al., 2018). Some of the general hypotheses behind this synergistic activity suggest that NAg disrupts the bacterial cell envelope and in turn assists in localising antibiotics to their cellular targets, or that NAg conjugates with the biologically active hydroxyl or amino groups present in antibiotics which improves their effective concentration and toxicity (Li et al., 2005; Dakal et al., 2016; Katva et al., 2017). Alternatively, it has been proposed that specific antibiotics can enhance the toxicity of NAg, such as penicillin, by increasing the cell membrane/wall permeability to the nanoparticle (Allahverdiyev et al., 2011; Wan et al., 2016). Wan et al. (2016) observed increasing efficacy of the nanoparticle on *A. baumannii in vitro* when combined with polymyxin-B (PMB), a last-resort membrane permeabilising antibiotic. The study also demonstrated the nanoparticle-antibiotic synergistic effect *in vivo* using *A. baumannii* infected mouse models, increasing mice survival

from 0% when treated with PMB (250 μg/kg) alone to 100% when treated with NAg-PMB (2 mg/kg + 50 μg/kg) after a 24 h infection period (Wan et al., 2016). This *in vivo* evidence is important, as it alludes to the therapeutic implications of potential NAg-antibiotic combination treatments for otherwise untreatable bacterial infections (Allahverdiyev et al., 2011; Wan et al., 2016; Baptista et al., 2018). Some other examples of NAg-antibiotic combinations include studies by McShan et al. (2015), who showed a greater extent of MDR *Salmonella typhimurium* growth inhibition with NAg-tetracycline and NAg-neomycin treatments than the nanoparticle alone, and Thomas et al., who reported improved efficacy of various NAg-antibiotic combinations on *S. aureus* and MDR *Staphylococcus epidermidis* (Allahverdiyev et al., 2011; Wan et al., 2016; Baptista et al., 2018).

## Effect of NAg on *A. baumannii* and Other Bacterial Biofilms

The pathogenicity and adaptability of bacteria to antimicrobial agents is significantly attributed to their ability to form biofilms – a surface-attached biological colony made up of one or more bacterial species enclosed by a protective sticky organic matrix called the extracellular polymeric substance (EPS; O'Toole et al., 2000; Donlan, 2002). Biofilms are the predominant mode of growth for over 99% of bacteria, conferring protection against environmental stressors, foreign agents, and toxins, therefore, playing an important role in antibiotic resistance and chronic human infection (Garrett et al., 2008; López et al., 2010; Romanova and Gintsburg, 2011). Antibiotic resistance in biofilms is garnered by several factors, including physical protection by the EPS matrix acting as a diffusion barrier, the stochastic generation of antibiotic tolerant subpopulations (persister cells), the rapid horizontal exchange of genetic material, as well as cell-to-cell communication *via* quorum sensing (Hausner and Wuertz, 1999; Miller and Bassler, 2001; Dufour et al., 2010; Flemming and Wingender, 2010; Lewis, 2010; López et al., 2010). Quorum sensing is a process which allows bacteria to communicate with each other and regulate a range of physiological activities, including conjugation, virulence, and biofilm production (Miller and Bassler, 2001). Biofilm-associated bacteria produce chemical signal molecules called auto inducers which control the expression of these physiological genes (Rutherford and Bassler, 2012).

There is growing attention towards the antibacterial effects of NAg on biofilms. Similar to reports on free-living (planktonic) bacterial systems, many studies have indicated that smaller-sized nanoparticles are more effective at biofilm killing when compared to larger particles, most likely due to the greater SAV and better EPS penetration of the former (see "Size, Shape, and Surface Properties of NAg" section; Choi et al., 2010; Markowska et al., 2013; Martinez-Gutierrez et al., 2013; Radzig et al., 2013). Again, however, it is important to note that the EPS of mature biofilms generally provides colonies with increased protection, rendering them more tolerant to NAg toxicity relative to their planktonic counterparts, as previously seen with *P. aeruginosa* biofilms and other bacterial species (Radzig et al., 2013; Pompilio et al., 2018). Studies have also correlated the anti-biofilm activity of NAg to cellular ROS generation. Qayyum et al. (2017), for example, observed substantial obliteration of *E. coli* and *Streptococcus mutans* biofilms upon exposure to NAg, which was associated with a detected increase in cellular ROS within the biofilm structure, leading to bacterial cell lysis and damage to the protein, polysaccharide, and eDNA constituents of the EPS (Xu et al., 2012; Ezraty et al., 2017).

Studies have also indicated the possible prevention and eradication of biofilm-associated infections with NAg. Wintachai et al. (2019) reported over 90% inhibition of viable MDR *A. baumannii* (NPRCOE 160575) at low NAg doses (0.09 μg/ml or 0.5x the reported MIC), which prevented the attachment and subsequent biofilm formation of (media-suspended) *A. baumannii* on the surface of human lung epithelia (cell line A549). Indeed, the team observed negligible toxicity of the nanoparticle towards to the lung cells (50% cytotoxicity concentration [$CC_{50}$] = 5.72 μg/ml) which is important when considering the medical application of NAg (Wintachai et al., 2019). Singh et al. (2018) reported a greater extent of eradication of *A. baumannii* biofilms with NAg [minimum biofilm eradication concentration (MBEC) = 2 mg/ml] when compared to tetracycline, erythromycin, and doxycycline, citing extensive EPS destruction and reduction in viable cells following nanoparticle treatment. The work also recognised a synergistic effect between erythromycin and NAg against the biofilms, with the antibiotic's efficacy increasing 32-fold in the presence of the nanoparticle (erythromycin MBEC = 128 mg/ml; erythromycin + NAg MBEC = 4 mg/ml). This again emphasises the potential value of NAg-antibiotic combinations (see "Effect of NAg on *A. baumannii* and other Drug-Resistant Bacteria" section; Singh et al., 2018). Likewise, Qayyum et al. (2017) had shown that catheters coated in NAg hindered the formation of the *E. coli* and *S. mutans* biofilms, which further highlights the healthcare capabilities of the nanoparticle.

Similar to planktonic cells (see "General Antibacterial Mechanisms of NAg (Cell surface)" section), studies have also specified greater $Ag^+$ toxicity towards biofilms of various bacterial species when compared to NAg, most likely due to more effective penetration of the ions through the protective EPS layer than the nanoparticles, though there is minimal data on $Ag^+$ activity on *A. baumannii* biofilms overall (Radzig et al., 2013; Kędziora et al., 2018). A paper by Vila Domínguez et al. (2020) reported $Ag^+$-induced protein damage (thiol group interaction) and DNA condensation on planktonic *A. baumannii* and other bacterial species, leading to subsequent cell death. Vaidya et al. (2017) compared the individual and synergistic efficacy of $Ag^+$, gold ($Au^+$), copper ($Cu^+$), platinum ($Pt^{2+}$), and palladium ($Pl^{2+}$) ions on planktonic and biofilm-forming *A. baumannii* (as well as on *E. faecium* and *K. pneumonia* planktonic and biofilm cells). $Ag^+$ and $Ag^+$-$Cu^+$ were found to be most effective individual and synergistic antibacterial ions against *A. baumannii* biofilms, respectively (Vaidya et al., 2017). Similarly, a study by Shih and Lin (2010) reported the ability of $Ag^+$-$Cu^+$ to inhibit planktonic and biofilm growth of *A. baumannii* (as well as other bacterial species) in a model plumbing system, providing insights into feasible bacterial biofilm control measures in water distribution systems.

There are a number of other studies that demonstrate effective inhibition and/or eradication of *A. baumannii* biofilms by NAg; however, each use different concentration ranges and methodologies (Salunke et al., 2014; Singh et al., 2016;

Ramachandran and Sangeetha, 2017). For example, Salunke et al. (2014) reported ~98% inhibition of *A. baumannii* biofilm formation at very high NAg concentrations (5,120 μg/ml) using a 96-well plate (1,024 μg/200 μl) experimental setup, while Ramachandran and Sangeetha (2017) observed biofilm inhibition at 'only' 100 μg/ml concentration of the nanoparticle in a glass test tube setup. Albeit, we should not ignore the fact that these experiments utilised nanoparticles with different physicochemical properties (e.g., NAg sizes of ~64 and ~7 nm, respectively), these inconsistencies in methodology highlight the challenges involved in assessing the antimicrobial efficacy of NAg. Currently, there is no standard protocol to follow for researchers to directly compare the antimicrobial activity of NAg, as the physicochemical characteristics of the nanoparticle, the bacterial growth medium and even the incubation conditions used, would influence its activity (Morones et al., 2005; Loo et al., 2018; Duval et al., 2019).

In summary, NAg has promising potential for prophylactic use and treatment of infections caused by MDR bacteria and their biofilms. The nanoparticle is considered highly effective in inhibiting the colonisation of many antibiotic-resistant bacteria, while also showing strong synergism with conventional antibiotics (Rai et al., 2012; Baptista et al., 2018). However, as previously described in "Introduction" section, advances in nanotechnology have enabled the manipulation and subsequent incorporation of NAg in not only medical devices, but also, increasingly, in everyday arbitrary consumer products (Dakal et al., 2016; Gunawan et al., 2017; Khan et al., 2017). To address this, researchers have investigated the toxic impact of NAg on environmental organisms, plant and animal models, and human cells, with studies still on-going to determine the toxicity threshold and long-term environmental and human health effects of NAg (Burdușel et al., 2018; Ferdous and Nemmar, 2020). The increasingly widespread use of the nanoparticle has also prompted a growing concern over the development of NAg-resistant bacteria, just like in the case of antibiotics, as described henceforth (Graves et al., 2015; Gunawan et al., 2017; Panáček et al., 2018; Valentin et al., 2020).

## BACTERIAL ADAPTATIONS TO NAg

Bacterial resistance to silver, specifically to $Ag^+$, has been described quite extensively, while evidence of NAg-specific resistance is still emerging. Up to this stage, studies have described the presence of both exogenous and endogenous genetic determinants of $Ag^+$ resistance, which is thought to be relevant to NAg also (Gupta et al., 1999; Gunawan et al., 2013; Graves et al., 2015; Panáček et al., 2018; Valentin et al., 2020). The earliest reported case of silver resistance was in an *E. coli* strain isolated from a burn patient in 1969, who was treated with wound dressings coated in 0.5% silver nitrate ($AgNO_3$; Jelenko, 1969). Two strains of *Enterobacter cloacae* isolated from a burns ward by Rosenkranz et al. (1974) were found to be resistant to the topical ointment silver sulfadiazine (AgSD). A year later, McHugh et al. (1975) reported on an *S. typhimurium* strain isolated from three burn victims with resistance to $AgNO_3$, which also displayed resistance to mercury chloride ($HgCl_2$) and various antibiotics.

The molecular basis of silver resistance was first described by Gupta et al. (1999), who discovered an $Ag^+$ resistance coding region (*sil* operon) present in a 180 kb plasmid called pMG101. This plasmid was extracted from the silver-resistant *S. typhimurium* strain previously isolated by McHugh et al. (1975) and Gupta et al. (1999). The silver resistance mechanism was first reported by Li et al., who found that the loss of OMPs combined with the upregulation of copper efflux proteins (Cus system) in *E. coli* conferred resistance to $Ag^+$ (Li et al., 1997; Randall et al., 2015). Over the years, several cases of $Ag^+$ resistance derived from the Sil/Cus systems (and other mechanisms) have been detected in various bacterial species, including *A. baumannii* (Deshpande et al., 1993; Deshpande and Chopade, 1994; Hosny et al., 2019). Gunawan et al. (2013) were the first to observe NAg resistance in the soil-borne bacterium *B. subtilis* elicited by oxidative-stress mechanisms, which was thought to be associated by the detected presence of *sil* genes. Further studies are published which provide evidence of NAg resistance determinants in different bacteria, which will be described in the following (Graves et al., 2015; Panáček et al., 2018; Valentin et al., 2020).

### Chromosomal (Endogenous) Silver Resistance

The endogenous silver resistance mechanism first discovered in *E. coli* by Li et al. relates to the presence of the Cus efflux system and the loss of major OMPs (Li et al., 1997; Randall et al., 2015). Prolonged exposure of various *E. coli* strains to sub-lethal doses of $AgNO_3$ and AgSD ($Ag^+$ potent agents) led to the mutational development of $Ag^+$ resistance in the bacteria. The mutant $Ag^+$-resistant strains displayed a loss of the major porins OmpF or both OmpF and OmpC, along with the expression of a natural copper binding/efflux (Cus) system which conferred cross-resistance to $Ag^+$ (**Figure 2**; Li et al., 1997; Randall et al., 2015; Kędziora et al., 2018). The *cusCFBA* operon is a gene cluster which encodes an active efflux system designed to export copper ions ($Cu^+$), and $Ag^+$ (Mijnendonckx et al., 2013; Randall et al., 2015). The proteins encoded, CusA, CusB, and CusC, are subunits of a tri-component resistance-nodulation-division (RND)-type efflux system, and CusF, which is periplasmic $Ag^+/Cu^+$ chaperone (Munson et al., 2000; Kędziora et al., 2018). Transcription of *cusCFBA* is regulated by a dual-component system called CusRS (encoded by *cusRS* operon), which sense (CusS) and respond (CusR) to increased levels of $Ag^+/Cu^+$ (Munson et al., 2000; Franke et al., 2003). Exposure of *E. coli* to $Ag^+$ can cause a missense mutation in *cusS*, promoting gene transcription and CusS synthesis (and CusR upregulation), where CusS/R then prompts increased expression of *cusCFBA* for active $Ag^+/Cu^+$ binding and efflux (Randall et al., 2015). CusF is a metal-binding chaperone, which binds $Ag^+/Cu^+$ ions to its methionine or cysteine sites and delivers them to CusCBA to be shuttled out of the cell (Lok et al., 2008; Mijnendonckx et al., 2013; Randall et al., 2015). The repression of the major porins OmpF/C in the outer membrane complements the Cus system,

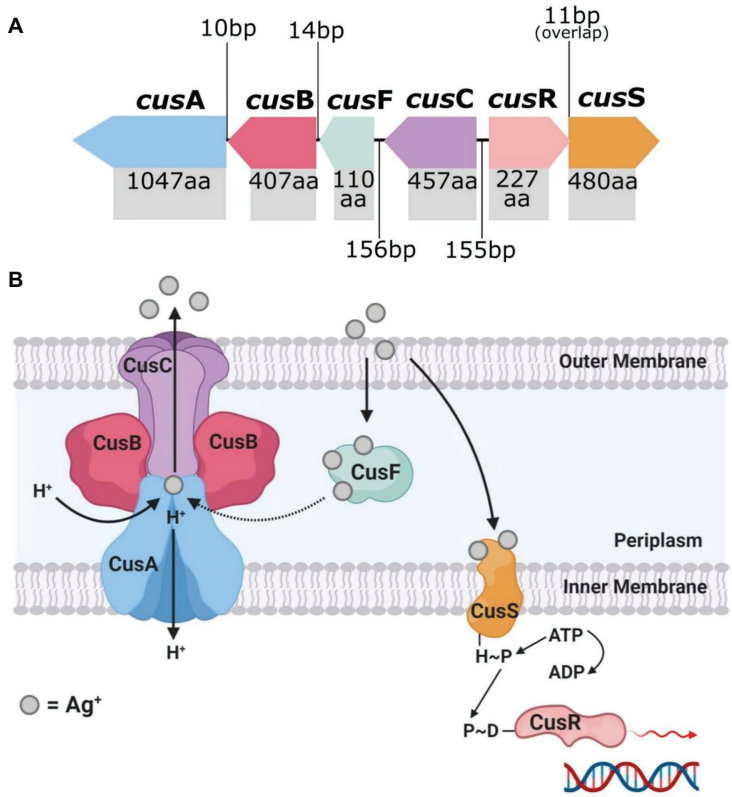


**FIGURE 2 |** The top image **(A)** shows the genetic arrangement of the *cus* operon and includes the intergenic DNA base pair (bp) gaps/overlaps and each *cus* gene's protein product amino acid (aa) length. The bottom image **(B)** is a graphical representation of the protein arrangement and functions of the encoded membrane bound Cus efflux system. Created in Inkscape **(A)** and BioRender **(B)**. Adapted from Randall et al. (2015).

as mentioned (Lok et al., 2008; Radzig et al., 2013; Randall et al., 2015). These porins are involved in the transport of cations and small molecules, such as drugs and toxins, across the cell membrane (Koebnik et al., 2000). Transcription of *ompF/C* is regulated by EnvZ/OmpR, whereby EnvZ responds to osmotic changes (i.e., presence of cations) and phosphorylates the transcription unit of OmpR, which then activates the expression of OmpF/C (Cai and Inouye, 2002). Mutation to *envZ*/*ompR* in response to $Ag^+$ exposure leads to loss of function to this regulatory system, which results in a reduction of *ompF/C* expression, causing a loss in outer membrane permeability (Li et al., 1997; Lok et al., 2008; Randall et al., 2015). This consequently limits the cytoplasmic access of $Ag^+$ and reduces the susceptibility of *E. coli* to $Ag^+$ toxicity (Li et al., 1997; Radzig et al., 2013; Randall et al., 2015).

Graves et al. (2015) reported on induced resistance to $AgNO_3$ in another *E. coli* strain upon prolonged exposure and, in addition, observed resistance to NAg. The team found non-synonymous point mutations (results in amino acid sequence changes of the protein product) in three genes; *cusS*, as well as *purL*, which encodes the protein phosphoribylsylforml-glycineamide synthetase involved in purine nucleotide biosynthesis, and *rpoB*, which codes for an RNA polymerase beta subunit. As previously discussed, CusS is part of the dual-component sensor/responder regulator for the CusCFBA $Ag^+/Cu^+$ efflux system (Franke et al., 2003; Lok et al., 2008). Resistance to $Ag^+$ in the *E. coli* strain was significant and defined, with a >26-fold increase in $Ag^+$ concentration at which the resistant bacterium could proliferate (compared to the wild-type strain), while the NAg-resistant strains could grow at a lower 1.4–4.7-fold increase in dose. It was unclear as to what exact mechanisms conferred the observed resistance to NAg in *E. coli*. As the leaching of $Ag^+$ from NAg is an integral part of the nanoparticles antibacterial activity, it is thought that the CusCFBA $Ag^+$ efflux system played some role in the NAg resistance effect (Graves et al., 2015).

According to Randall et al. (2015), the Cus system is not unique to the *E. coli* genome and has been found in strains of other bacteria, including the soil and human gut bacterium, *Citrobacter freundii*, and the pathogenic gut bacterium, *Shigella sonnei*. However, no changes in OMP expression in these bacteria (no loss of the porins) were observed, which could perhaps explain their susceptibility to $Ag^+$, suggesting that the Cus system alone is not sufficient for a bacterium to confer resistance to silver (Randall et al., 2015). The *cus* operon and OMP mechanisms are specific to Gram-negative bacteria; however, silver resistance, to both $Ag^+$ and NAg, has also been observed in Gram-positive bacteria. Apart from the original discovery in *B. subtilis* by Gunawan et al., studies have also detected resistance in the clinically-relevant species, *S. aureus*

(see "Other Mechanisms of Silver Resistance against NA" section), and silver resistance in these bacteria has been associated with *sil* genes and mutations of physiological genes (Loh et al., 2009; Randall et al., 2013; Valentin et al., 2020).

Resistance to $Ag^+$ has been previously reported in *A. baumannii*, which will be discussed further; however, no endogenous silver resistance mechanisms have been detected to date in this bacterium (Deshpande and Chopade, 1994; Shakibaie et al., 2003; Hosny et al., 2019). Alquethamy et al. (2019) provided the first report of a highly conserved chromosomally-encoded copper resistance system in *A. baumannii* which was distinct from the other known copper resistance mechanisms, including the Cus system. The mechanism involves two transcriptional regulators of copper-resistance, CueR and CopRS, as well as a P-type ATPase $Cu^+$ efflux protein called CopA (Williams et al., 2016; Alquethamy et al., 2019). The existence of this conserved chromosomal $Cu^+$ efflux system suggests that a mutational response to copper exposure may have occurred at some point earlier in the phylogeny of *A. baumannii* and has been maintained through natural selection. The copper and silver efflux mechanisms, i.e., Cus and Sil systems, are homologous as they share common protein sequences and elicit copper/silver cross-resistance in bacteria; therefore, it is possible that the CueR/CopRS/CopA could also be involved in a silver resistance effect in *A. baumannii*.

## Plasmid-Mediated (Exogenous) Silver Resistance

The $Ag^+$-resistant *S. typhimurium* strain isolated by McHugh et al. (1975) is the source of the most cited and researched silver resistance mechanism to date. In 1999, Gupta et al. isolated the HI-2 incompatibility group (IncHI-2) plasmid pMG101 from this bacterium and found that it contained various genes that encode resistance to several heavy metals and antibiotics (Gupta et al., 1999, 2001). The plasmid segment conferring silver resistance determinants contained the *sil* operon, which consists of nine genes that encode a $Ag^+$ binding and efflux system (**Figure 3**; Gupta et al., 1999; Silver, 2003; Niño-Martínez et al., 2019). In reading order, these genes are *silE*, *silS*, *silR*, *silC*, *silF*, *silB*, *silA*, *ORF105 (silG)*, *and silP*, and encode their proteins in three transcriptional units (SilE, SilRS, and SilCFBAGP; Silver, 2003; Andrade et al., 2018). The characterisation and organisation of the Sil system are in fact based on the earlier discovered Cus system, as the two efflux systems share close peptide homologies, as mentioned previously (Mijnendonckx et al., 2013; Randall et al., 2015; Kędziora et al., 2018). However, in contrast

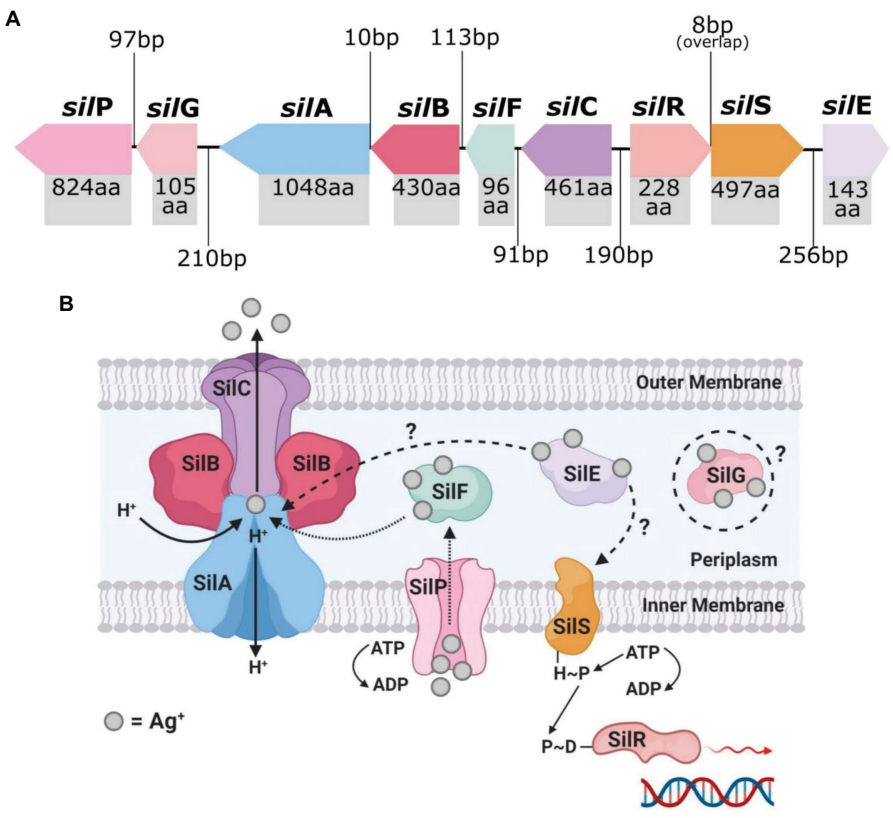


**FIGURE 3 |** The top image **(A)** shows the genetic arrangement of the *sil* operon and includes the intergenic DNA base pair (bp) gaps/overlaps and each *sil* gene's protein product amino acid (aa) length. The bottom image **(B)** is a graphical representation of the known and predicted protein arrangement and functions of the encoded membrane bound Sil efflux system. Created in Inkscape **(A)** and BioRender **(B)**. Adapted from Randall et al. (2015).

to the Cus system, the exogenous Sil system does not associate with the loss of OMP porins (i.e., OmpF/C) to evoke $Ag^+$ resistance (Randall et al., 2015).

SilE is a periplasmic protein chaperone that binds to free $Ag^+$ present in the periplasm and is currently the only Sil protein which has had its function fully validated (Gupta et al., 1999; Randall et al., 2015). SilRS are dual-component $Ag^+$ sensor (SilS) and responder (SilR) transcriptional regulators for SilCFBAGP, and are direct homologs of CusRS (Silver, 2003; Kędziora et al., 2018). SilCFBA shares ~80% protein homology with CusCFBA and functions as a multi-component RND-type $Ag^+$ efflux system (Randall et al., 2015; Kędziora et al., 2018). SilA is an inner membrane cation/proton efflux antiporter, SilB functions as membrane fusion protein which clamps SilA together with SilC, an OMP channel (Andrade et al., 2018). SilF is another periplasmic $Ag^+$-binding chaperone (similar to SilE), and binds with $Ag^+$ that have passed through the outer membrane from outside the cell (Kędziora et al., 2018). SilP is an inner membrane-bound P-type ATPase efflux which transports $Ag^+$ from the cytoplasm to the periplasm for binding with the chaperones SilE/F (Mijnendonckx et al., 2013). The *sil* operon also contains an unspecific open-reading frame *ORF105* which codes for a protein with currently no defined function (Gupta et al., 1999; Mijnendonckx et al., 2013; Andrade et al., 2018). The encoded protein shares a ~45% amino acid sequence homology with the $Cu^+$ chaperone CopG, and both contain a CXXC motif (two amino residues between two cysteine), which is known to be involved in heavy metal binding (Su et al., 2007; Randall et al., 2015; Andrade et al., 2018). To fit the *sil* gene nomenclature, Randall et al. (2015) proposed that *ORF105* be given the name *silG* and described as an $Ag^+$-binding chaperone, similar to SilE/F, until proven otherwise.

## Presence of Sil System in *A. baumannii* and Other Species

The *sil* operon has been found in other IncHI plasmids like pMG101 (**Table 2**), and due to horizontal gene transfer of these plasmids between bacteria, whole or part of the operon has been detected among many bacterial species (Gupta et al., 2001; Mijnendonckx et al., 2013). Since the initial discovery of *sil* genes in *S. typhimurium*, studies have further detected the genes in other *Salmonella* spp., and in other Gram-negative bacteria, including *E. cloacae*, *E. coli*, *P. aeruginosa*, *K. pneumoniae*, *Serratia marcescens*, and *A. baumannii*, as well as Gram-positive bacteria, such as *B. subtilis* and *S. aureus* (Deshpande and Chopade, 1994; Gunawan et al., 2013; Finley et al., 2015; Hosny et al., 2019; Valentin et al., 2020). Hosny et al. (2019) discovered *sil* operon-harbouring plasmids in various clinical species isolated from burns/wounds of hospital patients, including two MDR *A. baumannii* strains. Conjugative horizonal transfer of the *sil* operon was observed between the silver-resistant *A. baumannii* strains and non-silver-resistant *E. coli*. This resulted in the expression of the *sil* genes and subsequent development of a $Ag^+$ resistance phenotype in the latter bacterium (Hosny et al., 2019). Deshpande and Chopade (1994) had in fact reported the conjugal transfer of silver resistance determinants many years prior. Their work observed the transfer of plasmid pUPI199, which contained undefined silver resistance genes, from an *A. baumannii* strain (BL88) to *E. coli* with, once again, subsequent expression of the silver resistance phenotype (Deshpande and Chopade, 1994). A study by Shakibaie et al. (2003) also detected the presence of another plasmid-associated silver resistance

**TABLE 2** | Properties of known HI incompatibility group (IncHI) plasmids containing genes coding for silver resistance, including either the complete *sil* operon or some *sil* genes.

| Genus/species | Plasmid | *sil* genes | Size (bp) | Conjugative | GenBank acc. no. | Reference |
|---|---|---|---|---|---|---|
| *S. typhimurium* | pMG101 | *ESRCABGP* | 14,211 | Y | AF067954 | Gupta et al., 1999 |
| *Serratia marcescens* | R476b | *E* | 424 | Y | AY009372 | Gupta et al., 2001 |
| | | *P* | 1,362 | | AH011380 | |
| | | *S* | 1,154 | | AH011381 | |
| *Salmonella enterica* | MIP233 | *E* | 424 | Y | AY009382 | Gupta et al., 2001 |
| | | *P* | 1,356 | | AH011384 | |
| | | *S* | 1,154 | | AH011385 | |
| *S. enterica* | pWR23 | *E* | 424 | Y | AY009387 | Gupta et al., 2001 |
| | | *P* | 1,356 | | AH011388 | |
| | | *S* | 1,154 | | AH011389 | |
| *S. enterica* | MIP235 | *E* | 424 | Y | AY009392 | Gupta et al., 2001 |
| | | *P* | 1,356 | | AH011386 | |
| | | *S* | 1,154 | | AH011387 | |
| *S. marcescens* | R478 | *ESRCABGP* | 274,762 | Y | BX664015 | Gilmour et al., 2004 |
| *E. coli* | pAPEC-O1-R | *ESRCABGP* | 241,387 | Y | DQ517526 | Johnson et al., 2006 |
| *Salmonella typhi* | R27 | *ESRCABGP* | 180,461 | Y | AF250878 | Sherburne et al., 2000 |
| *A. baumannii* | pUPI199 | nk[1] | ~50,000 | Y | nk[2] | Deshpande and Chopade, 1994 |

[1]*Unknown if detected silver resistance genes are sil genes.*
[2]*Accession number could not be found in GenBank.*

mechanism in an *A. baumannii* strain (BL54), which is unrelated to the Sil system, and was thought to involve in the intracellular accumulation of $Ag^+$ and binding of the ions to metalloproteins to form inert silver complexes. No follow-up inquiries have been made on either of these non-*sil* derived silver resistance determinants, and, therefore, it is difficult to assess the significance of these resistance mechanisms.

## Other Mechanisms of Silver Resistance Against NAg

Most studies have established that bacterial resistance to silver can develop through genetic mutations, as well as through horizontal gene transfer (i.e., *via* plasmids; see "Chromosomal (Endogenous) Silver Resistance" and "Plasmid-mediated (Exogenous) Silver Resistance" sections). However, there is evidence that an increase in expression of native bacterial processes can also contribute to silver resistance. For example, a study by Muller et al. outlined that the redox-active metabolite pyocyanin, produced by *P. aeruginosa*, could reduce extracellular $Ag^+$ to non-toxic $Ag^0$ and, in turn, confer resistance to the ions (Muller and Merrett, 2014). Another example was the increased production of EPS by planktonic *E. coli*, which acted as a permeability barrier to $Ag^+$, causing neutralisation and agglomeration of the ion into inert particulates (Kang et al., 2013). A study by Panáček et al. (2018) revealed an intrinsic NAg resistance mechanism in *E. coli* involving overproduction of the protein flagellin, which led to the aggregation of the nanoparticles. Flagellin is an adhesive protein, forming part of the structural component in the bacterial motility organelle flagella and is known to be involved in biofilm formation (Metlina, 2004; Lu and Swartz, 2016; Panáček et al., 2018). This resistance mechanism was considered epigenetic, as it was independent of any genetic mutations, and provided no observable resistance to $Ag^+$ due to the solubility of the ions (Panáček et al., 2018).

As mentioned in "Chromosomal (Endogenous) Silver Resistance" section, evidence of silver resistance in Gram-positive bacteria have been reported, although less frequent in comparison to Gram-negative bacteria. Loh et al. (2009) examined the frequency of *sil* gene occurrences in 36 *S. aureus* strains isolated from human and animal sources. Three strains were found to contain only the *silE* gene (95–100% homology with *silE* in pMG101), which appeared to confer transient resistance upon exposure to $Ag^+$ through ion binding; however, the exposure eventually resulted in cell death (Loh et al., 2009). In another study, however, Hosny et al. (2019) isolated four clinical MDR *S. aureus* strains, each displaying stable resistance to $Ag^+$, and found one strain expressed the complete *sil* operon, while the remaining three expressed some of the *sil* genes. The study on *B. subtilis* by Gunawan et al. (2013) is the only other research inquiry apart from that of Valentin et al. (2020) that reported the development of NAg resistance in Gram-positive bacteria. Valentin et al. (2020) showed the development of stable resistance to NAg (and $Ag^+$) in *S. aureus* (ATCC 25923) through prolonged exposure, with no known presence of the *sil* genes in its genomes. The bacterium developed physiological genetic mutations, the first reported case of NAg-induced single nucleotide polymorphisms in a Gram-positive bacterium (Valentin et al., 2020). More specifically, mutations in *purR*, which encodes a purine repressor regulator protein, were hypothesised to lead to an upregulation in purine nucleotide synthesis to cope with DNA targeted NAg activity. The study also detected mutations in *tcyA*, which codes for an L-cystine binding protein, lowering the influx of extracellular cystine which helped reduce oxidative stress by ROS generated from both high levels of intracellular cysteine and by NAg and $Ag^+$ (Park and Imlay, 2003; Sinha et al., 2003; Valentin et al., 2020).

## Silver and Other Metals as Drivers of Antibiotic Resistance

While bacterial resistance to silver (NAg and $Ag^+$) is itself a troubling issue, there has been emerging evidence to show that silver and other heavy metals (e.g., lead, cadmium, chromium, mercury, etc.) can co-select for antibiotic resistance (Ma et al., 2016; Siddiqui et al., 2019). The emergence of heavy metal/antibiotic resistance was first described in 1974, when Koditschek and Guyre (1974) isolated *E. coli* from a sludge-contaminated estuarine and found it had "indirectly" acquired antibiotic resistance due to heavy metal exposure. Agriculture and aquaculture practices across the globe frequently use metal-containing fertilisers, pesticides, and feed additives, and have consequently contributed to profound environmental accumulation of heavy metals. Heavy metals are stable and are not subject to rapid degradation, thus their presence in soil and water is thought to be significantly greater than antibiotics, and may, therefore, contribute to long-term exposure and selective pressure on bacteria (Baker-Austin et al., 2006; Seiler and Berendonk, 2012). The co-selection of antibiotic resistance by heavy metals is often associated with 'dual' metal/antibiotic resistance phenomena – cross-resistance, co-resistance, or co-regulation/co-expression (**Figure 4**; Baker-Austin et al., 2006). Cross-resistance occurs when the same genes encode resistance mechanisms to multiple agents, and in the case of metal/antibiotic resistance, one key example is the expression of Tet efflux pumps, which export tetracyclines and zinc ions ($Zn^{2+}$; Chapman, 2003). Co-resistance arises when different genes present in the same genetic element confer resistance to multiple agents at once, and are often found in mobile genetic elements (plasmids, transposons, or integrons; Baker-Austin et al., 2006). As an example, plasmid pMG101, from which the *sil* genes were first discovered, was found to also contain resistance genes for mercury and tellurite, and for a number of antibiotics, including ampicillin and chloramphenicol (Gupta et al., 1999). Likewise, plasmid pUPI199 isolated from *A. baumannii* by Deshpande and Chopade (1994), which harboured (undefined) silver resistance genes, had also been found to contain resistance genes for 12 other metals and 10 antibiotics. Co-regulation is when regulatory genes (in a chromosome or plasmid) of different resistance mechanisms are transcriptionally linked, meaning, in this case, exposure to a metal can trigger the expression of both metal resistance genes (MRGs) and antibiotic resistance genes (ARGs; Baker-Austin et al., 2006). For example, overexpression of the gene *robA* [encodes the right origin-binding (Rob) transcriptional regulator protein] in *E. coli* was found to activate multiple

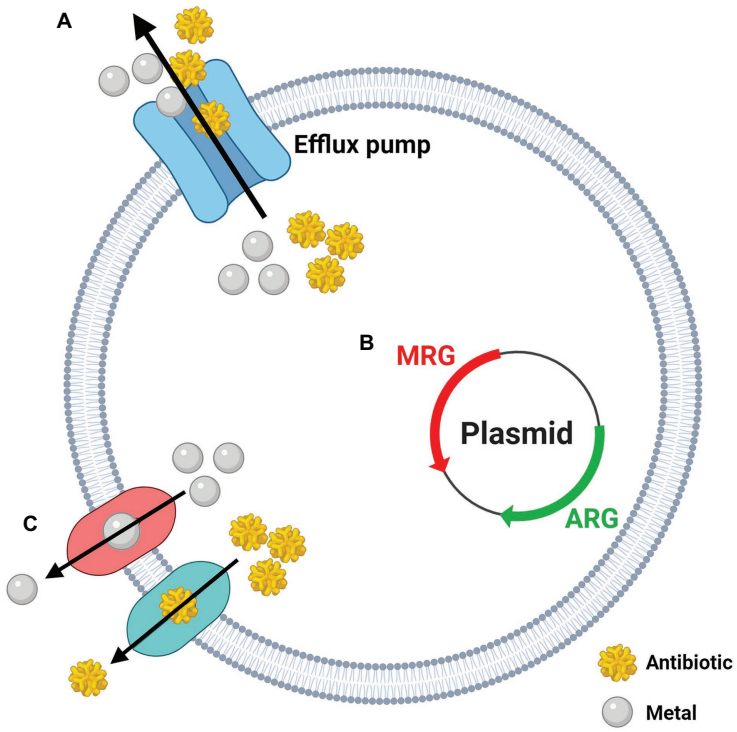


**FIGURE 4 |** The three potential mechanisms behind the co-selection of heavy metal and antibiotic resistance. **(A)** Cross-resistance: one gene/mechanism confers resistance to metals and antibiotics at once (i.e., efflux pumps); **(B)** Co-resistance: genes coding for metal resistance (MRG) and antibiotic resistance (ARG) are grouped together on the same genetic element (i.e., plasmids); **(C)** Co-regulation: expression of individual metal and antibiotic resistance systems are managed by a common gene or regulator. Created in BioRender. Adapted from Pal et al. (2017; Lic. No. 4986171126814).

mechanisms which gave rise to resistance phenotypes to silver, mercury, and cadmium, as well as various antibiotics and organic solvents (Nakajima et al., 1995).

A recent paper by Siddiqui et al. (2019) reported an increased co-selection of extended-spectrum beta lactamases (ESBLs; confer resistance to β-lactam antibiotics such as penicillins, carbapenems, cephalosporins, etc.) and silver resistance determinants (*sil* genes) in the polluted Yamuna River in India. From the collected bacterial isolates, 121 were found to be ESBL producers, including various *Acinetobacter*, *Enterobacteriaceae*, and *Bacillus* species, with the most prevalent ESBL gene being $bla_{\text{CTX-M}}$ (encodes class A β-lactamases; commonly targets cephalosporins, i.e., cefotaxime). Out of the 73 isolates containing $bla_{\text{CTX-M}}$ genes, 53 were found to have at least one *sil* gene (*silE*, *silP*, or *silS*), and worryingly, the most common 'dual' presence of ESBL/*sil* genes in these isolates were $bla_{\text{CTX-M}}$ + $bla_{\text{TEM}}$ (encodes other class A β-lactamases; commonly target penicillins) + *silE* + *silP* + *silS*. All ESBLs and *sil* genes were present in plasmids, and this work found these resistance genes could be horizontally transferred to a plasmid-free *E. coli*, rendering the bacterium resistant to β-lactams (including penicillins and cephalosporins) and $Ag^{+}$, confirming the co-resistance effect (Siddiqui et al., 2019). Another study by Deshpande et al. (1993) described a correlation between β-lactamase production and metal ion resistance in various clinical strains of *A. baumannii* and other *Acinetobacter* spp. The bacterial strains that were sensitive to toxic metals (including silver, mercury, and cadmium) were associated with lower levels β-lactamase gene expression, while those that were resistant to the metals were associated with higher expression levels of the ARGs. This correlation was particularly evident in *A. baumannii* (Deshpande et al., 1993; Abdar et al., 2019). Deshpande et al. suggested that the resistant *A. baumannii* strains were carrying plasmids that contained both β-lactamase and MRGs (Deshpande et al., 1993; Deshpande and Chopade, 1994; Veress et al., 2020). Other bacterial species have also been found to carry plasmids that harbour *sil* genes and ARGs. For example, Gilmour et al. (2004) found that the plasmid R478 isolated from the opportunistic pathogenic bacterium *S. marcescens* carried the entire *sil* operon, along with mercury, tellurite, and copper resistance genes, as well as tetracycline, chloramphenicol, and kanamycin resistance genes. Similarly, Johnson et al. (2006) also found the entire *sil* operon in plasmid pAPEC-O1-R isolated from *E. coli*, which also carried copper resistance genes and several ARGs, including gentamicin, streptomycin, and tetracycline resistance genes. Most antibiotic-resistant *A. baumannii* strains belong to the GC1 complex, many of which carry a large resistance gene island (AbaR) which contains several ARGs, including ESBLs (e.g., $bla_{\text{TEM}}$), and MRGs for mercury, cadmium, and zinc, and could perhaps alternatively explain the observations made by Deshpande et al. (1993) and Hamidian and Hall (2018). The high incidence of infections by MDR *A. baumannii* throughout

the Iraqi-Afghan conflict is one of the most important examples regarding heavy metal-driven antibiotic resistance co-selection in this species (Howard et al., 2012). Destroyed infrastructure and metal-based military equipment (i.e., munitions, ordnance, and explosives) are known to contaminate environments through heavy metal leaching (Gębka et al., 2016; Vänskä et al., 2019). It has been proposed that metal exposure on *A. baumannii* in contaminated soil or water, for example, could have promoted the co-selection of antibiotic resistance, which resulted in the increased prevalence of MDR-resistant *A. baumannii* infections in soldiers exposed to these environments during combat (Bazzi et al., 2020).

Silver nanoparticle has also been shown to promote the co-emergence of antibiotic resistance in bacteria (Ma et al., 2016; Chen et al., 2019b; Pietsch et al., 2020). A study by Ma et al. (2016) found that treatment of waste water with NAg (and $Ag^+$) using lab-scale sequencing batch reactors (SBRs), resulted in an increased shift in various ARGs among isolated Burkholderia spp., Streptomyces spp., and Gemmatimonas spp. More specifically, metagenomics data associated the detection of HAE1 family protein (multi-drug efflux protein), *strA* gene (encodes aminoglycoside 3'-phosphotransferase; aminoglycoside resistance), and *acrB* gene (encodes multidrug efflux pump subunit AcrB) with the increased presence of NAg, while increased abundance of undecaprenol kinase and undecaprenyl-disphosphatase (resistance to bacitracin) and *ermF* gene (encodes rRNA adenine N-6-methyltransferase; macrolide resistance) was associated with $Ag^+$ presence (Ma et al., 2016). Interestingly, the team also found that the total abundance of MRGs (including *sil* genes) were highest in the SBRs treated with NAg, suggesting that the nanoparticle has the most potential for ARG co-selection compared to $Ag^+$ (Ma et al., 2016). There is also evidence to show that the formation of biofilms functions as a mechanism for co-selecting antibiotic and metal resistance (Baker-Austin et al., 2006; Pietsch et al., 2020). The EPS matrix of biofilms acts as a sequestering barrier to heavy metals and antibiotics, and alarmingly, studies have found that exposure of metals on biofilms can encourage EPS synthesis, improving the biofilms adhesive, structural, and protective integrity (Yang and Alvarez, 2015; Song et al., 2016). Moreover, because of the proximity of biofilm-cells, there is a much greater magnitude of DNA conjugation between bacteria. Research shows that these events can increase under stressful conditions (i.e., exposure to antibacterial agents), which is advantageous to the co-selection process (Song et al., 2016; Singh et al., 2017). Studies have also found that exposure of NAg/$Ag^+$, and other heavy metal agents, on biofilms can stimulate quorum sensing, increasing expression of genes involved in biofilm formation and conjugation of ARGs (Qiu et al., 2015; Yang and Alvarez, 2015). Yang and Alvarez (2015) revealed that the treatment of *P. aeruginosa* biofilms with sub-lethal doses of NAg stimulated an upregulation in quorum sensing, resulting in increased EPS production and subsequent biofilm formation. They also found it induced an up to 3.4-fold increase in expression of the multi-drug efflux gene *mexA* (Yang and Alvarez, 2015). The regulation and promotion of biofilm formation and change in bacterial gene expression (including lateral transfer of ARGs) have been observed in *A. baumannii* in response to cationic iron ($Fe^+$) exposure previously, for example, but not to silver (NAg or $Ag^+$; Qiu et al., 2012, 2015).

While bacteria have been exposed to toxic heavy metals long before human existence, anthropogenic pollution of environments has evidently created prolonged selective pressures on bacteria, consequently promoting the co-emergence of heavy metal and antibiotic resistance (Baker-Austin et al., 2006). It is, therefore, critical to recognise the implications heavy metals (including silver) have on bacteria in both the environment and in clinical settings, as the co-selection of ARGs and promotion of biofilm growth could further strain the healthcare system and exacerbate the current drug resistance crisis.

## KNOWLEDGE GAP AND FINAL REMARKS

Global antibiotic resistance is not a future threat, but one that has at last transpired. From improper prescriptions for non-bacterial infections and overuse in agriculture/food industries, to the diminishing pharmaceutical investment into their development, the misuse of antibiotics ultimately calls for the need of novel and alternative antibacterial agents (Ventola, 2015; World Health Organization, 2017; Centers for Disease Control and Prevention, 2019). Major advancement in nanotechnology has led to significant progress in designing many antibacterial nanoparticles. The metal-based silver nanoparticle (NAg) is currently the most developed nanoparticle due to its multi-targeting antibacterial mechanisms and proven efficacy against a broad-spectrum of bacteria (Silva, 2004). Many studies have shown that NAg is highly toxic to several Gram-positive and Gram-negative bacterial species, including the ESKAPE pathogens – a consortium of bacteria that frequently exhibit multi-drug resistance and are the leading cause of nosocomial (hospital-related) infection (Rai et al., 2012). Among this group (carbapenem-resistant), *A. baumannii* is of key concern, having been recently declared the "number one" critical level priority pathogen. Thus calling for the immediate development of alternative antibacterial treatments for this highly infectious and resistant pathogen (Gonzalez-Villoria and Valverde-Garduno, 2016; Hamidian and Nigro, 2019). *A. baumannii* and other globally prevalent pathogens have become the main targets of the unique and effective antibacterial nanoparticle.

Notwithstanding the strong antibacterial efficacy of NAg, there has been a growing concern over the ability of bacteria to adapt to the nanoparticle due to its increasingly widespread use (Gunawan et al., 2017). Bacterial resistance to the ionic form of silver, $Ag^+$, has been recognised for many years, and in the last decade, research inquiries have indeed observed the development of resistance mechanisms against NAg in several environmental and clinically-relevant Gram-negative and Gram-positive bacteria (Gupta et al., 1999; Gunawan et al., 2013; Graves et al., 2015). Further, studies have shown that biofilms – a resilient surface-attached bacterial community, can also adapt to silver (both NAg and $Ag^+$) despite the effective biofilm inhibiting and eradicating activity of the silver agents

compared to many conventional antibiotics (Radzig et al., 2013; Yang and Alvarez, 2015). Biofilms are a major healthcare issue, as they frequently develop in cases of uncontrolled and chronic infections (López et al., 2010).

To the best of our knowledge, only the planktonic form of *A. baumannii* has been found to exhibit $Ag^+$ resistance characteristics due to the presence of the exogenous (plasmid-based) $Ag^+$ efflux Sil system, and, as found in some cases, other undefined/non-Sil related mechanisms (Deshpande and Chopade, 1994; Hosny et al., 2019). No presence of endogenous (chromosomal) silver resistance mechanisms have been identified in *A. baumannii*, so far. However, we are not ignoring the fact that chromosomally encoded copper efflux systems have been detected in this bacterium, which could infer the possibility of chromosomal silver resistance due to the similarities between copper and silver efflux mechanisms (Williams et al., 2016; Alquethamy et al., 2019). To date, no work has been undertaken to determine if *A. baumannii* can develop resistance or specific adaptation(s) to NAg exposure. Our team is currently studying the nanoparticles toxicity on *A. baumannii* in both its planktonic and dominant biofilm form of growth, and in turn, the adaptation characteristic(s) of the bacterium which could develop in response to prolonged exposure. While it is possible that the Sil system plays a role in resistance to NAg, given that the nanoparticle exerts its toxicity differently from $Ag^+$, it is likely that resistance to NAg involves additional mechanisms that are still largely unexplored.

In addition, evidence has emerged showcasing the potential for heavy metals to co-select for antibiotic resistance genes (ARGs), facilitated by 'dual' metal/antibiotic resistance mechanisms which are related to cross-resistance (same genes/mechanism conferring resistance to both metal and antibiotics), co-resistance (metal and antibiotic resistance determinants located in the same genetic element), or co-regulation (the regulatory genes of metal and antibiotic resistance determinants are transcriptionally linked; Baker-Austin et al., 2006). The combined effects of heavy metal exposure on bacteria in potentially driving both metal resistance and antibiotic resistance is a troubling issue, and further highlights the important implications of heavy metal overexposure on bacteria and to subsequently minimise this risk. Both NAg and $Ag^+$ have been found to facilitate the co-selection of various ARGs, most frequently seen at this stage in polluted water systems (Ma et al., 2016; Siddiqui et al., 2019). Over the years, studies have indeed shown that *Acinetobacter* spp. (including *A. baumannii*) can display cross-resistance to $Ag^+$ (and other heavy metals) and several antibiotics, but there is yet to be any evidence of NAg-induced co-selection of ARGs in this bacterial genus.

The increasing prevalence of silver resistance combined with growing evidence of the co-emergence of heavy metal and antibiotic resistance highlights the serious issues behind antibacterial overuse. Our knowledge of bacterial resistance to silver and other heavy metals will help equip us to study the complex adaptation mechanisms of bacteria against NAg. Elucidating the mechanisms of NAg resistance could enable the development of technologies that mitigate these problematic adaptation responses. The generated knowledge of how the nanoparticle targets bacteria, and, in turn, how bacteria develop responses to its multi-targeting mechanisms can help guide the physicochemical engineering process of NAg (e.g., morphology, oxidation state, and surface charge) to fine tune its antibacterial activity and, therefore, limit bacterial adaptation. Identification of the molecular basis of NAg resistance will allow us to target the biological signalling molecules and metabolites that trigger adaptation responses, including quorum sensing molecules and/or epigenetic and genetic regulators. The generated knowledge will also help inform strategies for a better risk vs. benefits assessment regarding the application of NAg-containing consumer products, limiting its misuse and inadequate disposal. With no discovery of new effective antibiotics over the last 30 years, we need to protect the efficacy of this valuable alternative antimicrobial agent so that we may continue to use it in the fight against untreatable infections.

## AUTHOR CONTRIBUTIONS

OM, MH, and CG: conceptualisation. OM: writing (original draft preparation). OM, RM, MH, and CG: writing (review and editing). MH and CG: supervision. All authors have read and agreed to the published version of the manuscript.

## FUNDING

This work was supported by research funding through an Australian Research Council (ARC) Discover Project grant (DP180100474). MH was supported by an ARC DECRA fellowship (DE200100111).

## REFERENCES

Abdar, M. H., Taheri-Kalani, M., Taheri, K., Emadi, B., Hasanzadeh, A., Sedighi, A., et al. (2019). Prevalence of extended-spectrum beta-lactamase genes in *Acinetobacter baumannii* strains isolated from nosocomial infections in Tehran, Iran. *GMS Hyg. Infect. Control* 14:Doc02. doi: 10.3205/dgkh000318

Al-Anazi, K. A., and Al-Jasser, A. M. (2014). Infections caused by *Acinetobacter baumannii* in recipients of hematopoietic stem cell transplantation. *Front. Oncol.* 4:186. doi: 10.3389/fonc.2014.00186

Allahverdiyev, A. M., Kon, K. V., Abamor, E. S., Bagirova, M., and Rafailovich, M. (2011). Coping with antibiotic resistance: combining nanoparticles with antibiotics and other antimicrobial agents. *Expert Rev. Anti-Infect. Ther.* 9, 1035–1052. doi: 10.1586/eri.11.121

Alquethamy, S. F., Khorvash, M., Pederick, V. G., Whittall, J. J., Paton, J. C., Paulsen, I. T., et al. (2019). The role of the CopA copper efflux system in *Acinetobacter baumannii* virulence. *Int. J. Mol. Sci.* 20:575. doi: 10.3390/ijms20030575

Alsan, M., and Klompas, M. (2010). *Acinetobacter baumannii*: an emerging and important pathogen. *J. Clin. Outcomes Manag.* 17:363.

Andrade, L. N., Siqueira, T. E., Martinez, R., and Darini, A. L. C. (2018). Multidrug-resistant CTX-M-(15, 9, 2)-and KPC-2-producing *Enterobacter hormaechei* and *Enterobacter asburiae* isolates possessed a set of acquired heavy metal tolerance genes including a chromosomal *sil* operon (for acquired silver resistance). *Front. Microbiol.* 9:539. doi: 10.3389/fmicb.2018.00539

Asif, M., Alvi, I. A., and Rehman, S. U. (2018). Insight into *Acinetobacter baumannii*: pathogenesis, global resistance, mechanisms of resistance, treatment

options, and alternative modalities. *Infect. Drug Resist.* 11, 1249–1260. doi: 10.2147/IDR.S166750

Baker-Austin, C., Wright, M. S., Stepanauskas, R., and McArthur, J. (2006). Co-selection of antibiotic and metal resistance. *Trends Microbiol.* 14, 176–182. doi: 10.1016/j.tim.2006.02.006

Baptista, P. V., McCusker, M. P., Carvalho, A., Ferreira, D. A., Mohan, N. M., Martins, M., et al. (2018). Nano-strategies to fight multidrug resistant bacteria—"A Battle of the Titans". *Front. Microbiol.* 9:1441. doi: 10.3389/fmicb.2018.01441

Bazzi, W., Abou Fayad, A. G., Nasser, A., Haraoui, L.-P., Dewachi, O., Abou-Sitta, G., et al. (2020). Heavy metal toxicity in armed conflicts potentiates AMR in *A. baumannii* by selecting for antibiotic and heavy metal co-resistance mechanisms. *Front. Microbiol.* 11:68. doi: 10.3389/fmicb.2020.00068

Berrisford, J. M., Baradaran, R., and Sazanov, L. A. (2016). Structure of bacterial respiratory complex I. *Biochim. Biophys. Acta* 1857, 892–901. doi: 10.1016/j.bbabio.2016.01.012

Burdușel, A.-C., Gherasim, O., Grumezescu, A. M., Mogoantă, L., Ficai, A., and Andronescu, E. (2018). Biomedical applications of silver nanoparticles: An up-to-date overview. *Nanomaterials* 8:681. doi: 10.3390/nano8090681

Cai, S. J., and Inouye, M. (2002). EnvZ-OmpR interaction and osmoregulation in *Escherichia coli*. *J. Biol. Chem.* 277, 24155–24161. doi: 10.1074/jbc.M110715200

Cassini, A., Colzani, E., Pini, A., Mangen, M.-J. J., Plass, D., McDonald, S. A., et al. (2018). Impact of infectious diseases on population health using incidence-based disability-adjusted life years (DALYs): results from the Burden of Communicable Diseases in Europe study, European Union and European Economic Area countries, 2009 to 2013. *Euro Surveill.* 23, 17-00454. doi: 10.2807/1560-7917.ES.2018.23.16.17-00454

Cassini, A., Högberg, L. D., Plachouras, D., Quattrocchi, A., Hoxha, A., Simonsen, G. S., et al. (2019). Attributable deaths and disability-adjusted life-years caused by infections with antibiotic-resistant bacteria in the EU and the European Economic Area in 2015: a population-level modelling analysis. *Lancet Infect. Dis.* 19, 56–66. doi: 10.1016/S1473-3099(18)30605-4

Cavassin, E. D., de Figueiredo, L. F. P., Otoch, J. P., Seckler, M. M., de Oliveira, R. A., Franco, F. F., et al. (2015). Comparison of methods to detect the in vitro activity of silver nanoparticles (AgNP) against multidrug resistant bacteria. *J. Nanobiotechnol.* 13:64. doi: 10.1186/s12951-015-0120-6

Centers for Disease Control and Prevention (2019). "Antibiotic resistance threats in the United States, 2019". Centres for Disease Control and Prevention, US Department of Health and Human Services.

Chapman, J. S. (2003). Disinfectant resistance mechanisms, cross-resistance, and co-resistance. *Int. Biodeterior. Biodegradation* 51, 271–276. doi: 10.1016/S0964-8305(03)00044-1

Chen, M., Yu, X., Huo, Q., Yuan, Q., Li, X., Xu, C., et al. (2019a). Biomedical potentialities of silver nanoparticles for clinical multiple drug-resistant *Acinetobacter baumannii*. *J. Nanomater.* 2019, 1–7. doi: 10.1155/2019/3754018

Chen, N., Zhou, M., Dong, X., Qu, J., Gong, F., Han, Y., et al. (2020). Epidemiological and clinical characteristics of 99 cases of 2019 novel coronavirus pneumonia in Wuhan, China: a descriptive study. *Lancet* 395, 507–513. doi: 10.1016/S0140-6736(20)30211-7

Chen, Q.-L., Zhu, D., An, X.-L., Ding, J., Zhu, Y.-G., and Cui, L. (2019b). Does nano silver promote the selection of antibiotic resistance genes in soil and plant? *Environ. Int.* 128, 399–406. doi: 10.1016/j.envint.2019.04.061

Choi, O., Yu, C.-P., Fernández, G. E., and Hu, Z. (2010). Interactions of nanosilver with *Escherichia coli* cells in planktonic and biofilm cultures. *Water Res.* 44, 6095–6103. doi: 10.1016/j.watres.2010.06.069

Clancy, C. J., Buehrle, D. J., and Nguyen, M. H. (2020). PRO: the COVID-19 pandemic will result in increased antimicrobial resistance rates. *JAC Antimicrob. Resist.* 2:dlaa049. doi: 10.1093/jacamr/dlaa049

Dakal, T. C., Kumar, A., Majumdar, R. S., and Yadav, V. (2016). Mechanistic basis of antimicrobial actions of silver nanoparticles. *Front. Microbiol.* 7:1831. doi: 10.3389/fmicb.2016.01831

Deshpande, L. M., and Chopade, B. A. (1994). Plasmid mediated silver resistance in *Acinetobacter baumannii*. *Biometals* 7, 49–56. doi: 10.1007/BF00205194

Deshpande, L. M., Kapadnis, B. P., and Chopade, B. A. (1993). Metal resistance in *Acinetobacter* and its relation to β-lactamase production. *Biometals* 6, 55–59. doi: 10.1007/BF00154233

Donlan, R. M. (2002). Biofilms: microbial life on surfaces. *Emerg. Infect. Dis.* 8:881. doi: 10.3201/eid0809.020063

Dufour, D., Leung, V., and Lévesque, C. M. (2010). Bacterial biofilm: structure, function, and antimicrobial resistance. *Endod. Top.* 22, 2–16. doi: 10.1111/j.1601-1546.2012.00277.x

Duval, R. E., Gouyau, J., and Lamouroux, E. (2019). Limitations of recent studies dealing with the antibacterial properties of silver nanoparticles: fact and opinion. *Nanomaterials* 9:1775. doi: 10.3390/nano9121775

Ebrahimi, A., Jafferi, H., Habibian, S., and Lotfalian, S. (2018). Evaluation of anti biofilm and antibiotic potentiation activities of silver nanoparticles against some nosocomial pathogens. *Iranian J. Pharm. Sci.* 14, 7–14. doi: 10.22034/IJPS.2018.33684

El Badawy, A. M., Silva, R. G., Morris, B., Scheckel, K. G., Suidan, M. T., and Tolaymat, T. M. (2010). Surface charge-dependent toxicity of silver nanoparticles. *Environ. Sci. Technol.* 45, 283–287. doi: 10.1021/es1034188

Ezraty, B., Gennaris, A., Barras, F., and Collet, J.-F. (2017). Oxidative stress, protein damage and repair in bacteria. *Nat. Rev. Microbiol.* 15, 385–396. doi: 10.1038/nrmicro.2017.26

Fahmy, H. M., Mosleh, A. M., Abd Elghany, A., Shams-Eldin, E., Serea, E. S. A., Ali, S. A., et al. (2019). Coated silver nanoparticles: synthesis, cytotoxicity, and optical properties. *RSC Adv.* 9, 20118–20136. doi: 10.1039/C9RA02907A

Fair, R. J., and Tor, Y. (2014). Antibiotics and bacterial resistance in the 21st century. *Perspect. Medicin. Chem.* 6, 25–64. doi: 10.4137/PMC.S14459

Feng, Q. L., Wu, J., Chen, G., Cui, F., Kim, T., and Kim, J. (2000). A mechanistic study of the antibacterial effect of silver ions on *Escherichia coli* and *Staphylococcus aureus*. *J. Biomed. Mater. Res.* 52, 662–668. doi: 10.1002/1097-4636(20001215)52:4<662::AID-JBM10>3.0.CO;2-3

Ferdous, Z., and Nemmar, A. (2020). Health impact of silver nanoparticles: a review of the biodistribution and toxicity following various routes of exposure. *Int. J. Mol. Sci.* 21:2375. doi: 10.3390/ijms21072375

Finley, P. J., Norton, R., Austin, C., Mitchell, A., Zank, S., and Durham, P. (2015). Unprecedented silver resistance in clinically isolated *Enterobacteriaceae*: major implications for burn and wound management. *Antimicrob. Agents Chemother.* 59, 4734–4741. doi: 10.1128/AAC.00026-15

Flemming, H.-C., and Wingender, J. (2010). The biofilm matrix. *Nat. Rev. Microbiol.* 8:623. doi: 10.1038/nrmicro2415

Franke, S., Grass, G., Rensing, C., and Nies, D. H. (2003). Molecular analysis of the copper-transporting efflux system CusCFBA of *Escherichia coli*. *J. Bacteriol.* 185, 3804–3812. doi: 10.1128/JB.185.13.3804-3812.2003

Gaidhani, S., Singh, R., Singh, D., Patel, U., Shevade, K., Yeshvekar, R., et al. (2013). Biofilm disruption activity of silver nanoparticles synthesized by *Acinetobacter calcoaceticus* PUCM 1005. *Mater. Lett.* 108, 324–327. doi: 10.1016/j.matlet.2013.07.023

Garcia-Garcia, T., Poncet, S., Derouiche, A., Shi, L., Mijakovic, I., and Noirot-Gros, M.-F. (2016). Role of protein phosphorylation in the regulation of cell cycle and DNA-related processes in bacteria. *Front. Microbiol.* 7:184. doi: 10.3389/fmicb.2016.00184

Garrett, T. R., Bhakoo, M., and Zhang, Z. (2008). Bacterial adhesion and biofilms on surfaces. *Prog. Nat. Sci.* 18, 1049–1056. doi: 10.1016/j.pnsc.2008.04.001

Ge, L., Li, Q., Wang, M., Ouyang, J., Li, X., and Xing, M. M. (2014). Nanosilver particles in medical applications: synthesis, performance, and toxicity. *Int. J. Nanomedicine* 9, 2399–2407. doi: 10.2147/IJN.S55015

Gębka, K., Bełdowski, J., and Bełdowska, M. (2016). The impact of military activities on the concentration of mercury in soils of military training grounds and marine sediments. *Environ. Sci. Pollut. Res.* 23, 23103–23113. doi: 10.1007/s11356-016-7436-0

Gilmour, M. W., Thomson, N. R., Sanders, M., Parkhill, J., and Taylor, D. E. (2004). The complete nucleotide sequence of the resistance plasmid R478: defining the backbone components of incompatibility group H conjugative plasmids through comparative genomics. *Plasmid* 52, 182–202. doi: 10.1016/j.plasmid.2004.06.006

Golkar, Z., Bagasra, O., and Pace, D. G. (2014). Bacteriophage therapy: a potential solution for the antibiotic resistance crisis. *J. Infect. Dev. Ctries.* 8, 129–136. doi: 10.3855/jidc.3573

Gonzalez-Villoria, A. M., and Valverde-Garduno, V. (2016). Antibiotic-resistant *Acinetobacter baumannii* increasing success remains a challenge as a nosocomial pathogen. *J. Pathog.* 2016, 1–10. doi: 10.1155/2016/7318075

Gottesman, T., Fedorowsky, R., Yerushalmi, R., Lellouche, J., and Nutman, A. (2021). An outbreak of carbapenem-resistant *Acinetobacter baumannii* in a

COVID-19 dedicated hospital. *Infect. Prev. Pract.* 3:100113. doi: 10.1016/j.infpip.2021.100113

Graves, J. L. Jr., Tajkarimi, M., Cunningham, Q., Campbell, A., Nonga, H., Harrison, S. H., et al. (2015). Rapid evolution of silver nanoparticle resistance in *Escherichia coli*. *Front. Genet.* 6:42. doi: 10.3389/fgene.2015.00042

Gunawan, C., Faiz, M. B., Mann, R., Ting, S. R., Sotiriou, G. A., Marquis, C. P., et al. (2020). Nanosilver targets the bacterial cell envelope: the link with generation of reactive oxygen radicals. *ACS Appl. Mater. Interfaces* 12, 5557–5568. doi: 10.1021/acsami.9b20193

Gunawan, C., Marquis, C. P., Amal, R., Sotiriou, G. A., Rice, S. A., and Harry, E. J. (2017). Widespread and indiscriminate nanosilver use: genuine potential for microbial resistance. *ACS Nano* 11, 3438–3445. doi: 10.1021/acsnano.7b01166

Gunawan, C., Teoh, W. Y., Marquis, C. P., and Amal, R. (2013). Induced adaptation of *Bacillus* sp. to antimicrobial nanosilver. *Small* 9, 3554–3560. doi: 10.1002/smll.201300761

Gupta, A., Matsui, K., Lo, J.-F., and Silver, S. (1999). Molecular basis for resistance to silver cations in *Salmonella*. *Nat. Med.* 5, 183–188. doi: 10.1038/5545

Gupta, A., Phung, L. T., Taylor, D. E., and Silver, S. (2001). Diversity of silver resistance genes in IncH incompatibility group plasmids. *Microbiology* 147, 3393–3402. doi: 10.1099/00221287-147-12-3393

Guzman, M., Dille, J., and Godet, S. (2012). Synthesis and antibacterial activity of silver nanoparticles against gram-positive and gram-negative bacteria. *Nanomedicine* 8, 37–45. doi: 10.1016/j.nano.2011.05.007

Hamida, R. S., Ali, M. A., Goda, D. A., Khalil, M. I., and Redhwan, A. (2020). Cytotoxic effect of green silver nanoparticles against ampicillin-resistant *Klebsiella pneumoniae*. *RSC Adv.* 10, 21136–21146. doi: 10.1039/D0RA03580G

Hamidian, M., and Hall, R. M. (2018). The AbaR antibiotic resistance islands found in *Acinetobacter baumannii* global clone 1–structure, origin and evolution. *Drug Resist. Updat.* 41, 26–39. doi: 10.1016/j.drup.2018.10.003

Hamidian, M., and Nigro, S. J. (2019). Emergence, molecular mechanisms and global spread of carbapenem-resistant *Acinetobacter baumannii*. *Microb. Genom.* 5:e000306. doi: 10.1099/mgen.0.000306

Hausner, M., and Wuertz, S. (1999). High rates of conjugation in bacterial biofilms as determined by quantitative in situ analysis. *Appl. Environ. Microbiol.* 65, 3710–3713. doi: 10.1128/AEM.65.8.3710-3713.1999

Heritier, C., Poirel, L., and Nordmann, P. (2006). Cephalosporinase over-expression resulting from insertion of ISAba1 in *Acinetobacter baumannii*. *Clin. Microbiol. Infect.* 12, 123–130. doi: 10.1111/j.1469-0691.2005.01320.x

Holt, K. B., and Bard, A. J. (2005). Interaction of silver (I) ions with the respiratory chain of *Escherichia coli*: an electrochemical and scanning electrochemical microscopy study of the antimicrobial mechanism of micromolar $Ag^+$. *Biochemistry* 44, 13214–13223. doi: 10.1021/bi0508542

Hosny, A. E.-D. M., Rasmy, S. A., Aboul-Magd, D. S., Kashef, M. T., and El-Bazza, Z. E. (2019). The increasing threat of silver-resistance in clinical isolates from wounds and burns. *Infect. Drug Resist.* 2019, 1985–2001. doi: 10.2147/IDR.S209881

Howard, A., O'Donoghue, M., Feeney, A., and Sleator, R. D. (2012). *Acinetobacter baumannii*: an emerging opportunistic pathogen. *Virulence* 3, 243–250. doi: 10.4161/viru.19700

Hsu, J. (2020). How covid-19 is accelerating the threat of antimicrobial resistance. *BMJ* 369:m1983. doi: 10.1136/bmj.m1983

Hujer, K. M., Hujer, A. M., Hulten, E. A., Bajaksouzian, S., Adams, J. M., Donskey, C. J., et al. (2006). Analysis of antibiotic resistance genes in multidrug-resistant *Acinetobacter* sp. isolates from military and civilian patients treated at the Walter Reed Army Medical Center. *Antimicrob. Agents Chemother.* 50, 4114–4123. doi: 10.1128/AAC.00778-06

Jain, U. (2020). Risk of COVID-19 due to shortage of personal protective equipment. *Cureus* 12:e8837. doi: 10.7759/cureus.8837

Jelenko, C. 3rd. (1969). Silver nitrate resistant *E. coli*: report of case. *Ann. Surg.* 170, 296–299. doi: 10.1097/00000658-196908000-00021

Johnson, T. J., Wannemeuhler, Y. M., Scaccianoce, J. A., Johnson, S. J., and Nolan, L. K. (2006). Complete DNA sequence, comparative genomics, and prevalence of an IncHI2 plasmid occurring among extraintestinal pathogenic *Escherichia coli* isolates. *Antimicrob. Agents Chemother.* 50, 3929–3933. doi: 10.1128/AAC.00569-06

Kang, F., Alvarez, P. J., and Zhu, D. (2013). Microbial extracellular polymeric substances reduce $Ag^+$ to silver nanoparticles and antagonize bactericidal activity. *Environ. Sci. Technol.* 48, 316–322. doi: 10.1021/es403796x

Katva, S., Das, S., Moti, H. S., Jyoti, A., and Kaushik, S. (2017). Antibacterial synergy of silver nanoparticles with gentamicin and chloramphenicol against *Enterococcus faecalis*. *Pharmacogn. Mag.* 13, S828–S833. doi: 10.4103/pm.pm_120_17

Kędziora, A., Speruda, M., Krzyżewska, E., Rybka, J., Łukowiak, A., and Bugla-Płoskońska, G. (2018). Similarities and differences between silver ions and silver in nanoforms as antibacterial agents. *Int. J. Mol. Sci.* 19:444. doi: 10.3390/ijms19020444

Khan, I., Saeed, K., and Khan, I. (2017). Nanoparticles: properties, applications and toxicities. *Arab. J. Chem.* 2017, 1–24. doi: 10.1016/j.arabjc.2017.05.011

Kirstein, J., and Turgay, K. (2005). A new tyrosine phosphorylation mechanism involved in signal transduction in *Bacillus subtilis*. *J. Mol. Microbiol. Biotechnol.* 9, 182–188. doi: 10.1159/000089646

Koditschek, L. K., and Guyre, P. (1974). Resistance transfer fecal coliforms isolated from the Whippany River. *Water Res.* 8, 747–752. doi: 10.1016/0043-1354(74)90019-0

Koebnik, R., Locher, K. P., and Van Gelder, P. (2000). Structure and function of bacterial outer membrane proteins: barrels in a nutshell. *Mol. Microbiol.* 37, 239–253. doi: 10.1046/j.1365-2958.2000.01983.x

Lara, H. H., Ayala-Núñez, N. V., Turrent, L. D. C. I., and Padilla, C. R. (2010). Bactericidal effect of silver nanoparticles against multidrug-resistant bacteria. *World J. Microbiol. Biotechnol.* 26, 615–621. doi: 10.1007/s11274-009-0211-3

Lemire, J. A., Harrison, J. J., and Turner, R. J. (2013). Antimicrobial activity of metals: mechanisms, molecular targets and applications. *Nat. Rev. Microbiol.* 11, 371–384. doi: 10.1038/nrmicro3028

Lewis, K. (2010). Persister cells. *Annu. Rev. Microbiol.* 64, 357–372. doi: 10.1146/annurev.micro.112408.134306

Li, P., Li, J., Wu, C., Wu, Q., and Li, J. (2005). Synergistic antibacterial effects of β-lactam antibiotic combined with silver nanoparticles. *Nanotechnology* 16:1912. doi: 10.1088/0957-4484/16/9/082

Li, X.-Z., Nikaido, H., and Williams, K. E. (1997). Silver-resistant mutants of *Escherichia coli* display active efflux of $Ag^+$ and are deficient in porins. *J. Bacteriol.* 179, 6127–6132. doi: 10.1128/JB.179.19.6127-6132.1997

Li, W.-R., Sun, T.-L., Zhou, S.-L., Ma, Y.-K., Shi, Q.-S., Xie, X.-B., et al. (2017). A comparative analysis of antibacterial activity, dynamics, and effects of silver ions and silver nanoparticles against four bacterial strains. *Int. Biodeterior. Biodegradation* 123, 304–310. doi: 10.1016/j.ibiod.2017.07.015

Loh, J. V., Percival, S. L., Woods, E. J., Williams, N. J., and Cochrane, C. A. (2009). Silver resistance in MRSA isolated from wound and nasal sources in humans and animals. *Int. Wound J.* 6, 32–38. doi: 10.1111/j.1742-481X.2008.00563.x

Lok, C.-N., Ho, C.-M., Chen, R., He, Q.-Y., Yu, W.-Y., Sun, H., et al. (2006). Proteomic analysis of the mode of antibacterial action of silver nanoparticles. *J. Proteome Res.* 5, 916–924. doi: 10.1021/pr0504079

Lok, C.-N., Ho, C.-M., Chen, R., Tam, P. K. -H., Chiu, J. -F., and Che, C.-M. (2008). Proteomic identification of the Cus system as a major determinant of constitutive *Escherichia coli* silver resistance of chromosomal origin. *J. Proteome Res.* 7, 2351–2356. doi:10.1021/pr700646b, PMID: 18419149

Loo, Y. Y., Rukayadi, Y., Nor-Khaizura, M.-A.-R., Kuan, C. H., Chieng, B. W., Nishibuchi, M., et al. (2018). In vitro antimicrobial activity of green synthesized silver nanoparticles against selected gram-negative foodborne pathogens. *Front. Microbiol.* 9:1555. doi: 10.3389/fmicb.2018.01555

López, D., Vlamakis, H., and Kolter, R. (2010). Biofilms. *Cold Spring Harb. Perspect. Biol.* 2:a000398. doi: 10.1101/cshperspect.a000398

Lu, Y., and Swartz, J. R. (2016). Functional properties of flagellin as a stimulator of innate immunity. *Sci. Rep.* 6:18379. doi: 10.1038/srep18379

Łysakowska, M. E., Ciebiada-Adamiec, A., Klimek, L., and Sienkiewicz, M. (2015). The activity of silver nanoparticles (Axonnite) on clinical and environmental strains of *Acinetobacter* spp. *Burns* 41, 364–371. doi: 10.1016/j.burns.2014.07.014

Ma, Y., Metch, J. W., Yang, Y., Pruden, A., and Zhang, T. (2016). Shift in antibiotic resistance gene profiles associated with nanosilver during wastewater treatment. *FEMS Microbiol. Ecol.* 92:fiw022. doi: 10.1093/femsec/fiw022

Marambio-Jones, C., and Hoek, E. M. (2010). A review of the antibacterial effects of silver nanomaterials and potential implications for human health and the environment. *J. Nanopart. Res.* 12, 1531–1551. doi: 10.1007/s11051-010-9900-y

Markowska, K., Grudniak, A. M., and Wolska, K. I. (2013). Silver nanoparticles as an alternative strategy against bacterial biofilms. *Acta Biochim. Pol.* 60, 523–530. doi: 10.18388/abp.2013_2016

Martinez-Gutierrez, F., Boegli, L., Agostinho, A., Sánchez, E. M., Bach, H., Ruiz, F., et al. (2013). Anti-biofilm activity of silver nanoparticles against different microorganisms. *Biofouling* 29, 651–660. doi: 10.1080/08927014.2013.794225

McHugh, G. L., Moellering, R., Hopkins, C., and Swartz, M. (1975). *Salmonella typhimurium* resistant to silver nitrate, chloramphenicol, and ampicillin: a new threat in burn units? *Lancet* 305, 235–240. doi: 10.1016/S0140-6736(75)91138-1

McShan, D., Zhang, Y., Deng, H., Ray, P. C., and Yu, H. (2015). Synergistic antibacterial effect of silver nanoparticles combined with ineffective antibiotics on drug resistant *Salmonella typhimurium* DT104. *J. Environ. Sci. Health C Environ. Carcinog. Ecotoxicol. Rev.* 33, 369–384. doi: 10.1080/10590501.2015.1055165

Metlina, A. (2004). Bacterial and archaeal flagella as prokaryotic motility organelles. *Biochemistry* 69, 1203–1212. doi: 10.1007/s10541-005-0065-8

Michael, C. A., Dominey-Howes, D., and Labbate, M. (2014). The antimicrobial resistance crisis: causes, consequences, and management. *Front. Public Health* 2:145. doi: 10.3389/fpubh.2014.00145

Mijnendonckx, K., Leys, N., Mahillon, J., Silver, S., and Van Houdt, R. (2013). Antimicrobial silver: uses, toxicity and potential for resistance. *Biometals* 26, 609–621. doi: 10.1007/s10534-013-9645-z

Miller, M. B., and Bassler, B. L. (2001). Quorum sensing in bacteria. *Annu. Rev. Microbiol.* 55, 165–199. doi: 10.1146/annurev.micro.55.1.165

Mody, V. V., Siwale, R., Singh, A., and Mody, H. R. (2010). Introduction to metallic nanoparticles. *J. Pharm. Bioallied Sci.* 2, 282–289. doi: 10.4103/0975-7406.72127

Morones, J. R., Elechiguerra, J. L., Camacho, A., Holt, K., Kouri, J. B., Ramírez, J. T., et al. (2005). The bactericidal effect of silver nanoparticles. *Nanotechnology* 16, 2346–2353. doi: 10.1088/0957-4484/16/10/059

Muller, M., and Merrett, N. D. (2014). Pyocyanin production by *Pseudomonas aeruginosa* confers resistance to ionic silver. *Antimicrob. Agents Chemother.* 58, 5492–5499. doi: 10.1128/AAC.03069-14

Munson, G. P., Lam, D. L., Outten, F. W., and O'Halloran, T. V. (2000). Identification of a copper-responsive two-component system on the chromosome of *Escherichia coli* K-12. *J. Bacteriol.* 182, 5864–5871. doi: 10.1128/JB.182.20.5864-5871.2000

Nakajima, H., Kobayashi, K., Kobayashi, M., Asako, H., and Aono, R. (1995). Overexpression of the *robA* gene increases organic solvent tolerance and multiple antibiotic and heavy metal ion resistance in *Escherichia coli*. *Appl. Environ. Microbiol.* 61, 2302–2307. doi: 10.1128/AEM.61.6.2302-2307.1995

Nikaido, H. (1994). Porins and specific diffusion channels in bacterial outer membranes. *J. Biol. Chem.* 269, 3905–3908. doi: 10.1016/S0021-9258(17)41716-9

Niño-Martínez, N., Salas Orozco, M. F., Martínez-Castañón, G.-A., Torres Méndez, F., and Ruiz, F. (2019). Molecular mechanisms of bacterial resistance to metal and metal oxide nanoparticles. *Int. J. Mol. Sci.* 20:2808. doi: 10.3390/ijms20112808

O'Toole, G., Kaplan, H. B., and Kolter, R. (2000). Biofilm formation as microbial development. *Annu. Rev. Microbiol.* 54, 49–79. doi: 10.1146/annurev.micro.54.1.49

Pal, C., Asiani, K., Arya, S., Rensing, C., Stekel, D. J., Larsson, D. J., et al. (2017). Metal resistance and its association with antibiotic resistance. *Adv. Microb. Physiol.* 70, 261–313. doi: 10.1016/bs.ampbs.2017.02.001

Pal, S., Tak, Y. K., and Song, J. M. (2007). Does the antibacterial activity of silver nanoparticles depend on the shape of the nanoparticle? A study of the gram-negative bacterium *Escherichia coli*. *Appl. Environ. Microbiol.* 73, 1712–1720. doi: 10.1128/AEM.02218-06

Panáček, A., Kvítek, L., Smékalová, M., Večeřová, R., Kolář, M., Röderová, M., et al. (2018). Bacterial resistance to silver nanoparticles and how to overcome it. *Nat. Nanotechnol.* 13, 65–71. doi: 10.1038/s41565-017-0013-y

Park, S., and Imlay, J. A. (2003). High levels of intracellular cysteine promote oxidative DNA damage by driving the Fenton reaction. *J. Bacteriol.* 185, 1942–1950. doi: 10.1128/JB.185.6.1942-1950.2003

Pazos-Ortiz, E., Roque-Ruiz, J. H., Hinojos-Márquez, E. A., López-Esparza, J., Donohué-Cornejo, A., Cuevas-González, J. C., et al. (2017). Dose-dependent antimicrobial activity of silver nanoparticles on polycaprolactone fibers against gram-positive and gram-negative bacteria. *J. Nanomater.* 2017, 1–9. doi: 10.1155/2017/4752314

Peleg, A. Y., Seifert, H., and Paterson, D. L. (2008). *Acinetobacter baumannii*: emergence of a successful pathogen. *Clin. Microbiol. Rev.* 21, 538–582. doi: 10.1128/CMR.00058-07

Percival, S. L., Bowler, P. G., and Dolman, J. (2007). Antimicrobial activity of silver-containing dressings on wound microorganisms using an in vitro biofilm model. *Int. Wound J.* 4, 186–191. doi: 10.1111/j.1742-481X.2007.00296.x

Perez, S., Innes, G. K., Walters, M. S., Mehr, J., Arias, J., Greeley, R., et al. (2020). Increase in hospital-acquired carbapenem-resistant Acinetobacter baumannii infection and colonization in an acute care hospital during a surge in COVID-19 admissions—New Jersey, February–July 2020. *Morb. Mortal. Wkly Rep.* 69:1827. doi: 10.15585/mmwr.mm6948e1

Pietsch, F., O'Neill, A. J., Ivask, A., Jenssen, H., Inkinen, J., Kahru, A., et al. (2020). Selection of resistance by antimicrobial coatings in the healthcare setting. *J. Hosp. Infect.* 106, 115–125. doi: 10.1016/j.jhin.2020.06.006

Pompilio, A., Geminiani, C., Bosco, D., Rana, R., Aceto, A., Bucciarelli, T., et al. (2018). Electrochemically synthesized silver nanoparticles are active against planktonic and biofilm cells of *Pseudomonas aeruginosa* and other cystic fibrosis-associated bacterial pathogens. *Front. Microbiol.* 9:1349. doi: 10.3389/fmicb.2018.01349

Qayyum, S., Oves, M., and Khan, A. U. (2017). Obliteration of bacterial growth and biofilm through ROS generation by facilely synthesized green silver nanoparticles. *PLoS One* 12:e0181363. doi: 10.1371/journal.pone.0181363

Qiu, Z., Shen, Z., Qian, D., Jin, M., Yang, D., Wang, J., et al. (2015). Effects of nano-TiO2 on antibiotic resistance transfer mediated by RP4 plasmid. *Nanotoxicology* 9, 895–904. doi: 10.3109/17435390.2014.991429

Qiu, Z., Yu, Y., Chen, Z., Jin, M., Yang, D., Zhao, Z., et al. (2012). Nanoalumina promotes the horizontal transfer of multiresistance genes mediated by plasmids across genera. *Proc. Natl. Acad. Sci. U. S. A.* 109, 4944–4949. doi: 10.1073/pnas.1107254109

Radzig, M., Nadtochenko, V., Koksharova, O., Kiwi, J., Lipasova, V., and Khmel, I. (2013). Antibacterial effects of silver nanoparticles on gram-negative bacteria: influence on the growth and biofilms formation, mechanisms of action. *Colloids Surf. B Biointerfaces* 102, 300–306. doi: 10.1016/j.colsurfb.2012.07.039

Rai, M., Deshmukh, S., Ingle, A., and Gade, A. (2012). Silver nanoparticles: the powerful nanoweapon against multidrug-resistant bacteria. *J. Appl. Microbiol.* 112, 841–852. doi: 10.1111/j.1365-2672.2012.05253.x

Rai, M., Yadav, A., and Gade, A. (2009). Silver nanoparticles as a new generation of antimicrobials. *Biotechnol. Adv.* 27, 76–83. doi: 10.1016/j.biotechadv.2008.09.002

Ramachandran, R., and Sangeetha, D. (2017). Antibiofilm efficacy of silver nanoparticles against biofilm forming multidrug resistant clinical isolates. *Pharm. Innov.* 6, 36–43.

Randall, C. P., Gupta, A., Jackson, N., Busse, D., and O'Neill, A. J. (2015). Silver resistance in Gram-negative bacteria: a dissection of endogenous and exogenous mechanisms. *J. Antimicrob. Chemother.* 70, 1037–1046. doi: 10.1093/jac/dku523

Randall, C. P., Oyama, L. B., Bostock, J. M., Chopra, I., and O'Neill, A. J. (2013). The silver cation ($Ag^+$): antistaphylococcal activity, mode of action and resistance studies. *J. Antimicrob. Chemother.* 68, 131–138. doi: 10.1093/jac/dks372

Ray, P. D., Huang, B.-W., and Tsuji, Y. (2012). Reactive oxygen species (ROS) homeostasis and redox regulation in cellular signaling. *Cell. Signal.* 24, 981–990. doi: 10.1016/j.cellsig.2012.01.008

Rice, L. B. (2008). Federal funding for the study of antimicrobial resistance in nosocomial pathogens: no ESKAPE. *J. Infect. Dis.* 197, 1079–1081. doi: 10.1086/533452

Romanova, I., and Gintsburg, A. (2011). Bacterial biofilms as a natural form of existence of bacteria in the environment and host organism. *Zh. Mikrobiol. Epidemiol. Immunobiol.* 3, 99–109.

Rosenkranz, H. S., Coward, J. E., Wlodkowski, T. J., and Carr, H. S. (1974). Properties of silver sulfadiazine-resistant *Enterobacter cloacae*. *Antimicrob. Agents Chemother.* 5, 199–201. doi: 10.1128/AAC.5.2.199

Różalska, B., Sadowska, B., Budzyńska, A., Bernat, P., and Różalska, S. (2018). Biogenic nanosilver synthesized in Metarhizium robertsii waste mycelium extract–As a modulator of *Candida albicans* morphogenesis, membrane lipidome and biofilm. *PLoS One* 13:e0194254. doi: 10.1371/journal.pone.0194254

Rutherford, S. T., and Bassler, B. L. (2012). Bacterial quorum sensing: its role in virulence and possibilities for its control. *Cold Spring Harb. Perspect. Med.* 2:a012427. doi: 10.1101/cshperspect.a012427

Salunke, G. R., Ghosh, S., Kumar, R. S., Khade, S., Vashisth, P., Kale, T., et al. (2014). Rapid efficient synthesis and characterization of silver, gold, and bimetallic nanoparticles from the medicinal plant *Plumbago zeylanica* and

their application in biofilm control. *Int. J. Nanomedicine* 9:2635. doi: 10.2147/IJN.S59834

Sánchez-López, E., Gomes, D., Esteruelas, G., Bonilla, L., Lopez-Machado, A. L., Galindo, R., et al. (2020). Metal-based nanoparticles as antimicrobial agents: an overview. *Nanomaterials* 10:292. doi: 10.3390/nano10020292

Santajit, S., and Indrawattana, N. (2016). Mechanisms of antimicrobial resistance in ESKAPE pathogens. *Biomed. Res. Int.* 2016:2475067. doi: 10.1155/2016/2475067

Schäfer, B., Tentschert, J., and Luch, A. (2011). Nanosilver in consumer products and human health: more information required! *Environ. Sci. Technol.* 45, 7589–7590. doi: 10.1021/es200804u

Seiler, C., and Berendonk, T. U. (2012). Heavy metal driven co-selection of antibiotic resistance in soil and water bodies impacted by agriculture and aquaculture. *Front. Microbiol.* 3:399. doi: 10.3389/fmicb.2012.00399

Shakibaie, M., Dhakephalker, B., Kapadnis, B., and Chopade, B. (2003). Silver resistance in *Acinetobacter baumannii* BL54 occurs through binding to a Ag-binding protein. *Iran. J. Biotechnol.* 1, 41–46.

Sharifipour, E., Shams, S., Esmkhani, M., Khodadadi, J., Fotouhi-Ardakani, R., Koohpaei, A., et al. (2020). Evaluation of bacterial co-infections of the respiratory tract in COVID-19 patients admitted to ICU. *BMC Infect. Dis.* 20:646. doi: 10.1186/s12879-020-05374-z

Sherburne, C. K., Lawley, T. D., Gilmour, M. W., Blattner, F., Burland, V., Grotbeck, E., et al. (2000). The complete DNA sequence and analysis of R27, a large IncHI plasmid from *Salmonella typhi* that is temperature sensitive for transfer. *Nucleic Acids Res.* 28, 2177–2186. doi: 10.1093/nar/28.10.2177

Shih, H.-Y., and Lin, Y. E. (2010). Efficacy of copper-silver ionization in controlling biofilm-and plankton-associated waterborne pathogens. *Appl. Environ. Microbiol.* 76, 2032–2035. doi: 10.1128/AEM.02174-09

Shrivastava, S., Bera, T., Roy, A., Singh, G., Ramachandrarao, P., and Dash, D. (2007). Characterization of enhanced antibacterial effects of novel silver nanoparticles. *Nanotechnology* 18:225103. doi: 10.1088/0957-4484/18/22/225103

Siddiqui, M., Mondal, A., Sultan, I., Ali, A., and Haq, Q. (2019). Co-occurrence of ESBLs and silver resistance determinants among bacterial isolates inhabiting polluted stretch of river Yamuna, India. *Int. J. Environ. Sci. Technol.* 16, 5611–5622. doi: 10.1007/s13762-018-1939-9

Silhavy, T. J., Kahne, D., and Walker, S. (2010). The bacterial cell envelope. *Cold Spring Harb. Perspect. Biol.* 2:a000414. doi: 10.1101/cshperspect.a000414

Silva, G. A. (2004). Introduction to nanotechnology and its applications to medicine. *Surg. Neurol.* 61, 216–220. doi: 10.1016/j.surneu.2003.09.036

Silva Santos, K., Barbosa, A. M., Pereira da Costa, L., Pinheiro, M. S., Oliveira, M. B. P. P., and Ferreira Padilha, F. (2016). Silver nanocomposite biosynthesis: antibacterial activity against multidrug-resistant strains of *Pseudomonas aeruginosa* and *Acinetobacter baumannii*. *Molecules* 21:1255. doi: 10.3390/molecules21091255

Silver, S. (2003). Bacterial silver resistance: molecular biology and uses and misuses of silver compounds. *FEMS Microbiol. Rev.* 27, 341–353. doi: 10.1016/S0168-6445(03)00047-0

Singh, R., Nadhe, S., Wadhwani, S., Shedbalkar, U., and Chopade, B. A. (2016). Nanoparticles for control of biofilms of *Acinetobacter* species. *Materilas* 9:383. doi: 10.3390/ma9050383

Singh, S., Singh, S. K., Chowdhury, I., and Singh, R. (2017). Understanding the mechanism of bacterial biofilms resistance to antimicrobial agents. *Open Microbiol. J.* 11, 53–62. doi: 10.2174/1874285801711010053

Singh, R., Vora, J., Nadhe, S. B., Wadhwani, S. A., Shedbalkar, U. U., and Chopade, B. A. (2018). Antibacterial activities of bacteriagenic silver nanoparticles against nosocomial *Acinetobacter baumannii*. *J. Nanosci. Nanotechnol.* 18, 3806–3815. doi: 10.1166/jnn.2018.15013

Sinha, S. C., Krahn, J., Shin, B. S., Tomchick, D. R., Zalkin, H., and Smith, J. L. (2003). The purine repressor of *Bacillus subtilis*: a novel combination of domains adapted for transcription regulation. *J. Bacteriol.* 185, 4087–4098. doi: 10.1128/JB.185.14.4087-4098.2003

Slavin, Y. N., Asnis, J., Häfeli, U. O., and Bach, H. (2017). Metal nanoparticles: understanding the mechanisms behind antibacterial activity. *J. Nanobiotechnol.* 15:65. doi: 10.1186/s12951-017-0308-z

Song, T., Duperthuy, M., and Wai, S. N. (2016). Sub-optimal treatment of bacterial biofilms. *Antibiotics* 5:23. doi: 10.3390/antibiotics5020023

Su, D., Berndt, C., Fomenko, D. E., Holmgren, A., and Gladyshev, V. N. (2007). A conserved cis-proline precludes metal binding by the active site thiolates in members of the thioredoxin family of proteins. *Biochemistry* 46, 6903–6910. doi: 10.1021/bi700152b

Syafiuddin, A., Salim, M. R., Beng Hong Kueh, A., Hadibarata, T., and Nur, H. (2017). A review of silver nanoparticles: research trends, global consumption, synthesis, properties, and future challenges. *J. Chin. Chem. Soc.* 64, 732–756. doi: 10.1002/jccs.201700067

Tang, S., and Zheng, J. (2018). Antibacterial activity of silver nanoparticles: structural effects. *Adv. Healthc. Mater.* 7:1701503. doi: 10.1002/adhm.201701503

Tiwari, V., Tiwari, M., and Solanki, V. (2017). Polyvinylpyrrolidone-capped silver nanoparticle inhibits infection of carbapenem-resistant strain of *Acinetobacter baumannii* in the human pulmonary epithelial cell. *Front. Immunol.* 8:973. doi: 10.3389/fimmu.2017.00973

Towner, K. (2009). Acinetobacter: an old friend, but a new enemy. *J. Hosp. Infect.* 73, 355–363. doi: 10.1016/j.jhin.2009.03.032

Vaidya, M. Y., McBain, A. J., Butler, J. A., Banks, C. E., and Whitehead, K. A. (2017). Antimicrobial efficacy and synergy of metal ions against *Enterococcus faecium*, *Klebsiella pneumoniae* and *Acinetobacter baumannii* in planktonic and biofilm phenotypes. *Sci. Rep.* 7, 1–9. doi: 10.1038/s41598-017-05976-9

Valentin, E., Bottomley, A. L., Chilambi, G. S., Harry, E., Amal, R., Sotiriou, G. A., et al. (2020). Heritable nanosilver resistance in priority pathogen: a unique genetic adaptation and comparison with ionic silver and antibiotic. *Nanoscale* 12, 2384–2392. doi: 10.1039/C9NR08424J

Vänskä, M., Diab, S. Y., Perko, K., Quota, S. R., Albarqouni, N. M., Myöhänen, A., et al. (2019). Toxic environment of war: maternal prenatal heavy metal load predicts infant emotional development. *Infant Behav. Dev.* 55, 1–9. doi: 10.1016/j.infbeh.2019.01.002

Ventola, C. L. (2015). The antibiotic resistance crisis: part 1: causes and threats. *Pharm. Ther.* 40:277.

Veress, A., Nagy, T., Wilk, T., Kömüves, J., Olasz, F., and Kiss, J. (2020). Abundance of mobile genetic elements in an *Acinetobacter lwoffii* strain isolated from Transylvanian honey sample. *Sci. Rep.* 10:2969. doi: 10.1038/s41598-020-59938-9

Vila Domínguez, A., Ayerbe Algaba, R., Miró Canturri, A., Rodríguez Villodres, Á., and Smani, Y. (2020). Antibacterial activity of colloidal silver against gram-negative and gram-positive bacteria. *Antibiotics* 9:36. doi: 10.3390/antibiotics9010036

Wan, G., Ruan, L., Yin, Y., Yang, T., Ge, M., and Cheng, X. (2016). Effects of silver nanoparticles in combination with antibiotics on the resistant bacteria *Acinetobacter baumannii*. *Int. J. Nanomedicine* 11:3789. doi: 10.2147/IJN.S104166

Williams, C. L., Neu, H. M., Gilbreath, J. J., Michel, S. L., Zurawski, D. V., and Merrell, D. S. (2016). Copper resistance of the emerging pathogen *Acinetobacter baumannii*. *Appl. Environ. Microbiol.* 82, 6174–6188. doi: 10.1128/AEM.01813-16

Wintachai, P., Paosen, S., Yupanqui, C. T., and Voravuthikunchai, S. P. (2019). Silver nanoparticles synthesized with *Eucalyptus critriodora* ethanol leaf extract stimulate antibacterial activity against clinically multidrug-resistant *Acinetobacter baumannii* isolated from pneumonia patients. *Microb. Pathog.* 126, 245–257. doi: 10.1016/j.micpath.2018.11.018

World Health Organization (2017). "Prioritization of pathogens to guide discovery, research and development of new antibiotics for drug-resistant bacterial infections, including tuberculosis". World Health Organization.

Xiu, Z.-M., Zhang, Q.-B., Puppala, H. L., Colvin, V. L., and Alvarez, P. J. (2012). Negligible particle-specific antibacterial activity of silver nanoparticles. *Nano Lett.* 12, 4271–4275. doi: 10.1021/nl301934w

Xu, H., Qu, F., Xu, H., Lai, W., Wang, Y. A., Aguilar, Z. P., et al. (2012). Role of reactive oxygen species in the antibacterial mechanism of silver nanoparticles on *Escherichia coli* O157: H7. *Biometals* 25, 45–53. doi: 10.1007/s10534-011-9482-x

Yang, Y., and Alvarez, P. J. (2015). Sublethal concentrations of silver nanoparticles stimulate biofilm development. *Environ. Sci. Technol. Lett.* 2, 221–226. doi: 10.1021/acs.estlett.5b00159

Yun'an Qing, L. C., Li, R., Liu, G., Zhang, Y., Tang, X., Wang, J., et al. (2018). Potential antibacterial mechanism of silver nanoparticles and the optimization of orthopedic implants by advanced modification technologies. *Int. J. Nanomedicine* 13, 3311–3327. doi: 10.2147/IJN.S165125

Zhang, X.-F., Liu, Z.-G., Shen, W., and Gurunathan, S. (2016). Silver nanoparticles: synthesis, characterization, properties, applications, and therapeutic approaches. *Int. J. Mol. Sci.* 17:1534. doi: 10.3390/ijms17091534

Zhao, X., and Drlica, K. (2014). Reactive oxygen species and the bacterial response to lethal stress. *Curr. Opin. Microbiol.* 21, 1–6. doi: 10.1016/j.mib.2014.06.008

Zhen, X., Lundborg, C. S., Sun, X., Hu, X., and Dong, H. (2019). Economic burden of antibiotic resistance in ESKAPE organisms: a systematic review. *Antimicrob. Resist. Infect. Control* 8:137. doi: 10.1186/s13756-019-0590-7

Zheng, W., Sun, W., and Simeonov, A. (2018). Drug repurposing screens and synergistic drug-combinations for infectious diseases. *Br. J. Pharmacol.* 175, 181–191. doi: 10.1111/bph.13895

**Conflict of Interest:** The authors declare that the research was conducted in the absence of any commercial or financial relationships that could be construed as a potential conflict of interest.

frontiers in Microbiology

ORIGINAL RESEARCH
published: 06 May 2021
doi: 10.3389/fmicb.2021.658772

# The Dissemination and Molecular Characterization of Clonal Complex 361 (CC361) Methicillin-Resistant *Staphylococcus aureus* (MRSA) in Kuwait Hospitals

*Eiman Sarkhoo[1], Edet E. Udo[1]*, Samar S. Boswihi[1], Stefan Monecke[2,3], Elke Mueller[2,3] and Ralf Ehricht[2,3,4]*

[1] Faculty of Medicine, Department of Microbiology, Kuwait University, Kuwait City, Kuwait, [2] Leibniz Institute of Photonic Technology (IPHT), Jena, Germany, [3] InfectoGnostics Research Campus Jena, Jena, Germany, [4] Institute of Physical Chemistry, Friedrich Schiller University Jena, Jena, Germany

OPEN ACCESS

**Edited by:**
Tarja Sironen,
University of Helsinki, Finland

**Reviewed by:**
Mohamamd Emaneini,
Tehran University of Medical Sciences, Iran
Raiane Cardoso Chamon,
Fluminense Federal University, Brazil

***Correspondence:**
Edet E. Udo
Udo.ekpenyong@ku.edu.kw

**Specialty section:**
This article was submitted to Antimicrobials, Resistance and Chemotherapy, a section of the journal Frontiers in Microbiology

**Received:** 26 January 2021
**Accepted:** 14 April 2021
**Published:** 06 May 2021

**Citation:**
Sarkhoo E, Udo EE, Boswihi SS, Monecke S, Mueller E and Ehricht R (2021) The Dissemination and Molecular Characterization of Clonal Complex 361 (CC361) Methicillin-Resistant Staphylococcus aureus (MRSA) in Kuwait Hospitals. Front. Microbiol. 12:658772. doi: 10.3389/fmicb.2021.658772

Methicillin-resistant *Staphylococcus aureus* (MRSA) belonging to clonal complex 361 (CC361-MRSA) is rare among patients' populations globally. However, CC361-MRSA has been isolated with an increasing trend among patients in Kuwait hospitals since 2010. This study investigated the molecular characteristics of CC361-MRSA isolated from patients in Kuwait hospitals in 2016–2018 to understand their genetic relatedness and virulence determinants. Of 5,223 MRSA isolates investigated by DNA microarray, 182 (3.4%) isolates obtained in 2016 (*N* = 55), 2017 (*N* = 56), and 2018 (*N* = 71) were identified as CC361-MRSA. The CC361-MRSA isolates were analyzed further using antibiogram, *spa* typing and multi locus sequence typing (MLST). Most of the isolates were resistant to fusidic acid (64.8%), kanamycin (43.4%), erythromycin (36.3%), and clindamycin (14.3%) encoded by *fusC*, *aphA3*, and *erm(B)/erm(C)* respectively. Nine isolates (4.9%) were resistant to linezolid mediated by *cfr.* The isolates belonged to 22 *spa* types with t3841 (*N* = 113), t315 (*N* = 16), t1309 (*N* = 14), and t3175 (*N* = 5) constituting 81.3% of the *spa* types, four genotypes (strain types), CC361-MRSA-[V/VT + fus] (*N* = 112), CC361-MRSA-IV, WA MRSA-29 (*N* = 36), CC361-MRSA-V, WA MRSA-70/110 (*N* = 33) and CC361-MRSA-[V + fus] variant (*N* = 1). MLST conducted on 69 representative isolates yielded two sequence types: ST361 (11/69) and ST672 (58/69). All CC361-MRSA isolates were positive for *cap8*, *agr1*, and the enterotoxin *egc* gene cluster (*seg, sei, selm, seln, selo,* and *selu*). The *tst1* was detected in 19 isolates. The immune evasion cluster (IEC) genes type B (*scn*, *chp*, and *sak*) and type E (*scn* and *sak*) were detected in 20 and 152 isolates, respectively. The CC361-MRSA circulating in Kuwait hospitals consisted of two closely related sequence types, ST361 and ST672 with ST672-MRSA [V/VT + fus] as the dominant genotype. The dissemination of these newly emerged clones and the emergence of linezolid resistance limits therapeutic options, as well as present significant challenges for the control of MRSA infections in Kuwait hospitals.

**Keywords: CC361-MRSA, molecular typing, DNA microarray, MLST, spa typing**

## INTRODUCTION

Methicillin-resistant *Staphylococcus aureus* (MRSA) remains a major universal healthcare problem as it causes a wide range of infections including skin and soft tissue infections (SSTI), pneumonia, bacteremia, endocarditis, and osteomyelitis (McCaig et al., 2006; Hassoun et al., 2017). The epidemiology of MRSA has changed significantly since its description in the 1960s. MRSA has evolved from being an exclusive healthcare-acquired pathogen (healthcare-acquired MRSA (HA-MRSA) (McCaig et al., 2006), to being acquired outside the healthcare facilities in the communities (Community-associated MRSA, CA-MRSA) (Udo et al., 1993; McCaig et al., 2006; David and Daum, 2010). Recently, MRSA has also evolved to become a livestock-associated pathogen designated Livestock-associated MRSA (Armand-Lefevre et al., 2005; van Cleef et al., 2011). HA-MRSA are characteristically multi-resistant to antibiotics and carry SCC*mec* types I, II or III (Monecke et al., 2011). In contrast, CA-MRSA are usually more susceptible to non-beta-lactam antibiotics and carry SCC*mec* types IV, V, or VI (David and Daum, 2010). The Livestock-associated MRSA (LA-MRSA) initially caused major problems in agriculture and were the leading cause of bovine mastitis (Fluit, 2012) but have now become prominent among livestock, people associated with livestock and those with no previous contact with livestock (Graveland et al., 2011; Köck et al., 2013; Wagenaar et al., 2009; Boswihi et al., 2020a).

Molecular typing tools including staphylococcal protein A (spa) typing, multilocus sequence typing (MLST), pulsed-field gel electrophoresis, staphylococcal cassette chromosome mec (SCC*mec*) typing, DNA microarray, and whole genome sequencing (WGS) have been used in the epidemiologic surveillance of MRSA strains to detect and monitor emerging and reemerging infections as well as monitoring geographic spread and shifts of epidemic and endemic clones (Pfaller, 1999; van Belkum et al., 2001; Monecke et al., 2011; Boswihi et al., 2016, 2020a,b; Rebic et al., 2016). The application of these typing techniques to type MRSA from different geographic regions have shown that most of the MRSA infections reported worldwide were caused by a limited number of pandemic MRSA clones belonging to clonal complexes 5 (CC5), CC8/ST239, CC22, CC30, and CC45 (Robinson and Enright, 2003; Monecke et al., 2011; Guthrie et al., 2020) although CA-MRSA isolates belong to more diverse genetic backgrounds compared to HA-MRSA (Monecke et al., 2011; Udo, 2013; Tong et al., 2015; Guthrie et al., 2020).

Methicillin-resistant *Staphylococcus aureus* strains belonging to CC361 (CC361-MRSA) were described as rare and were reported sporadically in humans (Afroz et al., 2008; Weber et al., 2010; Coombs et al., 2011; Monecke et al., 2011; Shambat et al., 2012; Kinnevey et al., 2014), Rhesus monkeys (Roberts et al., 2019), Cattle (Tegegne et al., 2017), and in ready-to-eat food items (Islam et al., 2019). However, the CC361-MRSA have been increasingly isolated from human patients in the Arabian Gulf countries of Saudi Arabia (Senok et al., 2019), United Arab Emirates (Senok et al., 2020) and Kuwait (Boswihi et al., 2018, 2020a,b).

The first two known isolates of CC361-MRSA were isolated in Kuwait in 2010 from two patients in two different hospitals (Boswihi et al., 2016). Since then, the proportion of MRSA isolates belonging to CC361-MRSA has been increasing annually (Boswihi et al., 2018, 2020a,b). In this study, we investigated CC361-MRSA isolated from patients in public hospitals in Kuwait from 1 January, 2016 to 31 December, 2018, using staphylococcal protein A (*spa*) typing, multi-locus sequence typing (MLST) and DNA microarray to determine their antibiotic resistance and virulence profiles, and genetic relatedness.

## MATERIALS AND METHODS

### MRSA Isolates

The MRSA isolates used in this study were obtained as part of routine diagnostic microbiology investigations. The MRSA were cultured and identified, using traditional diagnostic bacteriological methods including Gram stain, growth on Mannitol Salt Agar, positive DNAse and tube coagulase tests. The isolation and identification of the isolates were performed in the diagnostic microbiology laboratories where initial antibiotic susceptibility testing was also performed with VITEK MS (bioMérieux, Marcy l'Etoile, France). Pure cultures of isolates on blood agar plates were submitted to the Gram-Positive Bacteria Research laboratory, located at the Department of Microbiology, Faculty of Medicine, Kuwait University, where the isolates were retested for purity and preserved in 40% glycerol (v/v in brain heart infusion broth) at −80°C for further analysis. The isolates were recovered by two subcultures on brain heart infusion agar at 35°C before analysis. In total, 5,223 MRSA isolates were received from 13 different hospitals in Kuwait between 1 January, 2016 and 31 December, 2018. DNA microarray analysis performed on the 5,223 isolates revealed that 182 (3.4%) isolates were identified as CC361-MRSA. The 182 CC361-MRSA isolates were investigated further and reported in this study. The 182 CC361 isolates were collected from patients in Adan hospital ($N$ = 37; 20.3%), Mubarak hospital ($N$ = 32; 17.6%), Sabah hospital ($N$ = 23; 12.4%), Maternity hospital ($N$ = 20; 10.9%), Al-Amiri hospital ($N$ = 19; 10.4%), Al-Razi hospital ($N$ = 15; 8.2%), Chest Disease hospital ($N$ = 13; 7.1%), Al-Jahra hospital ($N$ = 8; 4.4%), Al-Farwaniya hospital ($N$ = 8; 4.4%), KOC hospital ($N$ = 3; 1.6%), Ibn-Sina hospital ($N$ = 2; 1.1%), Dasman Diabetic Centre ($N$ = 1; 0.5%) and Army Force hospital ($N$ = 1; 0.5%).

### Antibiotic Susceptibility Testing

The CC361-MRSA isolates were retested for susceptibility to antibiotics by the disk diffusion method, and interpreted according to the Clinical Laboratory Standards Institute (Clinical and Laboratory Standard Institute (CLSI), 2015)., The following antibiotic disks obtained from Oxoid (Basingstoke, United Kingdom) were used: Benzyl penicillin (2U), cefoxitin (30 μg), kanamycin (30 μg), mupirocin (200 μg), gentamicin (10 μg), erythromycin (15 μg), clindamycin (2 μg), chloramphenicol (30 μg), tetracycline (10 μg), trimethoprim (2.5 μg), fusidic acid (10 μg), rifampicin (5 μg), ciprofloxacin

(5 μg), teicoplanin (30 μg), and linezolid (30 μg). Penicillinase production was tested with the Nitrocefin solution (OXOID-Thermo Scientific) according to the manufacture's instruction. The minimum inhibitory concentration (MIC) for cefoxitin, vancomycin, teicoplanin, linezolid, and mupirocin were determined using E-test strips (bioMerieux, Marcy l'Etoile, France) and interpreted as described previously CLSI (Clinical and Laboratory Standard Institute (CLSI), 2015). *S. aureus* strains ATCC25923 and ATCC29213 were used as quality control strains for disk diffusion and MIC testing, respectively. Susceptibility to fusidic acid was interpreted according to the British Society to Antimicrobial Chemotherapy (BSAC) (British Society to Antimicrobial Chemotherapy [BSAC], 2013).

## Molecular Typing

### Staphylococcus Protein A (*spa*) Typing

*Spa* typing was performed using protocol and primers published previously (Harmsen et al., 2003). Bacterial DNA isolation for amplification studies was performed as described previously (Boswihi et al., 2018). Three to five identical colonies of an overnight culture were picked using a sterile loop and suspended in a microfuge tube containing 50 μL of lysostaphin (150 μg/mL) and 10 μL of RNase (10 μg/mL) solution. The tube was incubated at 37°C in the heating block (ThermoMixer, Eppendorf, Hamburg, Germany) for 20 min. To each sample, 50 μL of proteinase K (20 mg/mL) and 150 μL of Tris buffer (0.1 M) were added and mixed by pipetting. The tube was then incubated at 60°C in the water bath (VWR Scientific Co., Shellware Lab, United States) for 10 min. The tube was transferred to a heating block at 95°C for 10 min to inactivate proteinase K activity. Finally, the tube was centrifuged, and the supernatant containing extracted DNA was stored at 4°C till used for PCR.

The PCR protocol consisted of an initial denaturation at 94°C for 4 min, followed by 25 cycles of denaturation at 94°C for 1 min, annealing at 56°C for 1 min, and extension for 3 min at 72°C, and a final cycle with a single extension for 5 min at 72°C. Five μL of the PCR product was analyzed by 1.5% agarose gel electrophoresis to confirm amplification. The amplified PCR product was purified using Micro Elute Cycle-Pure Spin kit (Omega Bio-tek, Inc., United States) and the purified DNA was then used for sequencing PCR. The sequencing PCR product was then purified using Ultra-Sep Dye Terminator Removal kit (Omega Bio-tek, Inc., United States). The Purified DNA was sequenced in an automated 3130x1 genetic analyzer (Applied Biosystem, United States). The sequenced *spa* gene was analyzed using the Ridom Staph Type software (Ridom GmbH, Wurzburg, Germany).

### DNA Microarray

DNA microarray analysis was performed using the Identibac *S. aureus* genotyping kit 2.0 and the ArrayMate reader (Alere Technology, Jena, Germany) as described previously by Monecke et al. (2011). The DNA microarray analysis was used for the simultaneous detection of SCC*mec* types, antibiotic resistance genotypes and virulence related genes, including PVL, genes encoding species markers, and to allocate clonal complex (CC). *S. aureus* genotyping array is presented in an ArrayStrip format which contains 336 probes printed onto an array located in the bottom of the ArrayStrip. MRSA isolates were grown on blood agar plates at 35°C overnight. DNA extraction of the overnight culture was performed as described by the manufacturer using Identibac *S. aureus* genotyping kit 2.0 (Alere, GmbH, Germany). Linear amplification of the purified DNA was performed in a total of 10 μL of the reaction volume containing 4.9 μL of B1 (labeling reagent), 0.1 μL of B2 (DNA polymerase), and 5 μL of the purified DNA. The PCR protocol consisted of an initial denaturation for 5 min at 96°C, followed by 50 cycles of denaturation for 60 s at 96°C, annealing for 20 s at 50°C, and extension for 40 s at 72°C. hybridization and washing of the labeled arrays were performed as previously described (Monecke et al., 2011). The array was scanned using the ArrayMate reader (CLONDIAG, Alere, Germany) and the image of the arrays was recorded and analyzed using IconoClust software plug-in (CLONDIAG). The result was interpreted as negative, positive, or ambiguous by the software.

### Multilocus Sequencing Typing (MLST)

MLST was performed for representative isolates belonging to different spa types. The amplification of the seven housekeeping genes was performed using previously described M13-tailed primers (Tan et al., 2006). The amplified targets were sequenced with one pair of M13-tailed primers: 5′-TGTAAAACGACGGCCAGT-3′ and 3′-CAGGAAACAGCTATGACC-5′. The sequencing PCR protocol consisted of initial denaturation for 1 min at 94°C, followed by 25 cycles of denaturation for 10 s at 96°C, annealing at 55°C for 5 s, and extension for 4 min at 66°C. DNA sequencing was performed using a 313091 genetic analyzer (Applied Biosystems, Foster City, CA, United States) in accordance with the manufacturer's protocol. The sequences were submitted to http://www.pubmlst.net/ where an allelic profile was generated and the sequence type (ST) assigned.

# RESULTS

## Sources of CC361 MRSA Isolates

The isolates were obtained in 2016 ($N = 55$; 30.3%), 2017 ($N = 56$; 30.7%), and 2018 ($N = 71$; 39.0%) from nasal swabs ($N = 63$; 34.6%), wound swabs ($N = 25$; 13.7%), groin swabs ($N = 11$; 6.0%), tracheal aspirates ($N = 9$; 4.9%), pus ($N = 8$; 4.4%), axilla ($N = 6$; 3.3%), ear swab ($N = 6$; 3.3%), high vaginal swab (HVS) ($N = 6$;3.3%), sputum ($N = 5$; 2.7%), skin ($N = 5$; 2.7%), urine ($N = 5$; 2.7%), throat ($N = 4$; 2.2%), blood ($N = 4$; 2.2%), fluid ($N = 3$; 1.6%), and eye swab ($N = 2$; 1.1%). No clinical sources were provided for 20 isolates.

## Molecular Characteristics of the CC361-MRSA Isolates

The isolates belonged to three SCC*mec* types, 22 *spa* types and two sequence types. The distribution of the isolates and their

molecular characteristic is presented in **Table 1**. The SCC*mec* types were type V/VT (*N* = 112; 61.5%), type V (*N* = 34; 18.7 %), and type IV (*N* = 36, 19.8%).

**TABLE 1 |** Molecular characteristics of CC361-MRSA isolates from 2016 to 2018.

| Molecular types | ST | 2016 | 2017 | 2018 | Total |
|---|---|---|---|---|---|
| MRSA Genotypes | | | | | |
| CC361-MRSA [V/VT + fus] | | 31 | 29 | 52 | 112 |
| *Spa* types | | | | | |
| t3841 | 672 | 27 | 25 | 34 | 86 |
| t1309 | 672 | 1 | 1 | 2 | 4 |
| t12219 | 672 | | | 1 | 1 |
| t4336 | 672 | | 1 | 1 | 2 |
| t13751 | 672 | | | 1 | 1 |
| t14090 | 672 | | 1 | | 1 |
| t15253 | 672 | | | 1 | 1 |
| t15778 | 672 | 1 | | | 1 |
| t17533 | 672 | | | 1 | 1 |
| t3175 | 672 | 1 | | | 1 |
| t422 | 672 | | | 1 | 1 |
| t440 | 672 | | | 1 | 1 |
| t5357 | 672 | | | 1 | 1 |
| t779 | 672 | | | 1 | 1 |
| ND | 672 | 1 | 1 | 7 | 9 |
| | | | | | |
| CC361-MRSA-[V + fus] | | 1 | | | 1 |
| *Spa* types | | | | | |
| t3841 | 672 | 1 | | | 1 |
| CC361-MRSA-IV, WA MRSA-29 | | 12 | 12 | 12 | 36 |
| *Spa* types | ST | | | | |
| t3841 | 672 | 7 | 5 | 5 | 17 |
| t11113 | 672 | 1 | | | 1 |
| t12219 | 672 | | 1 | | 1 |
| t1309 | 672 | 1 | 2 | 4 | 7 |
| t14090 | 672 | 1 | | | 1 |
| t1427 | 672 | | 1 | | 1 |
| t311 | 672 | | | 1 | 1 |
| t3175 | 672 | 2 | 1 | 1 | 4 |
| ND | 672 | | 2 | | 2 |
| Molecular types | ST | 2016 | 2017 | 2018 | Total |
| MRSA Genotypes | | | | | |
| CC361-MRSA-V, WA MRSA-70/110 | | 11 | 15 | 7 | 33 |
| *Spa* types | | | | | |
| t315 | 361 | 7 | 9 | | 16 |
| t3841 | 672 | 3 | 3 | 2 | 8 |
| t003 | 672 | 1 | | | 1 |
| t12219 | 672 | | 1 | | 1 |
| t1309 | 672 | | | 3 | 3 |
| t17279 | 672 | | 1 | | 1 |
| t422 | 672 | | 1 | | 1 |
| t463 | 361 | | | 1 | 1 |
| t7191 | 672 | | | 1 | 1 |
| Total | | 55 | 56 | 71 | 182 |

*ST, sequence type; ND, not determined.*

The four genotypes were CC361-MRSA [V/VT + fus] (*N* = 112; 61.5%) as the most common genotype, followed by CC361-MRSA-IV, WA MRSA-29 (*N* = 36; 19.8%), CC361-MRSA-V, WA MRSA-70/110 (*N* = 33; 18.1%), and CC361-MRSA-[V + fus] (*N* = 1; 0.5%).

MLST was performed on 58 representative isolates chosen based on *spa* types chosen to include isolates from all clinical samples in all hospitals with the same *spa* types. The MLST identified two closely related sequence types; ST672 (MLST profile: arc-4, aroe-3, glpf-1, gmk-1, pta-11, tpi-72, yqil-11; *N* = 47) and ST361 (MLST profile: arc-4, aroe-3, glpf-1, gmk-1, pta-11, tpi-72, yqil-64; *N* = 11). The sequence types for the rest of the isolates was based on the associated *spa* types. The results showed that most of the isolates belonged to ST672 while 17 isolates belonged to ST361. All CC361-MRSA [V/VT + fus], CC361-MRSA-[V + fus), CC361-MRSA-IV, WA MRSA-29 and 16 of CC361-MRSA-V, WAMRSA −70/110 belonged to ST672 while 17 of CC361-MRSA-V, WAMRSA -70/110 isolates belonged to ST361. **Table 1** also shows the yearly distribution of the clones.

The CC361MRSA [V/VT + fus] genotype showed an increasing trend, while the CC361-MRSA-IV, WA MRSA-29 genotype showed a uniform distribution over the three years. In contrast, the prevalence of the CC361-MRSA-V, WA MRSA-70/110 genotype varied by year but declined in 2018.

The 22 *spa* types consisted of t3841 (*N* = 112; 61.5%) as the dominant *spa* type. The other *spa* types were t315 (*N* = 16; 8.8%), t1309 (*N* = 14; 7.7%), t3175 (*N* = 5; 2,7%), t12219 (*N* = 3; 16.5%), t14090 (*N* = 2; 1.1%), t422 (*N* = 2; 1.1%), t4336 (*N* = 2; 1.1%), t003 (*N* = 1; 0.5%), t11113 (*N* = 1; 0.5 %), t13751 (*N* = 1; 0.5%), t1427 (*N* = 1; 0.5%), t15253 (*N* = 1; 0.5%), t15778 (*N* = 1; 0.5%), t17279 (*N* = 1; 0.5%), t17533 (*N* = 1; 0.5 %), t311 (*N* = 1; 0.5%), t440 (*N* = 1; 0.5%), t463 (*N* = 1; 0.5%), t5357 (*N* = 1; 0.5%), t7191 (*N* = 1; 0.5%), t779 (*N* = 1; 0.5%), and 11 isolates (6%) had no determined *spa* type. The dominant spa type, t3841 was distributed among the four genotypes. It constituted the major *spa* type in CC361-MRSA [V/VT + fus] (86/112) and CC361-MRSA-IV, WA MRSA-29 (17/36) but was the second common spa type among the CC361-MRSA-V, WA MRSA-70/110 isolates. The second common spa type, t315 was associated only with the CC361-MRSA-V, WA MRSA-70/110 clone and ST631 (**Table 1**). The ST631-MRSA-V, WA MRSA-70/110/t315 was detected only in 2016 and 2017.

## Antibiotic Resistance Phenotypes and Genotypes of the CC361-MRSA Isolates

All 182 CC361- MRSA isolates were susceptible to vancomycin and teicoplanin (MIC: ≤2 mg/L) and rifampicin. Besides beta-lactam resistance, resistance was observed to fusidic acid (*N* = 118; 64.8%), kanamycin (*N* = 79; 43.4%), erythromycin (*N* = 66; 36.3%), clindamycin (*N* = 26; 14.3%), gentamicin (*N* = 12; 6.6%), chloramphenicol (*N* = 9; 4.9%), linezolid (MIC: ≥16 mg/L; *N* = 9), trimethoprim (*N* = 5; 2.7%), and tetracycline (*N* = 5; 2.7%). Ten isolates expressed high-level mupirocin resistance. Of the 26 isolates that showed resistance

to clindamycin, 15 isolates revealed inducible resistance while 11 isolates expressed constitutive resistance.

The distribution of the antibiotic resistance genes of the CC361-MRSA isolates is presented in **Table 2**. There was general concordance between resistance phenotypes and genotypes. The penicillin resistance encoding genes *blaZ* and its regulatory genes, *blaI* and *blaR* were found in 177 isolates, while aminoglycoside (gentamicin and kanamycin) encoding genes *aacA-aphD, aphA3*, and *aadD* were detected in 12, 65, and 2 isolates, respectively. The five isolates that were negative for *blaZ*, *blaI*, and *blaR*, were susceptible to penicillin G and negative for penicillinase production but were positive for *mecA* and SCC*mec* genetic elements.

Of the 66 erythromycin-resistant isolates, 22 isolates carried *ermC*, one isolate carried *ermB*. While 48 and 46 isolates carried *msrA* and *mphC* encoding genes, respectively, *mefA* (macrolide efflux protein A), *vatA* (virginiamycin A acetyltransferase), *vatB* (acetyltransferase inactivating streptogramin A) and *linA* (lincosaminide nucleotidyltransferase) were detected sporadically among the CC361 isolates. Two isolates harbored *fusB* (*far1*) gene. Tetracycline resistance gene *tetK*, was detected in five isolates, while trimethoprim resistance gene *dfrS1* was also found in five isolates.

Whereas all of the CC361-MRSA [V/VT + fus) isolates were resistant to fusidic acid mediated by *fusC*, the CC361-MRRSA-V-WA-MRSA-70/110 isolates were more resistant to erythromycin mediated by erm(C), high-level mupirocin resistance mediated by *mupA*, and chloramphenicol and linezolid mediated by *cfr*.

## Prevalence of Virulence-Related Genes

The prevalence of the virulence factors amongst the CC361 MRSA isolates are presented in **Table 3**. All 182 isolates were positive for genes encoding the accessory gene regulator type I (*agr*I) and capsular polysaccharide type 8 (*cap*8) but lacked genes for Panton Valentine Leukocidin (PVL).

The most common enterotoxin gene, egc gene cluster (*seg, sei, selm, seln, selo*, and *selu*), was detected in all 182 CC361 isolates. This was followed by *sel* (*N* = 20; 11%) and *sec* (*N* = 19; 10.4%). Genes for Toxic shock-syndrome toxin (*tst1*) was detected in 19 isolates. The *sec* and *sel* were more common in the CC361-MRSA-V WA MRSA-70/110 isolates. Similarly, 17 of the 19 tst1-positive isolates belonged to CC361-MRSA-V WA MRSA-70/110. Only two of the CC361-MRSA [V/VT + fus] isolates harbored the *tst1*. On the other hand, *sek* and *seq* genes were common among the CC361-MRSA-V, WA MRSA-29 isolates (**Table 3**).

The isolates varied in the carriage of genes for the immune evasion cluster (IEC). Twenty isolates carried immune evasion cluster genes of type B (*scn*, *chp*, and *sak*), whilst 152 isolates carried the immune evasion cluster genes of genes for type E (*scn* and *sak*). Ten isolates were negative for the IEC genes.

The hemolysin encoding genes *hlgA*, *hl*, and *hlIII*, were detected in all 182 isolates. However, *hlb* was detected in 181 of the 182 isolates while *hla* was detected in 172 isolates (94.5%). In addition, all 182 isolates were positive for genes encoding clumping factors A and B (*clfA* and *clfB*), fibronectin-binding proteins A and B (*fnbA* and *fnbB*), *Staphylococcus aureus* surface protein G (*sasG*) and major histocompatibility complex class II analog protein (*map*). All isolates lacked *cna* that codes for the collagen-binding adhesin.

# DISCUSSION

This study has demonstrated a steady expansion of the CC361-MRSA lineage among patients in Kuwait hospitals in recent years. Until recently, CC361-MRSA was reported sporadically from human patients in Oman (Udo et al., 2014), Abu Dhabi (Weber et al., 2010), Australia (Monecke et al., 2011), Ireland (Kinnevey et al., 2014), Bangladesh (Afroz et al., 2008), Kuwait (Boswihi et al., 2016), Saudi Arabia (Senok et al., 2019), and Switzerland (Etter et al., 2020) as well as in monkeys in Nepal (Roberts et al., 2019), in cattle in Czech Republic (Tegegne et al., 2017), and in ready-to-eat food in Bangladesh (Islam et al., 2019). However, this report represents the largest number of CC361-MRSA reported to date. The number of CC361-MRSA obtained from human patients increased from two isolates identified for the first time in Kuwait in 2010 (Boswihi et al., 2016), to 55 in 2016, 56 in 2017 and 71 in 2018. Similarly, increases in the proportion of CC361-MRSA in human patients have been observed in the UAE and Saudi Arabia (Senok et al., 2020), making the CC361-MRSA no longer a rare but an evolving clone in the Arabian Gulf region.

The isolates were obtained from different clinical samples including wound swabs, nasal swabs, blood culture, vaginal swabs, sputum, tracheal aspirates, and urine highlighting the capacity of the CC361-MRSA isolates to colonize or cause superficial as well as invasive infections.

DNA microarray analysis revealed different genotypes dominated by CC361-MRSA [V/VT + Fus] which constituted 61.5% of the isolates. The other genotypes detected were CC361-MRSA-V WA MRSA-29 (*N* = 36; 19.8%), CC361-MRSA-V WA MRSA-70/110 (*N* = 33; 18.1%) and CC361-MRSA-[V + fus] variant (*N* = 1; 0.5%). Although there were no significant differences in the distribution of the four CC361 genotypes from 2016 to 2018, the CC361-MRSA [V/VT + fus] isolates increased from 31 in 2016 to 71 in 2018 (**Table 1**) suggesting its higher transmission capacity. The acquisition of the variant V/VT genetic element represents an evolutionary event that probably confers greater capacity to spread. Although this clone appears to be restricted to the countries of the Gulf at this time, it has the potential to spread widely as the highly virulent USA300 MRSA clone that emerged initially as a less virulent and less resistant clone (Strauß et al., 2017). The USA300 MRSA clone gradually acquired multiple antibiotic resistance, SCC*mec* Iva genetic element, genes for PVL, arginine catabolic mobile element, and a specific mutation in capsular polysaccharide gene, *capSE* and became highly transmissible following its introduction to North America from Central Europe (Strauß et al., 2017).

Despite the smaller numbers reported in Saudi Arabia (8 0f 12 isolates) (Senok et al., 2019) and the UAE (20 of 35 isolates) (Senok et al., 2020) compared to those in Kuwait, CC361-MRSA [V/VT + fus] isolates were also the most common strain type reported in these countries. Similarly, the second common genotype in this study, CC361-MRSA-IV, WA-MRSA 29, was also the second most common CC361-MRSA in the UAE

**TABLE 2 |** Distribution of antibiotic resistance genes of CC361-MRSA isolates from 2016 to 2018.

| Locus | CC361-MRSA [V/VT + fus] (*N* = 112) | CC361-MRSA-IV, WA MRSA-29 (*N* = 36) | CC361-MRSA-V, WA MRSA-70/110 (*N* = 33) | CC361-MRSA-[V + fus] (*N* = 1) | Total (*N* = 182) |
|---|---|---|---|---|---|
| Penicillin resistance | | | | | |
| *blaZ* | 110 | 34 | 32 | 1 | 177 |
| *blaI* | 110 | 34 | 32 | 1 | 182 |
| *blaR* | 110 | 34 | 32 | 1 | 182 |
| *mecA* | 112 | 36 | 3 | 1 | 182 |
| MLS-resistance | | | | | |
| *erm*(B) | 0 | 0 | 1 | 0 | 1 |
| *erm*(C) | 4 | 2 | 16 | 0 | 22 |
| *linA* | 0 | 0 | 1 | 0 | 1 |
| *msr*(A) | 35 | 8 | 4 | 1 | 48 |
| *mph(C)* | 33 | 8 | 4 | 1 | 46 |
| *vatA* | 0 | 1 | 0 | 0 | 1 |
| *vatB* | 0 | 1 | 0 | 0 | 1 |
| *vga*(A) | 11 | 1 | 0 | 0 | 12 |
| Aminoglycosides resistance | | | | | |
| *aacA-aphD* | 4 | 2 | 6 | 0 | 12 |
| *aadD* | 1 | 1 | 0 | 0 | 2 |
| *aphA3* | 33 | 10 | 21 | 1 | 65 |
| Trimethoprim resistance | | | | | |
| *dfrS1* | 5 | 0 | 0 | 0 | 5 |
| Fusidic acid resistance | | | | | |
| *fusC* | 112 | 1 | 2 | 1 | 116 |
| *fusB (far1)* | 1 | 1 | 0 | 0 | 2 |
| Tetracycline resistance | | | | | |
| *tet*(K) | 3 | 0 | 2 | 0 | 5 |
| Phenicol resistance | | | | | |
| *Cfr* | 0 | 0 | 9 | 0 | 9 |
| Mupirocin resistance | | | | | |
| *mupA* | | 0 | 10 | 0 | 10 |
| Quaternary ammonium compound resistance | | | | | |
| *qacA* | 1 | 0 | 0 | 0 | 1 |
| *qacC* | 2 | 0 | 0 | 1 | 3 |
| Streptothricin resistance | | | | | |
| *sat* | 33 | 9 | 21 | 1 | 64 |
| Fosfomycin resistance | | | | | |
| *fosB* | 112 | 36 | 33 | 1 | 182 |
| Locus | CC361-MRSA [V/VT + fus] (*N* = 112) | CC361-MRSA-IV, WA MRSA-29 (*N* = 36) | CC361-MRSA-V, WA MRSA-70/110 (*N* = 33) | CC361-MRSA-[V + fus] (*N* = 1) | Total (*N* = 182) |
| SCC*mec*-complex associated genes | | | | | |
| *mec*A | 112 | 36 | 33 | 1 | 182 |
| *ugp*Q | 112 | 36 | 33 | 1 | 182 |
| *plsSCC* (COL) | 0 | 0 | 0 | 1 | 1 |
| delta_*mec*R | 0 | 36 | 0 | 0 | 36 |
| *Q9XB68-dcs* | 0 | 36 | 0 | 0 | 36 |
| *ccr*C | 112 | 0 | 33 | 1 | 146 |
| *ccr*B-2 | 0 | 36 | 0 | 0 | 36 |

*(Continued)*

**TABLE 2** | Continued

| Locus | CC361-MRSA [V/VT + fus] (*N* = 112) | CC361-MRSA-IV, WA MRSA-29 (*N* = 36) | CC361-MRSA-V, WA MRSA-70/110 (*N* = 33) | CC361-MRSA- [V + fus] (*N* = 1) | Total (*N* = 182) |
|---|---|---|---|---|---|
| *ccr*A-2 | 0 | 36 | 0 | 0 | 36 |
| *ccr*A-3 | 0 | 1 | 0 | 0 | 1 |
| *ccr*AA | 112 | 0 | 33 | 1 | 146 |

*blaZ, beta-lactamase gene; blaI, beta lactamase repressor (inhibitor); blaR, beta-lactamase regulatory protein; mecA, penicillin binding protein 2; erm(B) + erm(C), rRNA methyltransferase associated with macrolide/lincosamide resistance; linA, lincosaminide nucleotidyltransferase; msr(A), macrolide efflux pump; mph(C), macrolide phosphotransferase II; vatA, virginiamycin A acetyltransferase; vatB, acetyltransferase inactivating streptogramin A; vga(A), ABC transporter conferring resistance to streptogramin A; aacA-aphD, aminoglycoside adenyl-/phosphotransferase (gentamicin, tobramycin); aadD, aminoglycoside adenyltransferase (neomycin, kanamycin, and tobramycin); aphA3, aminoglycoside phosphotransferase (neomycin, kanamycin); dfrS1, dihydrofolate reductase mediating trimethoprim resistance; fusC + fusB (far1), fusidic acid resistance gene; tet(K), tetracycline efflux protein; Cfr, 23S rRNA methyltransferase; mupA, isoleucyl-tRNA synthetase; qacA, multidrug efflux protein A; qacC, multidrug efflux protein C; sat, streptothricin acetyltransferase; fosB, metallothiol transferase; ugpQ, glycerophosphoryl diester phosphodiesterase (associated with mecA); plsSCC (COL), plasmin-sensitive surface protein; delta_mecR, truncated signal transducer protein MecR1; Q9XB68-dcs, hypothetical protein from SCCmec elements; ccrC, cassette chromosome recombinase gene C; ccrB-2, cassette chromosome recombinase gene B-2; ccrA-2, cassette chromosome recombinase gene A-2; ccrA-3, cassette chromosome recombinase gene A-3; ccrAA, Putative protein homologue to cassette chromosome recombinase A genes.*

(Senok et al., 2020), suggesting similar trends in the evolution of the CC361-MRSA in these countries.

MLST identified two closely related sequence types; ST672 (slv of ST361) and ST361 among the four different strain types, while *spa* typing revealed 22 spa types. Most of the isolates (112/182) belonged to ST672/ t3841 (**Table 1**) followed by ST361/t315 (16/182). We observed that whereas ST672/t3841 isolates were found in all four strain types, ST361/t315 isolates were only detected among CC361-MRSA-V, WA MRSA-70/110 strain type that were isolated only in 2016 and 2017. It is interesting that one of the two CC361 – MRSA isolates that were isolated in Kuwait in 2010 was ST361-MRSA-IV/t315 (Boswihi et al., 2016) whereas the current isolates are ST361-MRSA-V/t315 suggesting that the current isolates were acquired independently, and did not evolve from the 2010 isolate. Other studies have reported CC361-MRSA strains as belonging to ST361-MRSA-IV (Afroz et al., 2008; Coombs et al., 2011; Kinnevey et al., 2014; Al-Zahrani et al., 2019) or ST672-MRSA-V (Coombs et al., 2011; Shambat et al., 2012; Balakuntla et al., 2014; Santosaningsih et al., 2016; Sunagar et al., 2016). ST361-MRSA/t315 isolates have also been reported from processed fish fingers and Chapatti in Dhaka, Bangladesh (Islam et al., 2019) probably because of human contamination of the ready-to-eat foods.

The CC361-MRSA strains appear to have appeared independently in the GCC countries. It was first reported in Abu Dhabi, UAE, from patients in 2009 (Weber et al., 2010) followed by the report in two patients in Kuwait in 2010 (Boswihi et al., 2016) and in two patients in Oman in 2011 (Udo et al., 2014). However, prior to their emergence in the GCC countries, an isolate of ST361-MRSA-IV was isolated from a patient in Bangladesh in 2004 (Afroz et al., 2008) and two isolates of ST672-MRSA-V were reported among MRSA isolates obtained in 2004–2006 in India (Shambat et al., 2012) supporting the recent emergence of CC361-MRSA in the GCC countries.

The isolates belonged to 22 different *spa* types with t3841 (*N* = 112; 61.51%), t315 (*N* = 16; 8.8%), and t1309 (*N* = 14; 7.7%) constituting 78 percent of the isolates. Whereas t3841 and t1309 were associated with ST672 distributed in three strain types, t315 was associated only with ST361 in a single strain type, CC361-MRSA-V, WA MRSA 70/110, in this study. Similarly, t315 has been associated only with ST361 in studies conducted in Australia (Coombs et al., 2011), Ireland (Kinnevey et al., 2014), Austria (Zarfel et al., 2016), and from cattle in Czech Republic (Tegegne et al., 2017) where *spa* typing were also reported. In contrast, ST672 isolates were associated with t1309 in studies that reported *spa* types in Australia (Coombs et al., 2011) and India (Shambat et al., 2012). These studies support the recent acquisition of the ST672-MRSA [V/VT + Fus]/t3841 strain in Kuwait. The origin of the dominant t3841 isolates in this study is not clear since previous ST672 isolates have largely been associated with t1309 (Coombs et al., 2011; Shambat et al., 2012). However, a previous study in Kuwait detected t3841 among MSSA isolates in the country (Vali et al., 2017). It is possible that the t3841 MRSA isolates in this study emerged from a locally circulating MSSA isolate that acquired *mecA*. An isolate of t3841 MSSA had also been reported in India (Shambat et al., 2012).

Besides the diversity in *spa t*ypes, the insolates in this study harbored different SCC*mec* types consisting of SCC*mec* types IV, V and V/VT that are usually associated with community-associated genotypes. Apart from SCC*mec* V/VT, SCC*mec* types IV and V were also reported in CC361-MRSA from human patients in Western Australia (Monecke et al., 2011), Ireland (Kinnevey et al., 2014) and Bangladesh (Afroz et al., 2008), Abu Dhabi (Weber et al., 2010), Oman (Udo et al., 2014) and Saudi Arabia (Senok et al., 2019) and in animals in Nepal (Roberts et al., 2019) and Czech Republic (Tegegne et al., 2017). CC361 isolates were also reported to harbor SCC*mec* VIII in Australia where it is known as WA MRSA-28 (Nimmo and Coombs, 2008). These observations demonstrate the ability of CC361 to acquire different SCC*mec* elements. The detection of SCC*mec* V/VT together with *spa* type t3841 only in the current isolates supports the recent emergence of these strains in the GCC countries.

The CC361-MRSA isolates were resistant to different antibiotics including gentamicin, kanamycin, erythromycin, clindamycin, tetracycline, trimethoprim fusidic acid and high-level mupirocin and harbored *aacA-aphD*, *aphA3*, *msrA*, *tet(K)*, *dfrS1*, *fusC*, and *mupA* mediating resistance to the corresponding

**TABLE 3 |** Virulence factors amongst the CC361-MRSA strains.

| Locus | CC361-MRSA [V/VT + Fus] (*N* = 112) | CC361-MRSA-IV, WA MRSA-29 (*N* = 36) | CC361-MRSA-V, WA MRSA-70/110 (*N* = 33) | CC361-MRSA- [V + fus] (*N* = 1) | Total (*N* = 182) |
|---|---|---|---|---|---|
| Enterotoxins | | | | | |
| *sea* | 1 | 2 | 3 | 0 | 6 |
| *seb* | 1 | 7 | 0 | 0 | 8 |
| *sec* | 2 | 0 | 17 | 0 | 19 |
| *sed* | 2 | 1 | 0 | 0 | 3 |
| *see* | 0 | 1 | 0 | 0 | 1 |
| *sel* | 2 | 0 | 18 | 0 | 20 |
| *sek* | 0 | 7 | 0 | 0 | 7 |
| *seq* | 0 | 7 | 0 | 0 | 7 |
| **egc gene cluster* | 112 | 36 | 33 | 1 | 182 |
| Toxic shock syndrome toxin-1 (TSST-1) | | | | | |
| *tst1* | 2 | 0 | 17 | 0 | 19 |
| Lukocidins | | | | | |
| Luk-PV (P83) | 12 | 1 | 0 | 0 | 13 |
| lukF | 112 | 36 | 33 | 1 | 182 |
| lukS | 112 | 36 | 33 | 1 | 182 |
| lukD | 112 | 36 | 33 | 1 | 182 |
| lukE | 112 | 36 | 33 | 1 | 182 |
| lukX | 109 | 36 | 32 | 1 | 178 |
| lukY | 111 | 36 | 31 | 1 | 180 |
| Immune Evasion Cluster (IEC) | | | | | |
| *chp-scn-sak* (Type B) | 2 | 2 | 16 | 0 | 20 |
| *scn-sak* (Type E) | 102 | 32 | 17 | 1 | 152 |
| Negative for IEC genes | 8 | 2 | - | - | 10 |
| Hemolysins | | | | | |
| *hlgA* | 111 | 36 | 33 | 1 | 182 |
| *Hla* | 110 | 35 | 26 | 1 | 172 |
| *Hlb* | 111 | 36 | 33 | 1 | 181 |
| *Hl* | 112 | 36 | 33 | 1 | 182 |
| *hlIII* | 112 | 36 | 33 | 1 | 182 |
| Adhesion factors | | | | | |
| *clfA* | 112 | 36 | 33 | 1 | 182 |
| *clfB* | 112 | 36 | 33 | 1 | 182 |
| *fnbA* | 112 | 36 | 33 | 1 | 182 |
| *fnbB* | 112 | 36 | 33 | 1 | 182 |
| *sasG* | 112 | 36 | 33 | 1 | 182 |
| *Map* | 112 | 36 | 33 | 1 | 182 |
| *cna* | 0 | 0 | 0 | 0 | 0 |

**egc gene cluster: seg, sei, selm, seln, selo, selu.*
*hlgA, hemolysin gamma; hla, hemolysin alpha; hlb, hemolysin beta; hl/hlIII, putative membrane protein; sak, staphylokinase; chp, chemotaxis-inhibiting protein; scn, staphylococcal complement inhibitor, clfA, clumping factor A; clfB, clumping factor B; fnbA, fibronectin-binding protein A; fnbB, fibronectin-binding protein B; sasG, Staphylococcus aureus surface protein G; map, major histocompatibility complex class II; can, collagen-binding adhesin.*

antibiotics as has been reported in isolates from Saudi Arabia (Senok et al., 2019), Abu Dhabi (Monecke et al., 2011), and Australia (Coombs et al., 2011). All the 112 ST672-MRSA-[V/VT + fus] isolates harbored *fusC* and was responsible for the high prevalence of fusidic acid resistance in this study. Fusidic acid resistance mediated by *fusC* was also reported in CC361-MRSA isolates obtained from dental room environment and human patients in Saudi Arabia (Senok et al., 2019). Fusidic acid resistance has remained a major problem in MRSA isolates in Kuwait for some years, and has been suggested to be due to independent acquisition of fusidic acid determinants in isolates belonging to diverse backgrounds, and the consumption of over the counter fusidic acid preparations which are available without prescription in the country (Boswihi et al., 2018).

We detected linezolid resistance in nine CC361-MRSA-V, WA MRSA-70/110 isolates that were resistant to chloramphenicol and linezolid, and were positive for *cfr* that encodes resistance to linezolid, chloramphenicol, lincosamides, and streptogramin

A (Pillai et al., 2002; Long et al., 2006; Morales et al., 2010). This is the first report of linezolid resistance in *S. aureus* in Kuwait. Linezolid resistance mediated by *cfr* was recently reported in a recent MRSA isolate obtained in the United Arab Emirate (Senok et al., 2020) indicating that linezolid resistance is emerging in these countries and should raise awareness of an emerging problem. In contrast, none of the CC361-MRSA-V, WA MRSA-70 reported in Australia expressed resistance to linezolid or high-level mupirocin (Coombs et al., 2011). Since its approval for clinical use, Linezolid has remained an important treatment option for treating infections caused by MRSA and glycopeptide-resistant enterococci (Pillai et al., 2002). Therefore, the emergence of linezolid resistance in MRSA observed in this study is concerning because it will limit treatment options available for MRSA infections. The 10 high-level mupirocin-resistant isolates harbored *mupA* that codes for this resistance. The *mupA* mediated high-level mupirocin resistance have been previously in MRSA belonging to other genetic backgrounds in Kuwait (Udo et al., 2001; Udo and Sarkhoo, 2010).

The CC361-MRSA isolates in this study were negative for genes encoding PVL similar to CC631-MRSA isolates reported previously in Oman (Udo et al., 2014), UAE (Senok et al., 2020), Australia (Coombs et al., 2011), and most of the isolates in Saudi Arabia (Senok et al., 2019). However, two isolates consisting of, an isolate of CC361-MRSA-V/VT (PVL+) isolated in Saudi Arabia (Senok et al., 2019) and an isolate of ST361-MRSA-/t315 isolated from ready-to-eat food sample in Bangladesh (Islam et al., 2019), were positive for PVL suggesting that PVL is rare among CC361-MRSA isolates.

The isolates were all positive for agr type 1 (*agr1*) and capsular polysaccharide type 8 (*cap8*), egc gene cluster (*seg*, *sei*, *selm*, *seln*, *selo*, and *selu*), hemolysins genes *hlgA*, *Hl*, *hlIII* and adhesion factor genes *clfA*, *clfB*, *fnbA*, *fnbB*, *sasG*, and *Map*. *clfA*, *clfB*, *fnbA*, and *fnbB* and were negative for *cna* that encodes collagen binding adhesin, as have also been reported previously for other CC361-MRSA isolates (Afroz et al., 2008; Coombs et al., 2011; Monecke et al., 2011; Shambat et al., 2012; Boswihi et al., 2016; Senok et al., 2019) indicating that these are constitutional characteristics of CC361 isolates. In addition, the CC361-MRSA isolates in this study varied in the carriage of enterotoxin genes, *sea*, *seb*, *sec*, *sed*, *sel*, *sek*, and *seq* similar to the reports of studies on prevalence of enterotoxins genes in CC361-MRSA isolates in several countries (Boswihi et al., 2018; Senok et al., 2019, 2020; Etter et al., 2020) including CC361-MRSA obtained from monkeys and ready-to-eat food (Islam et al., 2019; Roberts et al., 2019).

Only 19 of the 182 isolates, consisting of 17 CC361-MRSA-V, WA MRSA-70/110, and two CC361-MRSA [V/VT + Fus], were positive for *tst1* in this study. Similarly, small numbers of C361 MRSA carrying the *tst1* gene were in Bangladesh (Islam et al., 2019) and in monkeys in Nepal (Roberts et al., 2019).

Most of the CC361- MRSA isolates in this study harbored type E (*scn*, *sak*) ($N$ = 152; 83.5%) or type B (*scn*, *chp*, and *sak*) ($N$ = 20; 11.0%) immune evasion cluster genes. Likewise, CC361-MRSA reported in Australia (Coombs et al., 2011) Saudi Arabia (Senok et al., 2019), and United Arab Emirates (Senok et al., 2020) also carry either type E or type B immune evasion cluster (IEC) genes. The immune evasion cluster genes binds specifically with compounds of the human innate immune system to protect bacteria from the human innate immune system (Resch et al., 2013; Sieber et al., 2020) and are therefore used to distinguish *S. aureus* of human from those of animal origin since human isolates harbor the IEC genes (Resch et al., 2013). The presence of IEC carrying *S. aureus* in animals usually suggests human contamination (Resch et al., 2013; Sieber et al., 2020). Viewed from this perspective, the presence of type E (*scn* and *sak*) IEC in CC361- MRSA that were recovered from monkeys (Roberts et al., 2019) which is similar to the IEC content of 94.5% of our isolates may suggest a human origin for the monkey isolates. Although CC361-MRSA have also been isolated from cattle (Tegegne et al., 2017), and ready to-eat-food (Islam et al., 2019) the IEC genes contents of these isolates were not reported. Hence it is not possible to speculate their origin. Ten of the isolates in this study consisting of five ST672-MRSA-V/VT + Fus/t3841 and five ST672-MRSA-IV, WAMRSA 29/t14690/t14271/t1309/t3175/3841 were negative for IEC genes suggesting the loss of the bacteriophage that bears the IEC genes.

## CONCLUSION

In conclusion, this study reports an increase in the prevalence of the CC361-MRSA isolates with the dominance and transmission of a newly emerged ST672-MRSA [V/VT + fus] genotype in Kuwait hospitals. The CC361-MRSA isolates expressed resistance to different antibiotics including linezolid resistance observed for the first time in Kuwait. The isolates were negative for genes encoding PVL but harbored common enterotoxins encoding genes (e.g., *egc* gene cluster). The detection of the various virulence genes in these isolates and their isolation from different clinical samples indicate their capacity to cause serious infections like other virulent MRSA lineages. Continuous surveillance is necessary to monitor and evaluate emerging MRSA clones in Kuwait to assist in developing better means of prevention and management.

## DATA AVAILABILITY STATEMENT

The original contributions presented in the study are included in the article/supplementary material, further inquiries can be directed to the corresponding author/s.

## AUTHOR CONTRIBUTIONS

SB carried out the laboratory work. ES, SM, EM, and RE performed the data analysis. EU performed the experimental design. ES, SM, SB, and EU carried out the manuscript writing and editing. All authors read and approved the final manuscript.

## ACKNOWLEDGMENTS

We are grateful to the technical staff in the MRSA Reference Laboratory located in Department of Microbiology, Faculty of Medicine, for their technical assistance.

## REFERENCES


Afroz, S., Kobayashi, N., Nagashima, S., Alam, M. M., Hossain, A. B., Rahman, M. A., et al. (2008). Genetic characterization of *Staphylococcus aureus* isolates carrying Panton-Valentine leukocidin genes in Bangladesh. *Jpn. J. Infect. Dis.* 61, 393–396.

Al-Zahrani, I. A., Azhar, E. I., Jiman-Fatani, A. A., Siddig, L. A., Yasir, M., Al-Ghamdi, A. K., et al. (2019). Impact of mass migrations on the clonal variation of clinical *Staphylococcus aureus* strains isolated from the Western region of Saudi Arabia. *J. Infect. Public Health* 12, 317–322. doi: 10.1016/j.jiph.2018.11.001

Armand-Lefevre, L., Ruimy, R., and Andremont, A. (2005). Clonal comparison of *Staphylococcus aureus* isolates from healthy pig farmers, human controls, and pigs. *Emerg. Infect. Dis.* 11, 711–714. doi: 10.3201/eid1105.040866

Balakuntla, J., Prabhakara, S., and Arakere, G. (2014). Novel rearrangements in the staphylococcal cassette chromosome mec type V elements of Indian ST772 and ST672 methicillin resistant *Staphylococcus aureus* strains. *PLoS One* 9:e94293. doi: 10.1371/journal.pone.0094293

Boswihi, S. S., Udo, E. E., Mathew, B., Noronha, B., Verghese, T., and Tappa, S. B. (2020a). Livestock-associated methicillin-resistant *Staphylococcus aureus* in patients admitted to Kuwait Hospitals in 2016-2017. *Front. Microbiol.* 10:2912. doi: 10.3389/fmicb.2019.02912

Boswihi, S. S., Udo, E. E., and Al-Sweih, N. (2016). Shifts in the clonal distribution of methicillin-resistant *Staphylococcus aureus* in Kuwait Hospitals: 1992-2010. *PLoS One* 11:e0162744. doi: 10.1371/journal.pone.0162744

Boswihi, S. S., Udo, E. E., and AlFouzan, W. (2020b). Antibiotic resistance and typing of the methicillin-resistant *Staphylococcus aureus* clones in Kuwait hospitals, 2016-2017. *BMC Microbiol.* 20:314. doi: 10.1186/s12866-020-02009-w

Boswihi, S. S., Udo, E. E., Monecke, S., Mathew, B., Noronha, B., Verghese, T., et al. (2018). Emerging variants of methicillin-resistant *Staphylococcus aureus* genotypes in Kuwait hospitals. *PLoS One* 13:e0195933. doi: 10.1371/journal.pone.0195933

British Society to Antimicrobial Chemotherapy [BSAC] (2013). Available online at: http://bsac.org.uk/susceptibility (accessed February 21, 2019).

Clinical and Laboratory Standard Institute (CLSI) (2015). *Performance Standards for Antimicrobial Susceptibility Testing: Twenty-Second Informational Supplement M100-S25*. Wayne, PA: CLSI.

Coombs, G. W., Monecke, S., Pearson, J. C., Tan, H. L., Chew, Y. K., Wilson, L., et al. (2011). Evolution and diversity of community-associated methicillin-resistant *Staphylococcus aureus* in a geographical region. *BMC Microbiol.* 11:215. doi: 10.1186/1471-2180-11-215

David, M. Z., and Daum, R. S. (2010). Community-associated methicillin-resistant *Staphylococcus aureus*: epidemiology and clinical consequences of an emerging epidemic. *Clin. Microbiol. Rev.* 23, 616–687. doi: 10.1128/CMR.00081-09

Etter, D., Corti, S., Spirig, S., Cernela, N., Stephan, R., and Johler, S. (2020). *Staphylococcus aureus* population structure and genomic profiles in asymptomatic carriers in Switzerland. *Front. Microbiol.* 11:1289. doi: 10.3389/fmicb.2020.01289

Graveland, H., Duim, B., Van Duijkeren, E., Heederik, D., and Wagenaar, J. A. (2011). Livestock-associated methicillin-resistant *Staphylococcus aureus* in animals and humans. *Int. J. Med. Microbiol.* 301, 630–634. doi: 10.1016/j.ijmm.2011.09.004

Guthrie, J. L., Teatero, S., Hirai, S., Fortuna, A., Rosen, D., Mallo, G. V., et al. (2020). Genomic epidemiology of invasive methicillin-resistant *Staphylococcus aureus* infections among hospitalized individuals in Ontario, Canada. *J. Infect. Dis.* 222, 2071–2081. doi: 10.1093/infdis/jiaa147

Fluit, A. C. (2012). Livestock-associated *Staphylococcus aureus*. *Clin. Microbiol. Infect.* 18, 735–744. doi: 10.1111/j.1469-0691.2012.03846.x

Harmsen, D., Claus, H., Witte, W., Rothgänger, J., Claus, H., Turnwald, D., et al. (2003). Typing of methicillin-resistant *Staphylococcus aureus* in a university hospital setting by using novel software for spa repeat determination and database management. *J. Clin. Microbiol.* 41, 5442–5448. doi: 10.1128/jcm.41.12.5442-5448.2003

Hassoun, A., Linden, P. K., and Friedman, B. (2017). Incidence, prevalence, and management of MRSA bacteremia across patient populations-a review of recent developments in MRSA management and treatment. *Crit. Care* 21:211.

Islam, M. A., Parveen, S., Rahman, M., Huq, M., Nabi, A., Khan, Z. U. M., et al. (2019). Occurrence and characterization of methicillin resistant *Staphylococcus aureus* in processed raw foods and ready-to-eat foods in an urban setting of a developing country. *Front. Microbiol.* 10:503. doi: 10.3389/fmicb.2019.00503

Kinnevey, P. M., Shore, A. C., Brennan, G. I., Sullivan, D. J., Ehricht, R., Monecke, S., et al. (2014). Extensive genetic diversity identified among sporadic methicillin-resistant *Staphylococcus aureus* isolates recovered in Irish hospitals between 2000 and 2012. *Antimicrob. Agents Chemother.* 58, 1907–1917. doi: 10.1128/aac.02653-13

Köck, R., Schaumburg, F., Mellmann, A., Köksal, M., Jurke, A., Becker, K., et al. (2013). Livestock-associated methicillin-resistant *Staphylococcus aureus* (MRSA) as causes of human infection and colonization in Germany. *PLoS One* 8:e55040. doi: 10.1371/journal.pone.0055040

Long, K. S., Poehlsgaard, J., Kehrenberg, C., Schwarz, S., and Vester, B. (2006). The cfr rRNA methyltransferase confers resistance to phenicols, lincosamides, oxazolidinones, pleuromutilins, and streptogramin A antibiotics. *Antimicrob. Agent Chemother.* 50, 2500–2505. doi: 10.1128/aac.00131-06

McCaig, L. F., McDonald, L. C., Mandal, S., and Jernigan, D. B. (2006). *Staphylococcus aureus*-associated skin and soft tissue infections in ambulatory care. *Emerg. Infect. Dis.* 12, 1715–1723. doi: 10.3201/eid1211.060190

Morales, G., Picazo, J. J., Baos, E., Candel, F. J., Arribi, A., PeláeZ, B., et al. (2010). Resistance to linezolid is mediated by the cfr gene in the first report of an outbreak of linezolid-resistant *Staphylococcus aureus*. *Clin. Infect. Dis.* 50, 821–825.

Monecke, S., Coombs, G., Shore, A. C., Coleman, D. C., Akpaka, P., Borg, M., et al. (2011). A field guide to pandemic, epidemic and sporadic clones of methicillin-resistant *Staphylococcus aureus*. *PLoS One* 6:e17936. doi: 10.1371/journal.pone.0017936

Nimmo, G. R., and Coombs, G. W. (2008). Community-associated methicillin-resistant *Staphylococcus aureus* (MRSA) in Australia. *Int. J. Antimicrob. Agents* 3, 401–410.

Pfaller, M. A. (1999). Molecular epidemiology in the care of patients. *Arch. Pathol. Lab. Med.* 123, 1007–1010. doi: 10.1043/0003-9985(1999)123<1007:MEITCO>2.0.CO;2

Pillai, S. K., Sakoulas, G., Wennersten, C., Eliopoulos, G. M., Moellering, R. C., Ferraro, M. J., et al. (2002). Linezolid resistance in *Staphylococcus aureus*: characterization and stability of resistant phenotype. *J. Infect. Dis.* 186, 1603–1607.

Rebic, V., Budimir, A., Aljicevic, M., Bektas, S., Vranic, S. M., and Rebic, D. (2016). Typing of methicillin resistant *Staphylococcus aureus* using DNA fingerprints by pulsed-field gel electrophoresis. *Acta Inform. Med.* 24, 248–252. doi: 10.5455/aim.2016.24.248-252

Resch, G., François, P., Morisset, D., Stojanov, M., Bonetti, E. J., Schrenzel, J., et al. (2013). Human-to-bovine jump of *Staphylococcus aureus* CC8 is associated with the loss of a β-hemolysin converting prophage and the acquisition of a new staphylococcal cassette chromosome. *PLoS One* 8:e58187. doi: 10.1371/journal.pone.0058187

Roberts, M. C., Joshi, P. R., Monecke, S., Ehricht, R., Müller, E., Gawlik, D., et al. (2019). MRSA strains in Nepalese rhesus macaques (*Macaca mulatta*) and their environment. *Front. Microbiol.* 10:2505. doi: 10.3389/fmicb.2019.02505

Robinson, D. A., and Enright, M. C. (2003). Evolutionary models of the emergence of methicillin-resistant *Staphylococcus aureus*. *Antimicrob. Agents Chemother.* 47, 3926–3934. doi: 10.1128/aac.47.12.3926-3934.2003

Santosaningsih, D., Santoso, S., Budayanti, N. S., Suata, K., Lestari, E. S., Wahjono, H., et al. (2016). Characterisation of clinical *Staphylococcus aureus* isolates harbouring mecA or Panton-Valentine leukocidin genes from four tertiary care hospitals in Indonesia. *Trop. Med. Int. Health* 21, 610–618.

Senok, A., Nassar, R., Celiloglu, H., Nabi, A., Alfaresi, M., Weber, S., et al. (2020). Genotyping of methicillin resistant *Staphylococcus aureus* from the United Arab Emirates. *Sci. Rep.* 10:18551.

Senok, A., Somily, A. M., Nassar, R., Garaween, G., Kim Sing, G., Müller, E., et al. (2019). Emergence of novel methicillin-resistant *Staphylococcus aureus* strains in a tertiary care facility in Riyadh, Saudi Arabia. *Infect. Drug Resist.* 12, 2739–2746. doi: 10.2147/idr.s218870

Shambat, S., Nadig, S., Prabhakara, S., Bes, M., Etienne, J., and Arakere, G. (2012). Clonal complexes and virulence factors of *Staphylococcus aureus* from several cities in India. *BMC Microbiol.* 12:64.doi: 10.1186/1471-2180-12-64

Sieber, R. N., Urth, T. R., Petersen, A., Møller, C. H., Price, L. B., Skov, R. L., et al. (2020). Phage-mediated immune evasion and transmission of livestock-associated methicillin-resistant *Staphylococcus aureus* in humans. *Emerg. Infect. Dis.* 26, 2578–2585.

Strauß, L., Stegger, M., Akpaka, P. E., Alabi, A., Breurec, S., Coombs, G., et al. (2017). Origin, evolution, and global transmission of community-acquired *Staphylococcus aureus* ST8. *Proc. Natl. Acad. Sci. U.S.A.* 114, E10596–E10604.

Sunagar, R., Hegde, N. R., Archana, G. J., Sinha, A. Y., Nagamani, K., and Isloor, S. (2016). Prevalence and genotype distribution of methicillin-resistant *Staphylococcus aureus* (MRSA) in India. *J. Glob. Antimicrob. Resist.* 7, 46–52.

Tan, J., Langvik, M., Yang, A., Turner, B., Rico, A., Jankowski, S., et al. (2006). "Fast, accurate, and automated workflow for multi locus sequence typing of *Staphylococcus aureus* using the applied biosystems genetic analyzers and SeqScape® software," in *Poster (P533) Presented at the 16th European Congress of Clinical Microbiology and Infectious Diseases (ECCMID)*, Nice.

Tegegne, H. A., Koláčková, I., and Karpíšková, R. (2017). Diversity of livestock associated methicillin-resistant *Staphylococcus aureus*. *Asian Pac. J. Trop. Med.* 10, 929–931. doi: 10.1016/j.apjtm.2017.08.013

Tong, S. Y., Davis, J. S., Eichenberger, E., Holland, T. L., and Fowler, V. G., Jr. (2015). *Staphylococcus aureus* infections: epidemiology, pathophysiology, clinical manifestations, and management. *Clin. Microbiol. Rev.* 28, 603–661. doi: 10.1128/CMR.00134-14

Udo, E. E. (2013). Community-acquired methicillin-resistant *Staphylococcus aureus*: the new face of an old foe? *Med. Princ. Pract.* 22, 20–29.

Udo, E. E., Al-Lawati, B. A., Al-Muharmi, Z., and Thukral, S. S. (2014). Genotyping of methicillin-resistant *Staphylococcus aureus* in the Sultan Qaboos University Hospital, Oman reveals the dominance of Panton-Valentine leucocidin-negative ST6-IV/t304 clone. *New Microbes New Infect.* 2, 100–105.

Udo, E. E., Jacob, L. E., and Mathew, B. (2001). Genetic analysis of methicillin-resistant *Staphylococcus aureus* expressing high- and low- level mupirocin resistance. *J. Med. Microbiol.* 50, 909–915. doi: 10.1099/0022-1317-50-10-909

Udo, E. E., Pearman, J. W., and Grubb, W. B. (1993). Genetic analysis of community isolates of methicillin-resistant *Staphylococcus aureus* in Western Australia. *J. Hosp. Infect.* 25, 97–108. doi: 10.1016/0195-6701(93)90100-e

Udo, E. E., and Sarkhoo, E. (2010). Genetic analysis of high-level mupirocin resistance in the ST80 clone of community-associated methicillin-resistant *Staphylococcus aureus*. *J. Med. Microbiol.* 59, 193–199.

Vali, L., Dashti, A. A., Mathew, F., and Udo, E. E. (2017). Characterization of heterogeneous MRSA and MSSA with reduced susceptibility to chlorhexidine in Kuwaiti Hospitals. *Front. Microbiol.* 8:1359. doi: 10.3389/fmicb.2017.01359

van Belkum, A., Struelens, M., de Visser, A., Verbrugh, H., and Tibayrenc, M. (2001). Role of genomic typing in taxonomy, evolutionary genetics, and microbial epidemiology. *Clin. Microbiol. Rev.* 14, 547–560. doi: 10.1128/CMR.14.3.547-560.2001

van Cleef, B. A., Monnet, D. L., Voss, A., Krziwanek, K., Allerberger, F., Struelens, M., et al. (2011). Livestock-associated methicillin-resistant *Staphylococcus aureus* in humans, Europe. *Emerg. Infect. Dis.* 17, 502–505.

Wagenaar, J. A., Yue, H., Pritchard, J., Broekhuizen-Stins, M., Huijsdens, X., Mevius, D., et al. (2009). Unexpected sequence types in livestock associated methicillin-resistant *Staphylococcus aureus* (MRSA): MRSA ST9 and a single locus variant of ST9 in pig farming in China. *Vet. Microbiol.* 139, 405–409. doi: 10.1016/j.vetmic.2009.06.014

Weber, S., Ehricht, R., Slickers, P., Abdel-Wareth, L., Donnelly, G., Pitout, M., et al. (2010). *Genetic Fingerprinting of MRSA from Abu Dhabi*. Vienna: ECCMID.

Zarfel, G., Luxner, J., Folli, B., Leitner, E., Feierl, G., Kittinger, C., et al. (2016). Increase of genetic diversity and clonal replacement of epidemic methicillin-resistant *Staphylococcus aureus* strains in South-East Austria. *FEMS. Microbiol. Lett.* 363:fnw137. doi: 10.1093/femsle/fnw137

**Conflict of Interest:** The authors declare that the research was conducted in the absence of any commercial or financial relationships that could be construed as a potential conflict of interest.

frontiers in Microbiology

ORIGINAL RESEARCH
published: 21 June 2021
doi: 10.3389/fmicb.2021.656610

# *In vivo* Emergence of Colistin Resistance in Carbapenem-Resistant *Klebsiella pneumoniae* Mediated by Premature Termination of the *mgrB* Gene Regulator

*Yingying Kong, Chao Li, Hangfei Chen, Wei Zheng, Qingyang Sun, Xinyou Xie*, Jun Zhang* and Zhi Ruan**

*Department of Clinical Laboratory, Sir Run Run Shaw Hospital, Zhejiang University School of Medicine, Hangzhou, China*

OPEN ACCESS

**Edited by:**
*Annamari Heikinheimo, University of Helsinki, Finland*

**Reviewed by:**
*Qiong Chen, Hangzhou First People's Hospital, China*
*Haijian Zhou, National Institute for Communicable Disease Control and Prevention (China CDC), China*

***Correspondence:**
*Zhi Ruan*
*r_z@zju.edu.cn*
*Jun Zhang*
*jameszhang2000@zju.edu.cn*
*Xinyou Xie*
*scottxie@zju.edu.cn*

**Specialty section:**
*This article was submitted to Antimicrobials, Resistance and Chemotherapy, a section of the journal Frontiers in Microbiology*

**Received:** *21 January 2021*
**Accepted:** *28 May 2021*
**Published:** *21 June 2021*

**Citation:**
*Kong Y, Li C, Chen H, Zheng W, Sun Q, Xie X, Zhang J and Ruan Z (2021) In vivo Emergence of Colistin Resistance in Carbapenem-Resistant Klebsiella pneumoniae Mediated by Premature Termination of the mgrB Gene Regulator. Front. Microbiol. 12:656610. doi: 10.3389/fmicb.2021.656610*

Multidrug-resistant (MDR) *Klebsiella pneumoniae* is a severe threat to public health worldwide. Worryingly, colistin resistance, one of the last-line antibiotics for the treatment of MDR *K. pneumoniae* infection, has been increasingly reported. This study aims to investigate the emergence of evolved colistin resistance in a carbapenem-resistant *K. pneumoniae* isolate during colistin treatment. In this study, a pair of sequential carbapenem-resistant *K. pneumoniae* isolates were recovered from the same patient before and after colistin treatment, named KP1-1 and KP1-2, respectively. Antibiotic susceptibility testing was performed by the microdilution broth method. Whole genome sequencing was performed, and putative gene variations were analyzed in comparison of the genome sequence of both isolates. The bacterial whole genome sequence typing and source tracking analysis were performed by BacWGSTdb 2.0 server. Validation of the role of these variations in colistin resistance was examined by complementation experiments. The association between colistin resistance and the expression level of PhoP/PhoQ signaling system and its regulated genes was evaluated by quantitative real-time PCR (qRT-PCR) assay. Our study indicated that KP1-1 displayed extensively antibiotic resistant trait, but only susceptible to colistin. KP1-2 showed additional resistance to colistin. Both isolates belonged to Sequence Type 11 (ST11). The whole genome sequence analysis uncovered multiple resistance genes and virulence genes in both isolates. No plasmid-mediated *mcr* genes were found, but genetic variations in five chromosomal genes, especially the Gln30* alteration in MgrB, were detected in colistin-resistant isolate KP1-2. Moreover, only complementation with wild-type *mgrB* gene restored colistin susceptibility, with colistin MIC decreased from 32 to 1 mg/L. Expression assays revealed an overexpression of the *phoP*, *phoQ*, and *pmrD* genes in the *mgrB*-mutated isolate KP1-2 compared to the wild-type isolate KP1-1, confirming the MgrB alterations was responsible for increased expression levels of those genes. This study provides direct *in vivo* evidence that Gln30* alteration of MgrB is a critical region responsible for colistin resistance in *K. pneumoniae* clinical strains.

**Keywords: *Klebsiella pneumoniae*, colistin resistance, *mgrB*, complementation, whole genome sequencing**

## INTRODUCTION

Carbapenem resistance in *Klebsiella pneumoniae* has increased worldwide, mainly due to the rapid dissemination of antimicrobial-resistant bacteria and carbapenem overconsumption, thus limiting the effectiveness of therapeutic regimens (Tzouvelekis et al., 2012; van Duin and Doi, 2017). Polymyxins (polymyxin B and colistin) are considered as the last-resort antibiotics to treat infections caused by carbapenem-resistant *K. pneumoniae* (Giamarellou, 2016; Poirel et al., 2017). Colistin initially exhibited robust antibacterial activity for carbapenem-resistant *K. pneumoniae*, however, the emergence of colistin-resistant isolates has been reported repeatedly as its use expanded (Cannatelli et al., 2013; Jayol et al., 2014; Olaitan et al., 2014a; Aires et al., 2016; Giamarellou, 2016; Haeili et al., 2017; Hamel et al., 2020).

In *K. pneumoniae*, resistance to polymyxins is mostly mediated by adding 4-amino-4-deoxy-L-arabinose (L-Ara4N) and/or phosphoethanolamine (PEtN) to the lipid A moiety of lipopolysaccharide (LPS), which reduces the affinity between polymyxins and LPS (Olaitan et al., 2014b; Poirel et al., 2017). This modification can be regulated by the PhoQ/PhoP and PmrAB signaling systems, which regulate the expression of *pmrCAB* and *pmrHFIJKLM* operons responsible for modification of lipid A (Jayol et al., 2014; Olaitan et al., 2014b; Poirel et al., 2017). MgrB is a small regulatory transmembrane protein and exerts negative feedback on the PhoQ/PhoP signaling system (Lippa and Goulian, 2009). Thus, genetic alterations of MgrB have been proved to be responsible for colistin resistance (Cannatelli et al., 2013, 2014; Poirel et al., 2015; Aires et al., 2016; Hamel et al., 2020). Moreover, plasmid mediated mobile colistin resistance (*mcr* gene) has been reported as a transmissible resistance mechanism in Enterobacteriaceae, including *K. pneumoniae* (Liu et al., 2016; Caniaux et al., 2017; Ga et al., 2019).

In this study, we investigated the genomic variations between a paired colistin-susceptible and -resistant *K. pneumoniae* isolates consecutively recovered from a single patient, and demonstrated the mechanism responsible for the emergence of high-level resistance to colistin during *in vivo* treatment.

## MATERIALS AND METHODS

### The Patient and Isolates

A 66-year-old female patient was hospitalized, in a tertiary hospital in Hangzhou, Zhejiang province, China, in 2019, with symptoms of pyosepticemia, pancreatic malignancy, leukopenia, thrombocytopenic purpura, hepatic failure, and renal insufficiency. Initially, the patient received tigecycline by intravenous injection. Isolates were cultured from the inpatient during her hospitalization. The first isolate KP1-1, cultured form the blood sample of the inpatient within 24 h after admission, displayed extensively antibiotic resistance (including tigecycline) but susceptible only to colistin. The antibiotic therapeutic strategy was then adjusted to that of intravenous colistin (500,000 Unit every 8 h for the first 4 days and every 12 h for the following days). After received colistin treatment for 9 days, the second isolate KP1-2 was cultured from the stool sample with a colistin MIC of 32 mg/L. At the end of the treatment period, the inpatient expired from pyosepticemia and pancreatic malignancy. The isolates were identified by VITEK 2 (bioMérieux, Marcy-l'Étoile, France) and Matrix-assisted laser desorption/ionization-time-of-flight mass spectrometry (MALDI-TOF-MS, Bruker, Billerica, MA, United States).

### Antimicrobial Susceptibility Testing

Antimicrobial susceptibility testing was performed by the microdilution broth method for the following antimicrobial agents: aztreonam, fosfomycin, ertapenem, ceftazidime, cefepime, cefoperazone-sulbactam, cefoxitin, levofloxacin, ciprofloxacin, amikacin, tetracycline, minocycline, tigecycline, colistin, cefotaxime, meropenem, imipenem, gentamicin, trimethoprim-sulfamethoxazole, piperacillin, and piperacillin-tazobactam. The results were interpreted according to Clinical and Laboratory Standards Institute (CLSI) guidelines, except for tigecycline and colistin, which were interpreted according to the European Committee on Antimicrobial Susceptibility Testing (EUCAST) guidelines. *Escherichia coli* (ATCC 25922) were used as quality control strains for antimicrobial susceptibility testing.

### Whole-Genome Sequencing

Genomic DNA was extracted using a QIAamp DNA MiniKit (Qiagen, Valencia, CA, United States) following the manufacturer's instructions. The bacterial genome was fragmented by sonication using a Covaris M220 sonicator (Covaris, Woburn, MA, United States) and the sheared DNA fragments were then used to prepare a shotgun paired-end library with an average insert size of 350 bp via a TruSeq DNA Sample Prep kit (Illumina, San Diego, CA, United States). The prepared library was sequenced using the Illumina NovaSeq 6000 platform (Illumina, San Diego, CA, United States) through the 150 bp paired-end protocol. The short reads were assembled using Unicycler v0.4.8 software (Wick et al., 2017).

The genome annotation was conducted using the NCBI Prokaryotic Genome Annotation Pipeline (PGAP) (Tatusova et al., 2016). Antibiotic resistance genes, virulence genes, and plasmid replicons were queried using ABRicate 1.0.1 in tandem with ResFinder 4.1, CARD 2020, VFDB 2019, and PlasmidFinder 2.1 databases, with a 90% threshold for gene identification and a 60% minimum length to respective database entries. With the genomic sequence of the first isolate KP1-1 as the reference, the reads of the second isolate KP1-2 was mapped against that of KP1-1 using CLC Genomics Workbench 12. The gene variations, including single nucleotide polymorphisms (SNPs) and insertion and deletion mutations were predicted, and the variations were verified by PCR and Sanger sequencing. *In silico* multilocus sequence typing (MLST) analysis and bacterial source tracking using core genome MLST (cgMLST) strategy were performed using BacWGSTdb 2.0 server (Ruan and Feng, 2016; Ruan et al., 2020;

**TABLE 1 |** Primers used in this study.

| Primer name | Sequence (5′ → 3′) | Amplicon size (bp) | Reference or source |
|---|---|---|---|
| **Conventional PCR** | | | |
| mgrB-SpeI-F | acactggcggccgttactagtAACACGTTTTGAAACAAGTCGATG | 373 | This study |
| mgrB-KpnI-R | tgactgggtcatggtggtaccCACCACCTCAAAGAGAAGGCG | | This study |
| aroP-SpeI-F | acactggcggccgttactagtATGGAAGGTCAACAGCACGG | 1413 | This study |
| aroP-KpnI-R | tgactgggtcatggtggtaccTTATTGTGCTTTTATGGTGGCG | | This study |
| fructokinase-SpeI-F | acactggcggccgttactagtATGAATGGAAAAATCTGGGTACTCG | 924 | This study |
| fructokinase-KpnI-R | tgactgggtcatggtggtaccTCATGGCGCCTTTGGCGG | | This study |
| lysR-SpeI-F | acactggcggccgttactagtATGAAACTGCGTCATCTGGAAAT | 957 | This study |
| lysR-KpnI-R | tgactgggtcatggtggtaccTTACCCCAGCGGCGCAAT | | This study |
| PTS system-SpeI-F | acactggcggccgttactagtATGAGTAAAGTGATCGATTCGCTTG | 1401 | This study |
| PTS system-KpnI-R | tgactgggtcatggtggtaccTCAGAATTTCAGTGCGTTAGCG | | This study |
| **qRT-PCR** | | | |
| phoP_F | ATTGAAGAGGTTGCCGCCCGC | 136 | 6 |
| phoP_R | GCTTGATCGGCTGGTCATTCACC | | |
| phoQ_F | ATATGCTGGCGAGATGGGAAAACGG | 138 | 6 |
| phoQ_R | CCAGCCAGGGAACATCACGCT | | |
| pmrA_F | TACGCCGAAAGAGTATGCCC | 170 | This study |
| pmrA_R | GGATCCGCGATTTGCCAATC | | This study |
| pmrB_F | TGC CAG CTG ATA AGC GTC TT | 95 | 10 |
| pmrB_R | TTC TGG TTG TTG TGC CCT TC | | |
| pmrC_F | GCG TGA TGA ATA TCC TCA CCA | 116 | 10 |
| pmrC_R | CAC GCC AAA GTT CCA GAT GA | | |
| pmrD_F | GAT CGC AGA GAT TGA AGC CT | 120 | 10 |
| pmrD_R | GCG TTG CGG ATC TTC AAA GT | | |
| pmrE_F | GCA TAC CGT AAT GCC GAC TA | 119 | 10 |
| pmrE_R | GGG TTG ATC TCT GTG ACA TC | | |
| pmrK_F | AGT ATC GGT CAG TGG CTG TT | 123 | 10 |
| pmrK_R | CCG CTT ATC ACG AAA GAT CC | | |
| mgrB_F | CCTGTTGCTGTGGACTCAGA | 73 | This study |
| mgrB_R | AGTGCAAATGCCGCTGAAAA | | This study |
| rpsL_F | CCGTGGCGGTCGTGTTAAAGA | 109 | 6 |
| rpsL_R | GCCGTACTTGGAGCGAGCCTG | | |

Feng et al., 2021). The phylogenetic relationship between *K. pneumoniae* KP1-1, KP1-2 and a total of 631 publicly available ST11 *K. pneumoniae* isolates recovered from China were analyzed.

## Complementation Assays

The high-copy plasmid pCR2.1-Hyg, constructed by inserting a hygromycin-resistant gene into the HindIII site of pCR2.1, was used as a genetic vector. *Escherichia coli* DH5α was used as the host for recombinant plasmids. The differential genes were amplified from the colistin-susceptible isolates KP1-1 using the primers shown in **Table 1**. The purified amplified fragments were, respectively, cloned into the plasmid pCR2.1-Hyg using the ClonExpress II One Step Cloning Kit (Vazyme, Nanjing, China). Then, the recombinant plasmids were separately transformed into the *E. coli* DH5α for amplification, and eventually introduced into the colistin-resistant isolates KP1-2 by electroporation. The plasmid pCR2.1-Hyg was also transformed into KP1-2 as blank control. Electro-transformants were selected on Mueller-Hinton agar supplemented with 40 g/mL of hygromycin.

## Transcriptional Analysis by Quantitative Real-Time PCR (qRT-PCR)

Expression levels of *phoP*, *phoQ*, *pmrA*, *pmrB*, *pmrC*, *pmrD*, *pmrE*, *pmrK*, and *mgrB* genes were determined by qRT-PCR with the primers listed in **Table 1**. Total RNA was extracted from the mid-log phase bacterial culture using the PureLink™ RNA Mini Kit (Thermo Fisher Scientific, Waltham, MA, United States) and treated with RNase-free DNase I (Takara Biotechnology, Dalian, China) to remove genomic DNA contamination. Then, the corresponding cDNAs were generated from 500 ng of RNA using the HiFiScript cDNA Synthesis Kit (CWBio, Beijing, China) according to the manufacturer's instructions. qRT-PCR was performed using MagicSYBR Mixture (CWBio, Beijing, China) on the Applied Biosystems™ QuantStudio™ 1 (Thermo Fisher Scientific, Waltham, MA, United States). Thermal cycling conditions were as follows: 95°C for 30 s for enzyme activation, followed by 40 cycles of denaturation at 95°C for 5 s and annealing at 60°C for 30 s. The relative gene expression levels were determined using the comparative threshold cycle ($\Delta\Delta C_t$) method with *rpsL* gene

normalization. The experiments were performed in triplicate and repeated three times.

## Accession Number

The draft genome sequence of *K. pneumoniae* KP1-1 and KP1-2 were deposited in the NCBI GenBank database under the accession numbers JAERIE000000000 and JAERIF000000000.

# RESULTS

## Isolate Characterizations

The minimum inhibitory concentrations (MICs) of the two isolates to 21 antibiotics were shown in **Table 2**. Antimicrobial susceptibility testing showed that the first isolate KP1-1 was extensively drug-resistant, including aztreonam, ertapenem, ceftazidime, cefepime, cefoperazone-sulbactam, cefoxitin, levofloxacin, ciprofloxacin, amikacin, tetracycline, minocycline, tigecycline, cefotaxime, meropenem, imipenem, gentamicin, trimethoprim-sulfamethoxazole, piperacillin, and piperacillin-tazobactam. However, it remains susceptible to colistin (MIC < 0.03 mg/L). After the colistin therapy for 9 days, the second isolate KP1-2 was recovered with an increased colistin MIC of 32 mg/L.

## Genomic Characteristics

The whole genome sequence data analysis classified isolates KP1-1 and KP1-2 to the same Sequence Type 11 (ST 11). Both KP1-1 and KP1-2 harbored multiple antimicrobial resistance genes, including aminoglycosides (*aadA2* and *rmtB*), β-lactams ($bla_{CTX-M-65}$, $bla_{KPC-2}$ and $bla_{TEM-1B}$), fluoroquinolones (*qnrS1*), fosfomycin (*fosA*), phenicols (*catA2*), sulfonamides (*sul2*), tetracyclines [*tet*(A)], and trimethoprim (*dfrA14*). Moreover, we also identified several virulence genes, including aerobactin (*iutA*, *iucA*, *iucB*, *iucC*, and *iucD*), hypermucoviscosity (*rmpA* and *rmpA2*), and yersiniabactin (*ybtA*, *ybtE*, *ybtP*, *ybtQ*, *ybtU*, *ybtT*, and *ybtX*). Phylogenetic analysis indicated that the majority of ST11 *K. pneumoniae* isolates in NCBI GenBank database were recovered from Sichuan and Hangzhou, and the most closely related strain to *K. pneumoniae* KP1-1 and KP1-2 is L20, another ST11 strain previously recovered from a human feces sample in Hangzhou in the year 2016, which differed by only 15 cgMLST loci (**Figure 1**).

## Genetic Variations in Colistin-Susceptible and -Resistant Isolates

Regarding to the colistin resistance, no plasmid-mediated genes (*mcr-1* to *mcr-10*) were found in isolate KP1-2. To explain the mechanism of colistin resistance, the raw sequence reads of KP1-1 and KP1-2 were mapped and putative variations were identified in seven genes (**Table 3**). Compared with the colistin-susceptible KP1-1, a premature stop codon was detected in the *mgrB* gene at the position 88 (C88T) in isolate KP1-2, leading to a non-sense mutation in the amino acid sequence for glutamine to stop at position 30 of the protein (Gln30*). The full-length

**TABLE 2** | MICs of the *K. pneumoniae* KP1-1 and KP1-2 to different antimicrobial agents.

| Isolate | MIC (mg/L) [a] | | | | | | | | | | | | | | | | | | |
|---|---|---|---|---|---|---|---|---|---|---|---|---|---|---|---|---|---|---|---|
| | ATM | FOF | ETP | CAZ | FEP | SCF | FOX | LVX | CIP | AMK | TET | TGC | MH | CST | CTX | MEM | IPM | GEN | SXT | PRL | PRL/TZP |
| KP1-1 | 32 | 16 | >256 | >256 | 256 | >256 | 256 | 64 | 128 | >256 | >256 | 8 | 64 | <0.03 | 64 | 128 | 128 | >256 | 16 | >512 | >512 |
| KP1-2 | 32 | 32 | >256 | 256 | 256 | >256 | 128 | 128 | 128 | >256 | >256 | 8 | 64 | 32 | 128 | 128 | 128 | >256 | 16 | >512 | 512 |

[a]*ATM, aztreonam; FOF, fosfomycin; ETP, ertapenem; CAZ, ceftazidime; FEP, cefepime; SCF, cefoperazone-sulbactam; FOX, cefoxitin; LVX, levofloxacin; CIP, ciprofloxacin; AMK, amikacin; TET, tetracycline; TGC, tigecycline; MH, minocycline; CST, colistin; CTX, cefotaxime; MEM, meropenem; IPM, imipenem; GEN, gentamicin; SXT, trimethoprim-sulfamethoxazole; PRL, piperacillin; PRL/TZP, piperacillin-tazobactam.*

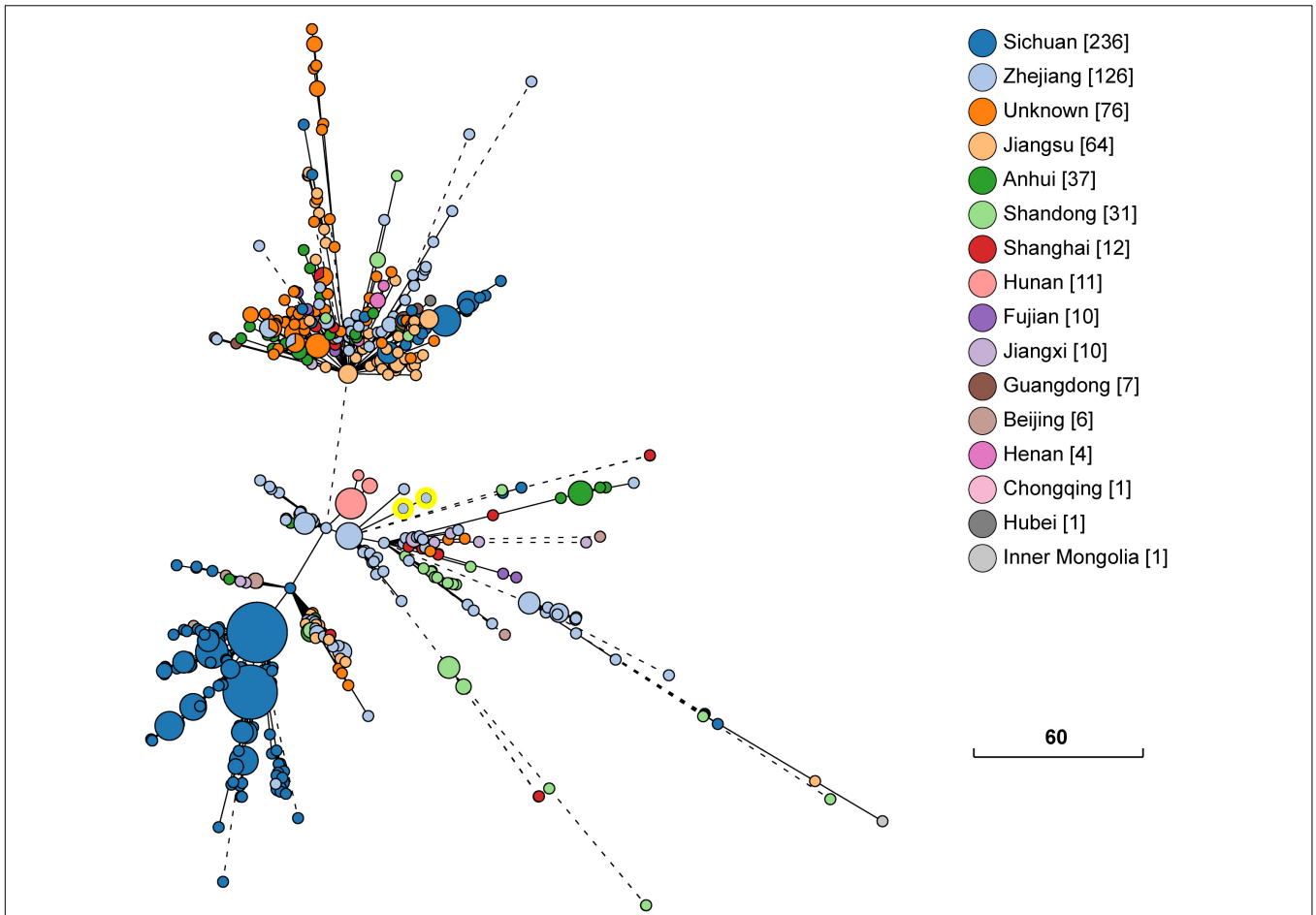


**FIGURE 1 |** Phylogenetic relationship between *K. pneumoniae* KP1-1, KP1-2 and a total of 631 ST11 *K. pneumoniae* strains retrieved from NCBI GenBank. The lines connecting the circles indicate the clonal relationship between different isolates. The scale bar represents a pairwise allelic difference of core genome multilocus sequence typing (cgMLST) loci. The number of isolates from each province is given in square brackets. The solid line indicates the pairwise allelic differences of two isolates is less than 50 alleles. Branches longer than 50 allelic differences are proportionally shortened and are represented by dashed lines. The two yellow circles indicate *K. pneumoniae* KP1-1, KP1-2.

**TABLE 3 |** Genetic alterations between the isolates KP1-1 and KP1-2.

| Genes | Annotation | Genotype | Genetic alterations |
|---|---|---|---|
| *mgrB* | PhoP/PhoQ regulator MgrB | Non-sense mutation | C88T (Gln30*) |
| *aroP* | Aromatic amino acid transporter AroP | Missense variant | A689T (Glu230Val) |
| *chbC* | PTS N,N′-diacetylchitobiose transporter subunit IIC | Missense variant | C413T (Ala138Val) |
| *lysR* | LysR family transcriptional regulator | Missense variant | G770A (Cys257Tyr) |
| – | Aminoimidazole riboside kinase | Frame shift variant | 714dupC (Ala239fs) |
| – | Fimbrial biogenesis outer membrane usher protein | Synonymous variant | T1641C (Ala547Ala) |
| *smvA* | Methyl viologen resistance protein | Synonymous variant | A711C (Thr237Thr) |

MgrB protein, which is 47 amino acids in wild type isolates, was therefore only 29 amino acids long in isolate KP1-2.

Moreover, Missense variants were detected in aromatic amino acid transporter AroP (A689T, Glu230Val), PTS N,N'-diacetylchitobiose transporter subunit ChbC (C413T, Ala138Val), transcriptional activator protein LysR (G770A, Cys257Tyr), and a frameshift variant was detected in aminoimidazole riboside kinase (714dupC, Ala239fs). Synonymous variants were found in fimbrial biogenesis outer membrane usher protein (T1641C) and Methyl viologen resistance protein SmvA (A711>C).

## Complementation Experiments

The significance of the non-silent alterations of the five genes detected in colistin-resistant KP1-2 was determined by

complementation experiments. The introduction of PCR2.1-Hyg-*mgrB*, which carries a cloned copy of the KP1-1 *mgrB* gene along with part of its flanking sequence, in isolate KP1-2 was able to restore susceptibility to colistin, with MIC decreased from 32 to 1 mg/L (**Table 4**). However, complementation with the rest four functional genes did not alter colistin susceptibility in KP1-2 isolates. This indicates that colistin resistance is not related to these alterations in the other four genes. On the contrary, transformed with the PCR2.1-Hyg, minor change of colistin MIC was found in KP1-2 (MIC decreased to 16 mg/L).

## Gln30* Substitution in MgrB Associated With *phoPQ* and *pmrD* Overexpression

Expression levels of the *phoPQ* operon and *pmr* genes were analyzed to assess the impact of the Gln30* substitution in MgrB. Analysis of *phoP*, *phoQ*, and *pmrD* transcription by qRT-PCR revealed a two- to three- fold increase in KP1-2 carrying an inactivated *mgrB* allele in comparison with KP1-1 and with the *mgrB* mutants complemented with a cloned copy of wild-type *mgrB* (**Table 5**). However, there was no upregulation in the expression of *pmrA, pmrB, pmrC, pmrE,* and *pmrK* genes. Interestingly, significant upregulation of *mgrB* was observed for KP1-2 (5-fold) and KP1-2 complemented with wild-type *mgrB* (10-fold).

# DISCUSSION

Over the past decade, increased rates of resistance to antibiotics in *K. pneumoniae* has been reported worldwide (Olaitan et al., 2014a; Giamarellou, 2016; van Duin and Doi, 2017). Colistin has regained a significant part of the therapeutic regimen for treatment of infection caused by carbapenem-resistant bacteria. However, it rapidly developed resistance due to the frequent use in clinical settings, becoming a major public health concern (Olaitan et al., 2014a; Giamarellou, 2016). In the present study, we monitored the evolved colistin resistance in a 66-year-old female inpatient infected with carbapenem-resistant *K. pneumoniae* during colistin treatment. Our data provide the direct evidence that genetic evolution in the *mgrB* gene can lead to a high level of colistin resistance and cause treatment failure.

**TABLE 4 |** The transformants of differential genes and the corresponding MICs of colistin.

| Strain | Colistin MIC (mg/L) |
|---|---|
| KP1-1 | <0.03125 |
| KP1-2 | 32 |
| KP1-2 (PCR2.1-Hyg) | 16 |
| KP1-2 (PCR2.1-Hyg-mgrB) | 1 |
| KP1-2 (PCR2.1-Hyg-aroP) | 32 |
| KP1-2 (PCR2.1-Hyg-fructokinase) | 32 |
| KP1-2 (PCR2.1-Hyg-lysR) | 32 |
| KP1-2 (PCR2.1-Hyg-pts system) | 32 |

**TABLE 5 |** Colistin MICs and the expression levels of *phoP, phoQ, pmrA, pmrB, pmrC, pmrD, pmrE, pmrK,* and *mgrB* genes of *K. pneumoniae* KP1-1, KP1-2, and of the corresponding transformants carrying either the PCR2.1-Hyg or PCR2.1-Hyg-mgrB plasmids[a].

| Stain | Chromosomal *mgrB* status | Colistin MIC (μg/mL) | Relative expression level (mean ± SD) | | | | | | | | |
|---|---|---|---|---|---|---|---|---|---|---|---|
| | | | *phoP* | *phoQ* | *pmrA* | *pmrB* | *pmrC* | *pmrD* | *pmrE* | *pmrK* | *mgrB* |
| KP1-1 | WT | <0.03125 | 1 | 1 | 1 | 1 | 1 | 1 | 1 | 1 | 1 |
| KP1-2 | Premature termination | 32 | 1.98 ± 0.18 | 3.25 ± 0.05 | 0.64 ± 0.03 | 0.57 ± 0.05 | 0.56 ± 003 | 2.26 ± 0.07 | 0.61 ± 0.05 | 0.96 ± 0.03 | 5.09 ± 0.22 |
| KP1-2 (PCR2.1-Hyg) | Premature termination | 16 | 1.93 ± 0.15 | 2.59 ± 0.17 | 0.76 ± 0.03 | 0.99 ± 0.08 | 1.14 ± 0.14 | 2.09 ± 0.11 | 0.98 ± 0.03 | 1.38 ± 0.10 | 4.9 ± 0.23 |
| KP1-2 (PCR2.1-Hyg-mgrB) | Premature termination | 1 | 1.07 ± 0.05 | 0.76 ± 0.02 | 0.70 ± 0.01 | 0.74 ± 0.02 | 1.12 ± 0.02 | 1.14 ± 0.10 | 0.98 ± 0.10 | 0.71 ± 0.07 | 10.43 ± 0.12 |

[a]*The expression levels for the phoP, phoQ, pmrA, pmrB, pmrC, pmrD, pmrE, pmrK, and mgrB genes were normalized against the value obtained with colistin-susceptible strain KP1-1.*

Colistin resistance is mainly mediated by chromosome or horizontal gene transfer. Chromosomal mutations in two-component systems (PmrA/PmrB and PhoP/PhoQ) and genes regulating these systems can lead to colistin resistance in *K. pneumoniae* (Olaitan et al., 2014a,b; Poirel et al., 2017). Moreover, plasmid-mediated *mcr* genes, which encodes a phosphoethanolamine transfer enzyme, have been identified to confer resistance to colistin via horizontal gene transfer (Liu et al., 2016; Caniaux et al., 2017; Ga et al., 2019). None of the plasmid encoded *mcr-1* to *mcr-10* genes were detected in KP1-2, which demonstrating that the colistin resistance is mediated by chromosomally encoded mechanisms.

By mapping the whole genome sequences of KP1-1 and KP1-2, five genes with non-silent alterations were exhibited in colistin-resistant KP1-2, including inactivated *mgrB* gene mediated by premature termination. MgrB, a small transmembrane protein with 47 amino acids, mediates potent negative feedback on the PhoQ/PhoP regulatory system, which regulates genes implicated in the LPS modifications and colistin resistance (Lippa and Goulian, 2009; Olaitan et al., 2014b; Poirel et al., 2017). Until now, the insertion of IS elements (especially the IS*5*-like element), non-sense mutations, and missense mutations have recently been reported in colistin resistance in *K. pneumoniae* isolates in diverse clinical and non-clinical isolates (Cannatelli et al., 2013, 2014; Olaitan et al., 2014a; Poirel et al., 2015; Aires et al., 2016; Haeili et al., 2017; Hamel et al., 2020). Among the above genetic variations, insertional inactivation of *mgrB* by IS elements, especially IS5-like elements, seemingly to be the most common mechanism of *mgrB* variation. Regarding the missense mutations, genetic alterations in MgrB, including Q30stop and C28stop, have been identified to be responsible for colistin resistance in *K. pneumoniae* isolates (Olaitan et al., 2014a; Aires et al., 2016). We suppose that premature termination within *mgrB*, found in the present study, result in MgrB inactivation and therefore lead to PhoP/PhoQ activation which in turn activates the PmrA/PmrB response regulator.

Complementation experiments showed that only transformation of wild *mgrB* gene had the ability to restore colistin susceptibility in KP1-2. This result agrees with that *mgrB* disruptions and mutations represent a strong association with colistin resistance mechanism in *K. pneumoniae* (Cannatelli et al., 2013, 2014; Olaitan et al., 2014a; Poirel et al., 2015; Aires et al., 2016; Haeili et al., 2017; Hamel et al., 2020). The Gln30* substitution, has been reported in several studies in different countries, found in the KP1-2 reinforced the hypothesis that position C88 in the *mgrB* (codon 30 in protein) is a critical region, which is prone to mutate upon colistin treatment (Olaitan et al., 2014a; Poirel et al., 2015; Aires et al., 2016; Haeili et al., 2017). Compared with the colistin resistance resulting from the *mcr* genes and two-component systems, the inactivation of MgrB leads to a higher level of colistin resistance (Olaitan et al., 2014a; Liu et al., 2016; Ga et al., 2019). In the current study, MgrB variation conferring colistin resistance occurred in a successful pandemic clone ST11, which will likely cause global presence of pan-drug-resistant *K. pneumoniae* and need continuous monitor.

The disruption of *mgrB* results in the activation of PhoP/PhoQ signaling system, which is known to indirectly activate the PmrA/PmrB via PmrD (Lippa and Goulian, 2009; Olaitan et al., 2014b). The activation of the PmrA/PmrB leads to the upregulation of *pmrCAB* and *pmrHFIJKLM-pmrE* operons that transfer of PEtN and L-Ara4N cationic groups to the LPS, which is responsible for the acquisition of colistin resistance in *K. pneumoniae* (Olaitan et al., 2014b; Poirel et al., 2017). Thus, it is generally accepted that loss of MgrB activates the cross-regulation of PhoPQ-PmrD-PmrAB signal transduction pathway in *K. pneumoniae*. However, activation of PhoP/PhoQ through *mgrB* mutation dose not significantly activate the production of PmrA/PmrB and confers colistin resistance. Therefore, PhoP/PhoQ activation alone is able to confer colistin resistance even without any additional effects caused by PmrA/PmrB activation (Cheung et al., 2020). In our study, we observed a signification association between colistin resistance, attributed to Gln30* substitution in MgrB, and upregulation of *phoPQ* operon and *pmrD* gene despite there being no upregulation of *pmrHFIJKLM* and *pmrCAB* operons. This can be explained by the fact that some unexplained mechanisms other than *pmrHFIJKLM* and *pmrCAB* might be involved in mediating colistin resistance in *K. pneumoniae*, which warrants further investigation.

In conclusion, our findings identified that Gln30* substitution in MgrB is responsible for the upregulation of PhoP/PhoQ signaling system and of the *pmrD* gene that confers colistin resistance in *K. pneumoniae*. To the best of our knowledge, this is the first report to provide direct *in vivo* evidence that the alteration of MgrB confers colistin resistance in a carbapenem-resistant *K. pneumoniae* isolate in China.

## DATA AVAILABILITY STATEMENT

The datasets presented in this study can be found in online repositories. The names of the repository/repositories and accession number(s) can be found in the article/supplementary material.

## AUTHOR CONTRIBUTIONS

ZR, JZ, and XX designed the experiments. YK, CL, and HC performed the experiments. ZR, WZ, and QS analyzed the data. YK and ZR wrote the manuscript. All authors read and approved the final manuscript.

## FUNDING

This study was supported by the National Natural Science Foundation of China (81871696 and 82072342) and Zhejiang Provincial Medical and Health Science and Technology Plan (2021KY943).

## REFERENCES


Aires, C. A., Pereira, P. S., Asensi, M. D., and Carvalho-Assef, A. P. (2016). mgrB Mutations Mediating polymyxin B resistance in *Klebsiella pneumoniae* isolates from rectal surveillance swabs in Brazil. *Antimicrob. Agents Chemother.* 60, 6969–6972. doi: 10.1128/aac.01456-16

Caniaux, I., van Belkum, A., Zambardi, G., Poirel, L., and Gros, M. F. (2017). MCR: modern colistin resistance. *Eur. J. Clin. Microbiol. Infect. Dis.* 36, 415–420. doi: 10.1007/s10096-016-2846-y

Cannatelli, A., D'Andrea, M. M., Giani, T., Di Pilato, V., Arena, F., Ambretti, S., et al. (2013). In vivo emergence of colistin resistance in *Klebsiella pneumoniae* producing KPC-type carbapenemases mediated by insertional inactivation of the PhoQ/PhoP mgrB regulator. *Antimicrob. Agents Chemother.* 57, 5521–5526. doi: 10.1128/aac.01480-13

Cannatelli, A., Giani, T., D'Andrea, M. M., Di Pilato, V., Arena, F., Conte, V., et al. (2014). MgrB inactivation is a common mechanism of colistin resistance in KPC-producing *Klebsiella pneumoniae* of clinical origin. *Antimicrob. Agents Chemother.* 58, 5696–5703. doi: 10.1128/aac.03110-14

Cheung, C. H. P., Heesom, K. J., and Avison, M. B. (2020). Proteomic investigation of the signal transduction pathways controlling colistin resistance in *Klebsiella pneumoniae*. *Antimicrob. Agents Chemother.* 64, e00790–20.

Feng, Y., Zou, S., Chen, H., Yu, Y., and Ruan, Z. (2021). BacWGSTdb 2.0: a one-stop repository for bacterial whole-genome sequence typing and source tracking. *Nucleic Acids Res.* 49, D644–D650.

Ga, L. M., Guldimann, C., Sullivan, G., Henderson, L. O., and Wiedmann, M. (2019). Identification of novel mobilized colistin resistance gene mcr9 in a multidrug-resistant, colistin-susceptible *Salmonella enterica* serotype typhimurium isolate. *mBio* 10, e000853–19.

Giamarellou, H. (2016). Epidemiology of infections caused by polymyxin-resistant pathogens. *Int. J. Antimicrob. Agents* 48, 614–621. doi: 10.1016/j.ijantimicag.2016.09.025

Haeili, M., Javani, A., Moradi, J., Jafari, Z., Feizabadi, M. M., and Babaei, E. (2017). MgrB Alterations mediate colistin resistance in *Klebsiella pneumoniae* isolates from Iran. *Front. Microbiol.* 8:2470.

Hamel, M., Chatzipanagiotou, S., Hadjadj, L., Petinaki, E., Papagianni, S., Charalampaki, N., et al. (2020). Inactivation of mgrB gene regulator and resistance to colistin is becoming endemic in carbapenem-resistant *Klebsiella pneumoniae* in Greece: a nationwide study from 2014 to 2017. *Int. J. Antimicrob. Agents* 55, 105930. doi: 10.1016/j.ijantimicag.2020.105930

Jayol, A., Poirel, L., Brink, A., Villegas, M. V., Yilmaz, M., and Nordmann, P. (2014). Resistance to colistin associated with a single amino acid change in protein PmrB among *Klebsiella pneumoniae* isolates of worldwide origin. *Antimicrob. Agents Chemother.* 58, 4762–4766. doi: 10.1128/aac.00084-14

Lippa, A. M., and Goulian, M. (2009). Feedback inhibition in the PhoQ/PhoP signaling system by a membrane peptide. *PLoS Genet* 5:e1000788. doi: 10.1371/journal.pgen.1000788

Liu, Y.-Y., Wang, Y., Walsh, T. R., Yi, L.-X., Zhang, R., Spencer, J., et al. (2016). Emergence of plasmid-mediated colistin resistance mechanism MCR-1 in animals and human beings in China: a microbiological and molecular biological study. *Lancet Infect. Dis.* 16, 161–168. doi: 10.1016/s1473-3099(15)00424-7

Olaitan, A. O., Diene, S. M., Kempf, M., Berrazeg, M., Bakour, S., Gupta, S. K., et al. (2014a). Worldwide emergence of colistin resistance in *Klebsiella pneumoniae* from healthy humans and patients in Lao PDR, Thailand, Israel, Nigeria and France owing to inactivation of the PhoP/PhoQ regulator mgrB: an epidemiological and molecular study. *Int. J. Antimicrob. Agents* 44, 500–507. doi: 10.1016/j.ijantimicag.2014.07.020

Olaitan, A. O., Morand, S., and Rolain, J. M. (2014b). Mechanisms of polymyxin resistance: acquired and intrinsic resistance in bacteria. *Front. Microbiol.* 5:643.

Poirel, L., Jayol, A., Bontron, S., Villegas, M. V., Ozdamar, M., Turkoglu, S., et al. (2015). The mgrB gene as a key target for acquired resistance to colistin in *Klebsiella pneumoniae*. *J. Antimicrob. Chemother.* 70, 75–80. doi: 10.1093/jac/dku323

Poirel, L., Jayol, A., and Nordmann, P. (2017). Polymyxins: antibacterial activity, susceptibility testing, and resistance mechanisms encoded by plasmids or chromosomes. *Clin. Microbiol. Rev.* 30, 557–596. doi: 10.1128/cmr.00064-16

Ruan, Z., and Feng, Y. (2016). BacWGSTdb, a database for genotyping and source tracking bacterial pathogens. *Nucleic Acids Res.* 44, D682–D687.

Ruan, Z., Yu, Y., and Feng, Y. (2020). The global dissemination of bacterial infections necessitates the study of reverse genomic epidemiology. *Brief. Bioinform.* 21, 741–750. doi: 10.1093/bib/bbz010

Tatusova, T., DiCuccio, M., Badretdin, A., Chetvernin, V., Nawrocki, E. P., Zaslavsky, L., et al. (2016). NCBI prokaryotic genome annotation pipeline. *Nucleic Acids Res.* 44, 6614–6624. doi: 10.1093/nar/gkw569

Tzouvelekis, L. S., Markogiannakis, A., Psichogiou, M., Tassios, P. T., and Daikos, G. L. (2012). Carbapenemases in *Klebsiella pneumoniae* and Other *Enterobacteriaceae*: an evolving crisis of global dimensions. *Clin. Microbiol. Rev.* 25, 682–707. doi: 10.1128/cmr.05035-11

van Duin, D., and Doi, Y. (2017). The global epidemiology of carbapenemase-producing *Enterobacteriaceae*. *Virulence* 8, 460–469. doi: 10.1080/21505594.2016.1222343

Wick, R. R., Judd, L. M., Gorrie, C. L., and Holt, K. E. (2017). Unicycler: Resolving bacterial genome assemblies from short and long sequencing reads. *PLoS Comput. Biol.* 13:e1005595. doi: 10.1371/journal.pcbi.1005595


**Conflict of Interest:** The authors declare that the research was conducted in the absence of any commercial or financial relationships that could be construed as a potential conflict of interest.

frontiers in Microbiology

ORIGINAL RESEARCH
published: 20 July 2021
doi: 10.3389/fmicb.2021.653595

# Emergence and Clonal Spread of CTX-M-65-Producing *Escherichia coli* From Retail Meat in Portugal

*Célia Leão[1,2], Lurdes Clemente[1,3], Laura Moura[1,4], Anne Mette Seyfarth[5], Inge M. Hansen[5], Rene S. Hendriksen[5] and Ana Amaro[1]**

[1] Laboratory of Bacteriology and Mycology, National Institute of Agrarian and Veterinary Research (INIAV, IP), Oeiras, Portugal, [2] MED – Mediterranean Institute for Agriculture, Environment and Development, Évora, Portugal, [3] Faculty of Veterinary Science, CIISA- Centre for Interdisciplinary Research in Animal Health, Lisbon, Portugal, [4] Faculty of Pharmacy, University of Lisbon, Lisbon, Portugal, [5] EURL-AR, European Reference Laboratory for Antimicrobial Resistance, Technical University of Denmark (DTU), National Food Institute, Lyngby, Denmark

The emergence and dissemination of resistance to third- and fourth-generation cephalosporins among *Enterobacteriaceae* from different sources impose a global public health threat. Here, we characterized by whole-genome sequencing four *Escherichia coli* strains harboring the $bla_{CTX-M-65}$ gene identified among 49 isolates from beef and pork collected at retail. The genomic content was determined using the Center for Genomic Epidemiology web tools. Additionally, the prediction and reconstruction of plasmids were conducted, the genetic platform of the $bla_{CTX-M-65}$ genes was investigated, and phylogenetic analysis was carried out using 17 other genomes with the same sequence type and harboring the $bla_{CTX-M-65}$ gene. All strains harbored $bla_{CTX-M-65}$, $bla_{OXA-1}$, and $bla_{TEM-1B}$, and one also carried the $bla_{SHV-12}$ gene. Other resistance genes, namely, *qnrS2*, *aac(6')-Ib-c*, *dfrA14*, *sul2*, *tetA*, and *mphA*, were present in all the genomes; the *mcr*-1.1 gene was identified in the colistin-resistant strains. They belong to sequence type 2179, phylogenetic group B1, and serotype O9:H9 and carried plasmids IncI, IncFIC(FII), and IncFIB. All strains share an identical genetic environment with IS*903* and IS*Ecp1* flanking the $bla_{CTX-M-65}$ gene. It seems likely that the $bla_{CTX-M-65}$ gene is located in the chromosome in all isolates based on deep *in silico* analysis. Our findings showed that the strains are clonally related and belong to two sub-lineages. This study reports the emergence of CTX-M-65-producing *E. coli* in Portugal in food products of animal origin. The chromosomal location of the $bla_{CTX-M-65}$ gene may ensure a stable spread of resistance in the absence of selective pressure.

**Keywords: *Escherichia coli*, retail meat, ESBL, WGS, CTX-M-65, chromosome**

OPEN ACCESS

***Edited by:***
*Tarja Sironen,*
*University of Helsinki, Finland*

***Reviewed by:***
*Jian-Hua Liu,*
*South China Agricultural University, China*
*Andres Felipe Opazo-Capurro,*
*University of Concepcion, Chile*

***Correspondence:**
*Ana Amaro*
*ana.amaro@iniav.pt*

***Specialty section:***
*This article was submitted to Antimicrobials, Resistance and Chemotherapy, a section of the journal Frontiers in Microbiology*

***Received:*** *14 January 2021*
***Accepted:*** *10 May 2021*
***Published:*** *20 July 2021*

***Citation:***
*Leão C, Clemente L, Moura L, Seyfarth AM, Hansen IM, Hendriksen RS and Amaro A (2021) Emergence and Clonal Spread of CTX-M-65-Producing Escherichia coli From Retail Meat in Portugal. Front. Microbiol. 12:653595. doi: 10.3389/fmicb.2021.653595*

## INTRODUCTION

Bacteria harboring antimicrobial resistance genes can be spread to humans, constituting a global public health concern (O'Neill, 2016). Of particular importance is the resistance to β-lactam antibiotics, enzymatic inactivation being the most common mechanism of resistance through which β-lactamases cause the cleavage of the β-lactam ring (Blair et al., 2015). Extended-spectrum β-lactamase (ESBL) is a group of enzymes that hydrolyze oxymino-beta-lactam antibiotics,

conferring resistance to a wide variety of β-lactams, including penicillins, first-, second-, third-, and fourth-generation cephalosporins, and monobactams (Bush, 2018). These enzymes can be inhibited by β-lactam inhibitors such as clavulanic acid, sulbactam, and tazobactam through the covalent link to the serine residue active site (Tooke et al., 2019). Mobile genetic elements, particularly plasmids, are involved in the spread of ESBL genes, resulting in the rapid increase of ESBL-producing bacteria among different sources (Rozwandowicz et al., 2018; Silva et al., 2019). ESBLs are classified into several enzymatic groups, of which CTX-M, OXA, SHV, and TEM are frequently observed, CTX-M being the most prevalent (Silva et al., 2019; Palmeira and Ferreira, 2020). Currently, 230 CTX-M variants have been described according to GenBank records (last accessed on January 4, 2021). In Europe, the most frequently reported variants of *Enterobacteriaceae* species isolated from food-producing animals and food products are CTX-M-1, CTX-M-14, CTX-M-15, and CTX-M-2, CTX-M-15 being associated with outbreaks of severe extraintestinal infections in humans caused by the multidrug-resistant (MDR) *Escherichia coli* ST131 (Silva et al., 2019; Palmeira and Ferreira, 2020). In Portugal, the CTX-M-1, CTX-M-14, and CTX-M-32 variants were reported as the most prevalent in commensal and pathogenic *E. coli* isolated from food-producing animals and food products (Clemente et al., 2019; Silva et al., 2019).

In 2008, a new variant of the CTX-M family identified as CTX-M-65, belonging to the CTX-M-9 group and cluster 14, was described for the first time in *E. coli* isolated from a human urine sample in the United States (Doi et al., 2008). CTX-M-65 differs from CTX-M-14 by two amino acid substitutions, namely, alanine by valine at position 77 (A77V) and serine by arginine at position 274 (S274R). In 2017, Tate and colleagues reported the emergence of a CTX-M-65 *Salmonella* Infantis isolated from food animals, retail chickens, and humans in the United States that is highly resistant to most of the studied β-lactam antimicrobials (Tate et al., 2017). In Europe, the CTX-M-65 variant has also been reported from Italy in *Salmonella* Infantis isolated from broilers and humans (Franco et al., 2015) and from the Netherlands in *E. coli* from cattle (Palmeira and Ferreira, 2020). Globally, the enzyme is widely distributed, with reports from China, Korea, and South America in *E. coli* isolated from humans, food-producing animals, retail chickens, and in a giant anteater from a zoo (Zheng et al., 2012; Bartoloni et al., 2013; Rao et al., 2014; Tate et al., 2017; Furlan et al., 2019; Park et al., 2019; Vinueza-Burgos et al., 2019; Wang et al., 2020). It is noteworthy to mention that a multidrug carbapenemase strain of *Klebsiella pneumoniae* co-producing CTX-M-65 was the causative agent of a severe nosocomial outbreak in China (Zhan et al., 2017).

In the present study, four CTX-M-65-producing *E. coli* isolated from beef and pork samples collected at retail in 2017 were characterized by whole-genome sequencing (WGS). Here, we described the molecular epidemiology of the resistance genes, the identification of the plasmids, and the $bla_{\mathrm{CTX-M-65}}$ genetic environment. Moreover, we determined and described the genetic relatedness with other *E. coli* genomes for better insights into the public health impact of an ESBL producer rarely found in Europe.

# MATERIALS AND METHODS

## Bacterial Isolates and Antimicrobial Susceptibility Testing

Two hundred and twenty beef and 220 pork samples were collected at retail stores across mainland Portugal in compliance with the European Commission Implementing Decision of November 12, 2013 to monitor and report antimicrobial resistance in zoonotic and commensal bacteria (Commission Decision 652/2013) in 2017. The isolation and identification of extended-spectrum β-lactamase/plasmid-mediated AmpC (ESBL/PMAβ) *E. coli* producers from meat samples were performed according to the laboratory protocols defined by the European Union Reference Laboratory for antimicrobial resistance (EURL-AR)[1]. Briefly, 25 g of each meat sample was mixed with 225 ml of buffered peptone water, followed by incubation at 37°C for 18–22 h. Enriched samples were plated onto MacConkey agar supplemented with 1 mg/L of cefotaxime (Glentham, Corsham, United Kingdom) and incubated at 44°C for 18–22 h. Presumptive *E. coli* colonies were selected for biochemical identification on ChromID® coli agar (bioMérieux, Marcy-l'Étoile, France), and after confirmation, the isolates were sub-cultured and stored at −80°C before further analyses.

The isolates were tested for antimicrobial susceptibility through the determination of the minimum inhibitory concentrations (MICs) using commercially available 96-well microplates, EUVSEC and EUVSEC2 (Sensititre®, Trek Diagnostic Systems, East Grinstead, United Kingdom) panels, and the results were interpreted according to EUCAST epidemiological breakpoints[2].

## Molecular Characterization of β-Lactam Resistance

Resistance mechanisms associated with ESBL/PMAβ enzymes were screened by PCR using primers targeting $bla_{\mathrm{TEM}}$, $bla_{\mathrm{SHV}}$, $bla_{\mathrm{OXA}}$, $bla_{\mathrm{CTX-M}}$, $bla_{\mathrm{ACC}}$, $bla_{\mathrm{FOX}}$, $bla_{\mathrm{MOX}}$, $bla_{\mathrm{DHA}}$, $bla_{\mathrm{CIT}}$, and $bla_{\mathrm{EBC}}$ (Dallenne et al., 2010). Amplified products were purified with ExoSAP-IT™ (Applied Biosystems™, Warrington, United Kingdom), followed by Sanger sequencing using the BigDye® Terminator v3.1 Cycle Sequencing Kit (Applied Biosystems). The sequencing of fragments was performed in an automatic sequencer ABI3100 (Applied Biosystems), and the identification of resistance genes was determined using the Basic Local Alignment Search Tool (BLAST) from the NCBI website (Altschul et al., 1990) and The Comprehensive Antibiotic Resistance Database (CARD) (Alcock et al., 2019).

## Whole-Genome Sequencing and Bioinformatics Analysis of the CTX-M-65 *E. coli* Producers

Four isolates identified as positive for $bla_{\mathrm{CTX-M-65}}$ by PCR and Sanger sequencing were further characterized by whole-genome sequencing. The isolates were recovered from pork and beef

[1] https://www.eurl-ar.eu/protocols.aspx

[2] https://mic.eucast.org/Eucast2/

samples, collected on the same day from the same retail store in the north of Portugal (INIAV_ECX027 and INIAV_ECX036) and on different days from different retail stores in Lisbon and Tejo Valley (INIAV_ECX016 and INIAV_ECX035).

The genome of two isolates (INIAV_016ECX and INIAV_027ECX) was sequenced at EURL-AR, DTU, Lyngby, Denmark, under the scope of the European Food Safety Authority (EFSA) confirmatory testing. Genomic DNA was extracted using an Invitrogen Easy-DNA Kit™ (Invitrogen, Carlsbad, CA, United States) and the DNA concentrations determined using the Qubit dsDNA BR assay kit (Invitrogen). Genomic DNA was prepared for Illumina pair-end sequencing using the Illumina (Illumina, Inc., San Diego, CA, United States) Nextera XT® Guide following the protocol revision C1. A sample of the pooled Nextera XT Libraries was loaded onto an Illumina MiSeq reagent cartridge using MiSeq Reagent Kit v3. The libraries were sequenced using an Illumina MiSeq platform (Illumina). The raw reads were *de novo* assembled using the assembler pipeline (version 1.4) available from the Center for Genomic Epidemiology (CGE)[3]. Raw sequence data from these two isolates were submitted to the European Nucleotide Archive (ENA)[4] under study accession numbers: ERS3535656 and ERS3535669.

DNA extraction of the remaining two isolates (INIAV_035ECX and INIAV_036ECX) was carried out at INIAV, Oeiras, Portugal, using the PureLink® Genomic DNA kit (Invitrogen) according to the manufacturer's instructions, with minor modifications. Briefly, the incubation period at 55°C was performed for 90 min and the DNA eluted with 50 μl of Tris-HCl buffer, pH 8.5. The DNA quality and quantity were assessed using a spectrophotometer [NanoDrop® 2000, Thermo Scientific, emergency use authorization (EUA), Waltham, MA, United States] and sequenced using the Illumina HiSeq sequencing technology (NovaSeq 6000 S2 PE150 XP sequencing mode, Eurofins Genomics Europe Sequencing GmbH, Ebersberg, Germany). The raw sequence data from these two isolates were submitted to the ENA under study accession numbers: ERS5493675 and ERS5493676. Raw data quality was assessed by FastQC[5]. BBDuk from the BBTools package[6] was used to remove possible contamination by adapter sequences and for trimming/removing low-quality reads, all performed with a minimum quality of Q20 using the Phred algorithm, with a minimum read length of 50 and with a *k*-mer length parameter of 19. All pre-processed reads were assembled with SPAdes 3.12.0 (Nurk et al., 2013).

The assembly stats of all the sequenced isolates were calculated using QUAST-5.0.2 (Mikheenko et al., 2018). Contigs with sizes lower than 500 bp were removed, and bioinformatics analysis using tools available at the CGE was performed. The acquired antimicrobial resistance genes and chromosomal point mutations, plasmid replicons, multilocus sequence type (MLST), serotype, *fum*C and *fim*H type, identification of virulence genes, and pathogenicity were assessed using ResFinder version 4.1 (80% threshold for%ID/60% minimum length) (Zankari et al., 2012; Bortolaia et al., 2020), PlasmidFinder version 2.1 (80% threshold for%ID) (Carattoli et al., 2014), MLST version 2.0 (Larsen et al., 2012), SerotypeFinder version 2.0 (85% threshold for%ID/60% minimum length) (Joensen et al., 2015), CHTyper version 1.0 (95% threshold for%ID) (Camacho et al., 2009), VirulenceFinder version 2.0 (90% threshold for%ID/60% minimum length) (Joensen et al., 2014), and PathogenFinder version 1.1 (Cosentino et al., 2013), respectively. The phylogenetic group was predicted using the ClermonTyping web-based tool (Beghain et al., 2018; Clermont et al., 2019).

Additionally, PLACNETw (Plasmid Constellation Network) was used to predict and reconstruct the plasmids (Vielva et al., 2017) in specifically assembled contigs of the bacterial genomes. For identifying the genetic platform of the CTX-M-65 enzyme, the contigs containing the $bla_{\mathrm{CTX-M-65}}$ gene were annotated using Prokka version 1.14.6 (Seemann, 2014), followed by analysis with Artemis (Carver et al., 2012) and EasyFig version 2.2.5 (Sullivan et al., 2011). A plasmid database, PLSDB, was also used to search for the plasmid nucleotide sequences contained in each of the selected contigs using the "mash screen" option (Galata et al., 2018).

A phylogenetic analysis based on the single nucleotide polymorphisms (SNPs) present in the genomes using CSI Phylogeny version 1.4 (10 reads of minimal depth at SNP positions, 10% minimal relative depth at SNP positions, 10 bp of minimal distance between SNPs, minimal SNP quality of 30, minimal read mapping quality of 25, and a minimal *Z*-score of 1.96) (Kaas et al., 2014) from the CGE website was conducted with the *E. coli* isolates from this study and 17 *E. coli* genomes with the same sequence type (ST2179) and harboring the $bla_{\mathrm{CTX-M-65}}$ gene, retrieved from EnteroBase (Zhou et al., 2020). The tree was visualized using FigTree version v1.4.3[7].

# RESULTS

## Characterization of Antimicrobial Resistance

From 49 isolates of *E. coli* phenotypically resistant to third-generation cephalosporins, a total of 10 different *bla* genes were identified in 42 ESBL and seven PMAβ producers: $bla_{\mathrm{CTX-M-1}}$ ($n = 8$), $bla_{\mathrm{CTX-M-15}}$ ($n = 5$), $bla_{\mathrm{CTX-M-27}}$ ($n = 2$), $bla_{\mathrm{CTX-M-55}}$ ($n = 1$), $bla_{\mathrm{CTX-M-9}}$ ($n = 1$), $bla_{\mathrm{CTX-M-14}}$ ($n = 7$), $bla_{\mathrm{CTX-M-32}}$ ($n = 9$), $bla_{\mathrm{CTX-M-65}}$ ($n = 4$), $bla_{\mathrm{SHV-12}}$ ($n = 5$), and $bla_{\mathrm{CMY-2}}$ ($n = 7$).

The $bla_{\mathrm{CTX-M-65}}$ gene was detected in four isolates (8.2%) recovered from beef (3/26) and pork (1/23) retail meat samples, and all exhibited a MDR phenotype, being resistant to ciprofloxacin, nalidixic acid, azithromycin, chloramphenicol, tetracycline, trimethoprim, and sulfamethoxazole. Resistance to colistin was observed in all, except isolate INIAV_ECX035 (**Table 1**).

[3]http://cge.cbs.dtu.dk/services/all.php

[4]http://www.ebi.ac.uk/ena

[5]http://www.bioinformatics.babraham.ac.uk/projects/fastqc

[6]http://jgi.doe.gov/data-and-tools/bb-tools/

[7]http://tree.bio.ed.ac.uk/software/figtree/

**TABLE 1 |** Results of the minimum inhibitory concentrations (μg/ml) obtained by antimicrobial susceptibility testing.

| Antibiotic | Breakpoints | INIAV_ECX016 | INIAV_ECX027 | INIAV_ECX035 | INIAV_ECX036 |
|---|---|---|---|---|---|
| Ampicillin | 8 | >64 | >64 | >64 | >64 |
| Cefepime | 0.125 | 4 | 2 | 4 | 8 |
| Cefotaxime | 0.25 | 64 | 64 | 64 | >64 |
| Cefoxitin | 8 | 8 | 8 | 8 | 8 |
| Ceftazidime | 0.5 | 1 | 1 | 32 | 2 |
| Ciprofloxacin | 0.064 | >8 | >8 | >8 | >8 |
| Nalidixic acid | 16 | >128 | >128 | >128 | >128 |
| Colistin | 2 | 4 | 4 | ≤1 | 4 |
| Ertapenem | 0.064 | ≤0.015 | ≤0.015 | ≤0.015 | ≤0.015 |
| Imipenem | 0.5 | 0.25 | 0.25 | 0.25 | 0.5 |
| Meropenem | 0.125 | ≤0.03 | ≤0.03 | ≤0.03 | ≤0.03 |
| Tetracycline | 8 | 64 | >64 | 64 | >64 |
| Sulfamethoxazole | 64 | >1,024 | >1,024 | >1,024 | >1,024 |
| Trimethoprim | 2 | >32 | >32 | >32 | >32 |
| Chloramphenicol | 16 | 128 | 128 | 128 | 128 |
| Gentamicin | 2 | 1 | 1 | 1 | 2 |
| Azithromycin | 16 | 32 | 32 | 64 | 64 |
| Tigecycline | 1 | 0.5 | 0.5 | 0.5 | 0.5 |
| Temocillin | 32 | 8 | 8 | 8 | 8 |
| Cefotaxime/clavulanic acid | 0.25 | ≤0.06 | ≤0.06 | 0.12 | 0.12 |
| Ceftazidime/clavulanic acid | 0.5 | ≤0.12 | 0.25 | ≤0.12 | 0.25 |

## Genome Analysis of the CTX-M-65 *E. coli* Producers

The assemblies of the reads originated between 70 and 120 contigs and a genome size of about 5 Gb. The genotypic traits of the four isolates, their resistome and mobilome, are summarized in **Table 2**. According to the ResFinder tool, three β-lactam-encoding genes were found in all isolates, namely, $bla_{CTX-M-65}$, $bla_{OXA-1}$, and $bla_{TEM-1B}$. Moreover, one isolate (INIAV_ECX035) also carried $bla_{SHV-12}$. The *mcr*-1.1 gene was identified in the three isolates resistant to colistin, and plasmid-mediated quinolone resistance (PMQR) genes, namely, *qnrS2* and *aac(6′)-Ib-cr*, were detected in all isolates. Additional genes conferring resistance to trimethoprim/sulfamethoxazole (*dfrA14* and *sul2*), tetracycline (*tetA*), and azithromycin (*mphA*) were also present. Point mutations were identified at the *gyrA* and *parC* subunits of DNA, namely, serine by lysine at position 83 (S83L) and serine by isoleucine at position 80 (S80I), respectively, conferring resistance to quinolones. Based on these results, the phenotype and genotype were in accordance.

According to the PlasmidFinder tool, IncFIC (FII) and IncFIB replicons were identified in all isolates, and p0111 was also predicted in one isolate (INIAV_ECX016). Isolate INIAV_ECX035 also harbored the IncI1-I plasmid, while the remaining isolates carried the IncI2 plasmid. All strains have identical profiles regarding MLST (ST2179), *fum*C65/*fim*H32 alleles, serotype (O9:H9), and phylogroup (B1). The somatic antigen of the INIAV_ECX036 isolate was not typable. VirulenceFinder predicted the presence of five virulence factors (*lpfA*, *iroN*, *iss*, *cma*, and *gad*) in all isolates except one (INIAV_ECX016), which carries four as *gad* is absent.

Using PLACNETw, a new assembly was generated from the raw reads, and a network was produced representing the contigs defined as belonging to the chromosome and plasmids, according to the reference genomes from the software database. The contigs were identified as belonging to plasmids based on the recognition of relaxase and/or replicon protein sequences. A manual pruning of the original network (**Figure 1A**) was performed according to Lanza et al. (2014) to reconstruct the graphical representation of the genome (**Figure 1B**). With the FASTA files obtained from this assembly, a new analysis with PlasmidFinder and ResFinder was performed to identify in which contigs were the antimicrobial resistance genes and plasmids located. Hereafter, it was possible to pinpoint the exact position of the resistance genes in the genome's graphical representation. Thus, based on the analysis of all isolates, the $bla_{CTX-M-65}$ gene, along with *flo*R and *mdf* A, was identified in contigs belonging to the chromosome, and the remaining resistance genes, including the other *bla* genes, were located in contigs belonging to plasmids (**Figure 1B**). In isolates INIAV_ECX016, INIAV_ECX027, and INIAV_ECX036, genes $bla_{CTX-M-65}$ and *flo*R were located in the same contig, and *mdf* A was in a different contig, while in isolate INIAV035, the three genes were in different contigs. Most resistance genes were located in IncFIC (FII) and IncFIB plasmids, except $bla_{SHV-12}$ and *mcr*1.1, which were carried in IncI-1 and IncI2, respectively.

The analysis of the genetic platform of the $bla_{CTX-M-65}$ genes using the EasyFig tool revealed that all isolates have the IS*903* (IS*5* family) and IS*Ecp1* (IS*1380* family) flanking the $bla_{CTX-M-65}$ gene, and all but one isolate also harbored the transposon TnAs3 (Tn3 family), IS*1006* (IS6 family) and IS*Vsa3* (IS*91* family). In this isolate (INIAV_ECX035), the contig starts

**TABLE 2 |** Genomic characterization of the four CTX-M-65-producing *E. coli* isolates by whole-genome sequencing.

| Features | | INIAV_ECX016 | INIAV_ECX027 | INIAV_ECX035 | INIAV_ECX036 |
|---|---|---|---|---|---|
| Antibiotic resistance determinants | Ampicillin, Cefepime, Cefotaxime, Cefoxitin, Ceftazidime | $bla_{CTX-M-65}$, $bla_{TEM-1B}$, $bla_{OXA-1}$ | $bla_{CTX-M-65}$, $bla_{TEM-1B}$, $bla_{OXA-1}$ | $bla_{CTX-M-65}$, $bla_{TEM-1B}$, $bla_{OXA-1}$, $bla_{SHV-12}$ | $bla_{CTX-M-65}$, $bla_{TEM-1B}$, $bla_{OXA-1}$ |
| | Ciprofloxacin, Nalidixic acid | *QnrS2*, *aac(6')Ib-cr*, *gyrA* S83L, *parC* S80I | *QnrS2*, *aac(6')Ib-cr*, *gyrA* S83L, *parC* S80I | *QnrS2*, *aac(6')Ib-cr*, *gyrA* S83L, *parC* S80I | *QnrS2*, *aac(6')Ib-cr*, *gyrA* S83L, *parC* S80I |
| | Colistin | *mcr*-1.1 | *mcr*-1.1 | – | *mcr*-1.1 |
| | Tetracycline | *tet(A)* | *tet(A)* | *tet(A)* | *tet(A)* |
| | Sulphamethoxazole | *sul2* | *sul2* | *sul2*, *sul1* | *sul2* |
| | Trimethoprim | *dfrA14* | *dfrA14* | *dfrA17* | *dfrA14* |
| | Chloramphenicol | *catB3*, *floR* | *catB3*, *floR* | *catB3*, *floR* | *catB3*, *floR* |
| | Azithromycin | *mph(A)* | *mph(A)* | *mph(A)* | *mph(A)* |
| | Rifampicin | *ARR-3* | *ARR-3* | *ARR-3* | *ARR-3* |
| | Aminoglycoside | *aph(3'')-Ib*, *aph(6)-Id* | *aph(3'')-Ib*, *aph(6)-Id* | *aadA5*, *aph(3'')-Ib*, *aph(6)-Id* | *aph(3'')-Ib*, *aph(6)-Id* |
| | Other | *mdf(A)* | *mdf(A)* | *mdf(A)* | *mdf(A)* |
| Plasmid replicons | | IncI2, pIncFIB, p0111, IncFIC | IncI2, pIncFIB, IncFIC | IncI1-I, IncFIB, IncFIC (FII) | IncI2, IncFIB, IncFIC(FII) |
| MLST | | ST2179 | ST2179 | ST2179 | ST2179 |
| Serotype | | O9:H9 | O9:H9 | O9:H9 | H9 |
| Virulence genes | | *lpfA*, *iroN*, *iss*, *cma* | *lpfA*, *iroN*, *iss*, *cma*, *gad* | *lpfA*, *iroN*, *iss*, *cma*, *gad* | *lpfA*, *iroN*, *iss*, *cma*, *gad* |
| *fum*C/*fim*H type | | *fum*C65/*fim*H32 | *fum*C65/*fim*H32 | *fum*C65/*fim*H32 | *fum*C65/*fim*H32 |
| Pathogenicity | | Yes (93.6%) | Yes (93.6%) | Yes (93.3%) | Yes (93.6%) |
| Phylogenetic group | | B1 | B1 | B1 | B1 |
| Sample source | | Bovine | Swine | Bovine | Bovine |
| No. of contigs | | 90 | 77 | 74 | 79 |
| Total length of genome (bp) | | 5,115,923 | 5,012,767 | 5,015,983 | 5,058,472 |
| N50 (bp) | | 140,276 | 142,205 | 282,032 | 232,144 |

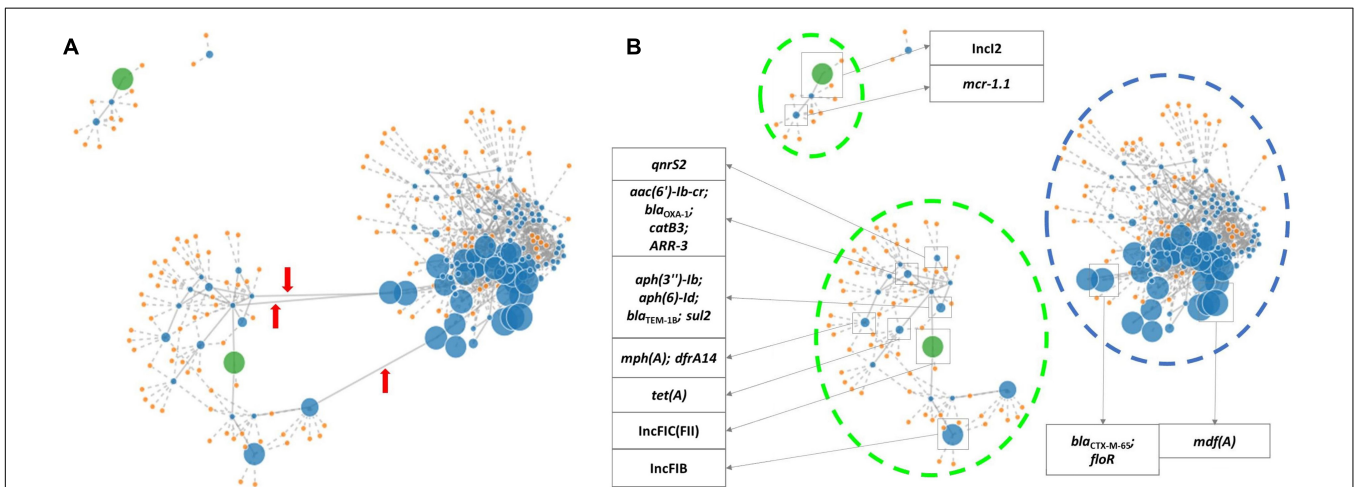


**FIGURE 1 |** PLACNETw (Plasmid Constellation Network) representation of the INIAV_ECX036 genome. **(A)** The original network. *Red arrows* indicate the contig linkages that were pruned. **(B)** The pruned network, where contigs containing the antimicrobial resistance genes and plasmids are identified according to ResFinder and PlasmidFinder. *Blue dots* indicate contigs (the dot size is proportional to the size of the contig); *orange dots* are the reference genomes from the tool database; *green dots* are contigs with relaxase and replicon protein of the plasmid; *blue broken lines* indicate contigs identified as chromosome; and *green broken lines* are contigs identified as plasmids.

in a different position, and its genetic platform seems to be not fully represented (**Figure 2A**). Consequently, the genetic platform is split and the downstream elements (TnAs3, IS*1006*, and IS*Vsa3*) are not represented in this contig, being in a different one. Looking at a larger region of the contigs (**Figure 2B**), it is possible to realize that all four contigs have high homology between each other. The alignment of each contig using EasyFig with the plasmid sequences identified by PlasmidFinder revealed

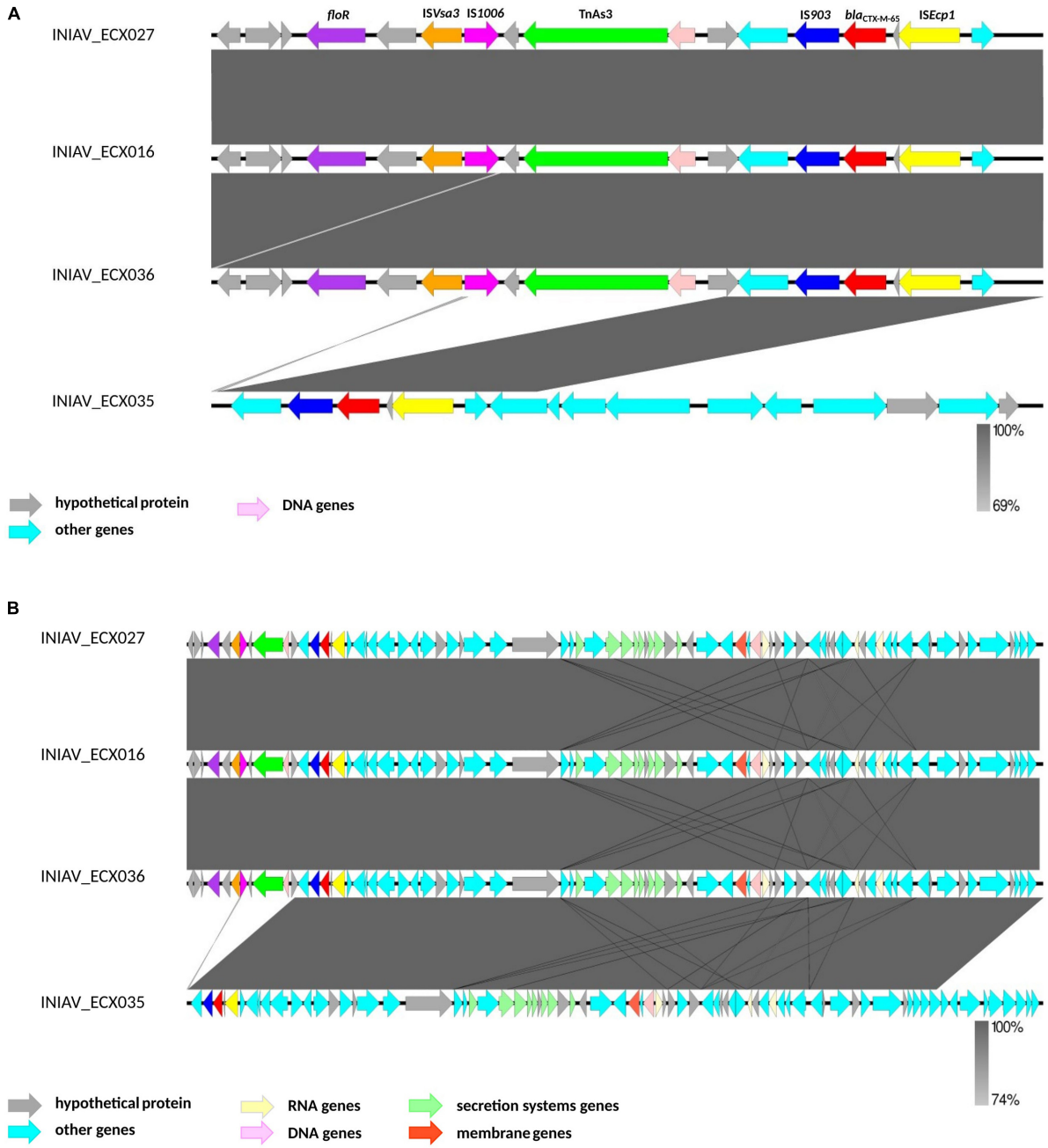


**FIGURE 2 |** Genetic platform of the $bla_{CTX-M-65}$ genes obtained by the analysis of the contigs containing the $bla_{CTX}$ gene using EasyFig. **(A)** A subregion of 17,000 bp of each contig to better identify the mobilization elements. **(B)** A subregion of 83,000 bp from the contigs.

no homology between those sequences. Comparison of the sizes of the contigs containing the $bla_{CTX-M-65}$ gene (ranging from 227,681 to 340,574 bp, except for the INIAV_ECX035 isolate with 82,631 bp in length) with the sizes of the plasmids identified in this study (ranging from 64,015 to 99,159 bp) revealed that the contigs are mostly wider than the plasmids. Furthermore, no plasmids were also identified, using the "mash screen" option of the PLSDB tool, in the contig's input sequence containing the $bla_{CTX-M-65}$ gene from each isolate.

An unrooted phylogenetic tree (radial cladogram option) using *E. coli* ATCC 25922 as the reference genome was constructed using 21 genomes from different geographic regions worldwide and isolated from multiple sources (**Figure 3**). Multiple phylogenetic groups can be distinguished in the tree: one group includes two strains, one from Nigeria and one from Colombia isolated from poultry and human samples; another phylogenetic group including European strains from the United Kingdom, Hungary, and Italy, isolated mainly

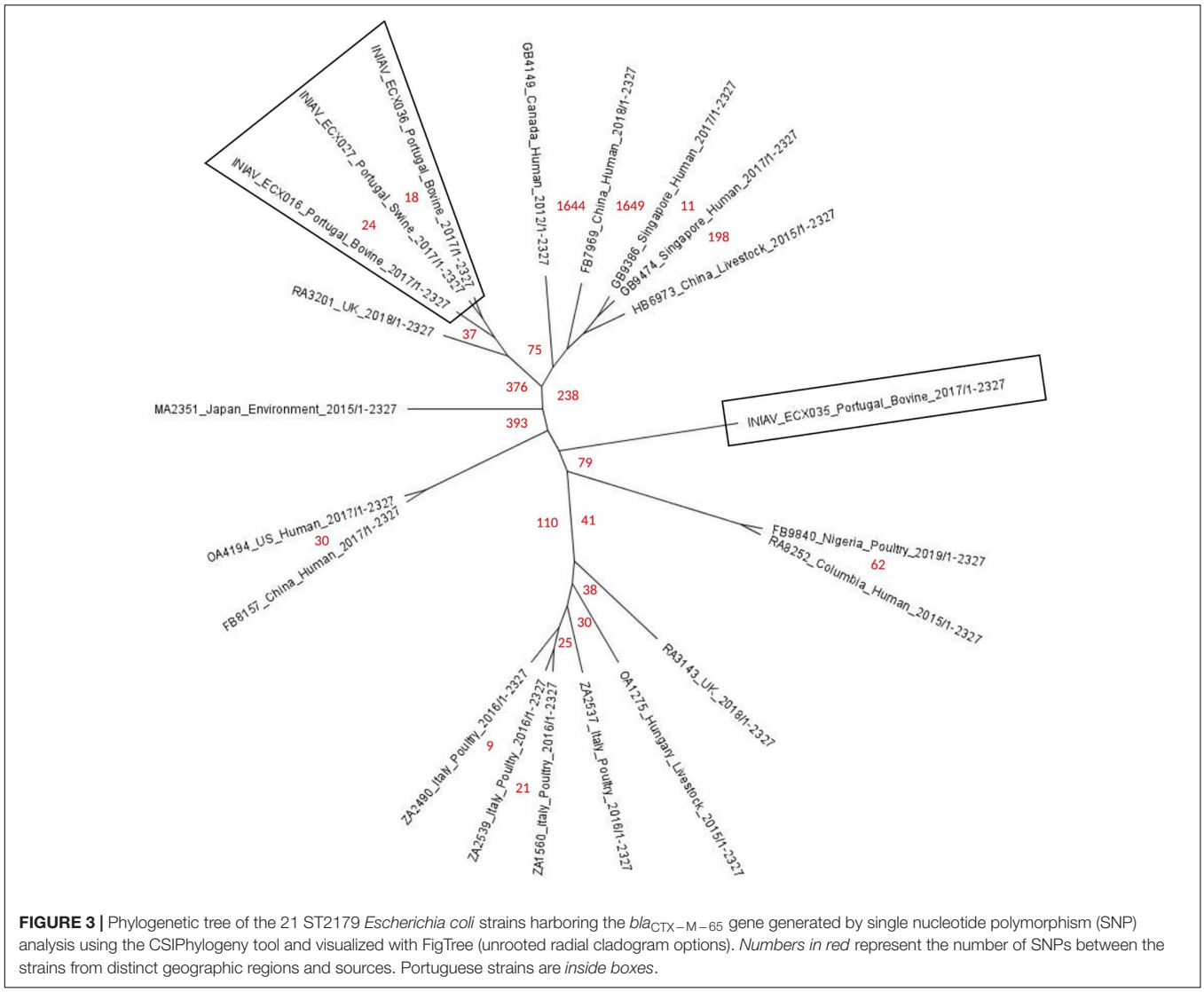


**FIGURE 3 |** Phylogenetic tree of the 21 ST2179 *Escherichia coli* strains harboring the $bla_{CTX-M-65}$ gene generated by single nucleotide polymorphism (SNP) analysis using the CSIPhylogeny tool and visualized with FigTree (unrooted radial cladogram options). *Numbers in red* represent the number of SNPs between the strains from distinct geographic regions and sources. Portuguese strains are *inside boxes*.

from poultry; other groups formed with one strain from the United States and one strain from China isolated from human samples; another group includes strains from China, Singapore, and Canada isolated from human and livestock samples; and two groups with only one strain each from Portugal and Japan isolated from bovine and environmental samples. All shared about 43,430 SNPs against the reference genome. The SNP analysis showed FB7969_China_Human_2018 as the strain having more SNPs, between 1,636 and 1,746. Most shared less than 112 SNPs with the four strains from this study, except for HB6973_China_Livestock_2015 and MA2351_Japan_Environment_2015 separated by between 219 and 394 SNPs. Three Portuguese strains were grouped with one strain from the UK (RA3201_UK_2018), separated by 37 and 45 SNPs. The fourth Portuguese strain (INIAV_ECX035) is separated from the remaining three from this study by 85 and 101 SNPs, being in a different phylogenetic group. The most closely related strains from this study are INIAV_ECX016 and INIAV_ECX036, sharing only 8 SNPs between each other; these two strains were obtained from beef samples collected from distinct geographic regions in Portugal.

## DISCUSSION

In this study, four CTX-M-65-producing *E. coli* were identified among 49 ESBL/PMAβ producers isolated from meat. Here, $bla_{CTX-M-65}$ is identified in Portugal for the first time in food of animal origin, with no reports linking to human infections; a complete characterization by WGS of the four MDR *E. coli* harboring this gene is described. *E. coli* harboring the $bla_{CTX-M-65}$ gene is commonly found in food-producing animals and meat from Southwest Asian and South American countries (Rao et al., 2014; Na et al., 2019; Vinueza-Burgos et al., 2019; Zurita et al., 2019). Although rarely occurring in Europe, previous studies have reported CTX-M-65-producing *E. coli* from Dutch beef calves (Ceccarelli et al., 2019) and wild birds from Switzerland (Zurfluh et al., 2019). In our study, three isolates were from beef and one from pork; therefore, we

cannot confirm the source of the CTX-M-65 *E. coli* detected in meat. There are several potential sources of bacteria in meat, including the animals from which the meat was derived, cross-contamination from other products, equipment and the environment, and the workers who are producing and handling the meat (EFSA and ECDC, 2019).

Based on PLACNETw, the $bla_{CTX-M-65}$ genes were located in contigs with homology to the chromosome. Moreover, the contigs containing this gene are wider than the plasmids identified in this study, and none of the four contigs showed homology to any sequence of the identified plasmids, reinforcing that the $bla_{CTX-M-65}$ gene is in the chromosome. The chromosomal location of $bla_{CTX-M}$ genes has already been reported, namely, $bla_{CTX-M-2}$ (Zhao and Hu, 2013; Ferreira et al., 2014), $bla_{CTX-M-14}$ and $bla_{CTX-M-15}$ (Hamamoto and Hirai, 2019), $bla_{CTX-M-55}$ (Zhang et al., 2019), and $bla_{CTX-M-65}$ (He et al., 2017).

The successful spread of ESBL enzymes is based on their ability to disseminate their resistance genes on mobile genetic elements to other bacteria, the skill to expand their spectrum of activity, and the acquisition of point mutations (Bush, 2018; Galal et al., 2018; Tooke et al., 2019). Nevertheless, the chromosomal location of the resistance genes can benefit the stable propagation of resistance, regardless of the bacterial host's habitat (Yoon et al., 2020). The genetic platform analysis revealed that all share an identical genetic environment with IS*903* and IS*Ecp1* flanking the $bla_{CTX-M-65}$ gene downstream and upstream, respectively. IS*Ecp1* is one of the most important insertion sequences associated with $bla_{CTX-M}$ genes (Canton et al., 2012; Zhao and Hu, 2013) and Tn3, a conjugative transposon. These mobile genetic elements found in the chromosome may promote excision and reintegration in a new chromosome or transference to other bacteria through a conjugative plasmid (Canton et al., 2012).

Particularly worrying is the co-occurrence of genes encoding resistance to other critically important antimicrobials, namely, fluoroquinolones, macrolides, and polymyxins, except for isolate INIAV_ECX035, which was susceptible to colistin. This isolate also carried the $bla_{SHV-12}$ gene, exhibiting a higher MIC to ceftazidime (MIC = 32 μg/ml) compared to the remaining isolates (MIC = 1–2 μg/ml), which is in accordance with the previously described (Maina et al., 2011).

Of note is that all isolates were resistant to azithromycin and harbored the *mph(A)* gene, confirming this gene's relevant role in macrolide susceptibility. As previously reported (Gomes et al., 2019), most of the *mph(A)*-carrying isolates show a MIC > 32 μg/L, as observed in our study, where the MIC values were between 32 and 64 μg/L. Moreover, other antimicrobial resistance genetic determinants were found in the isolates, including those also associated with resistance to antimicrobials frequently used in the rearing of food-producing animals, such as sulfamethoxazole (*sul1* and *sul2*), trimethoprim (*dfrA14* and *dfrA17*), phenicols (*catB3* and *floR*), tetracycline (*tetA*), and aminoglycosides [*aph*(3″)-Ib and *aph*(6)-Id] (ESVAC, 2020).

In all isolates, different replicon-typing plasmids were identified [IncFIC(FII) and IncFIB] carrying most of the resistance genes. IncF plasmids are frequently described from human and animal sources and are considered epidemic resistance plasmids, bearing the greatest variety of resistance genes in Enterobacteriaceae (Rozwandowicz et al., 2018). Although the precise gene location on plasmids was not determined in this study, based on PLACNETw, *mcr*-1.1 was located on IncI2 replicon-typing plasmid. IncI2 plasmids have been associated with the mobilization of *mcr* genes widely spread in Europe in *E. coli* isolates from animals and humans (Rozwandowicz et al., 2018; Migura-Garcia et al., 2020). The IncI-1 plasmid predominantly described in Europe was identified in the INIAV_ECX035 strain carrying $bla_{SHV-12}$, in accordance with previous reports (Rozwandowicz et al., 2018).

WGS analysis also revealed that all isolates belong to ST2179, phylogroup B1, and *fumC*65/*fimH*32 type, suggesting that all have a common clonal origin, with minor differences. Recently, *E. coli* ST2179 bearing the $bla_{CTX-M-65}$ gene but belonging to phylogroup A was reported from ducks in South Korea (Na et al., 2019). Isolates belonging to phylogroup B1 are commonly associated with non-pathogenic commensal *E. coli* reported from humans, animals, and food products (Bailey et al., 2010; Coura et al., 2015; Scheinberg et al., 2017; Belaynehe et al., 2018; Zurita et al., 2019).

The phylogenetic analysis revealed three isolates (INIAV_ECX016, INIAV_ECX027, and INIAV_ECX036) grouped in the same cluster, showing high genetic homology between each other. The UK strain (RA3201_UK_2018) was closely related to the Portuguese strains with 37–45 SNPs. The *in silico* analysis of the UK strain revealed the $bla_{CTX-M-65}$ gene to also be located in the chromosome. These findings suggest the clonal spread of CTX-M-65-producing *E. coli* isolates in Europe. INIAV_ECX035 is separated from INIAV_ECX027 by 101 SNPs and from the remaining two strains by 85 SNPs. Although from different animal species, the isolates from the same retail store (INIAV_ECX027 and INIAV_ECX036) are closely related, pointing out the hypothesis of cross-contamination. Moreover, the phylogenetic tree and the WGS analysis suggest that the four isolates belong to two sub-lineages, one composed of the three strains that grouped and the second with the fourth strain. INIAV_ECX035 showed some differences regarding the resistance genes and plasmids compared with the other three strains: the presence of the $bla_{SHV-12}$ gene conferring a higher resistance to ceftazidime and the absence of resistance to colistin, also the presence of the IncI1-I plasmid instead of the IncI2 plasmid carrying the *mcr*-1.1 gene. These genetic differences may justify the higher number of SNPs found and the existence of two evolutionary sub-lineages suggesting that the CTX-M-65 variant is emerging in our country.

The emergence and clonal spread of *E. coli* harboring $bla_{CTX-M-65}$ can be a problem for the livestock industry and human health, given their multidrug resistance profile to critically important antimicrobials and their presence in the food supply chain. To our knowledge, this is the first time that CTX-M-65 is identified in Portugal in food products of animal origin. The chromosomal addition of the $bla_{CTX-M-65}$ gene may ensure the spread of resistance in the absence of selective pressure. A better understanding of the factors that contribute to the emergence and dissemination of ESBL genes rarely seen

in Europe, but highly prevalent in Southwest Asian and South American countries, is strongly advisable and is worthy of close monitoring. Tourism and migration flow to Portugal and the trade treaties established between countries by importing meat and meat products may be sources of cross-contamination with uncommon MDR strains, facilitating their dissemination to the community.

## DATA AVAILABILITY STATEMENT

The datasets presented in this study can be found in online repositories. The names of the repository/repositories and accession number(s) can be found below. https://www.ebi.ac.uk/ERS3535656, ERS3535669, ERS5493675, and ERS5493676.

## AUTHOR CONTRIBUTIONS

CL contributed to the whole-genome sequencing (WGS) experiments, bioinformatics analysis, and interpretation of the data and wrote the manuscript. LM contributed to the laboratory experiments. AS, IH, and RH contributed to the WGS and bioinformatics analysis. LC and AA designed the study, interpreted the data, and reviewed and edited the manuscript. All authors read and approved the manuscript.

## FUNDING

This work was supported by the project PTDC/CVT-CVT/28469/2017 "CIAinVET—Food-producing animals as reservoirs of resistance to Critically Important Antibiotics" financed by the "Fundação para a Ciência e Tecnologia" (FCT), Portugal. CL was also funded by National Funds through FCT—Foundation for Science and Technology under the Project UIDB/05183/2020.

## ACKNOWLEDGMENTS

We are grateful to all staff involved in the sampling and laboratory work for their technical support.

## REFERENCES

Alcock, B. P., Raphenya, A. R., Lau, T. T. Y., Tsang, K. K., Bouchard, M., Edalatmand, A., et al. (2019). CARD 2020: antibiotic Resistome Surveillance with the Comprehensive Antibiotic Resistance Database. *Nucleic Acids Res.* 48, D517–D525. doi: 10.1093/nar/gkz935

Altschul, S. F., Gish, W., Miller, W., Myers, E. W., and Lipman, D. J. (1990). Basic local alignment search tool. *J. Mol. Biol.* 215, 403–410. doi: 10.1016/S0022-2836(05)80360-2

Bailey, J., Pinyon, J., Anantham, S., and Hall, R. (2010). Commensal *Escherichia coli* of healthy humans: a reservoir for antibiotic-resistance determinants. *J. Med. Microbiol.* 59, 1331–1339. doi: 10.1099/jmm.0.022475-0

Bartoloni, A., Pallecchi, L., Riccobono, E., Mantella, A., Magnelli, D., Di Maggio, T., et al. (2013). Relentless increase of resistance to fluoroquinolones and expanded-spectrum cephalosporins in *Escherichia coli*: 20 years of surveillance in resource-limited settings from Latin America. *Clin. Microbiol. Infect.* 19, 356–361. doi: 10.1111/j.1469-0691.2012.03807.x

Beghain, J., Bridier-Nahmias, A., Le Nagard, H., Denamur, E., and Clermont, O. (2018). Clermontyping: an easy-to-use and accurate in silico method for *Escherichia* genus strain phylotyping. *Microb. Genom.* 4:e000192. doi: 10.1099/mgen.0.000192

Belaynehe, K., Won Shin, S., and Sang Yoo, H. (2018). Interrelationship between tetracycline resistance determinants, phylogenetic group affiliation and carriage of class 1 integrons in commensal *Escherichia coli* isolates from cattle farms. *BMC Vet. Res.* 14:340. doi: 10.1186/s12917-018-1661-3

Blair, J. M., Webber, M. A., Baylay, A. J., Ogbolu, D. O., and Piddock, L. J. (2015). Molecular mechanisms of antibiotic resistance. *Nat. Rev. Microbiol.* 13, 42–51. doi: 10.1038/nrmicro3380

Bortolaia, V., Kaas, R. F., Ruppe, E., Roberts, M. C., Schwarz, S., Cattoir, V., et al. (2020). ResFinder 4.0 for predictions of phenotypes from genotypes. *J. Antimicrob. Chemother.* 75, 3491–3500. doi: 10.1093/jac/dkaa345

Bush, K. (2018). Past and present perspectives on β-lactamases. *Antimicrob. Agents Chemother.* 62, e01076–18. doi: 10.1128/AAC.01076-18

Camacho, C., Coulouris, G., Avagyan, V., Ma, N., Papadopoulos, J., Bealer, K., et al. (2009). BLAST+: architecture and applications. *BMC Bioinformatics* 10:421. doi: 10.1186/1471-2105-10-421

Canton, R., González-Alba, J. M., and Galán, J. C. (2012). CTX-M enzymes: origin and diffusion. *Front. Microbiol.* 3:110. doi: 10.3389/fmicb.2012.00110

Carattoli, A., Zankari, E., Garcia-Fernandez, A., Voldby, L. M., Lund, O., Villa, L., et al. (2014). PlasmidFinder and pMLST: in silico detection and typing of plasmids. *Antimicrob. Agents Chemother.* 58, 3895–3903. doi: 10.1128/AAC.02412-14

Carver, T., Harris, S. R., Berriman, M., Parkhill, J., and McQuillan, J. A. (2012). Artemis: an integrated platform for visualization and analysis of high-throughput sequence-based experimental data. *Bioinformatics* 28, 464–469. doi: 10.1093/bioinformatics/btr703

Ceccarelli, D., Kant, A., van Essen-Zandbergen, A., Dierikx, C., Hordijk, J., Wit, B., et al. (2019). Diversity of Plasmids and Genes Encoding Resistance to Extended Spectrum Cephalosporins in Commensal *Escherichia coli* From Dutch Livestock in 2007-2017. *Front. Microbiol.* 4:76. doi: 10.3389/fmicb.2019.00076

Clemente, L., Manageiro, V., Correia, I., Amaro, A., Albuquerque, T., Themudo, P., et al. (2019). Revealing mcr-1-positive ESBL-producing *Escherichia coli* strains among *Enterobacteriaceae* from food-producing animals (bovine, swine and poultry) and meat (bovine and swine), Portugal, 2010-2015. *Int. J. Food Microbiol.* 296, 37–42. doi: 10.1016/j.ijfoodmicro.2019.02.006

Clermont, O., Dixit, O. V. A., Vangchhia, B., Condamine, B., Dion, S., Bridier-Nahmias, A., et al. (2019). Characterization and rapid identification of phylogroup G in *Escherichia coli*, a lineage with high virulence and antibiotic resistance potential. *Environ. Microbiol.* 21, 3107–3117. doi: 10.11111/1462-2920.14713

Cosentino, S., Larsen, M. V., Aarestrup, F. M., and Lund, O. (2013). PathogenFinder - Distinguishing Friend from Foe Using Bacterial Whole Genome Sequence Data. *PLoS One* 8:e77302. doi: 10.1371/journal.pone.0077302

Coura, F., Diniz, S., Silva, M., Mussi, J., Barbosa, S., Lage, A., et al. (2015). Phylogenetic Group Determination of *Escherichia coli* Isolated from Animals Samples. *ScientificWorldJournal* 2015:258424. doi: 10.1155/2015/258424

Dallenne, C., Da Costa, A., Decré, D., Favier, C., and Arlet, G. (2010). Development of a set of multiplex PCR assays for the detection of genes encoding important β-lactamases in *Enterobacteriaceae*. *J. Antimicrob. Chemother.* 65, 490–495. doi: 10.1093/jac/dkp498

Doi, Y., Adams-Haduch, J. M., and Paterson, D. L. (2008). *Escherichia coli* isolate coproducing 16S rRNA Methylase and CTX-M-type extended-spectrum beta-lactamase isolated from an outpatient in the United States. *Antimicrob. Agents Chemother.* 52, 1204–1205. doi: 10.1128/AAC.01320-07

EFSA, and ECDC. (2019). The European Union summary report on antimicrobial resistance in zoonotic and indicator bacteria from humans, animals and food in 2017. *EFSA J.* 17:e05598. doi: 10.2903/j.efsa.2019.5598

ESVAC. (2020). *10th ESVAC Report Sales of veterinary antimicrobial agents in 31 European countries in 2018*. Amsterdam: European Medical Agency.

Ferreira, J. C., Penha Filho, R. A. C., Andrade, L. N., Berchieri, A., and Darini, A. L. C. (2014). Detection of chromosomal blaCTX-M-2 in diverse *Escherichia coli* isolates from healthy broiler chickens. *Clin. Microbiol. Infect.* 20, O623–O626. doi: 10.1111/1469-0691.12531

Franco, A., Leekitcharoenphon, P., Feltrin, F., Alba, P., Cordaro, G., Iurescia, M., et al. (2015). Emergence of a Clonal Lineage of Multidrug-Resistant ESBL-Producing *Salmonella* Infantis Transmitted from Broilers and Broiler Meat to Humans in Italy between 2011 and 2014. *PLoS One* 10:e0144802. doi: 10.1371/journal.pone.0144802

Furlan, J. P. R., Moura, Q., Gonzalez, I. H. L., Ramos, P. L., Lincopan, N., and Stehling, E. G. (2019). Draft genome sequence of a multidrug-resistant CTX-M-65-producing *Escherichia coli* ST156 colonizing a giant anteater (*Myrmecophaga tridactyla*) in a Zoo. *J. Glob. Antimicrob. Resist.* 17, 19–20. doi: 10.1016/j.jgar.2019.03.005

Galal, L., Abdel Aziz, N. A., and Hassan, W. M. (2018). Defining the relationship between phenotypic and genotypic resistance profiles of multidrug-resistant Enterobacterial clinical isolates. *Adv. Exp. Med. Biol.* 1214, 9–21. doi: 10.1007/5584_2018_208

Galata, V., Fehlmann, T., Backes, C., and Keller, A. (2018). PLSDB: a resource of complete bacterial plasmids. *Nucleic Acids Res.* 47, D195–D202. doi: 10.1093/nar/gky1050

Gomes, C., Ruiz-Roldán, L., Mateu, J., Ochoa, T., and Ruiz, J. (2019). Azithromycin resistance levels and mechanisms in *Escherichia coli*. *Sci. Rep.* 9:6089. doi: 10.1038/s41598-019-42423-3

Hamamoto, K., and Hirai, I. (2019). Characterization of chromosomally-located blaCTX-M and its surrounding sequence in CTX-M type extended-spectrum β-lactamase-producing *Escherichia coli* isolates. *J. Glob. Antimicrob. Resist.* 17, 53–57. doi: 10.1016/j.jgar.2018.11.006

He, D., Liu, L., Guo, B., Wu, S., Chen, X., Wang, J., et al. (2017). Chromosomal location of the fosA3 and blaCTX-M genes in *Proteus mirabilis* and clonal spread of *Escherichia coli* ST117 carrying fosA3-positive IncHI2/ST3 or F2:A-:B- plasmids in a chicken farm. *Int. J. Antimicrob. Agents* 49, 443–448. doi: 10.1016/j.ijantimicag.2016.12.009

Joensen, K. G., Scheutz, F., Lund, O., Hasman, H., Kaas, R. S., Nielsen, E. M., et al. (2014). Real-time whole-genome sequencing for routine typing, surveillance, and outbreak detection of verotoxigenic *Escherichia coli*. *J. Clin. Micobiol.* 52, 1501–1510. doi: 10.1128/JCM.03617-13

Joensen, K. G., Tetzschner, A. M., Iguchi, A., Aarestrup, F. M., and Scheutz, F. (2015). Rapid and easy in silico serotyping of *Escherichia coli* using whole genome sequencing (WGS) data. *J. Clin. Microbiol.* 53, 2410–2426. doi: 10.1128/JCM.00008-15

Kaas, R. S., Leekitcharoenphon, P., Aarestrup, F. M., and Lund, O. (2014). Solving the Problem of Comparing Whole Bacterial Genomes across Different Sequencing Platforms. *PLoS One* 9:e104984. doi: 10.1371/journal.pone.0104984

Lanza, V. F., Toro, M., Garcillán-Barcia, M. P., Mora, A., Blanco, J., Coque, T. M., et al. (2014). Plasmid Flux in *Escherichia coli* ST131 Sublineages, Analyzed by Plasmid Constellation Network (PLACNET), a New Method for Plasmid Reconstruction from Whole Genome Sequences. *PLoS Genet.* 10:e1004766. doi: 10.1371/journal.pgen.1004766

Larsen, M. V., Cosentino, S., Rasmussen, S., Friis, C., Hasman, H., Marvig, R. L., et al. (2012). Multilocus Sequence Typing of Total Genome Sequenced Bacteria. *J. Clin. Micobiol.* 50, 1355–1361. doi: 10.1128/jcm.06094-11

Maina, D., Revathi, G., Kariuki, S., and Ozwara, H. (2011). Genotypes and cephalosporin susceptibility in extended-spectrum β-lactamase producing *Enterobacteriaceae* in the community. *J. Infect. Dev. Ctries.* 6, 470–477. doi: 10.3855/jidc.1456

Migura-Garcia, M., González-López, J., Martinez-Urtaza, M., Aguirre Sánchez, J., Moreno-Mingorance, A., Perez de Rozas, A., et al. (2020). mcr-Colistin Resistance Genes Mobilized by IncX4, IncHI2, and IncI2 Plasmids in *Escherichia coli* of Pigs and White Stork in Spain. *Front. Microbiol.* 17:3072. doi: 10.3389/fmicb.2019.03072

Mikheenko, A., Prjibelski, A., Saveliev, V., Antipov, D., and Gurevich, A. (2018). Versatile genome assembly evaluation with QUAST-LG. *Bioinformatics* 34, i142–i150. doi: 10.1093/bioinformatics/bty266

Na, S., Moon, D., Choi, M., Oh, S., Jung, D., Sung, E., et al. (2019). Antimicrobial Resistance and Molecular Characterization of Extended-Spectrum β-Lactamase-Producing *Escherichia coli* Isolated from Ducks in South Korea. *Foodborne Pathog. Dis.* 16, 799–806. doi: 10.1089/fpd.2019.2644

Nurk, S., Bankevich, A., Antipov, D., Gurevich, A., Korobeynikov, A., Lapidus, A., et al. (2013). "Assembling genomes and mini-metagenomes from highly chimeric reads," in *Research in computational molecular biology*, eds M. Deng, R. Jiang, F. Sun, and X. Zhang (Berlin: Springer), 158–170. doi: 10.1007/978-3-642-37195-0_13

O'Neill, J. (2016). *Review on Antimicrobial Resistance. Tackling Drug-Resistant Infections Globally: Final report and Recommendations*. U.K.: Government of United Kingdom.

Palmeira, J. D., and Ferreira, H. M. N. (2020). Extended-spectrum beta-lactamase (ESBL)-producing *Enterobacteriaceae* in cattle production – a threat around the world. *Heliyon* 6:e03206. doi: 10.1016/j.heliyon.2020.e03206

Park, H., Kim, J., Ryu, S., and Jeon, B. (2019). The predominance of blaCTX-M-65 and blaCTX-M-55 in extended-spectrum β-lactamase-producing *Escherichia coli* from retail raw chicken in South korea. *J. Glob. Antimicrob. Resist.* 17, 216–220. doi: 10.1016/j.jgar.2019.01.005

Rao, L., Luchao, L., Zeng, Z., Chen, S., He, D., Chen, X., et al. (2014). Increasing prevalence of extended-spectrum cephalosporin-resistant *Escherichia coli* in food animals and the diversity of CTX-M genotypes during 2003-2012. *Vet. Microbiol.* 172, 534–541. doi: 10.1016/j.vetmic.2014.06.013

Rozwandowicz, M., Brouwer, M., Fischer, J., Wagenaar, J., Gonzalez-Zorn, B., Mevius, D., et al. (2018). Plasmids carrying antimicrobial resistance genes in *Enterobacteriaceae*. *J. Antimicrob. Chemother.* 73, 1121–1137. doi: 10.1093/jac/dkx488

Scheinberg, J., Dudley, E., Campbell, J., Roberts, B., Dimarzio, M., Debroy, C., et al. (2017). Prevalence and Phylogenetic Characterization of *Escherichia coli* and Hygiene Indicator Bacteria Isolated from Leafy Green Produce, Beef, and Pork Obtained from Farmers' *Markets in Pennsylvania*. *J. Food Prot.* 80, 237–244. doi: 10.4315/0362-028X.JFP-16-282

Seemann, T. (2014). Prokka: rapid prokaryotic genome annotation. *Bioinformatics* 30, 2068–2069. doi: 10.1093/bioinformatics/btu153

Silva, N., Carvalho, I., Currie, C., Sousa, M., Igrejas, G., and Poeta, P. (2019). "Extended-Spectrum-β-Lactamase and Carbapenemase-Producing *Enterobacteriaceae* in Food-Producing Animals in Europe," in *Antibiotic Drug Resistance, Chapter 12*, eds J. L. Capelo-Martínez and G. Igrejas (New Jerssey: John Wiley & Sons, Inc), 261–273. doi: 10.1002/9781119282549.ch12

Sullivan, M. J., Petty, N. K., and Beatson, S. A. (2011). Easyfig: a genome comparison visualizer. *Bioinformatics.* 27, 1009–1010. doi: 10.1093/bioinformatics/btr039

Tate, H., Folster, J. P., Hsu, C.-H., Chen, J., Hoffmann, M., Li, C., et al. (2017). Comparative analysis of extended-spectrum-β-lactamase CTX-M-65-producing *Salmonella enterica* serovar Infantis isolates from humans, food animals, and retail chickens in the United States. *Antimicrob. Agents Chemother.* 61, e00488–17. doi: 10.1128/AAC.00488-17

Tooke, C. L., Hinchliffe, P., Bragginton, E. C., Colenso, C. K., Hirvonen, V. H. A., Takebayashi, Y., et al. (2019). ß-Lactamases and ß-Lactamase Inhibitors in the 21st Century. *J. Mol. Biol.* 431, 3472–3500. doi: 10.1016/j.jmb.2019.04.002

Vielva, L., de Toro, M., Lanza, V. F., and de La Cruz, F. (2017). PLACNETw: a web-based tool for plasmid reconstruction from bacterial genomes. *Bioinformatics* 33, 3796–3798. doi: 10.1093/bioinformatics/btx462

Vinueza-Burgos, C., Ortega-Paredes, D., Narváez, C., and Zurita, J. (2019). Characterization of cefotaxime resistant *Escherichia coli* isolated from broiler farms in Ecuador. *PLos One* 14:e0207567. doi: 10.1371/journal.pone.0207567

Wang, W., Zhao, L., Hu, Y., Dottorini, T., Fanning, S., Xu, J., et al. (2020). Epidemiological Study on Prevalence, Serovar Diversity, Multidrug Resistance, and CTX-M-Type Extended-Spectrum beta-Lactamases of *Salmonella* spp. from Patients with Diarrhea, Food of Animal Origin, and Pets in Several Provinces of China. *Antimicrob. Agents Chemother.* 64, e00092–20. doi: 10.1128/AAC.00092-20

Yoon, E.-J., Gwon, B., Liu, C., Kim, D., Won, D., Park, S. G., et al. (2020). Beneficial Chromosomal Integration of the Genes for CTX-M Extended-Spectrum β-Lactamase in *Klebsiella pneumoniae* for Stable Propagation. *mSystems* 5, e00459–20. doi: 10.1128/mSystems.00459-20

Zankari, E., Hasman, H., Cosentino, S., Vestergaard, M., Rasmussen, S., Lund, O., et al. (2012). Identification of acquired antimicrobial resistance genes. *J. Antimicrob. Chemother.* 67, 2640–2644. doi: 10.1093/jac/dks261

Zhan, L., Wang, S., Guo, Y., Jin, Y., Duan, J., Hao, Z., et al. (2017). Outbreak by Hypermucoviscous *Klebsiella pneumoniae* ST11 Isolates with Carbapenem

Resistance in a Tertiary Hospital in China. *Front. Cell. Infect. Microbiol.* 7:182. doi: 10.3389/fcimb.2017.00182

Zhang, C.-Z., Ding, X.-M., Lin, X.-L., Sun, R.-Y., Lu, Y.-W., Cai, R.-M., et al. (2019). The Emergence of Chromosomally Located blaCTX-M-55 in *Salmonella* From Foodborne Animals in China. *Front. Microbiol.* 10:1268. doi: 10.3389/fmicb.2019.01268

Zhao, W. H., and Hu, Z. Q. (2013). Epidemiology and genetics of CTX-M extended-spectrum β-lactamases in Gram-negative bacteria. *Crit. Rev. Microbiol.* 39, 79–101. doi: 10.3109/1040841X.2012.691460

Zheng, H., Zeng, Z., Chen, S., Liu, Y., Yao, Q., Deng, Y., et al. (2012). Prevalence and characterisation of CTX-M β-lactamases amongst *Escherichia coli* isolates from healthy food animals in China. *Int J Antimicrob Agents* 39, 305–310. doi: 10.1016/j.ijantimicag.2011.12.001

Zhou, Z., Alikhan, N. F., Mohamed, K., Agama Study Group, and Achtman, M. (2020). The EnteroBase user's guide, with case studies on *Salmonella* transmissions, Yersinia pestis phylogeny and *Escherichia* core genomic diversity. *Genome Res.* 30, 138–152. doi: 10.1101/gr.251678.119

Zurfluh, K., Albini, S., Mattmann, P., Kindle, P., Nüesch-Inderbinen, M., Stephan, R., et al. (2019). Antimicrobial resistant and extended-spectrum β-lactamase producing *Escherichia coli* in common wild bird species in Switzerland. *Microbiolopen* 8:e845. doi: 10.1002/mbo3.84

Zurita, J., Anez, F., Sevillano, G., Ortega-Paredes, D., and Paz, A. (2019). Ready-to-eat street food: a potential source for dissemination of multidrug-resistant *Escherichia coli* epidemic clones in Quito. *Ecuador. Lett. Appl. Microbiol.* 70, 203–209. doi: 10.1111/lam.13263

**Conflict of Interest:** The authors declare that the research was conducted in the absence of any commercial or financial relationships that could be construed as a potential conflict of interest.

frontiers in Microbiology

ORIGINAL RESEARCH
published: 05 October 2021
doi: 10.3389/fmicb.2021.720449

# Genomic Analysis of Ciprofloxacin-Resistant *Salmonella enterica* Serovar Kentucky ST198 From Spanish Hospitals

*Xenia Vázquez[1,2], Javier Fernández[2,3,4], Margarita Bances[5], Pilar Lumbreras[2], Miriam Alkorta[6], Silvia Hernáez[7], Elizabeth Prieto[8], Pedro de la Iglesia[9], María de Toro[10], M. Rosario Rodicio[1,2*†] and Rosaura Rodicio[2,11*†]*

[1] Área de Microbiología, Departamento de Biología Funcional, Universidad de Oviedo (UO), Oviedo, Spain, [2] Instituto de Investigación Sanitaria del Principado de Asturias (ISPA), Oviedo, Spain, [3] Servicio de Microbiología, Hospital Universitario Central de Asturias (HUCA), Oviedo, Spain, [4] Research and Innovation, Artificial Intelligence and Statistical Department, Pragmatech AI Solutions, Oviedo, Spain, [5] Laboratorio de Salud Pública (LSP) del Principado de Asturias, Dirección General de Salud Pública, Oviedo, Spain, [6] Servicio de Microbiología, Hospital Universitario Donostia (HUD)-IIS Biodonostia, San Sebastián, Spain, [7] Servicio de Microbiología, Hospital Universitario de Álava (HUA), Vitoria-Gasteiz, Spain, [8] Servicio de Microbiología, Hospital Universitario San Agustín, Avilés, Spain, [9] Servicio de Microbiología, Hospital Universitario de Cabueñes, Gijón, Spain, [10] Plataforma de Genómica y Bioinformática, Centro de Investigación Biomédica de La Rioja (CIBIR), Logroño, Spain, [11] Departamento de Bioquímica y Biología Molecular, Universidad de Oviedo (UO), Oviedo, Spain

OPEN ACCESS

**Edited by:**
*Ravi Kant, University of Helsinki, Finland*

**Reviewed by:**
*Dhiraj Kumar Chaudhary, Korea University, South Korea*
*Leili Shokoohizadeh, Hamadan University of Medical Sciences, Iran*

***Correspondence:**
*Rosaura Rodicio*
*mrosaura@uniovi.es*
*M. Rosario Rodicio*
*rrodicio@uniovi.es*

*† These authors have contributed equally to this work and share senior authorship*

**Specialty section:**
*This article was submitted to Antimicrobials, Resistance and Chemotherapy, a section of the journal Frontiers in Microbiology*

**Received:** *04 June 2021*
**Accepted:** *13 September 2021*
**Published:** *05 October 2021*

**Citation:**
*Vázquez X, Fernández J, Bances M, Lumbreras P, Alkorta M, Hernáez S, Prieto E, de la Iglesia P, de Toro M, Rodicio MR and Rodicio R (2021) Genomic Analysis of Ciprofloxacin-Resistant Salmonella enterica Serovar Kentucky ST198 From Spanish Hospitals. Front. Microbiol. 12:720449. doi: 10.3389/fmicb.2021.720449*

*Salmonella enterica* serovar Kentucky (*S*. Kentucky) with sequence type (ST) 198 and highly resistant to ciprofloxacin (ST198-Cip$^R$) has emerged as a global MDR clone, posing a threat to public health. In the present study, whole genome sequencing (WGS) was applied to characterize all Cip$^R$ *S.* Kentucky detected in five Spanish hospitals during 2009–2018. All Cip$^R$ isolates ($n$ = 13) were ST198 and carried point mutations in the quinolone resistance-determining regions (QRDRs) of both *gyrA* (resulting in Ser83Phe and Asp87Gly, Asp87Asn, or Asp87Tyr substitutions in GyrA) and *parC* (with Thr57Ser and Ser80Ile substitutions in ParC). Resistances to other antibiotics (ampicillin, chloramphenicol, gentamicin, streptomycin, sulfonamides, and tetracycline), mediated by the $bla_{TEM-1B}$, *catA1, aacA5*, *aadA7, strA*, *strB*, *sul1*, and *tet*(A) genes, and arranged in different combinations, were also observed. Analysis of the genetic environment of the latter resistance genes revealed the presence of multiple variants of SGI1 (*Salmonella* genomic island 1)-K and SGI1-P, where all these resistance genes except *catA1* were placed. IS*26* elements, found at multiple locations within the SGI1 variants, have probably played a crucial role in their generation. Despite the wide diversity of SGI1-K- and SGI1-P-like structures, phylogenetic analysis revealed a close relationship between isolates from different hospitals, which were separated by a minimum of two and a maximum of 160 single nucleotide polymorphisms. Considering that *S. enterica* isolates resistant to fluoroquinolones belong to the high priority list of antibiotic-resistant bacteria compiled by the World Health Organization, continuous surveillance of the *S*. Kentucky ST198-CIP$^R$ clone is required.

**Keywords: *Salmonella enterica* serovar Kentucky, ST198, SGI1-K, IS*26*, fluoroquinolone resistance, multidrug resistance, whole genome sequencing, phylogenetic analysis**

## INTRODUCTION

*Salmonella enterica* is one of the major causes of bacterial gastrointestinal infections in humans, worldwide, with estimates of 93.8 million cases each year and 155,000 deaths (Majowicz et al., 2010). In the European Union (EU), after a long period of declining trend, the number of cases of human salmonellosis has stabilized over the past 5 years (European Food Safety Authority [EFSA] and European Centre for Disease Prevention and Control [ECDC], 2021). Along this period, salmonellosis remained the second most frequent food-borne zoonosis (only preceded by campylobacteriosis), with a total of 87,923 confirmed cases and a notification rate of 20.0 cases per 100,000 inhabitants reported in 2019 (European Food Safety Authority [EFSA] and European Centre for Disease Prevention and Control [ECDC], 2021). In Spain, from 2015 to 2018, the number of confirmed cases of human salmonellosis ranged between 8,730 (2018) and 9,818 (2016), while neither the complete data for 2019 nor the rate per 100,000 inhabitants are available (European Food Safety Authority [EFSA] and European Centre for Disease Prevention and Control [ECDC], 2021).

Human salmonellosis is usually a self-limiting infection that remains confined to the intestine and resolves in about one week, even in the absence of antimicrobial treatment. Nevertheless, invasive, severe infections may occur in immunocompromised patients, as well as in small children and the elderly, in which case the treatment may become life-saving. The high rate of resistance against traditional antimicrobials has prompted the use of newer broad-spectrum drugs, like third generation cephalosporins and fluoroquinolones (Hohmann, 2001), which are recommended by therapeutic international and national (including Spanish) guidelines as first choices for *Salmonella* severe infections (Gilbert et al., 2021; Mensa and Soriano, 2021). These compounds are listed by the World Health Organization (WHO) as "critically important antimicrobials" with the highest priority for human medicine (World Health Organization [WHO], 2016). Fortunately, resistance to cephalosporins remains low in *Salmonella* isolates recovered from humans (1.5 and 1.2% for cefotaxime and ceftazidime, respectively), food-animals and foods in the EU (European Food Safety Authority [EFSA] and European Centre for Disease Prevention and Control [ECDC], 2020). However, the proportion of human isolates resistant to ciprofloxacin, a second generation (2a) fluoroquinolone (Pham et al., 2019), was of 12.5% on average, with extremely high levels reported for certain serovars, particularly in *S. enterica* serovar (*S.* Kentucky; 85.7%) (European Food Safety Authority [EFSA] and European Centre for Disease Prevention and Control [ECDC], 2020). In *S.* Kentucky, resistance to ampicillin, sulfonamides, tetracyclines (also common in other *S. enterica* serovars) and gentamicin (infrequently found in *Salmonella*) are very high as well, leading to multidrug resistance (MDR).

The high frequency of MDR in *S.* Kentucky has been associated with the expansion of a single clone with sequence type (ST) 198 and belonging to *Xba*I-pulsed field gel electrophoresis cluster X1 (Weill et al., 2006; Le Hello et al., 2011, 2013a; Hawkey et al., 2019). Phylogenomic analysis indicated that this clone emerged in Egypt around 1989, linked to the acquisition of a variant of *Salmonella* genomic island 1 (SGI1-K), conferring resistance to multiple antibiotics, such as ampicillin, streptomycin, gentamicin, sulfonamides, and tetracycline (Le Hello et al., 2013a; Hawkey et al., 2019). The SGI1-K prototype (48.7 Kb) consists of a 27 kb backbone and a complex resistance region encompassing a In*4*-type integron, parts of the Tn*21*, Tn*1721*, Tn*5393*, and Tn*2* transposons, and two copies of IS*26* flanking the defective Tn*2* in opposite orientation (Hamidian et al., 2015). SGI1-K is inserted within the *S.* Kentucky chromosome, between the *trmE* (*thdF*) and *yidY* genes, with the resistance region flanked by *resG* and Δ*S044* pertaining to the island backbone (Hamidian et al., 2015). Multiple variants of SGI1-K have previously been reported, including the highly degenerated SGI1-P and SGI1-Q structures, which confer only resistance to ampicillin or lack antibiotic resistance genes, respectively (Doublet et al., 2008; Le Hello et al., 2011; Hawkey et al., 2019).

After acquisition of SGI1-K by *S.* Kentucky, the already MDR clone accumulated various mutations in the quinolone-resistance-determining regions (QRDRs) of genes encoding subunits of the target DNA gyrase (*gyrA*) and DNA topoisomerase IV (*parC*) (Le Hello et al., 2013b), which combined are responsible for resistance to ciprofloxacin. The Ser83Phe substitution in GyrA, which by itself confers resistance to nalidixic acid (Hamidian et al., 2015), was the first to occur, followed in time by the Ser80Ile substitution in ParC which, together with the former, increased the minimum inhibitory concentration (MIC) of ciprofloxacin. Nonetheless, high-level resistance only emerged after the advent of additional mutations in *gyrA*-87, and this was accompanied by clonal expansion of *S.* Kentucky ST198-Cip$^R$, and its subsequent spread from Egypt to many other geographical regions, including Europe (Le Hello et al., 2011; Hawkey et al., 2019). A second mutation found in the *parC* gene (Thr57Ser) has also been reported in *S.* Kentucky ST198 detected in French travelers returning from Africa, in a human patient in United States, as well as in retail chicken carcasses from Egypt (Weill et al., 2006; Ramadan et al., 2018; Shah et al., 2018). Such change, however, does not appear to be associated with quinolone resistance, as it was also identified in isolates susceptible to nalidixic acid (Weill et al., 2006). Although alterations in the target topoisomerases are the main cause of ciprofloxacin resistance in *S.* Kentucky, the involvement of the major multidrug AcrAB-TolC efflux pump, and of mutations affecting the *rpoB* gene coding for the β-subunit of the enzyme RNA polymerase, have also been reported (Weill et al., 2006; Baucheron et al., 2013; Brandis et al., 2021). Many other efflux pumps were identified in *S. enterica* (Li et al., 2018), but their contribution to high level CIP$^R$ in *S.* Kentucky has yet to be demonstrated.

Taking into account (i) that *S. enterica* resistant to fluoroquinolones is amongst the high priority pathogens listed by WHO (Tacconelli et al., 2018), (ii) that *S.* Kentucky ST198-Cip$^R$ represents an emerging threat to food safety and public health, and (iii) that ciprofloxacin is a treatment of choice for severe infections caused by *S. enterica* in adults, the present study applied whole genome sequence analyses to thoroughly characterize and compare ciprofloxacin resistant isolates of

this serovar, which were recovered in recent years at different hospitals located in Northern Spain. Particular attention was paid to the genetic environment of their antimicrobial resistance genes, and the mobile genetic elements associated with them.

# MATERIALS AND METHODS

## Bacterial Isolates and Antimicrobial Susceptibility Testing

A total of 13 isolates of *S.* Kentucky resistant to ciprofloxacin were analyzed. They were recovered between 2009 and 2018 from fecal samples of patients with gastroenteritis, attended at five Spanish hospitals or primary care centers associated with them (**Table 1**). Stool samples were cultured using selective media, such as selenite broth and Hecktoen agar (bioMerieux, Marcy l'Etoile, France), and subsequently identified by MALDI-TOF (Bruker Daltonics, Billerica, MA). Experimental serotyping of the isolates was performed either at the Spanish National Center of Microbiology (Madrid) or directly at the hospital. Susceptibility to antimicrobial agents was determined by automated MicroScan NC 53 (Beckman Coulter, Brea, CA, United States), and complemented with disk diffusion assays using Mueller-Hinton agar and commercially available discs (Oxoid, Madrid, Spain). Results were interpreted according to the Clinical and Laboratory Standards Institute Guidelines (Clinical and Laboratory Standards Institute [CLSI], 2019). MICs to ciprofloxacin were determined by Etest (bioMérieux, Marcy l'Étoile, France).

## Whole Genome Sequencing and Bioinformatics Analysis

WGS of the isolates was determined by Illumina either at the sequencing facility of the "Centro de Investigación Biomédica," La Rioja (CIBIR), Spain or Eurofins Genomics (Ebersberg, Germany). Total DNA was extracted from overnight cultures grown in Luria-Bertani (LB) broth, using the GenElute™ Bacterial Genomic DNA Kit (Sigma-Aldrich; Merck Life Science, Madrid, Spain), according to the manufacturer's instructions. Paired-end reads of 100 or 150 nt were sequenced with a HiSeq 2500 or a NovaSeq 6000 S2 PE150 XP, in the case of CIBIR and Eurofins, respectively. Reads were assembled with the VelvetOptimiser.pl script implemented in the "on line" version of PLACNET,[1] which also served for plasmid reconstruction (Vielva et al., 2017). The quality of the assemblies was evaluated with QUAST (Quality Assessment Tool for Genome Assemblies; Gurevich et al., 2013), and the output information is compiled in **Supplementary Table 1**. The genomes were deposited in GenBank under accession numbers provided in the same table and also below, and annotated by the NCBI Prokaryotic Genome Annotation Pipeline (PGAP[2]). Several tools from the Center for Genomic Epidemiology (CGE) of the Technical University of Denmark (DTU), such as MLST, ResFinder, PlasmidFinder, and pMLST, were used for bioinformatic analysis.[3] ResFinder detects chromosomal mutations that mediate antimicrobial resistance (such as mutations in *gyrA*, *gyrB*, *parC,* and *parE* genes involved in quinolone resistance), and identifies acquired genes [including plasmid-mediated quinolone resistance (PMQR) genes, such as *qnr*, *qepA*, *oqxAB,* and *aac(6′)-Ib-cr*], in bacterial genome sequences. After annotation of the genomes, analysis of relevant regions, including SGI1-K-related DNA, DNA encoding efflux pumps and their regulatory proteins (*acrAB*, *acrA*, *acrD*, *acrEF*, *acrR*, *acrS*, *ramR*, *ramA*, *soxR*, *sosS*, *marC*, *marRAB,* and *rob*) and of the *rpoB* gene, was performed with the aid of BLASTn, CLONE Manager (CloneSuit9), and MyDbFinder (CGE, DTU). For the latter, a database comprising all open reading frames from SGI1-K and flanking *orfs* (based on accession number AY463797), was specifically built for this study. The presence and orientation of more than one copy of IS*26* was used as an initial reference for the assembly of contigs belonging to the island in each genome. PCR amplification with the primers compiled in **Supplementary Table 2**, followed by Sanger sequencing of the obtained amplicons (carry out at STAB VIDA, Caparica, Portugal), were performed when required to reconstruct the intact islands.

## Phylogenetic Analysis

The relationship between the *S.* Kentucky isolates from Spanish hospitals was inferred using the CSI phylogeny tool (version 1.4), available at the CGE website (Kaas et al., 2014). The pipeline was run with default parameters, using the genome of *S.* Kentucky strain 201001922 (accession number CP028357) as reference for SNP calling. Additional genomes of *S.* Kentucky ST198 (see **Supplementary Table 3** for accession numbers), were also included in the analysis, and the resulting SNP matrix is shown in **Supplementary Table 4**. Bootstrap support for the consensus tree relied on 1,000 replicates (Felsenstein, 1985).

## Ethics Approval Statement

This study was approved by the Research Ethics Committee of the Principality of Asturias (Code CEImPA 2020.446).

# RESULTS

## General Properties of the Isolates

All isolates in this study ($n$ = 13) derived from human clinical samples analyzed at five hospitals in Northern Spain (**Table 1**). They were identified as *S.* Kentucky and selected on the basis of MIC values to ciprofloxacin >2 μg/ml. The assembly size of the sequenced genomes ranged from 4.785 Mb (HUD 1/14) to 4.857 Mb (HUA 10/18), and MLST performed *in silico* assigned all isolates to ST198. Plasmids were found in nine of them, in numbers ranging from one (LSP 213/09 and HUD 1/13) up to six (HUA 10/18). A plasmid of 85.3 kb, carried by the latter isolate, belonged to incompatibility group IncI. All other plasmids were smaller than 10.5 kb, and belonged to ColpVC, ColE, Col156, or had an unidentified replicon.

[1] https://castillo.dicom.unican.es/upload/

[2] https://www.ncbi.nlm.nih.gov/genome/annotation_prok/

[3] https://cge.cbs.dtu.dk/services/

**TABLE 1 |** Origin and resistance properties of *Salmonella enterica* serovar Kentucky ST198 isolates from Spanish hospitals.

| Isolate[a] | Travel history[b] | Resistance phenotype[c] | SGI1-K (SGI1-P) genes<br>Other genes | CIP MIC (μg/mL) | Amino acid substitutions | | Plasmid Inc (size in bp)[d] |
|---|---|---|---|---|---|---|---|
| | | | | | GyrA | ParC | |
| LSP 213/09 | na | CHL, TET, NAL, CIP | ***tet*(A),**<br>*catA1*, *aac(6′)-Iaa* | 8 | Ser83Phe<br>Asp87Gly | Thr57Ser<br>Ser80Ile | ColpVC (4,110) |
| LSP 150/10 | Morocco | AMP, GEN, STR, SUL, TET, NAL, CIP | ***bla*$_{TEM-1B}$, *aacA5*, *aadA7*, *sul1*, *tet*(A)**,<br>aac(6′)-Iaa | 12 | Ser83Phe<br>Asp87Asn | Thr57Ser<br>Ser80Ile | ColE (5,058); Col156 (5,769); nid (10,524) |
| LSP 105/15 | na | AMP, NAL, CIP | ***bla*$_{TEM-1B}$**,<br>*aac(6′)-Iaa* | 16 | Ser83Phe<br>Asp87Asn | Thr57Ser<br>Ser80Ile | nd |
| LSP 235/17 | na | TET, NAL, CIP | ***tet*(A),**<br>*aac(6′)-Iaa* | >32 | Ser83Phe<br>Asp87Asn | Thr57Ser<br>Ser80Ile | nid (3,893; 4,631) |
| LSP 314/17 | Bali | AMP, GEN, STR, SUL, TET, NAL, CIP | ***bla*$_{TEM-1B}$, *aacA5*, aadA7, *strA*, *strB*, *sul1*, *tet*(A)**,<br>*aac(6′)-Iaa* | 12 | Ser83Phe<br>Asp87Asn | Thr57Ser<br>Ser80Ile | nd |
| HUD 1/09 | Tanzania | GEN, STR, SUL, TET, NAL, CIP | ***aacA5*, *aadA7*, *strB*, *sul1*, *tet*(A)**,<br>*aac(6)-Iaa* | 6 | Ser83Phe<br>Asp87Tyr | Thr57Ser<br>Ser80Ile | nd |
| HUD 2/09 | South Africa | AMP, GEN, STR, SUL, TET, NAL, CIP | ***bla*$_{TEM-1B}$, *aacA5*, *aadA7*, *strB*, *sul1*, tet(A)**,<br>aac(6)-Iaa | 8 | Ser83Phe<br>Asp87Tyr | Thr57Ser<br>Ser80Ile | nd |
| HUD 1/13 | nth | AMP, NAL, CIP | ***bla*$_{TEM-1B}$**,<br>*aac(6)-Iaa* | 8 | Ser83Phe<br>Asp87Asn | Thr57Ser<br>Ser80Ile | nid (1,145) |
| HUD 1/14 | nth | AMP, GEN, STR, SUL, TET, NAL, CIP | ***bla*$_{TEM-1B}$, *aacA5, aadA7*, *sul1*, *tet*(A)**,<br>*aac(6)-Iaa* | 12 | Ser83Phe<br>Asp87Asn | Thr57Ser<br>Ser80Ile | ColE (4,132); nid (3,372; 4,010) |
| HUD 1/15 | nth | AMP, GEN, STR, SUL, TET, NAL, CIP | ***bla*$_{TEM-1B}$, *aacA5, aadA7, sul1,* *tet*(A)**,<br>*aac(6)-Iaa* | 12 | Ser83Phe<br>Asp87Asn | Thr57Ser<br>Ser80Ile | ColE (2,504); nid (3,371; 3,904; 4,179) |
| HUD 1/17 | Morocco | TET, NAL, CIP | ***tet*(A),**<br>*aac(6)-Iaa* | 8 | Ser83Phe<br>Asp87Asn | Thr57Ser<br>Ser80Ile | ColE (2,448); nid (4,110) |
| HUA 3/18 | Morocco | AMP, GEN, STR, SUL, TET, NAL, CIP | ***bla*$_{TEM-1B}$, *aacA5*, *aadA7*, *sul1*, *tet*(A)**,<br>*aac(6)-Iaa* | 12 | Ser83Phe<br>Asp87Asn | Thr57Ser<br>Ser80Ile | ColE (4,020); nid (2,117; 3,985) |
| HUA 10/18 | nth | SUL, TET, NAL, CIP | ***sul1*, *tet*(A)**,<br>*aac(6)-Iaa* | 8 | Ser83Phe<br>Asp87Asn | Thr57Ser<br>Ser80Ile | IncI1 (85,307); ColE (4,105); nid (2,185; 3,985; 4,164; 5,413) |

[a] *Isolates are designated with the initials of the center which supplied them, followed by a serial number/last two numbers of the year of recovery. LSP, Laboratory of Public Health of the Principality of Asturias, acting as regional reference center for Salmonella. LSP isolates come from "Hospital Universitario Central de Asturias," Oviedo, Asturias (LSP 213/09 and LSP 105/15), "Hospital Universitario de Cabueñes," Gijón, Asturias (LSP 150/10 and LSP 314/17); and "Hospital Universitario San Agustín," Avilés, Asturias (LSP 235/17). HUD, "Hospital Universitario Donostia," Basque Country; HUA, "Hospital Universitario de Álava," Basque Country.*

[b] *nth, no travel history; na, information not available.*

[c] *AMP, ampicillin; CHL, chloramphenicol; GEN, gentamicin; STR, streptomycin; SUL, sulfonamides; TET, tetracycline, NAL, nalidixic acid; CIP, ciprofloxacin.*

[d] *Inc, incompatibility group; nid, Inc not identified; nd, plasmid(s) not detected.*

With regard to antimicrobial susceptibility, six distinct resistance phenotypes were identified (**Table 1**). According to the bases of selection, resistance to ciprofloxacin, and also to nalidixic acid, was common to all isolates. MICs to ciprofloxacin ranged between 6 and >32 μg/ml. Resistances to ampicillin, gentamicin, streptomycin, sulfonamides, and tetracycline, arranged in different combinations, were also observed. Such resistances are expected to be conferred by SGI1-K or variants herein, including SGI1-P, which are characteristically associated with the ST198-Cip$^R$ clone. The most common phenotype, shared by six isolates, comprised all SGI1-K-encoded resistances. Apart from that, a single isolate (LSP 213/09) was resistant to chloramphenicol, whereas resistances to broad spectrum cephalosporins, carbapenems, or colistin were not detected.

## Genetic Bases of Ciprofloxacin Resistance

The 13 isolates characterized in the present study had four mutations in the QRDR, two in *gyrA* and two in *parC*. One of the *gyrA* mutations, leading to the Ser83Phe substitution in the protein, and the two mutations in *parC*, resulting in Ser80Ile and Thr57Ser replacements, were shared by all isolates. In contrast, three different changes affecting the 87 codon of *gyrA*: Asp87Asn, Asp87Tyr, and Asp87Gly were detected in ten, two, and one isolates, respectively. Travel to an African country (Morocco, Tanzania, and South Africa) or to Bali (Indonesia), prior the onset of the disease, was documented for six patients. For the remaining patients, this was not the case or the information was not available (**Table 1**). As indicated before, MIC values to ciprofloxacin of the *S.* Kentucky isolates analyzed in the present study ranged from 6 up to >32 μg/ml. Searching additional resistance mechanisms, which could justify the observed differences, revealed single mutations in the *acrR* (encoding a local regulator of the AcrAB-TolC efflux pump) and *marC* (unknown function) genes of LSP 235/17, the isolate with the higher MIC to ciprofloxacin (>32 μg/ml). A change of G→A in each of these genes led to the conservative substitution of Val by Ile in the proteins, so the high MIC value of the isolate is unlikely to be due to the detected mutations. Alterations in structural or regulatory genes (*acrA*, *acrB*, *acrS*, *acrE*, *acrF*, *tolC*, *ramR*, *ramA*, *soxR*, *soxS*, *marR*, *marA,* and *rob*), for other pumps, including their putative promoter regions, or mutations in the *rpoB* gene, were not observed. PMQR genes were neither detected. Thus, the bases for MIC variation in the analyzed isolates remain unknown.

## High Diversity of *Salmonella* Genomic Island 1-K (and *Salmonella* Genomic Island 1-P) in the Clinical Isolates of *Salmonella enterica* Serovar Kentucky

The diversity of resistance phenotypes shown by the clinical *S.* Kentucky isolates in the present study was mostly associated with a high variability of SGI1-K. As shown in **Figure 1**, each isolate has a distinct SGI1-K variant, which differed in structure and/or resistance gene content. The genomic island of LSP 314/17 was the only one that coincided with the SGI1-K prototype. Variations observed in all other isolates comprised deletions and inversions of variable size, affecting different components of the resistance region, the SGI1 backbone, and/or the flanking chromosomal DNA at the *yidY* end (in the case of HUD 1/17 and LSP 235/17). The islands of HUD 1/13 and LSP 105/15 were closely related. Both carried a Tn*2*-like transposon with the $bla_{TEM-1}$ gene as the only resistance element, and could then be assigned to SGI1-P. When compared with the control SGI1-K, most islands carry a copy of IS*26* between a deleted, and frequently inverted, resistance region, and the upstream SGI1-K backbone, which was also deleted in all but one isolate (LSP 150/10). In three isolates, a copy of IS*26* was found inside the island backbone (LSP 235/17, HUD 1/13, and LSP 105/15), and in one isolate (LSP 213/09) the 5′-end of the backbone was interrupted by the resistance region and the second segment, now contiguous to the 3′-end of the backbone, was inverted. In all, a total of 38 copies of IS*26* were identified, supporting the essential role of this element in the generation of the variants.

Apart from the resistance genes carried by SGI1-K- and SGI-P-like islands, the *catA1* gene was detected in a single isolate (LSP 213/09), resistant to chloramphenicol. The gene was located on a 5,047 bp contig which has to be of chromosomal origin, since the isolate carried a single ColpVC plasmid of 4,110 bp. The contig is flanked by IS*1* and IS*26*, and a 4,917 bp segment, consisting of IS*1*, *catA1*, $tnpA_{Tn21}$, and $\Delta tnpR_{Tn21}$, but excluding IS*26*, is 100% identical to regions found in plasmids, as well as in the chromosome of strains from different serovars of *S. enterica*, including *S.* Typhimurium, *S.* Wien, *S.* Wirchow, *S.* Typhi, and *S.* Paratyphi B (not shown). It is finally of note that all *S.* Kentucky isolates from the present study carried a cryptic *aac(6′)-1aa* gene of chromosomal location, which is widespread in *S. enterica* but fails to confer the resistance phenotype expected for AAC(6′)-Iaa, which effectively acetylates kanamycin, tobramycin, and amikacin (Salipante and Hall, 2003).

## Genomic Relationships Between the Isolates

As shown in **Figure 2**, the 13 isolates from Spanish hospitals were closely related, differing by a minimum of two single nucleotide polymorphisms (SNP) (HUD 1/13 versus LSP 105/15), and a maximum of 160 SNP (LSP 213/09 versus LSP 235/17; **Supplementary Table 4**). However, they could be separated into two clades, one including nine isolates from five hospitals, and the other comprising the remaining four, detected in three hospitals.

# DISCUSSION

In the present study, *S.* Kentucky ST198 resistant to ciprofloxacin and carrying SGI1-K- and SGI1-P-like structures were detected in five hospitals from Northern Spain. Travel to an African country before the onset of the disease was documented for five patients, while in another one the disease could have been acquired during a previous trip to Indonesia. The link between *S.* Kentucky ST198-Cip$^R$ and Africa is well established, as there is evidence indicating that the clone has emerged in Egypt, from where it has disseminated first into Northern,

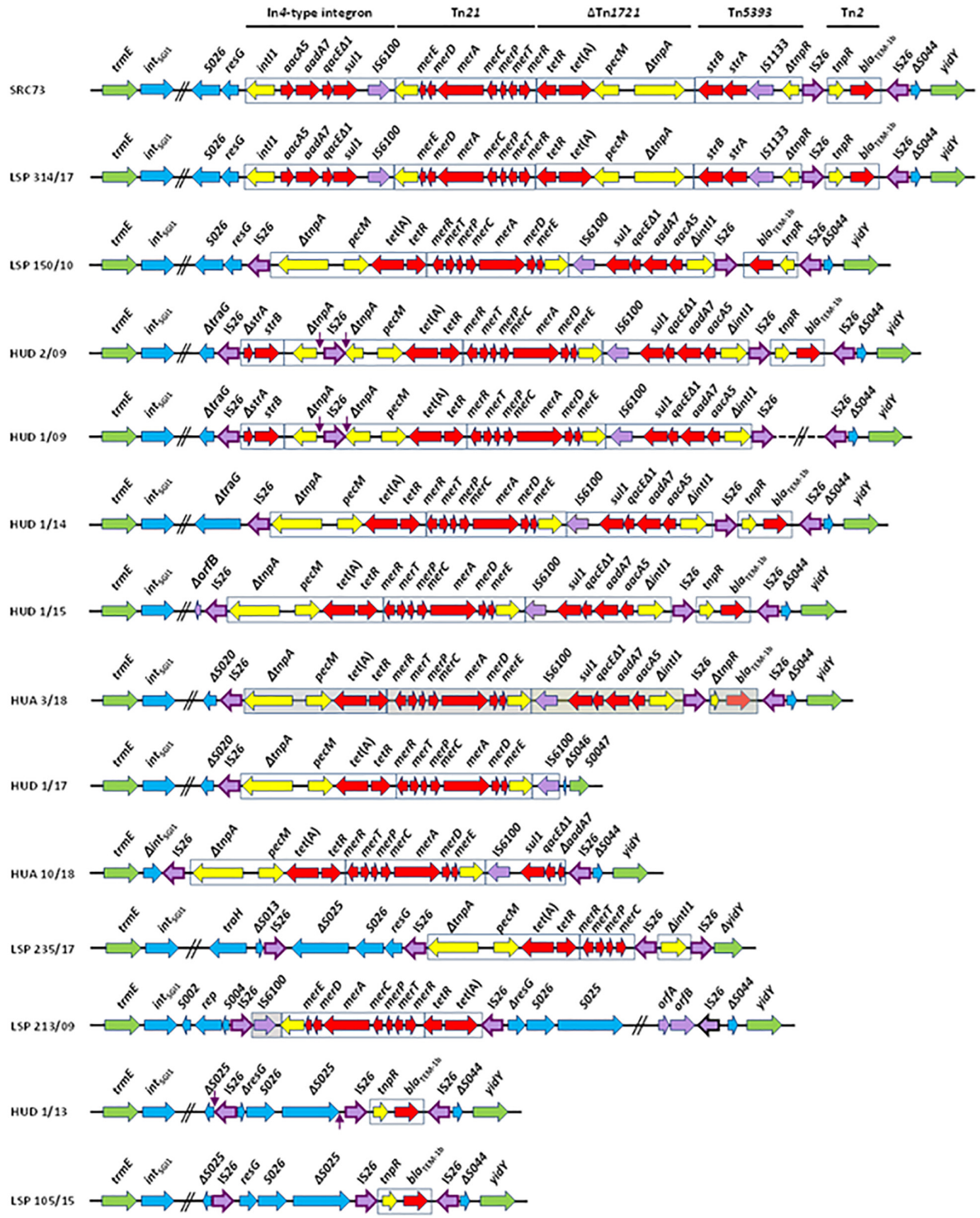


**FIGURE 1 |** SGI1-K (SGI1-P) variation in *Salmonella enterica* serovar Kentucky ST198-Cip$^R$ from Spanish hospitals. Coding regions are represented by arrows pointing in the direction of transcription and having different colors according to their function. Green, flanking chromosomal DNA; blue, SGI1 backbone; red, resistance genes; yellow, transposon and integron genes other than resistance genes; purple, insertion sequences with IS*26* highlighted by a darker border. Target site duplications are indicated by vertical arrows. Contiguous horizontal lines crossed by two parallel oblique lines indicate that not all genes are shown. In HUD 1/09, the dashed line crossed by two parallel oblique lines denotes that the corresponding sequence is unknown. LSP, Laboratory of Public Health of the Principality of Asturias, acting as regional reference center for *Salmonella*. LSP isolates come from "Hospital Universitario Central de Asturias," Oviedo, Asturias (LSP 213/09 and LSP 105/15), "Hospital Universitario de Cabueñes," Gijón, Asturias (LSP 150/10 and LSP 314/17) and "Hospital Universitario San Agustín," Avilés, Asturias (LSP 235/17). HUD, "Hospital Universitario Donostia," Basque Country; HUA, "Hospital Universitario de Álava," Basque Country.

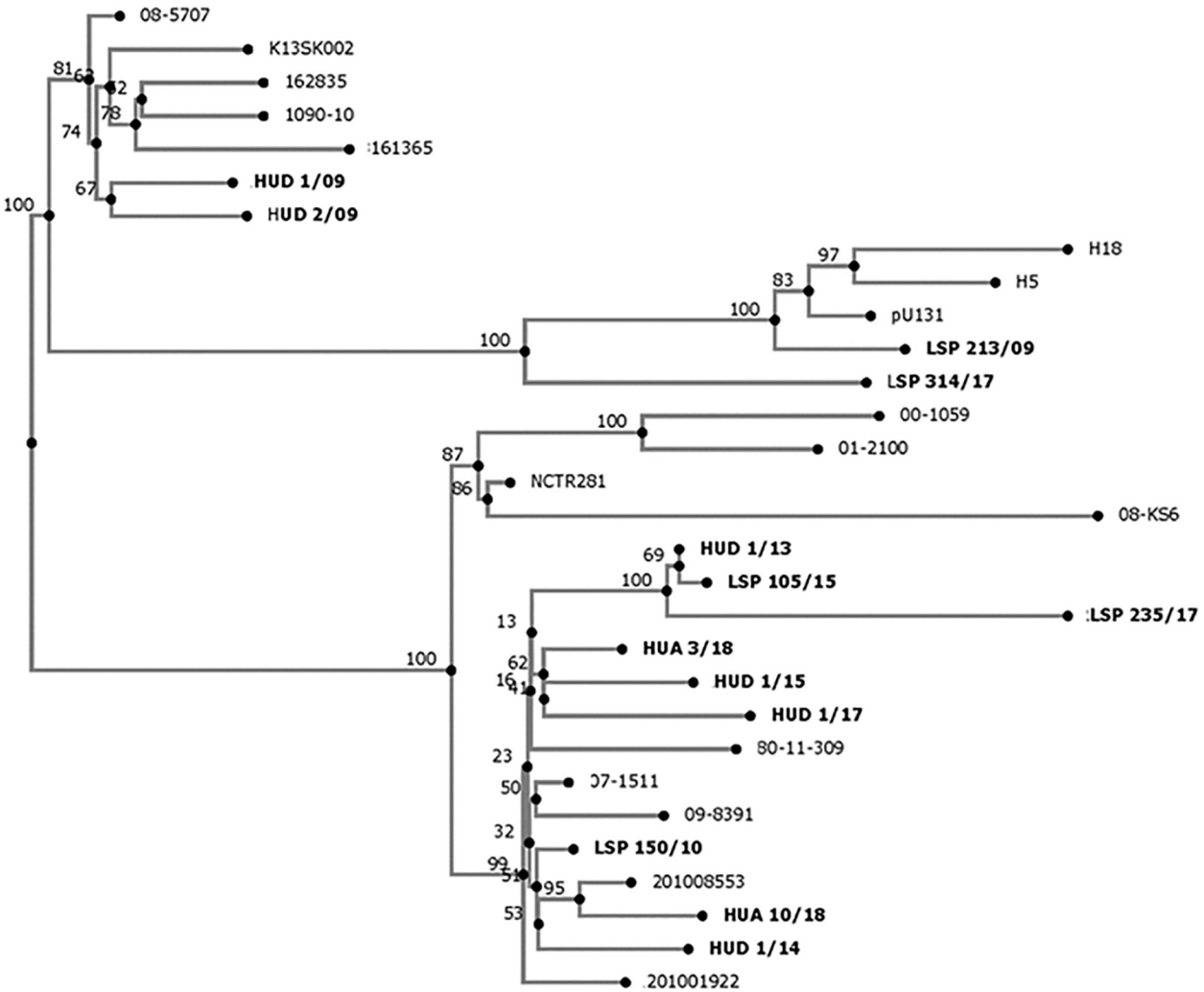


**FIGURE 2 |** Phylogenetic tree showing the relationships between *Salmonella enterica* serovar Kentucky ST198-Cip$^R$ isolates from Spanish hospitals (highlighted in bold), and other *S.* Kentucky ST198 isolates. The whole genome single nucleotide polymorphism based analysis was established with the CSI Phylogeny 1.4 (https://cge.cbs.dtu.dk/services/CSIPhylogeny/), using the genome of *S.* Kentucky strain 201001922 (accession number CP028357) as reference. Numbers at the nodes represent bootstrap values based on 1,000 replicates.

Southern, and Western Africa, and then into Asia and the European Union (Le Hello et al., 2011, 2012; Hawkey et al., 2019). With regard to Indonesia, two epidemiologically unrelated *S.* Kentucky-Cip$^R$ isolates were detected in French patients that reported travel to this region in the early 90' (Le Hello et al., 2012). Interestingly, these isolates did not belong to the *Xba*I pulsotype X1 characteristically associated with African isolates but to pulsotype X2 and they carried the SGI1-J4 and SGI1-J6 islands instead of the SGI1-K-like structures identified in the African epidemic clone (Le Hello et al., 2012). However, *S.* Kentucky ST198-Cip$^R$ isolates with pulsotype group X1 and SGI1-K have also been found in Indonesia (Le Hello et al., 2013a,b). In the present study, the Spanish isolate from a patient with previous travel history to Bali (LSP 314/17) was the only one containing the canonical SGI1-K, and probably belongs to the African clone. Interestingly, four patients did not report travel to a foreign country prior to the onset of the disease, consistent with intra-national spread of the ST198-Cip$^R$ clone.

SGI1-K was first reported in *S.* Kentucky SRC73, isolated in 2001 from spice imported into Australia from India and, since then, multiple variants have been detected (Levings et al., 2007; Doublet et al., 2008; Le Hello et al., 2011; Hawkey et al., 2019). Most if not all of those described herein could have been generated by the activity of IS*26*, an insertion sequence which is playing a key role in the evolution of complex resistance regions. IS*26* is well suited for this by using two mechanisms of movement: (i) the copy-in mechanism, which requires DNA replication and results in duplication of both IS*26* and 8 bp originally present at a randomly selected target site; and (ii) the targeted conservative mechanism, which involves two copies of IS*26* and occurs in the absence of IS*26* replication or target

site duplication (TSD) (Harmer et al., 2014, 2020; He et al., 2015). In the SGI1-K-like structures analyzed in this study, the number of IS*26* elements ranged from one (HUD 1/17) up to four (HUD 2/09, HUD 1/09, and LSP 235/17), and they were found inserted at multiple locations (**Figure 1**). It is of note that, of the total 38 IS*26* elements which have invaded the regions examined, only three of them were flanked by TSD, apparently derived from random insertion of IS*26* into particular genes, i.e., the *tnpA* gene of Tn*1721* in the SGI1-K variants of HUD 1/09 and HUD 2/09 (CGCTACCG), or the S025 *orf* belonging to the SGI1-P backbone of HUD 1/13 (GATAGCTA; although in this case the position and orientation of one of the TDS has been altered by further inversion). Insertion of IS*26* into $tnpA_{Tn1721}$ could have resulted from intermolecular copy in transposition, followed by resolution of the generated cointegrate through homologous recombination between the two directly oriented copies of the IS present in it. In contrast, the structure of HUD 1/13 could have originated by intramolecular copy in transposition of IS*26* into S025, using the *trans* pathway. Intramolecular copy in transposition events could also have been responsible for the generation of other inversions (*trans* attack) and deletions (*cis* attack) observed in the structures analyzed (He et al., 2015), while homologous recombination between oppositely oriented copies of IS*26* is likely to have originated the inversion of the $bla_{TEM-1}$ segment in the SGI1-K-like variant of LSP 150/10.

The *S.* Kentucky ST198-Cip$^R$ clone is actively evolving, not only by altering the SGI1-K- and SGI-P-like structures, usually affecting their resistance gene content, but also through acquisition of plasmids, some of which encoding resistance to last resort antibiotics, like third generation cephalosporins and carbapenems (Hawkey et al., 2019). In the present study, plasmids with ColE, Col156, ColpVC, IncI1 or not identified replicons, were found in most isolates (69.2%). However, none of the detected plasmids were involved in resistance or conferred any other noticeable property to the carrier bacteria. In *S.* Heidelberg, which is a poultry-associated pathogen, like *S.* Kentucky ST198-Cip$^R$ (Foley et al., 2011; Shah et al., 2017), carriage of ColE1 or ColpVC plasmids was shown to increase fitness of the bacteria in poultry litter (Oladeinde et al., 2018), and this might also be the case for the *S.* Kentucky isolates carrying such plasmids in the present study.

A global phylogenomic analysis of *S.* Kentucky ST198 has revealed that all MDR-Cip$^R$ isolates carrying SGI1-K or variants herein belonged to a single monophylogenetic clade, and provided evidence that multiple independent transfers of this emergent pathogen out of Africa have occurred (Hawkey et al., 2019). The 13 *S.* Kentucky ST198-Cip$^R$ isolates from Spanish hospitals, each carrying a distinct variant of SGI1-K, appear to belong to the African clone and were accordingly closely related. Interestingly, the closest isolates, HUD 1/13 and LSP 105/15, only differing by two SNP and carrying highly similar, but not identical SGI1-P variants, originated from hospitals placed in different regions of Spain, Basque Country and Asturias, respectively. Thus, after reaching Spain, the *S.* Kentucky ST198-CIP$^R$ isolates are apparently spreading within the country, while their genomic islands continue to evolve, mainly as a consequence of the striking activity of IS*26*. As indicated before, such isolates belong to the high priority list of antibiotic-resistant bacteria compiled by WHO (Tacconelli et al., 2018), and so their continuous surveillance is required. The present study shows how implementation of WGS in clinical microbiology laboratories can efficiently help to conduct epidemiological studies of emerging pathogens, and to elucidate the genomic bases of antimicrobial drug resistance.

## DATA AVAILABILITY STATEMENT

The datasets presented in this study can be found in online repositories. The names of the repository/repositories and accession number(s) can be found below: https://www.ncbi.nlm.nih.gov/genbank/, JACYBW000000000; https://www.ncbi.nlm.nih.gov/genbank/, JACYBX000000000; https://www.ncbi.nlm.nih.gov/genbank/, JACYBY000000000; https://www.ncbi.nlm.nih.gov/genbank/, JACYBZ000000000; https://www.ncbi.nlm.nih.gov/genbank/, JACYCA000000000; https://www.ncbi.nlm.nih.gov/genbank/, JACYBO000000000; https://www.ncbi.nlm.nih.gov/genbank/, JACYBP000000000; https://www.ncbi.nlm.nih.gov/genbank/, JACYBQ000000000; https://www.ncbi.nlm.nih.gov/genbank/, JACYBR000000000; https://www.ncbi.nlm.nih.gov/genbank/, JACYBS000000000; https://www.ncbi.nlm.nih.gov/genbank/, JACYBT000000000; https://www.ncbi.nlm.nih.gov/genbank/, JACYBU000000000; and https://www.ncbi.nlm.nih.gov/genbank/, JACYBV000000000.

## ETHICS STATEMENT

This study was reviewed and approved by the Research Ethics Committee of the Principality of Asturias (Code CEImPA 2020.446).

## AUTHOR CONTRIBUTIONS

JF, MR, and RR designed the experiments. XV, MB, PL, MA, SH, EP, PI, and RR carried out the experiments. XV, MT, MR, and RR performed WGS analyses. XV, JF, MR, and RR drafted the manuscript. All authors approved the final version of this manuscript.

## FUNDING

This research was supported by project FIS PI17/00474 of the "Fondo de Investigación Sanitaria, Instituto de Salud Carlos III, Ministerio de Economía y Competitividad," Spain, co-funded by European Regional Development Fund of the European Union: a way to making Europe. XV was the recipient of grant BP17-018

from the Program "Severo Ochoa" for support of Research and Teaching in the Principality of Asturias, Spain.

## ACKNOWLEDGMENTS

The authors are grateful to Joaquim Ruiz (Laboratorio de Genética Molecular y Bioquímica, Universidad Científica del Sur, Lima, Peru) and Jürgen J. Heinisch (Department of Genetics, Faculty of Biology and Chemistry, University of Osnabrück, Germany) for their useful comments and helpful advice.

## SUPPLEMENTARY MATERIAL

The Supplementary Material for this article can be found online at: https://www.frontiersin.org/articles/10.3389/fmicb.2021.720449/full#supplementary-material

## REFERENCES

Baucheron, S., Le Hello, S., Doublet, B., Giraud, E., Weill, F. X., and Cloeckaert, A. (2013). *ramR* mutations affecting fluoroquinolone susceptibility in epidemic multidrug-resistant *Salmonella enterica* serovar Kentucky ST198. *Front. Microbiol.* 4:213. doi: 10.3389/fmicb.2013.00213

Brandis, G., Granstrom, S., Leber, A. T., Bartke, K., Garoff, L., Cao, S., et al. (2021). Mutant RNA polymerase can reduce susceptibility to antibiotics via ppGpp-independent induction of a stringent-like response. *J. Antimicrob. Chemother.* 76, 606–615. doi: 10.1093/jac/dkaa469

Clinical and Laboratory Standards Institute [CLSI] (2019). *Performance Standards for Antimicrobial Susceptibility Testing. CLSI Supplement M100*. Wayne PA: Clinical and Laboratory Standards Institute.

Doublet, B., Praud, K., Bertrand, S., Collard, J. M., Weill, F. X., and Cloeckaert, A. (2008). Novel insertion sequence- and transposon-mediated genetic rearrangements in genomic island SGI1 of *Salmonella enterica* serovar Kentucky. *Antimicrob. Agents Chemother.* 52, 3745–3754. doi: 10.1128/AAC.00525-08

European Food Safety Authority [EFSA] and European Centre for Disease Prevention and Control [ECDC] (2021). The European union one health 2019 zoonoses report. *EFSA J.* 19:6406. doi: 10.2903/j.efsa.2021.6406

European Food Safety Authority [EFSA] and European Centre for Disease Prevention and Control [ECDC] (2020). The European union summary report on antimicrobial resistance in zoonotic and indicator bacteria from humans, animals and food in 2017/2018. *EFSA J.* 18:e06007. doi: 10.2903/j.efsa.2020.6007

Felsenstein, J. (1985). Confidence limits on phylogenies: an approach using the bootstrap. *Evolution* 39, 783–791. doi: 10.1111/j.1558-5646.1985.tb00420.x

Foley, S. L., Nayak, R., Hanning, I. B., Johnson, T. J., Han, J., and Ricke, S. C. (2011). Population dynamics of *Salmonella enterica* serotypes in commercial egg and poultry production. *Appl. Environ. Microbiol.* 77, 4273–4279. doi: 10.1128/AEM.00598-11

Gilbert, D. N., Chambers, H. F., Saag, M. S., Pavia, A. T., Boucher, H. W., Douglas, B., et al. (2021). *The Sanford Guide to Antimicrobial Therapy*. Sperryville, VA: Antimicrobial Therapy, Inc.

Gurevich, A., Saveliev, V., Vyahhi, N., and Tesler, G. (2013). QUAST: quality assessment tool for genome assemblies. *Bioinformatics* 29, 1072–1075. doi: 10.1093/bioinformatics/btt086

Hamidian, M., Holt, K. E., and Hall, R. M. (2015). The complete sequence of *Salmonella* genomic island SGI1-K. *J Antimicrob. Chemother.* 70, 305–306. doi: 10.1093/jac/dku331

Harmer, C. J., Moran, R. A., and Hall, R. M. (2014). Movement of IS*26*-associated antibiotic resistance genes occurs via a translocatable unit that includes a single IS*26* and preferentially inserts adjacent to another IS*26*. *mBio* 5:e01801-14. doi: 10.1128/mBio.01801-14

Harmer, C. J., Pong, C. H., and Hall, R. M. (2020). Structures bounded by directly-oriented members of the IS*26* family are pseudo-compound transposons. *Plasmid* 111:102530. doi: 10.1016/j.plasmid.2020.102530

Hawkey, J., Le Hello, S., Doublet, B., Granier, S. A., Hendriksen, R. S., Fricke, W. F., et al. (2019). Global phylogenomics of multidrug-resistant *Salmonella enterica* serotype Kentucky ST198. *Microb. Genom.* 5:e000269. doi: 10.1099/mgen.0.000269

He, S., Hickman, A. B., Varani, A. M., Siguier, P., Chandler, M., Dekker, J. P., et al. (2015). Insertion sequence IS*26* reorganizes plasmids in clinically isolated multidrug-resistant bacteria by peplicative transposition. *mBio* 6:e00762. doi: 10.1128/mBio.00762-15

Hohmann, E. L. (2001). Nontyphoidal salmonellosis. *Clin. Infect. Dis.* 32, 263–269. doi: 10.1086/318457

Kaas, R. S., Leekitcharoenphon, P., Aarestrup, F. M., and Lund, O. (2014). Solving the problem of comparing whole bacterial genomes across different sequencing platforms. *PLoS One* 9:e104984. doi: 10.1371/journal.pone.0104984

Le Hello, S., Harrois, D., Bouchrif, B., Sontag, L., Elhani, D., Guibert, V., et al. (2013a). Highly drug-resistant *Salmonella enterica* serotype Kentucky ST198-X1: a microbiological study. *Lancet Infect. Dis.* 13, 672–679. doi: 10.1016/S1473-3099(13)70124-5

Le Hello, S., Bekhit, A., Granier, S. A., Barua, H., Beutlich, J., Zajac, M., et al. (2013b). The global establishment of a highly-fluoroquinolone resistant *Salmonella enterica* serotype Kentucky ST198 strain. *Front. Microbiol.* 4:395. doi: 10.3389/fmicb.2013.00395

Le Hello, S., Hendriksen, R. S., Doublet, B., Fisher, I., Nielsen, E. M., Whichard, J. M., et al. (2011). International spread of an epidemic population of *Salmonella enterica* serotype Kentucky ST198 resistant to ciprofloxacin. *J. Infect. Dis.* 204, 675–684. doi: 10.1093/infdis/jir409

Le Hello, S., Weill, F. X., Guibert, V., Praud, K., Cloeckaert, A., and Doublet, B. (2012). Early strains of multidrug-resistant *Salmonella enterica* serovar Kentucky sequence type 198 from Southeast Asia harbor *Salmonella* genomic island 1-J variants with a novel insertion sequence. *Antimicrob. Agents Chemother.* 56, 5096–5102. doi: 10.1128/AAC.00732-12

Levings, R. S., Partridge, S. R., Djordjevic, S. P., and Hall, R. M. (2007). SGI1-K, a variant of the SGI1 genomic island carrying a mercury resistance region, in *Salmonella enterica* serovar Kentucky. *Antimicrob. Agents Chemother.* 51, 317–323. doi: 10.1128/AAC.01229-06

Li, J., Hao, H., Sajid, A., Zhang, H., and Yuan, Z. (2018). "Fluoroquinolone resistance in *Salmonella*: mechanisms, fitness, and virulence," in *Salmonella – A Re-emerging Pathogen*, ed. M. T. Mascellino (Rijeka: IntechOpen). doi: 10.5772/intechopen.74699

Majowicz, S. E., Musto, J., Scallan, E., Angulo, F. J., Kirk, M., O'brien, S. J., et al. (2010). The global burden of nontyphoidal *Salmonella* gastroenteritis. *Clin. Infect. Dis.* 50, 882–889. doi: 10.1086/650733

Mensa, J., and Soriano, A. (2021). Guia de Terapeutica Antimicrobiana. Escofet Zamora – Antares. Editorial Antares, Editorial Madrid, Spain ISBN: 9788488825339.

Oladeinde, A., Cook, K., Orlek, A., Zock, G., Herrington, K., Cox, N., et al. (2018). Hotspot mutations and ColE1 plasmids contribute to the fitness of *Salmonella* Heidelberg in poultry

litter. *PLoS One* 13:e0202286. doi: 10.1371/journal.pone.0202286

Pham, T. D. M., Ziora, Z. M., and Blaskovich, M. A. T. (2019). Quinolone antibiotics. *Medchemcomm* 10, 1719–1739. doi: 10.1039/c9md00120d

Ramadan, H., Gupta, S. K., Sharma, P., Sallam, K. I., Hiott, L. M., Elsayed, H., et al. (2018). Draft genome sequences of two ciprofloxacin-resistant *Salmonella enterica* subsp. *enterica* serotype Kentucky ST198 isolated from retail chicken carcasses in Egypt. *J. Glob. Antimicrob. Resist.* 14, 101–103. doi: 10.1016/j.jgar.2018.06.012

Salipante, S. J., and Hall, B. G. (2003). Determining the limits of the evolutionary potential of an antibiotic resistance gene. *Mol. Biol. Evol.* 20, 653–659. doi: 10.1093/molbev/msg074

Shah, D. H., Paul, N. C., and Guard, J. (2018). Complete genome sequence of a Ciprofloxacin-resistant *Salmonella enterica* subsp. enterica Serovar Kentucky sequence type 198 strain, PU131, isolated from a human patient in Washington State. *Genome Announc.* 6:e00125-18. doi: 10.1128/genomeA.00125-18

Shah, D. H., Paul, N. C., Sischo, W. C., Crespo, R., and Guard, J. (2017). Population dynamics and antimicrobial resistance of the most prevalent poultry-associated *Salmonella* serotypes. *Poult. Sci.* 96, 687–702. doi: 10.3382/ps/pew342

Tacconelli, E., Carrara, E., Savoldi, A., Harbarth, S., Mendelson, M., Monnet, D. L., et al. (2018). Discovery, research, and development of new antibiotics: the WHO priority list of antibiotic-resistant bacteria and tuberculosis. *Lancet Infect. Dis.* 18, 318–327. doi: 10.1016/S1473-3099(17)30753-3

Vielva, L., De Toro, M., Lanza, V. F., and De La Cruz, F. (2017). PLACNETw: a web-based tool for plasmid reconstruction from bacterial genomes. *Bioinformatics* 33, 3796–3798. doi: 10.1093/bioinformatics/btx462

Weill, F. X., Bertrand, S., Guesnier, F., Baucheron, S., Cloeckaert, A., and Grimont, P. A. (2006). Ciprofloxacin-resistant *Salmonella* Kentucky in travelers. *Emerg. Infect. Dis.* 12, 1611–1612. doi: 10.3201/eid1210.060589

World Health Organization [WHO] (2016). *Critically Important Antimicrobials for Human Medicine. Advisory Group on Integrated Surveillance of Antimicrobial Resistance (AGISAR)*. Geneva: World Health Organization.

**Conflict of Interest:** The authors declare that the research was conducted in the absence of any commercial or financial relationships that could be construed as a potential conflict of interest.

**Publisher's Note:** All claims expressed in this article are solely those of the authors and do not necessarily represent those of their affiliated organizations, or those of the publisher, the editors and the reviewers. Any product that may be evaluated in this article, or claim that may be made by its manufacturer, is not guaranteed or endorsed by the publisher.

frontiers in Microbiology

ORIGINAL RESEARCH
published: 15 December 2021
doi: 10.3389/fmicb.2021.765291

# Species-Level Analysis of the Human Gut Microbiome Shows Antibiotic Resistance Genes Associated With Colorectal Cancer

*Chuanfa Liu[1,2,3†], Zhiming Li[2,3†], Jiahong Ding[2,3†], Hefu Zhen[2,3], Mingyan Fang[2,3*] and Chao Nie[2,3*]*

[1] College of Life Sciences, University of Chinese Academy of Sciences, Beijing, China, [2] BGI-Shenzhen, Shenzhen, China, [3] China National GeneBank, BGI-Shenzhen, Shenzhen, China

OPEN ACCESS

**Edited by:**
*Ravi Kant,*
*University of Helsinki, Finland*

**Reviewed by:**
*Shenghui Li,*
*China Agricultural University, China*
*Seungha Kang,*
*University of Queensland, Australia*

***Correspondence:**
*Mingyan Fang*
*fangmingyan@genomics.cn*
*Chao Nie*
*niechao@genomics.cn*

*†These authors share first authorship*

**Specialty section:**
*This article was submitted to Antimicrobials, Resistance and Chemotherapy, a section of the journal Frontiers in Microbiology*

**Received:** *26 August 2021*
**Accepted:** *11 November 2021*
**Published:** *15 December 2021*

**Citation:**
*Liu C, Li Z, Ding J, Zhen H, Fang M and Nie C (2021) Species-Level Analysis of the Human Gut Microbiome Shows Antibiotic Resistance Genes Associated With Colorectal Cancer. Front. Microbiol. 12:765291. doi: 10.3389/fmicb.2021.765291*

Colorectal cancer (CRC) is the second leading cause of cancer deaths and continuously increases new cancer cases globally. Accumulating evidence links risks of CRC to antibiotic use. Long-term use and abuse of antibiotics increase the resistance of the gut microbiota; however, whether CRC is associated with antibiotic resistance in gut microbiota is still unclear. In this study, we performed a *de novo* assembly to metagenomic sequences in 382 CRC patients and 387 healthy controls to obtain representative species-level genome bins (rSGBs) and plasmids and analyzed the abundance variation of species and antibiotic resistance genes (ARGs). Twenty-five species and 65 ARGs were significantly enriched in the CRC patients, and among these ARGs, 12 were multidrug-resistant genes (MRGs), which mainly included *acrB*, *TolC*, *marA*, *H-NS*, *Escherichia coli acrR* mutation, and *AcrS*. These MRGs could confer resistance to fluoroquinolones, tetracyclines, cephalosporins, and rifamycin antibiotics by antibiotic efflux and inactivation. A classification model was built using the abundance of species and ARGs and achieved areas under the curve of 0.831 and 0.715, respectively. Our investigation has identified the antibiotic resistance types of ARGs and suggested that *E. coli* is the primary antibiotic resistance reservoir of ARGs in CRC patients, providing valuable evidence for selecting appropriate antibiotics in the CRC treatment.

**Keywords: antibiotic resistance gene (ARG), colorectal cancer (CRC), human gut metagenome, species-level genome bins, *Escherichia coli***

## INTRODUCTION

Colorectal cancer (CRC) is one of the most common cancers worldwide and has led to nearly 1 million deaths in 2020 only (Ferlay et al., 2021). Many factors are associated with an elevated risk of CRC, including genetic predisposition, colorectal polyps, inflammatory bowel disease, smoking, and alcohol intake (Wang et al., 2014). Accumulating evidence suggests that long-term, frequent, and/or combined antibiotic use could also be risk factors for CRC (Wang et al., 2014;

Dik et al., 2016; Cao et al., 2018; Crockett and Nagtegaal, 2019; Zhang et al., 2019). Antibiotics, such as metronidazole, ciprofloxacin, and rifaximin, are frequently used to treat colitis and intestinal lesions (Bernstein et al., 2016; Nitzan et al., 2016). During the long-term development and progression of CRC, the detrimental effect of antibiotics may be present even at the early stage of colitis, adenomatous polyps, or other precursors of the CRC. It is worth noting that antibiotic use could increase the richness of antibiotic-resistance bacterial species and the abundance of antibiotic resistance genes (ARGs) in the gut microbiota (Casals-Pascual et al., 2018; Dubinsky et al., 2020). Subsequent to antibiotic use and increased resistance, bowel dysbacteria may occur, and concomitantly, colonization resistance, and mucus production of the colon mucosal may be impaired (Becattini et al., 2016; Schwartz et al., 2020). Existing literature indicates that gut microbiota dysbiosis and colon mucosal surface changes are associated with the occurrence and progression of CRC (Yachida et al., 2019; Cheng et al., 2020; Xing et al., 2021). Therefore, research on drug-resistant microbiota and resistance genes may help to understand the progression of CRC.

The compositional patterns of antibiotic-resistant species and ARGs in the gut microbiota of CRC patients were scantly studied. To examine their potential effects exerted upon CRC patients and healthy people, we have downloaded published human gut metagenomic data of CRC patients and healthy controls to study the antibiotic resistance species and ARG distribution in the gut microbiota. We performed the metagenomic assembly to obtain representative species-level genome bins (rSGBs) to investigate ARG abundance in each species. Based on the Genome Taxonomy Database (GTDB) and Comprehensive Antibiotic Resistance Database (CARD), we annotated species and ARGs in rSGBs and analyzed their abundance. These analyses have revealed how the burden of antibiotic resistance changes in the intestine of CRC patients, stressing significant associations between these changes and microbiota composition. Our study has characterized the resistance of the gut microbiota in CRC patients and may shed new light on the proper antibiotic use for avoiding drug resistance.

# RESULTS

## Reconstruction and Annotation of Microbial Genomes and Plasmids

In this study, we downloaded metagenomic data of 382 CRC patients (the CRC group) and 387 healthy controls (CTR group) from eight studies (**Table 1** and **Supplementary Table 1**). The genome reconstruction was performed using a pipeline reported by Pasolli et al. (2019) and carried out a *de novo* single-sample metagenomes assembly and binning. More than 23.5 million contigs (mean ± SD, 30,688.6 ± 13,972.6) were assembled from these samples; 5,880 high-quality metagenome-assembled genomes (MAGs) and 5,390 medium-quality MAGs were obtained (**Supplementary Table 2**). After clustering and filtering the rSGBs for the high-quality MAGs, we obtained 696 rSGBs with genome sizes ranging from 0.95 to 6.41 Mb (2.39 ± 0.43 Mb) (**Supplementary Tables 2–4**). We then aligned the high-quality sequencing reads to the 696 rSGBs. The read mapping rate in our results (76.6% ± 7.8%, **Supplementary Table 2**) was similar to that of a large-scale gut microbiota study (range, 67.76–87.51%) (Pasolli et al., 2019). Based on the quality of the mapping rate, it is acceptable to use our data for subsequent species and ARG annotations.

Thereafter, we classified rSGBs using the GTDB Toolkit (GTDB-Tk, see *Methods* for details on the taxonomy nomenclature used) (Chaumeil et al., 2019). However, 60 rSGBs (8.62%) could not be assigned to an existing species, and 402 (57.75%) rSGBs belonged to uncultured species (**Figure 1** and **Supplementary Table 5**). All 696 rSGBs were classified into 13 phyla and 306 genera. In line with previous studies (Yeoh et al., 2020), Firmicutes (including Firmicutes A), Bacteroidota, Actinobacteriota, and Proteobacteria were predominant phyla, and the total relative abundance accounted for more than 90% of the gut microbiota (mean ± SD, CRC group: 93.69% ± 8.76%; CTR group: 96.67% ± 5.75%) (**Supplementary Figure 1A**). *Bacteroides*, *Phocaeicola*, *Faecalibacterium*, *Prevotella*, *Alistipes*, and *Blautia A* were the dominant genera in the gut (**Figure 2A**). It indicated that our rSGBs covered the dominate species in the gut microbiota.

In addition, we assembled the plasmids of gut microbiota using metaplasmidSPAdes (Antipov et al., 2019). We obtained 24,692 plasmid-sourced contigs (N50 = 42,448 bp; max = 473,623 bp; min = 2,564 bp) with a mean of 32 contigs in each sample. The plasmid-sourced genes were predicted and clustered with MetaGeneMark and cd-hit, respectively (Li and Godzik, 2006; Zhu et al., 2010). A non-redundant plasmid-sourced gene catalog (159,890 genes, N50 = 701 bp) was obtained. Next, we applied reference-based taxonomy annotation of the gene catalog using the NCBI-NT database. Finally, 157,504 (98.5%) of the genes in the gene catalog could be uniquely and reliably assigned to a species. We found those genes mainly from *Escherichia coli*, *Faecalibacterium prausnitzii*, *Bacteroides dorei*, *Bacteroides fragilis*, *Bacteroides uniformis*, and *Klebsiella pneumoniae*.

## Alterations of Gut Microbial Composition in Colorectal Cancer and CTR Groups

We analyzed the effect size of cohorts and host characteristics on the variance of the gut microbiome by permutational multivariate analysis of variance (PERMANOVA) test, where results revealed the factor "cohort" to have a predominant impact on the species and ARG composition of the subjects (**Supplementary Figure 2**). To test the accuracy of results in the analysis, we select two cohorts randomly to confirm our species and ARG results [PRJEB7774 ($n$ = 109) and PRJEB12449 ($n$ = 104)]. The analysis of the α and β diversity of microbial composition revealed that the CRC group had a slightly lower species diversity than the CTR group [Shannon–Wiener index ($H'$), $p$ = 0.24, **Figure 2B**], which was consistent with the literature (Gao et al., 2015). The dimensionality-reduction analysis [principal coordinate analysis (PCoA) and non-metric multidimensional scaling (NMDS) analysis] of the rSGBs relative abundance of the CRC and CTR groups showed that the CRC and CTR groups

**TABLE 1 |** Characteristics of the data sets included in this study.

| Accession number[a] | Group (n[b]) | Age (years) (mean ± SD[c]) | Gender (F/M,%[d]) | BMI (kg/m$^2$) (mean ± SD[c]) | Read counts (mean ± SD[c]) |
|---|---|---|---|---|---|
| PRJEB7774 Feng et al. (2015) | CRC (46) | 67.07 ± 10.91 | 39.13/60.87 | 26.46 ± 3.54 | 49,936,552 ± 7,270,051 |
| | CTR (63) | 67.06 ± 6.37 | 41.27/58.73 | 27.57 ± 3.74 | 46,090,975 ± 7,068,141 |
| PRJNA389927 Hannigan et al. (2018) | CRC (28) | 58.86 ± 11.02 | 28.57/71.43 | 28.57/71.43 | 4,851,235 ± 2,209,656 |
| | CTR (28) | 55.46 ± 9.52 | 60.71/39.29 | 60.71/39.29 | 5,848,176 ± 3,578,299 |
| PRJEB10878 Yu et al. (2017) | CRC (74) | 66.04 ± 10.60 | 35.14/64.86 | 23.98 ± 3.16 | 49,225,941 ± 10,554,038 |
| | CTR (54) | 61.76 ± 5.67 | 38.89/61.11 | 23.46 ± 2.96 | 53,622,545 ± 8,128,850 |
| PRJEB6070 Zeller et al. (2014) | CRC (91) | 64.66 ± 12.23 | 40.66/59.34 | 26.04 ± 4.49 | 43,899,076 ± 19,556,571 |
| | CTR (66) | 58.61 ± 12.79 | 50.00/50.00 | 24.68 ± 3.17 | 48,152,424 ± 23,181,408 |
| PRJEB27928 Wirbel et al. (2019) | CRC (22) | 66.55 ± 10.6 | 50.00/50.00 | 25.33 ± 4.93 | 48,769,786 ± 18,597,297 |
| | CTR (60) | 57.57 ± 11.08 | 46.67/53.33 | 24.88 ± 3.2 | 28,494,527 ± 7,144,313 |
| PRJNA447983 Thomas et al. (2019) | CRC (29) | 71.45 ± 8.23 | 20.69/79.31 | 25.71 ± 4.14 | 46,797,011 ± 22,256,056 |
| | CTR (24) | 67.92 ± 7.01 | 45.83/54.17 | 25.32 ± 3.51 | 58,117,998 ± 40,294,533 |
| PRJDB4176 Yachida et al. (2019) | CRC (40) | 59.05 ± 12.83 | 47.50/52.50 | 22.36 ± 2.72 | 40,249,523 ± 12,291,484 |
| | CTR (40) | 63.63 ± 12.36 | 42.50/57.50 | 22.90 ± 2.44 | 46,232,480 ± 14,228,285 |
| PRJEB12449 Vogtmann et al. (2016) | CRC (52) | 61.85 ± 13.58 | 28.85/71.15 | 24.89 ± 4.25 | 52,664,424 ± 16,619,909 |
| | CTR (52) | 61.23 ± 11.03 | 28.85/71.15 | 25.34 ± 4.28 | 52,629,971 ± 12,022,921 |

[a] *References of the study.*
[b] *Counts of samples.*
[c] *Standard deviation.*
[d] *Ratio of the percentage of female and male.*

were separated (PERMANOVA analysis $p = 0.01$, $R = 0.0731$) (**Figure 2C** and **Supplementary Figure 1B**).

Then, the composition of microbiota between CRC patients and healthy controls was compared at phylum and genus levels. On the phylum levels, Bacteroidota, Desulfobacterota, and Fusobacteriota phyla were enriched in the CRC group, and Firmicutes A phylum was enriched in the CTR group (Wilcoxon test, adjusted $p < 0.05$; **Supplementary Figure 1C**). On the genus level, *Anaerotignum*, *Bilophila*, *Bulleidia*, *Flavonifractor*, *Gemella*, *Intestinimonas*, *Parvimonas*, *Peptostreptococcus*, *Porphyromonas*, *Prevotella*, and *Ruthenibacterium* genera were enriched in the CRC group; meanwhile, *Agathobacter*, *Anaerostipes*, *Butyricicoccus A*, *Butyrivibrio A*, *CAG-41*, *Eubacterium G*, *Eubacterium R*, *Faecalibacterium*, *GCA-900066135*, *Lachnospira*, *TF01-11*, and *UBA11524* genera were enriched in the CTR group significantly (Wilcoxon test, adjusted $p < 0.05$; **Supplementary Figure 1C**).

Next, we compared the microbiota composition between CRC patients and healthy controls at species levels using the linear discriminant analysis effect size (LefSe) algorithm (Segata et al., 2011). Within the 25 species enriched in the CRC group (**Figure 2D** and **Supplementary Table 6**), nine species had been reported to be increased in the CRC group before, that is, *E. coli* (GTDB classification: *E. coli D*), *Parabacteroides distasonis*, *B. fragilis*, *Porphyromonas* species, *Alistipes finegoldii*, *Alistipes onderdonkii*, *Akkermansia muciniphila*, *Bacteroides thetaiotaomicron*, *Mediterraneibacter torques* (previously named *Ruminococcus torques*), and *Ruminococcus B gnavus* (Zhang et al., 2018; Ai et al., 2019; Dai et al., 2019; Sahankumari et al., 2019; Wong and Yu, 2019; Yang et al., 2019). Moreover, two species were the first discovered species that were enriched in the CRC group, that is, *CAG-180 sp000432435* and *CAG-177 sp003514385*. Among the 35 species enriched in the CTR group (**Figure 2D** and **Supplementary Table 6**), *Anaerostipes hadrus*, *Bifidobacterium catenulatum*, *Fusicatenibacter saccharivorans*, and butyrate-producing species *F. prausnitzii*, *Agathobacter rectalis*, and *Agathobacter faecis* had been reported in the literature as enriched in the healthy controls and possibly beneficial to the gut health (Ai et al., 2019; Kim et al., 2020; Ma et al., 2021). Focusing on the 60 microbiota that exhibited significantly different abundances between the CRC and CTR groups in all samples, we further compared the relative abundances of these microbiota between the CRC and CTR groups in PRJEB7774 and PRJEB12449 cohorts using the Wilcoxon rank-sum tests. We found that the enrichment of 85 and 83.3% of the significantly different species (CRC and CTR) in the PRJEB7774 and PRJEB12449 cohorts were congruent with those in the composite cohort of all samples (**Supplementary Figure 3**).

## Antibiotic Resistance Genes Conferred to Multiple Antibiotics

To analyze the antibiotic resistance information in microbiota, we characterized the ARGs and analyzed their abundance in the rSGBs and plasmids by annotating them to the CARD (Alcock et al., 2020), obtaining 164 ARGs in 189 rSGBs (**Supplementary Tables 7, 8**). The top 11 ARGs accounted for 51.16% of all abundance, mainly including *adeF*, *TolC*, *E. coli soxS* mutation, *AcrS*, *E. coli soxR* mutation, and *marA* (**Figure 3A** and **Supplementary Figure 4A**). The *adeF* had the highest relative abundance, which could encode the membrane fusion proteins of the multidrug efflux complex AdeFGH (Coyne et al., 2010). Within the plasmid-sourced genes, we obtained 43 ARGs in 49 genes (0.03% of all plasmid genes) that conferred resistance to antibiotics (**Supplementary Table 8**), and the ARG *tetQ* had the highest abundance.

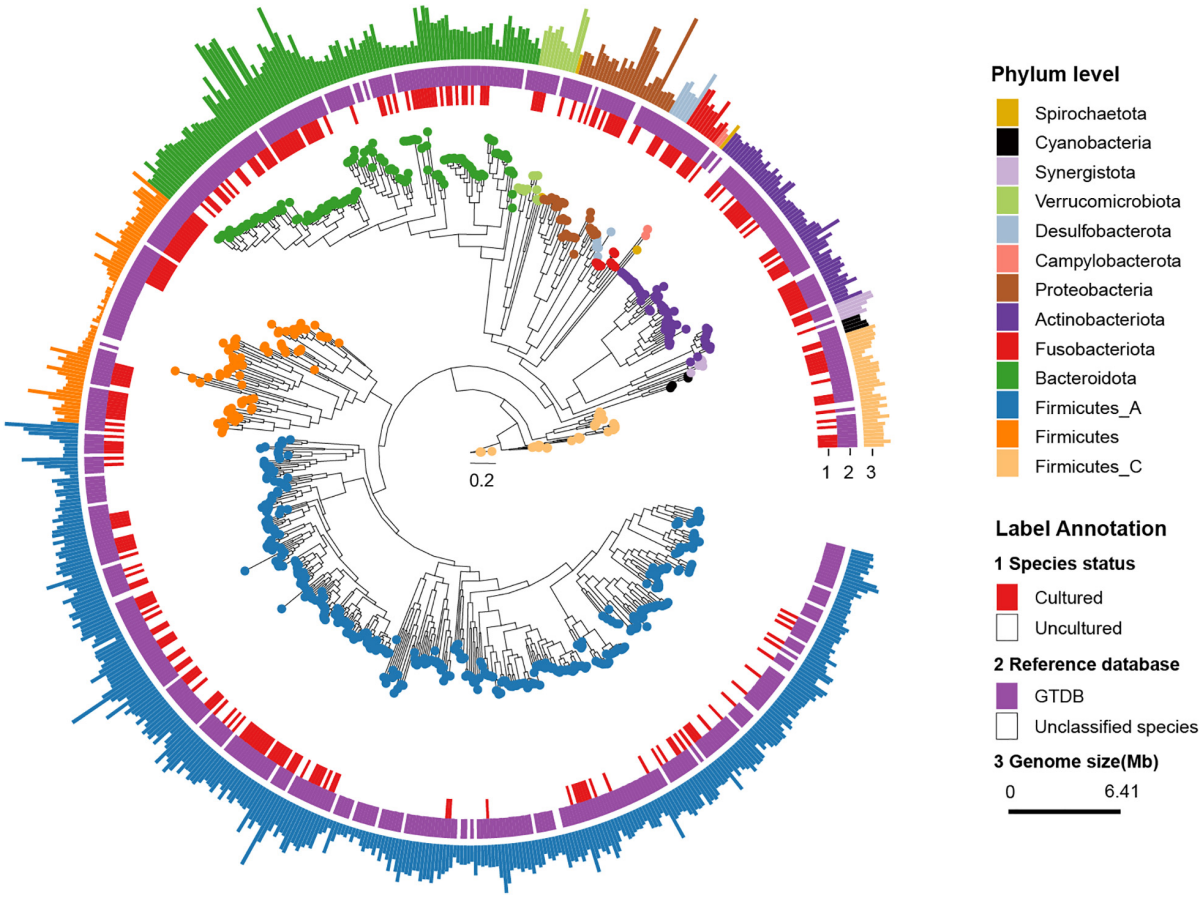


**FIGURE 1 |** Phylogenetic tree of representative genomes. The phylogenetic tree in the center showed 696 rSGBs. The colored points on the tree represent different phyla. The innermost circle (labeled "1") means whether the species was cultured (red color, marked as Cultured) or not (white color, marked as Uncultured) in the previous study. The middle circle (labeled "2") means whether the species could be annotated to the known genome (purple color, marked as "GTDB") or not (white color, marked as "Unclassified species") in the GTDB. In the outmost circle (label "3"), the length of bars represents the genome size (bp), and colors represent different phyla.

We analyzed the resistance mechanisms and resistance drug types of identified ARGs and found that these ARGs in the rSGBs and plasmids could confer resistance to 33 and 18 types of antibiotics, respectively. Notably, 53.05% of rSGB-sourced ARGs (87 out of 164) could confer resistance to more than one antibiotic (**Supplementary Table 7**). ARGs could affect antibiotic resistance through the mechanisms of antibiotic efflux, inactivation, target alteration, target protection, target replacement, and reduced permeability to antibiotics.

Regarding the percentage of abundance, the antibiotic efflux accounted for 53.36% of rSGB-sourced ARGs resistance mechanism, and antibiotic inactivation and antibiotic targets alteration accounted for 21.21 and 14.49%, respectively (**Figure 3B** and **Supplementary Figure 4B**). Eighty percent of the total rSGB-sourced ARG abundance could be ascribed to the top 10 resistance drug types, including nucleoside antibiotics (17.3%), cephalosporins (16.77%), macrolides (11.64%), phenicol antibiotics (8.06%), fluoroquinolones (5.97%), penams (5.2%), rifamycins (2.96%), and other antibiotics (**Figure 3C** and **Supplementary Figure 4C**).

We found that those with top resistance types were also the most consumed antibiotics globally (Van Boeckel et al., 2014). For example, ARGs in the gut of the CRC group could confer six types of global high-consumption antibiotics, including penicillins, cephalosporins, macrolides, fluoroquinolones, tetracyclines, and rifamycins. The antibiotic resistance types in our findings were consistent with the global antibiotic consumption. Among these antibiotics, 19.23% belong to the Access Class, 30.77% belong to the Watch Class, and 23.08% are part of the Reserve Class (World Health Organization AWaRe classification, version 2019; **Supplementary Table 9** and **Supplementary Figure 4D**; World Health Organization, 2019).

## The Divergence and Heterogeneity of Antibiotic Resistance Gene in the Colorectal Cancer and CTR Groups

We performed a group comparison in the abundance of ARGs, antibiotic mechanisms, and their resistance drug types to analyze ARG variations. First, the component of ARGs in the CRC and

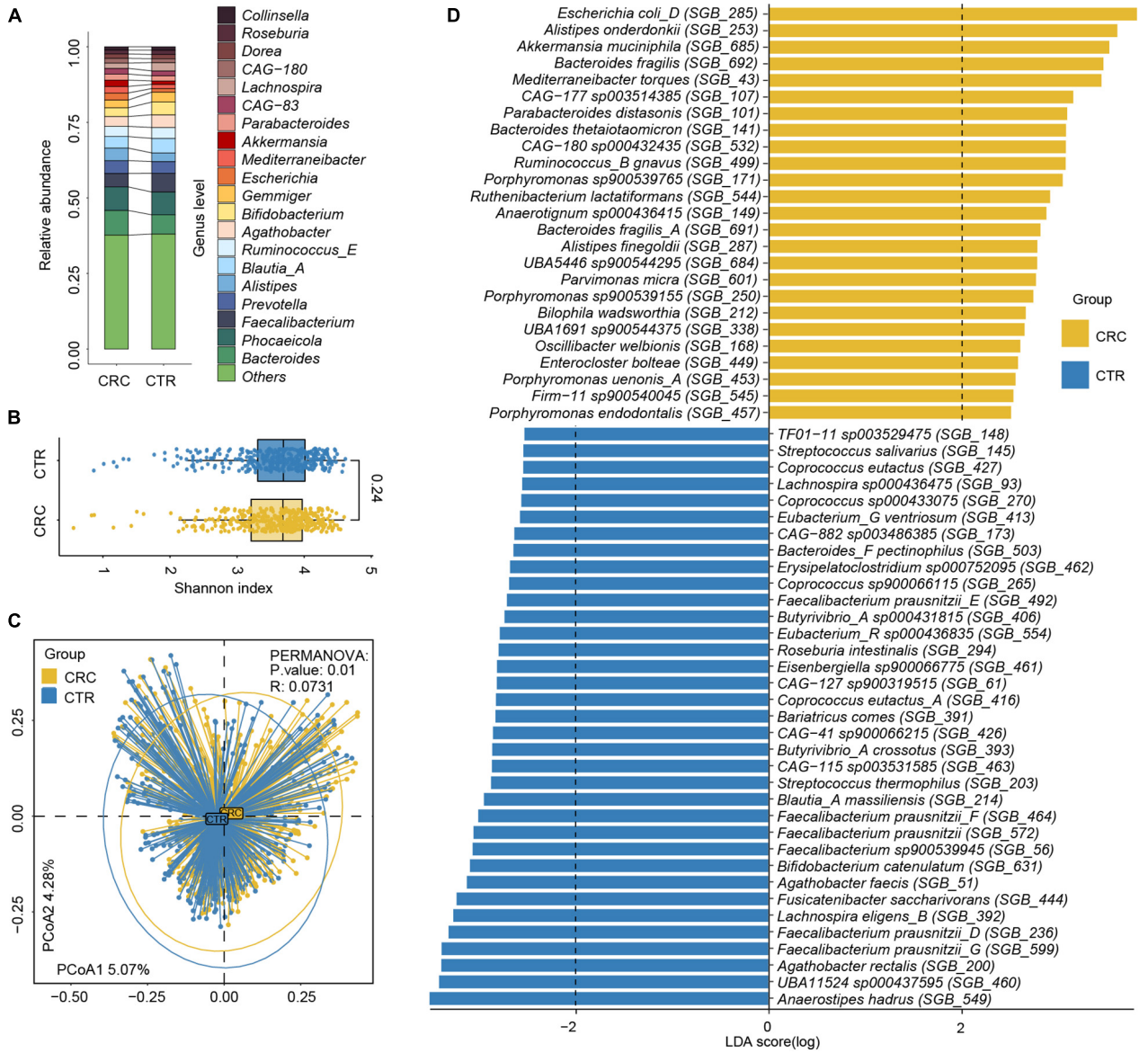


**FIGURE 2 |** Relative abundance difference of rSGBs in the CRC and CTR groups. **(A)** The relative abundance of rSGBs on the genus level. **(B)** The Shannon–Wiener indices of rSGBs abundance in CRC (yellow color) and CTR (blue color) groups were similar (Wilcoxon rank-sum test, $p = 0.24$). **(C)** Principal coordinate analysis (PCoA) plot depicted the Bray–Curtis distances of rSGBs in the CRC (yellow) and CTR (blue) groups. *P*-value and R represent PERMANOVA analysis *p*-value and $R^2$ value, respectively. **(D)** LefSe analysis results showed the distribution difference of rSGBs, the colors yellow and blue represent the CRC and CTR groups, respectively.

CTR groups were analyzed. Compared with the CTR group, the CRC group had a higher rSGB-sourced ARG diversity [Shannon–Wiener index ($H'$), $p < 0.001$, **Figure 3D**], which indicated that gut microbiota in the CRC group had more complexity of ARGs. The β diversity of ARG abundance showed that the ARGs in the CRC group differed from those in the CTR group (NMDS, PERMANOVA: $p = 0.01$, $R = 0.0058$) (**Figure 3E**).

We then analyzed the rSGB-sourced ARG abundance grouped by resistance mechanisms and resistance drug types in the CRC and CTR groups. Eighty percent (33 of 39) resistance mechanisms and resistance drugs were significantly enriched in the CRC group, mainly including antibiotic efflux and inactivation mechanism, tetracyclines, fluoroquinolones, penams, carbapenem, and cephalosporins (**Figure 3F**). The abundance of ARGs in the rSGBs was significantly enriched in the CRC group on the mechanisms and resistance drug type scales.

To further demonstrate the variability in the resistance burden between the CRC and CTR groups, we analyzed the abundance difference of every ARG. Fifty ARGs from rSGBs were significantly enriched in the CRC group (Wilcoxon test, adjusted $p < 0.05$) (**Figure 4**). Correspondingly, the total abundance of ARGs from plasmids was higher in the CRC group than that in

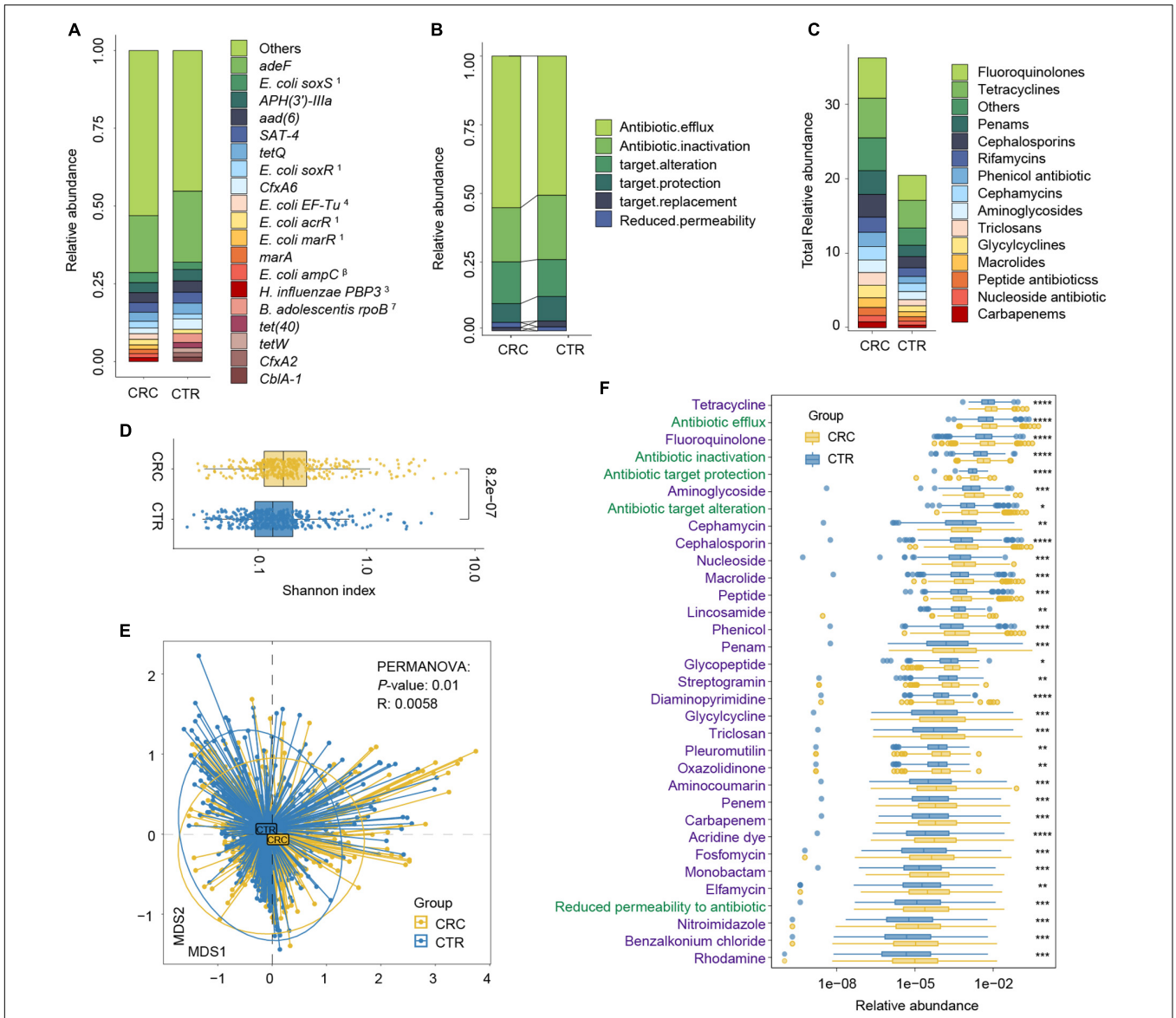


**FIGURE 3 |** Antibiotic resistance variations in CRC and CTR groups. **(A)** The average abundance percentage of ARGs in the CRC and CTR groups. **(B)** Resistance mechanism abundance percentage in the CRC and CTR groups, respectively. **(C)** The abundance of resistance drug types in CRC and CTR groups. **(D)** Shannon–Wiener index (*H'*) difference of ARG abundance in the CRC (yellow color) and CTR (blue color) group. **(E)** NMDS results of ARG abundance in the CRC (yellow color) and CTR (blue color) group. **(F)** Resistance drug types (green color label) and resistance mechanisms (purple color label) abundance had statistical differences in the CRC (yellow color) and CTR (blue color) groups. The following symbols denoted statistical significance: $^{*}p < 0.05$, $^{**}p < 0.01$, $^{***}p < 0.001$, $^{****}p < 0.0001$. In **(A)**, the superscript labels from numbers 1 to 7 and β represent the resistance drug types of mutations: [1]antibiotic resistance, [2] multiple antibiotics, [3]β-lactam antibiotics, [4]pulvomycins, [5]fosfomycin antibiotics, [6]fluoroquinolones, [7]rifampicins; [β] β-lactamases.

the CTR group (**Figure 5A**), and 70% of ARGs (16 of 23) were enriched in the CRC group significantly (Wilcoxon test, adjusted $p < 0.05$) (**Figure 5B**). In our two validation cohorts, 100 and 96% rSGB-sourced ARGs as well as 60.9 and 73.9% plasmid-sourced ARGs in PRJEB7774 and PRJEB12449 cohorts were enriched congruently with all the samples (**Supplementary Figures 5, 6**). The ARGs from both the rSGBs and plasmids in the validation cohorts showed a notable consistency with those in all samples.

Among these rSGB-sourced ARGs, 90% (45 of 50) were found in the *E. coli*, mainly composing of *TolC*, *E. coli soxS* mutation, *marA*, *AcrS*, *acrB*, and *mdtM*. The remaining five ARGs, including *adeF*, *CcrA*, *cepA*, *tet(W/N/W)*, and *tetQ*, were found in *P. distasonis, B. fragilis A*, *B. fragilis*, *UMGS693 sp900544555*, and *A. onderdonkii,* respectively. Although the ARGs existing in *E. coli*, *Bacteroides* species, and *Alistipes* species had been reported, their association with CRC was not robust (Dubinsky et al., 2020; Parker et al., 2020). In terms of resistance mechanisms and resistance drug types, these rSGB-sourced ARGs enriched in CRC could confer resistance to 33 types of antibiotics by five mechanisms, and 37 of 50 ARGs encoded antibiotic efflux

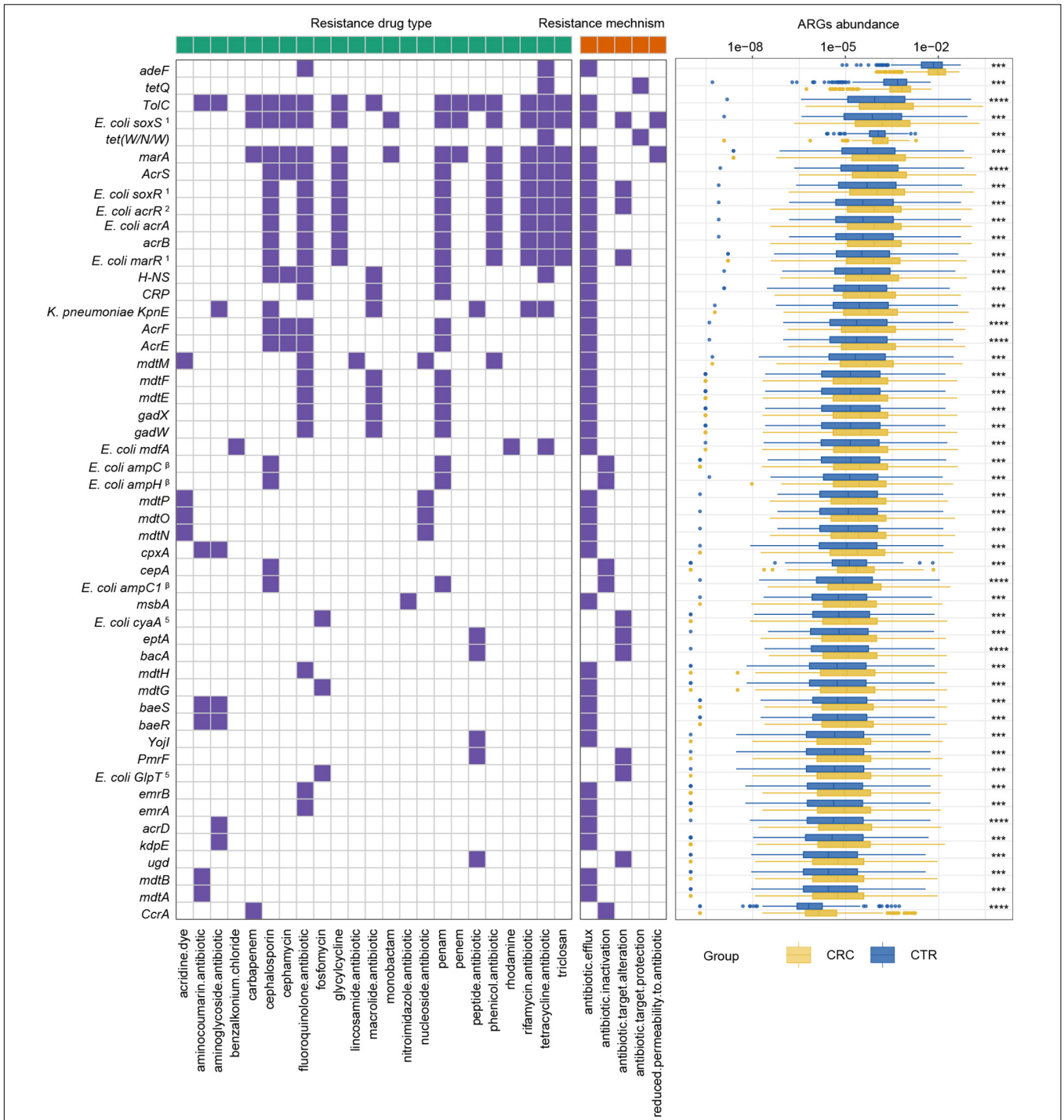


**FIGURE 4 |** ARGs with significant differences and their resistance mechanism and resistance drug type abundance. The left (with a green label) and the right (with an orange label) panels of heatmap represented drug resistance type and resistance mechanism, respectively. The purple or white color denoted with and without certain characteristic. The boxplot showed abundance difference of ARGs in the CRC (yellow) and CTR (blue) groups. The following symbols denoted statistical significance: ***$p < 0.001$, ****$p < 0.0001$. The superscript label from numbers 1 to 7 and β was the same as **Figure 3A**.

mechanism (**Figure 4**). In addition, in rSGB-sourced ARGs, 22 ARGs had resistance to fluoroquinolones, 20 ARGs to penams, 17 ARGs to cephalosporins, 15 ARGs to tetracyclines, and 10 ARGs to rifamycins, respectively.

For the 23 plasmid-sourced ARGs, 39% of ARGs (9 of 23) were found in *E. coli*, mainly composing *acrB*, *msbA*, *AcrF*, and *E. coli acrR* mutation. These ARGs could confer resistance to 18 antibiotics by five mechanisms (**Figure 5B**),

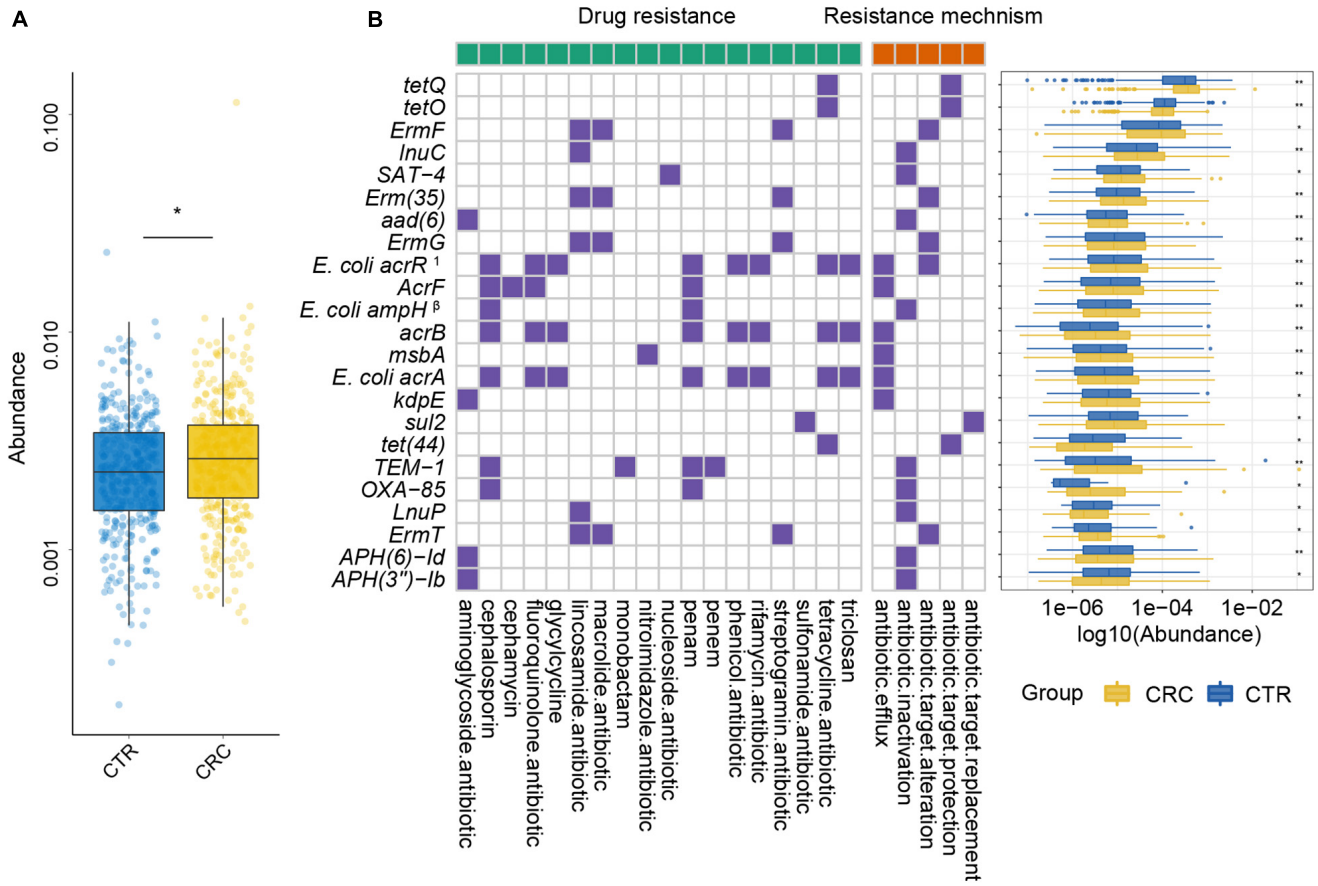


**FIGURE 5 |** Plasmid ARGs with significant differences and their resistance mechanism and resistance drug type abundance. **(A)** The abundance variation of total ARGs from plasmids in the CRC (yellow color) and CTR (blue color) groups. **(B)** The left (with a green label) and the right (with an orange label) panels of the heatmap represented drug resistance type and resistance mechanism, respectively. The purple or white color denoted with or without certain characteristic. The boxplot showed abundance difference of ARGs in the CRC (yellow color) and CTR (blue color) groups. In **(B)**, the superscript label 1 and β represent the resistance drug types of mutations: [1]multiple antibiotics; [β] β-lactamases. The following symbols denoted statistical significance: $^{*}p < 0.05$, $^{**}p < 0.01$.

where the antibiotics included cephalosporins, fluoroquinolones, macrolides, tetracycline, and penams. Seven ARGs had resistance to penams and cephalosporins, six ARGs to tetracyclines and lincosamides, respectively.

Interestingly, penicillins, cephalosporins, and fluoroquinolones had been reported to be associated with the onset of colitis (Nitzan et al., 2016). Meanwhile, fluoroquinolones, cephalosporins, tetracyclines, and rifamycins were the most commonly used antibiotics in colitis treatment (Theochari et al., 2018). These results suggested that the increase in resistance burden might be due to antibiotic treatment of precancerous colitis and antibiotic use related to intestinal colitis and CRC by an unknown mechanism.

To further investigate the multidrug resistance of ARGs, we denoted ARGs that could confer resistance to five or more antibiotic drug types as multidrug-resistant genes (MRGs) (**Supplementary Table 7**). A total of 21 species from rSGBs were found that carried 41 MRGs, of which 12 MRGs were significantly enriched in the CRC group (**Supplementary Figure 7**). In the plasmid-sourced ARGs, three MRGs were found (*acrB*, *E. coli acrR* mutation, and *E. coli acrA*) enriched in the CRC group. All these MRGs enriched in the CRC group were derived from *E. coli* and *K. pneumoniae* (**Figures 5B**, **6A**). Meanwhile, compared with the CTR group, the rSGB-sourced MRG abundance in *E. coli* was significantly higher in the CRC group (**Figure 6B**). These MRGs could confer resistance to 19 types of antibiotic drugs, which included fluoroquinolones, cephalosporins, tetracyclines, penams, phenicol antibiotics, and rifamycins (**Figures 5B**, **6A**). Among these MRGs, *mdtM* could confer resistance to 15 types of antibiotics, where both *E. coli marR* mutant and *K. pneumoniae KpnE* could confer resistance to 12 types of antibiotics, and *H-NS* conferred resistance to 9 types of antibiotics (**Figure 6A**). The intergroup difference of MAGs was completely confirmed in the PRJEB7774 and PRJEB12449 cohorts, respectively (**Supplementary Figure 8**). This finding showed that the abundance of MRGs and species with MARs was enriched in the CRC group, which suggested that the increase in MRG abundance was also associated with the CRC. Findings thus far indicated that the CRC group had a higher antibiotic resistance burden and had resistance to multiple antibiotics.

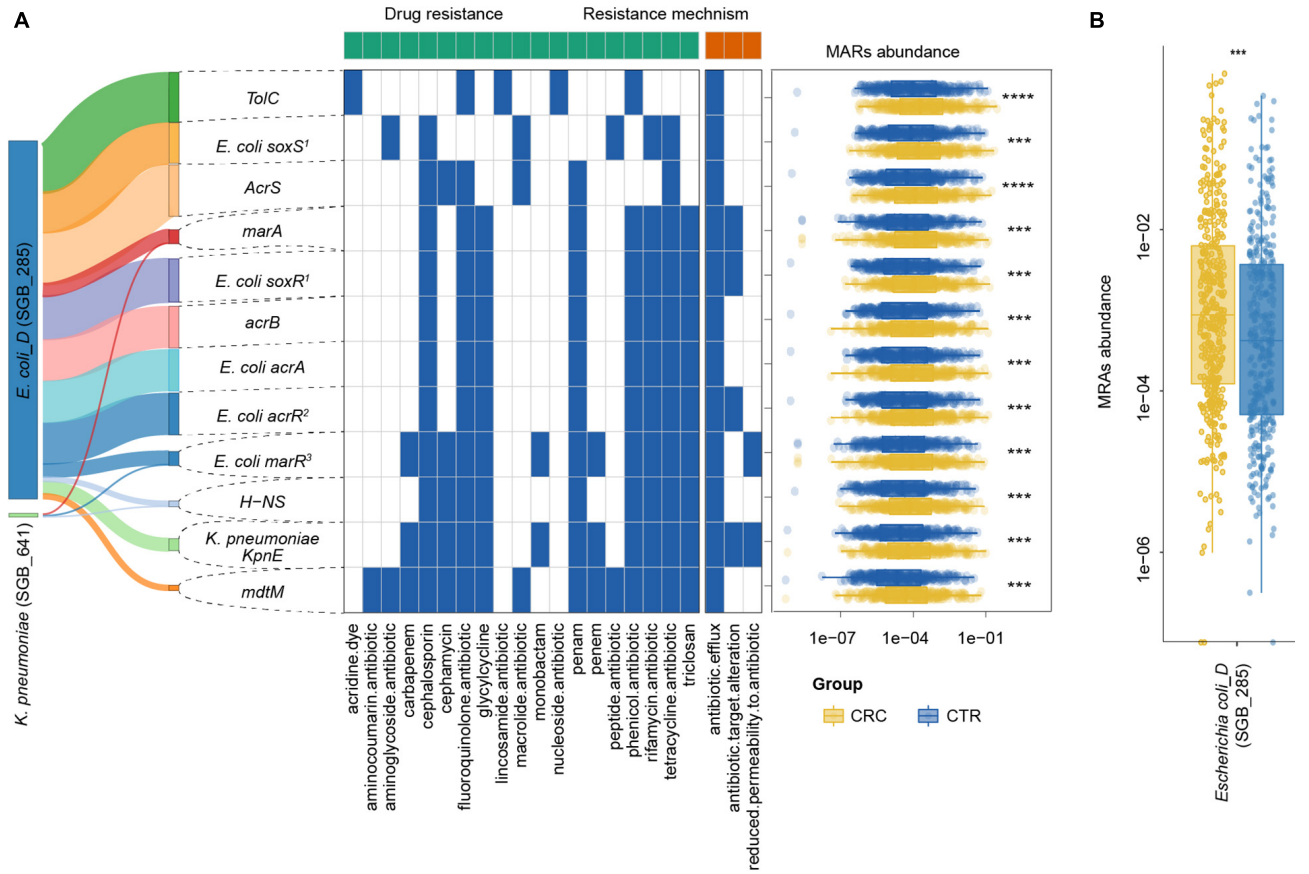


**FIGURE 6 |** MRG distribution in the CRC and CTR groups. **(A)** Distribution, resistance drug types, and resistance mechanism of MRGs in CRC (yellow color) and CTR (blue color) groups. The left Sankey showed the source percentage of MARs. The middle heatmap exhibited the drug resistance type and mechanism of MARs. The blue color denoted MAR had that characteristic. The right boxplot showed the abundance of MARs. **(B)** MRGs in *Escherichia coli* (SGB_285) were enriched in the CRC groups significantly. The following symbols denoted statistical significance: ***$p < 0.001$, ****$p < 0.0001$.

## Species Encoded by Antibiotic Resistance Genes Were Enriched in the Colorectal Cancer Group

We further analyzed the sum of ARG abundance in the CRC-associated and unassociated species, where species enriched in the CRC and CTR groups were denoted as the "CRC-associated" cluster and others as the "unassociated" cluster. In the CRC-associated cluster, there were 30% of species (18 of 60 species) carrying ARGs; accordingly, there were 27% of species (171 of 636 rSGBs) with ARGs in the unassociated cluster (**Figure 7A**). Among all ARG types, 61 ARG types are found in CRC-associated clusters, and 122 ARG types are in unassociated clusters, whereas 19 are common to both clusters (**Figure 7B**). Moreover, the results showed that the CRC-associated cluster and unassociated cluster were divided in the PCoA analysis (PERMANOVA analysis, $p = 0.01$, **Figure 7C**), and the total abundance of ARGs in the CRC-associated cluster was significantly higher than that in the unassociated cluster (Wilcoxon test, $p < 0.0001$, **Figure 7D**).

The analysis of ARG abundance in the CRC group reported that *E. coli*, *A. onderdonkii*, *P. distasonis*, and *A. finegoldii* had a relatively high abundance of ARGs (median value) (**Figure 7E**). Notably, these four species were also significantly enriched in the CRC groups, primarily *E. coli*, which was encoded by as many as 37 ARGs and 13 MRGs. Although the ARG type counts in the CRC-associated cluster were lower than that in the unassociated cluster, the former cluster carried a higher abundance of ARGs. Therefore, *E. coli* in the CRC-associated cluster may act as an antibiotic resistance reservoir in the gut microbiota because of its high abundance of drug resistance genes. Taken together, we reported here that more ARGs encoded CRC-associated species than unassociated species, and *E. coli* was a critical antibiotic reservoir in the gut.

## Predictive Effectiveness of Species and Antibiotic Resistance Genes

To demonstrate the plausible clinical prediction of ARGs and species, we next built a series of random-forest prediction models using all the species, rSGB-sourced ARGs, and these features enriched in two groups. First, we tested the classification effect of the abundance of species and ARGs. The results showed that the classification performance of species features (area under the

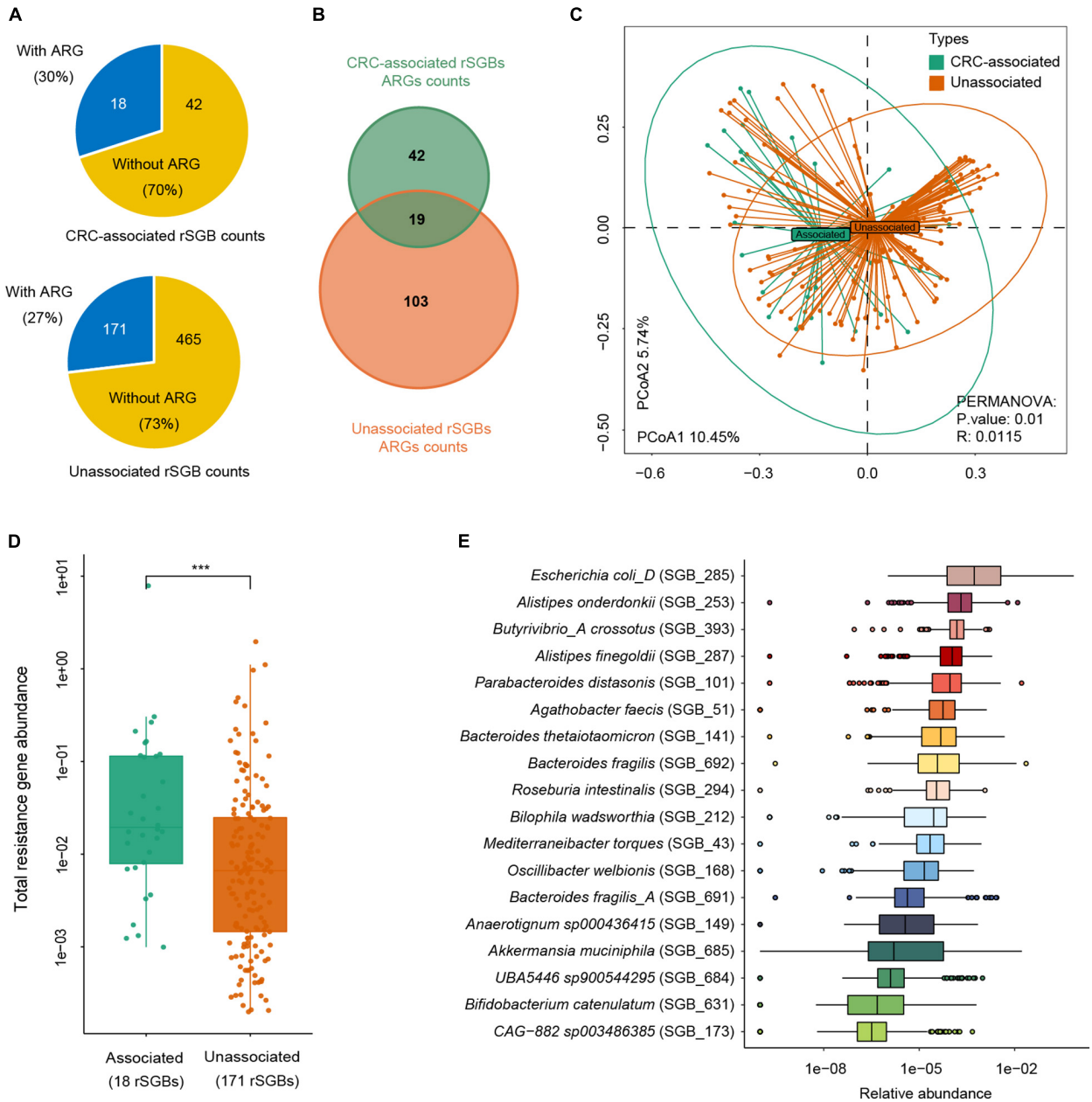


**FIGURE 7 |** Abundance difference of ARGs in rSGBs that associated with CRC or not. **(A)** The rSGB count and percentage in the CRC-associated and unassociated clusters; the blue or yellow colors represented the proportion of rSGBs with or without ARGs. **(B)** ARG counts in the CRC-associated and unassociated clusters. **(C)** PCoA plot depicting Bray–Curtis distances of ARG abundances in the CRC-associated (green color) and unassociated (dark yellow color) clusters. **(D)** Total ARG abundance in the CRC-associated (green color) and unassociated (dark yellow color) clusters (***$p < 0.001$). **(E)** Relative abundance of ARGs in every CRC-associated rSGBs in the CRC groups.

curve [AUC] = 0.802) outperformed that of the ARG features (AUC = 0.663) (**Supplementary Figures 9A,B**).

To improve the precision, we rebuilt two models using 118 selected species (32 carried ARGs) features and 19 selected ARG features, using the random forest method (**Supplementary Table 10** and **Supplementary Figures 9C,D**). From **Figure 8**, it could be observed that the species model was more effective (AUC = 0.831) than the ARGs model (AUC = 0.715), when classifying the CRC and CTR groups. Our species-based classification model performed better than the previous report, where the AUC ≥ 0.8 (Wirbel et al., 2019). The model accuracy based on ARG features in our study was approximate to that of a previously reported species model, although the accuracy of our model was unsatisfying (Thomas et al., 2019). In summary, species and ARGs in microbiota could predict CRC patients with modest precision.

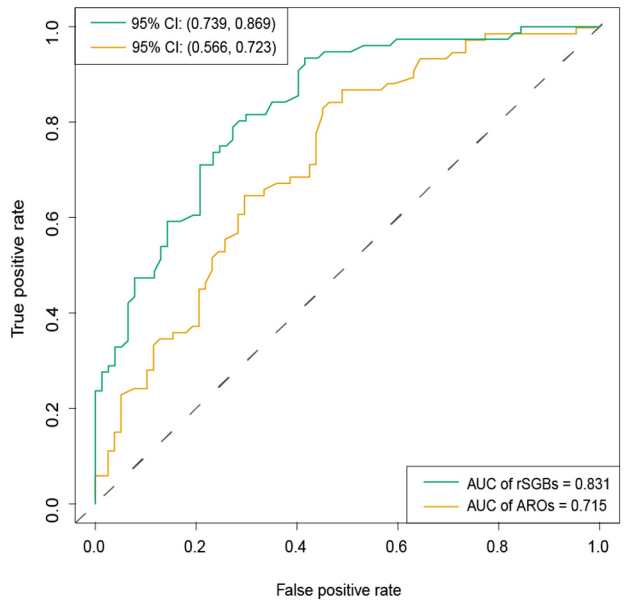


**FIGURE 8 |** AUC of classification model by selected rSGBs and ARGs features. The random forest model was built based on species (green color) and ARGs (dark yellow). CI, confidential interval.

## DISCUSSION

Antibiotic resistance is one of the most critical public health threats to human beings in recent years (Hernando-Amado et al., 2019). Although evidence has shown that antibiotic use may increase the risk of CRC, whether antibiotic resistance is also related is far from clear (Dik et al., 2016; Zhang et al., 2019; Armstrong et al., 2020; Wan et al., 2020). Here, we discovered 696 rSGBs, 24,692 plasmids, and 187 ARGs in the gut microbiota, where 25 species were enriched in the CRC group, and 13 species carried ARGs, such as *E. coli*, *A. onderdonkii*, *B. fragilis*, *A. muciniphila*, and *M. torques*. The abundance of ARGs was enriched in the CRC group, and *E. coli* was the essential ARG carrier.

To analyze the ARGs on the species level, we reconstructed the genomes *via* single-sample assembly from the metagenomes as reported in the literature (Pasolli et al., 2019; Zhu et al., 2019). However, plasmids also harbor many ARGs. It is reported that while the bacterial genome is assembled, its plasmids often remain unidentified because it is not clear which contigs in the genome assembly have arisen from plasmids (Antipov et al., 2016, 2019). We used metaplasmidSPAdes, which could identify novel plasmids and assemble plasmids from metagenomic data sets in order to annotate as many ARGs as possible.

With the species-level genomes reconstructed, representative genomes had a high genome quality of more than 90% completeness and less than 5% contamination. As a result, we found 25 species enriched in the CRC group, such as *E. coli*, *P. distasonis*, *A. muciniphila*, *B. thetaiotaomicron*, etc. These species had been reported to induce CRC by producing inflammatory polysaccharides, cell cycle inhibiting factors, and cytolethal distending toxins (Wassenaar, 2018; Sahankumari et al., 2019). For species enriched in the CTR group, mounting evidence showed the potential benefits of *F. prausnitzii* for improving intestinal healthy *via* producing butyrate (Ferreira-Halder et al., 2017; Kim et al., 2020). *B. catenulatum*, as a significant commensal bacterium of *F. prausnitzii*, could improve its growth, gut colonization, and butyrate production by producing short-chain fatty acids (Kim et al., 2020). Moreover, *Lachnospira eligens* (formerly *Eubacterium eligens*) could effectively suppress intestinal inflammation and prevent colitis and CRC (Feng et al., 2016). Although more than 90% of species we found had been reported or cultured before, we had also discovered unknown species enriched in the CRC group, such as *UBA5446 sp900544295* and *Anaerotignum sp000436415*, with both of the species carrying ARGs. It indicated that reconstructing genomes was useful to find out more species carrying ARGs and increased the probability of illustrating the ARG distribution in gut microbiota.

In these species of rSGBs, we detected 164 ARGs, which was slightly higher than another large cohort study on antibiotics (149 ARG types) (Hu et al., 2013). In our results, 30.49% of ARGs were enriched in the CRC group significantly. These CRC-associated species had a high antibiotic resistance abundance. The *adeF* gene was the largest abundant ARG in the CRC group. In another cohort of a healthy population, the highest abundance of ARG was *TcR* (Hu et al., 2013). The ARG abundance difference in different populations may be due to the disease-specific variations in antibiotic resistance under different antibiotic exposures (Shamsaddini et al., 2021).

Antibiotic resistance could be acquired *via* gut microbiota through the use of broad-spectrum antibiotics, including cephalosporins, fluoroquinolones, penams, and rifaximin, to name a few. We noticed that the nucleoside antibiotic type had the highest abundance of antibiotics, followed by the cephalosporins, macrolides, and phenicol antibiotic types. Although a previous meta-analysis reported no significant associations between CRC and some antibiotics, for example, quinolones, tetracyclines, and macrolide antibiotics (Wan et al., 2020), a significantly higher abundance of these antibiotic resistance drugs was detected in the CRC group. In this study, penams were significantly higher in the CRC group, which may be caused by higher penicillin usage in CRC patients (Wan et al., 2020). Another interesting finding was that we found no evident difference in resistance to rifaximin between the CRC and CTR groups. Rifaximin, a rifamycin antibiotic, was popularly used in travelers' diarrhea and irritable bowel syndrome. It had been reported to neither affect ARGs nor increase the ARG burden because the use of rifaximin would rarely bring about the development of drug resistance compared with other antibiotics (Shamsaddini et al., 2021). The high ARG burden in CRC patients suggested that it is recommended to consider possible antibiotic resistance when selecting appropriate antibiotic treatments, such as short-term alternating antibiotics and microbiome-based interventions (Dubinsky et al., 2020).

We found that ARGs were resistant to antibiotics in Reserve Class. Reserve Class antibiotics were treated as the "last resort"

options and usually used for highly selected patients (life-threatening infections due to multidrug-resistant bacteria). They were closely monitored and prioritized as targets of stewardship programs to ensure their continued effectiveness (World Health Organization, 2019). However, drug-resistance species in the CRC group were resistant to the "last resort" antibiotics, such as penems, glycylcyclines, and streptogramins. Increasing resistance of intestinal bacteria to "last resort" antibiotics reduces the number of antibiotics that can be used to control intestinal infections. Therefore, even the use of reserve group antibiotics still calls for caution.

Our study was limited to illustrating the association between CRC and antibiotic use for lacking information on antibiotic administration in these studies. A more directed study was needed to establish their association in the future. As our metagenomic data were collected from eight cohorts, the abundance of rSGBs and ARGs was affected by the host properties. Two cohorts were selected to analyze the abundance variation of rSGBs and ARGs, and consistent results were obtained. In our study, *E. coli* carried many MRGs and was significantly enriched in the CRC group. Although phylotype D *E. coli* (*E. coli D*) was one of these species with cyclomodulin-encoding genes and could produce cytotoxic necrotizing factors, phylotype B2 *E. coli* was the main strain associated with CRC (Wassenaar, 2018). Therefore, whether the phylotype D *E. coli* is associated with CRC warrants further investigation.

## CONCLUSION

We analyzed the species and ARGs distribution in the gut microbiota of CRC and CTR groups and found that the CRC group's gut microbiota had higher ARGs and MRG abundance than that of the CTR group. And bacteria with ARGs were enriched in the CRC group, such as *E. coli*, *P. distasonis*, *B. thetaiotaomicron*, and *B. fragilis*. Meanwhile, CRC-associated species carried abundant ARGs. *E. coli* was the primary antibiotic resistance reservoir of species in the CRC patients. Using species and ARGs could classify CRC patients from healthy controls. It showed that the gut microbiota in CRC patients could confer resistance to fluoroquinolones, cephalosporins, penams, and tetracyclines. Our investigation proposes antibiotic resistance guidance to CRC patients, and this may help develop antibiotic use strategies to reduce the detrimental effects of antibiotic resistance.

## MATERIALS AND METHODS

### Datasets and Samples Details

We downloaded a total of 769 metagenomic paired-end data, including 382 CRC patients (CRC group, aged 64 ± 11 years) and 387 healthy controls (CTR group, aged 61 ± 10 years) (**Table 1**). Data were selected from eight published studies with the NCBI SRA database accession codes PRJEB10878 (Yu et al., 2017), PRJNA389927 (Hannigan et al., 2018), PRJEB12449 (Vogtmann et al., 2016), PRJEB27928 (Wirbel et al., 2019), PRJEB6070 (Zeller et al., 2014), PRJNA447983 (Thomas et al., 2019), PRJEB7774 (Feng et al., 2015), and PRJDB4176 (Yachida et al., 2019). Participants who had a history of cancers, used antibiotics in the past period, or with gastrointestinal disease, including inflammatory bowel disease and intestinal infection, were excluded from the CTR groups (Zeller et al., 2014; Feng et al., 2015; Vogtmann et al., 2016; Yu et al., 2017; Hannigan et al., 2018; Thomas et al., 2019; Wirbel et al., 2019; Yachida et al., 2019). Basic information of participants, including gender, age, body mass index (BMI), vegetarian or not, smoking or not, health stat (health or CRC), and the American Joint Committee on Cancer Staging (AJCC Staging) information for CRC participation, was also collected (**Supplementary Table 1**).

### Metagenomes *de novo* Assembly, Binning, and Quality Evaluation

All the 769 paired-end fastq data went through quality control by fastp (Chen et al., 2018); the host sequence (human reference genome version: hg38) in the data was removed using soap2 (Li et al., 2009). Next, data were applied *de novo* assembled using metaSPAdes genome assembler (Nurk et al., 2017). Metagenomic binning was performed by MetaBAT2, which generated 36,461 bins in total. Completeness and contamination rates of bins were calculated by checkm qa workflow (Parks et al., 2015). We filtered bins into high-quality bins (completeness $>$ 90%, contamination $<$ 5%), medium-quality bins (completeness $>$ 50%, contamination $<$ 5%), and low-quality bins (the residual bins). To obtain more high-quality MAGs, we rebinned contigs using the same parameters mentioned previously for these contigs tagged "bin.unbinned" in the MetaBAT2 results and low-quality bins.

### Species-Level Genome Bin Cluster and Representation Selection

The completeness and contamination rates and the quality filtering of new bins were assessed again to remove low-completeness and high-contamination bins. Finally, we obtained 5,880 high-quality MAGs and 5,390 medium-quality MAGs. The 5,880 high-quality MAGs were clustered into species-level genome bins (SGBs) by a two-step clustering strategy based on genetic distance calculation by Metapi (Zhu et al., 2019). Then, representative genomes were selected for each cluster by SGB properties, including completeness, contamination, genome size, and strain heterogeneity index. The sequence with the maximal rank value was selected as representative genomes (rSGBs). The maximal rank value was computed according to a formula: $Rv = Cp - Ct + \log(Gs) - Th$, where $Rv$ means rank value, $Cp$ and $Ct$ represent completeness value and contamination value, and $Gs$ and $Th$ represent genome size and train heterogeneity.

### Taxonomy and Relative Abundance of Species

Taxonomy annotation for all the rSGBs was performed by GTDB-Tk (Chaumeil et al., 2019) based on the genome taxonomy database (GTDB, Release 95) (Parks et al., 2020). The high-quality reads were aligned to the rSGBs by bwa (default

parameters) (Li, 2013). Sequence-based contigs abundance profiling was performed by jgi_summarize_bam_contig_depths (default parameters) (Kang et al., 2019). Reads were mapped to the rSGBs, and the number of reads counted formed a mapping depth. Considering the different sequencing depths of different samples, we used the mapping depth matrix of normalization to estimate the abundances of contigs. For the rSGB profile, we used the species assignment of each contig from the rSGBs and took the median of the relative abundance of contigs from the same rSGBs to generate the abundance of certain rSGBs (**Supplementary Table 11**). Then the α diversity (Shannon–Wiener index) of relative abundance of species was computed by the vegan (Oksanen et al., 2018). Next, β diversity was computed by PCoA and NMDS based on ape packages (Paradis and Schliep, 2018).

## Plasmid Assembly and Acquisition of Non-redundant Gene Catalog in the Plasmids

To avoid the possible ARG omission in the progress of MAGs assembly, we assembled the whole plasmid sequence in the gut microbiota from the host genome and removed high-quality reads using the metaplasmidSPAdes assembler (Antipov et al., 2019). Then, we called the genes in the contigs by MetaGeneMark (Zhu et al., 2010) and processed the gene cluster to the genes by cd-hit (Li and Godzik, 2006) to get the non-redundant gene catalog of the plasmids. After that, we computed the relative abundance of non-redundant genes in all samples. The genes were annotated to the NCBI-NT database (20191213) to get the species source of plasmids.

## Antibiotic Resistance Gene Identity, Resistance Mechanism, and Drug Type Analysis

To annotate ARGs in rSGBs, we predicted the open reading frame by Prodigal (Hyatt et al., 2010) and then identified ARGs using Resistance Gene Identifier based on CARD (version 3.0.7) for both rSGBs and plasmid genes (Alcock et al., 2020). Then, antibiotic resistance ontology (ARG types) was matched to the species by contigs id. Based on the best hit antibiotic resistance ontology results, relative abundances of ARGs, drug types, and resistance mechanism types were obtained. In our research, the ARGs were used to represent ARGs types. We also matched resistance antibiotics of rSGBs to AWaRe classification according to the WHO AWaRe classification of antibiotics (2019 version) (**Supplementary Table 9**). We computed the α diversity (Shannon–Wiener index) of ARG relative abundance in the rSGBs by the vegan (Oksanen et al., 2018). Then, PCoA and NMDS were performed to compute β diversity by ape packages (Paradis and Schliep, 2018). Meanwhile, PERMANOVA was used to test the statistical significance of β diversity by the vegan package (Oksanen et al., 2018).

## Machine Learning Train Model

To assess the classification effect of species and rSGB-sourced ARGs, we built and trained a series of machine learning models using selected elements from relative abundance profiles of species and ARGs. Data splitting, preprocessing, feature selection, model training, model tuning, and variable importance estimation were finished using the caret package (Kuhn, 2020). Before model training, near-zero variance and high correlation (absolute value of correlations coefficient $> 0.75$), variables were removed. And then, data were centered and scaled. Next, the 10-fold cross-validation approach was used to select features, and random forest methods were applied to train models. Finally, we assessed the effect of models by the area under the receiver operating characteristic curve (AUC) value using the ROCR package (Sing et al., 2005).

## Statistical Analysis

During the analysis, we carried out Wilcoxon test and LefSe analysis for the relative abundance of all species (Segata et al., 2011), with cutoff $p < 0.05$ and absolute values of the LDA score $> 2.0$ (**Supplementary Table 6**). Then, we analyzed the ARG profile by calculating Wilcoxon test with a cutoff of adjusted $p < 0.05$. Finally, 50 ARGs were filtered from rSGBs. To access the effect of ARGs in the CRC-associated species, we marked the selected 60 species above as "CRC-associated" cluster and other species with ARGs as "unassociated" cluster. And then, we compared the sum of ARG abundance in these two clusters, and then a PCoA analysis was performed on the classes. During the analysis and figure visualization, ggplot2 (Wickham, 2016), ggtree (Yu, 2020), ggpubr (Kassambara, 2020), and networkD3 (Allaire et al., 2017) packages were used in our study.

# DATA AVAILABILITY STATEMENT

All the 5880 SGBs and 696 rSGBs data in this study have been deposited into CNGB Sequence Archive (CNSA) (Guo et al., 2020) of China National GeneBank DataBase (CNGBdb) (Chen et al., 2020) with accession number CNP0001862.

# ETHICS STATEMENT

The studies involving human participants were reviewed and approved by the Ethical Clearance the Institutional Review Board of BGI. Written informed consent for participation was not required for this study in accordance with the national legislation and the institutional requirements.

# AUTHOR CONTRIBUTIONS

CL and ZL downloaded and analyzed the data. CL wrote the manuscript. JD modified the manuscript. HZ and CN gave beneficial advice. ZL and MF conceived the study and commented on the manuscript. All authors contributed to the article and approved the submitted version.

## FUNDING

This research was supported by the National Key Research and Development Program of China (No. 2020YFC2002902) and the National Natural Science Foundation of China (No. 31800765).

## SUPPLEMENTARY MATERIAL

The Supplementary Material for this article can be found online at: https://www.frontiersin.org/articles/10.3389/fmicb.2021.765291/full#supplementary-material

## REFERENCES

Ai, D., Pan, H., Li, X., Gao, Y., Liu, G., and Xia, L. C. (2019). Identifying gut microbiota associated with colorectal cancer using a zero-inflated lognormal model. *Front. Microbiol.* 10:826. doi: 10.3389/fmicb.2019.00826

Alcock, B. P., Raphenya, A. R., Lau, T. T. Y., Tsang, K. K., Bouchard, M., Edalatmand, A., et al. (2020). CARD 2020: antibiotic resistome surveillance with the comprehensive antibiotic resistance database. *Nucleic Acids Res.* 48, D517–D525. doi: 10.1093/nar/gkz935

Allaire, J. J., Gandrud, C., Russell, K., and Yetman, C. (2017). *networkD3: D3 JavaScript Network Graphs from R*. R package version 0.4. Available online at: https://CRAN.R-project.org/package=networkD3

Antipov, D., Hartwick, N., Shen, M., Raiko, M., Lapidus, A., and Pevzner, P. A. (2016). plasmidSPAdes: assembling plasmids from whole genome sequencing data. *Bioinformatics* 32, 3380–3387. doi: 10.1093/bioinformatics/btw493

Antipov, D., Raiko, M., Lapidus, A., and Pevzner, P. A. (2019). Plasmid detection and assembly in genomic and metagenomic data sets. *Genome Res.* 29, 961–968. doi: 10.1101/gr.241299.118

Armstrong, D., Dregan, A., Ashworth, M., White, P., McGee, C., and de Lusignan, S. (2020). The association between colorectal cancer and prior antibiotic prescriptions: case control study. *Br. J. Cancer* 122, 912–917. doi: 10.1038/s41416-019-0701-705

Becattini, S., Taur, Y., and Pamer, E. G. (2016). Antibiotic-Induced changes in the intestinal microbiota and disease. *Trends Mol. Med.* 22, 458–478. doi: 10.1016/j.molmed.2016.04.003

Bernstein, C. N., Eliakim, A., Fedail, S., Fried, M., Gearry, R., Goh, K. L., et al. (2016). World gastroenterology organisation global guidelines inflammatory bowel disease: update August 2015. *J. Clin. Gastroenterol.* 50, 803–818. doi: 10.1097/MCG.0000000000000660

Cao, Y., Wu, K., Mehta, R., Drew, D. A., Song, M., Lochhead, P., et al. (2018). Long-term use of antibiotics and risk of colorectal adenoma. *Gut* 67, 672–678. doi: 10.1136/gutjnl-2016-313413

Casals-Pascual, C., Vergara, A., and Vila, J. (2018). Intestinal microbiota and antibiotic resistance: perspectives and solutions. *Hum. Microbiome J.* 9, 11–15. doi: 10.1016/j.humic.2018.05.002

Chaumeil, P. A., Mussig, A. J., Hugenholtz, P., and Parks, D. H. (2019). GTDB-Tk: a toolkit to classify genomes with the genome taxonomy database. *Bioinformatics* 36, 1925–1927. doi: 10.1093/bioinformatics/btz848

Chen, F. Z., You, L. J., Yang, F., Wang, L. N., Guo, X. Q., Gao, F., et al. (2020). CNGBdb: China national genebank database. *Yi Chuan* 42, 799–809. doi: 10.16288/j.yczz.20-080

Chen, S., Zhou, Y., Chen, Y., and Gu, J. (2018). fastp: an ultra-fast all-in-one FASTQ preprocessor. *Bioinformatics* 34, i884–i890. doi: 10.1093/bioinformatics/bty560

Cheng, Y., Ling, Z., and Li, L. (2020). The intestinal microbiota and Colorectal Cancer. *Front. Immunol.* 11:615056. doi: 10.3389/fimmu.2020.615056

Coyne, S., Rosenfeld, N., Lambert, T., Courvalin, P., and Perichon, B. (2010). Overexpression of resistance-nodulation-cell division pump AdeFGH confers multidrug resistance in *Acinetobacter baumannii*. *Antimicrob. Agents Chemother.* 54, 4389–4393. doi: 10.1128/AAC.00155-110

Crockett, S. D., and Nagtegaal, I. D. (2019). Terminology, molecular features, epidemiology, and management of serrated colorectal neoplasia. *Gastroenterology* 157, 949–966.e4. doi: 10.1053/j.gastro.2019.06.041.

Dai, Z., Zhang, J., Wu, Q., Chen, J., Liu, J., Wang, L., et al. (2019). The role of microbiota in the development of colorectal cancer. *Int. J. Cancer* 145, 2032–2041. doi: 10.1002/ijc.32017

Dik, V. K., van Oijen, M. G., Smeets, H. M., and Siersema, P. D. (2016). Frequent use of antibiotics is associated with colorectal cancer risk: results of a nested case-control study. *Dig. Dis. Sci,* 61, 255–264. doi: 10.1007/s10620-015-3828-3820

Dubinsky, V., Reshef, L., Bar, N., Keizer, D., Golan, N., Rabinowitz, K., et al. (2020). Predominantly antibiotic-resistant intestinal microbiome persists in patients with pouchitis who respond to antibiotic therapy. *Gastroenterology* 158, doi: 10.1053/j.gastro.2019.10.001 610-624 e613.

Feng, Q., Liang, S., Jia, H., Stadlmayr, A., Tang, L., Lan, Z., et al. (2015). Gut microbiome development along the colorectal adenoma-carcinoma sequence. *Nat. Commun.* 6:6528. doi: 10.1038/ncomms7528

Feng, Q., Zhang, D., Liu, C., Xiao, L., Tang, L., and Wang, J. (2016). *Use of Eubacterium in the Prevention and Treatment for Colorectal Cancer Related Diseases*. Geneva: World Intellectual Property Organization. PCT/CN2014/083689.

Ferlay, J., Colombet, M., Soerjomataram, I., Parkin, D. M., Piñeros, M., Znaor, A., et al. (2021). Cancer statistics for the year 2020: an overview. *Int. J. Cancer* doi: 10.1002/ijc.33588 [Online ahead of print].

Ferreira-Halder, C. V., Faria, A. V. S., and Andrade, S. S. (2017). Action and function of *Faecalibacterium prausnitzii* in health and disease. *Best Pract. Res. Clin. Gastroenterol.* 31, 643–648. doi: 10.1016/j.bpg.2017.09.011

Gao, Z., Guo, B., Gao, R., Zhu, Q., and Qin, H. (2015). Microbiota disbiosis is associated with colorectal cancer. *Front. Microbiol.* 6:20. doi: 10.3389/fmicb.2015.00020

Guo, X., Chen, F., Gao, F., Li, L., Liu, K., You, L., et al. (2020). CNSA: a data repository for archiving omics data. *Database (Oxford)* 2020:baaa055. doi: 10.1093/database/baaa055

Hannigan, G. D., Duhaime, M. B., Ruffin, M. T. T., Koumpouras, C. C., and Schloss, P. D. (2018). Diagnostic potential and interactive dynamics of the colorectal cancer virome. *mBio* 9:e02248-18 doi: 10.1128/mBio.02248-2218.

Hernando-Amado, S., Coque, T. M., Baquero, F., and Martinez, J. L. (2019). Defining and combating antibiotic resistance from one health and global health perspectives. *Nat. Microbiol.* 4, 1432–1442. doi: 10.1038/s41564-019-0503-509

Hu, Y., Yang, X., Qin, J., Lu, N., Cheng, G., Wu, N., et al. (2013). Metagenome-wide analysis of antibiotic resistance genes in a large cohort of human gut microbiota. *Nat. Commun.* 4:2151. doi: 10.1038/ncomms3151

Hyatt, D., Chen, G.-L., LoCascio, P. F., Land, M. L., Larimer, F. W., and Hauser, L. J. (2010). Prodigal: prokaryotic gene recognition and translation initiation site identification. *BMC Bioinformatics* 11:119. doi: 10.1186/1471-2105-11-119

Kang, D. D., Li, F., Kirton, E., Thomas, A., Egan, R., An, H., et al. (2019). MetaBAT 2: an adaptive binning algorithm for robust and efficient genome reconstruction from metagenome assemblies. *PeerJ* 7:e7359. doi: 10.7717/peerj.7359

Kassambara, A. (2020). *ggpubr: 'ggplot2' Based Publication Ready Plots. R Package Version 0.4.0*. Available online at: https://CRAN.R-project.org/package=ggpubr

Kim, H., Jeong, Y., Kang, S., You, H. J., and Ji, G. E. (2020). Co-Culture with bifidobacterium catenulatum improves the growth, gut colonization, and butyrate production of *Faecalibacterium prausnitzii*: in vitro and in vivo studies. *Microorganisms* 8:788. doi: 10.3390/microorganisms8050788

Kuhn, M. (2020). *caret: Classification and Regression Training. R package Version 6.0-86*. Available online at: https://CRAN.R-project.org/package=caret

Li, R., Yu, C., Li, Y., Lam, T. W., Yiu, S. M., Kristiansen, K., et al. (2009). SOAP2: an improved ultrafast tool for short read alignment. *Bioinformatics* 25, 1966–1967. doi: 10.1093/bioinformatics/btp336

Li, W., and Godzik, A. (2006). Cd-hit: a fast program for clustering and comparing large sets of protein or nucleotide sequences. *Bioinformatics* 22, 1658–1659. doi: 10.1093/bioinformatics/btl158

Li, H. (2013). Aligning sequence reads, clone sequences and assembly contigs with BWA-MEM. *arXiv* [Preprint]. arXiv:1303.3997. Available online at: https://arxiv.org/abs/1303.3997v2 (accesed May 26, 2013).

Ma, C., Chen, K., Wang, Y., Cen, C., Zhai, Q., and Zhang, J. (2021). Establishing a novel colorectal cancer predictive model based on unique gut microbial single

nucleotide variant markers. *Gut Microbes* 13, 1–6. doi: 10.1080/19490976.2020.1869505

Nitzan, O., Elias, M., Peretz, A., and Saliba, W. (2016). Role of antibiotics for treatment of inflammatory bowel disease. *World J. Gastroenterol.* 22, 1078–1087. doi: 10.3748/wjg.v22.i3.1078

Nurk, S., Meleshko, D., Korobeynikov, A., and Pevzner, P. A. (2017). metaSPAdes: a new versatile metagenomic assembler. *Genome Res.* 27, 824–834. doi: 10.1101/gr.213959.116

Oksanen, J., Blanchet, F. G., Friendly, M., Kindt, R., Legendre, P., McGlinn, D., et al. (2018). *vegan: Community Ecology Package. Ordination Methods, Diversity Analysis and Other Functions for Community and Vegetation Ecologists. Version 2.5-1*. Available online at: https://CRAN.R-project.org/package=vegan

Paradis, E., and Schliep, K. (2018). ape 5.0: an environment for modern phylogenetics and evolutionary analyses in R. *Bioinformatics* 35, 526–528. doi: 10.1093/bioinformatics/bty633

Parker, B. J., Wearsch, P. A., Veloo, A. C. M., and Rodriguez-Palacios, A. (2020). The genus alistipes: gut bacteria with emerging implications to inflammation, cancer, and mental health. *Front. Immunol.* 11:906. doi: 10.3389/fimmu.2020.00906

Parks, D. H., Chuvochina, M., Chaumeil, P.-A., Rinke, C., Mussig, A. J., and Hugenholtz, P. (2020). A complete domain-to-species taxonomy for Bacteria and Archaea. *Nat. Biotechnol.* 38, 1079–1086. doi: 10.1038/s41587-020-0501-508

Parks, D. H., Imelfort, M., Skennerton, C. T., Hugenholtz, P., and Tyson, G. W. (2015). CheckM: assessing the quality of microbial genomes recovered from isolates, single cells, and metagenomes. *Genome Res.* 25, 1043–1055. doi: 10.1101/gr.186072.114

Pasolli, E., Asnicar, F., Manara, S., Zolfo, M., Karcher, N., Armanini, F., et al. (2019). Extensive unexplored human microbiome diversity revealed by over 150,000 genomes from metagenomes spanning age, geography, and lifestyle. *Cell* 176, 649-662.e20. doi: 10.1016/j.cell.2019.01.001.

Sahankumari, A., Gamage, B. D., and Malavige, G. N. (2019). Association of the gut microbiota with colorectal cancer in a South Asian cohort of patients. *bioRxiv* [Preprint]. doi: 10.1101/694125

Schwartz, D. J., Langdon, A. E., and Dantas, G. (2020). Understanding the impact of antibiotic perturbation on the human microbiome. *Genome Med.* 12:82. doi: 10.1186/s13073-020-00782-x

Segata, N., Izard, J., Waldron, L., Gevers, D., Miropolsky, L., Garrett, W. S., et al. (2011). Metagenomic biomarker discovery and explanation. *Genome Biol.* 12:R60. doi: 10.1186/gb-2011-12-6-r60

Shamsaddini, A., Gillevet, P. M., Acharya, C., Fagan, A., Gavis, E., Sikaroodi, M., et al. (2021). Impact of antibiotic resistance genes in gut microbiome of patients with cirrhosis. *Gastroenterology* 161, 508-521.e7. doi: 10.1053/j.gastro.2021.04.013

Sing, T., Sander, O., Beerenwinkel, N., and Lengauer, T. (2005). ROCR: visualizing classifier performance in R. *Bioinformatics* 21, 3940–3941. doi: 10.1093/bioinformatics/bti623

Theochari, N. A., Stefanopoulos, A., Mylonas, K. S., and Economopoulos, K. P. (2018). Antibiotics exposure and risk of inflammatory bowel disease: a systematic review. *Scand. J. Gastroenterol.* 53, 1–7. doi: 10.1080/00365521.2017.1386711

Thomas, A. M., Manghi, P., Asnicar, F., Pasolli, E., Armanini, F., Zolfo, M., et al. (2019). Metagenomic analysis of colorectal cancer datasets identifies cross-cohort microbial diagnostic signatures and a link with choline degradation. *Nat. Med.* 25, 667–678. doi: 10.1038/s41591-019-0405-407

Van Boeckel, T. P., Gandra, S., Ashok, A., Caudron, Q., Grenfell, B. T., Levin, S. A., et al. (2014). Global antibiotic consumption 2000 to 2010: an analysis of national pharmaceutical sales data. *Lancet Infect. Dis.* 14, 742–750. doi: 10.1016/s1473-3099(14)70780-70787

Vogtmann, E., Hua, X., Zeller, G., Sunagawa, S., Voigt, A. Y., Hercog, R., et al. (2016). Colorectal Cancer and the human gut microbiome: reproducibility with whole-genome shotgun sequencing. *PLoS One* 11:e0155362. doi: 10.1371/journal.pone.0155362

Wan, Q. Y., Zhao, R., Wang, Y., Wu, Y., and Wu, X. T. (2020). Antibiotic use and risk of colorectal cancer: a meta-analysis of 412 450 participants. *Gut* 69, 2059–2060. doi: 10.1136/gutjnl-2020-320826

Wang, J. L., Chang, C. H., Lin, J. W., Wu, L. C., Chuang, L. M., and Lai, M. S. (2014). Infection, antibiotic therapy and risk of colorectal cancer: a nationwide nested case-control study in patients with Type 2 diabetes mellitus. *Int. J. Cancer* 135, 956–967. doi: 10.1002/ijc.28738

Wassenaar, T. M. (2018). E. coli and colorectal cancer: a complex relationship that deserves a critical mindset. *Crit. Rev. Microbiol.* 44, 619–632. doi: 10.1080/1040841X.2018.1481013

Wickham, H. (2016). *ggplot2: Elegant Graphics for Data Analysis*. New York, NY: Springer-Verlag.

Wirbel, J., Pyl, P. T., Kartal, E., Zych, K., Kashani, A., Milanese, A., et al. (2019). Meta-analysis of fecal metagenomes reveals global microbial signatures that are specific for colorectal cancer. *Nat. Med.* 25, 679–689. doi: 10.1038/s41591-019-0406-406

Wong, S. H., and Yu, J. (2019). Gut microbiota in colorectal cancer: mechanisms of action and clinical applications. *Nat. Rev. Gastroenterol. Hepatol.* 16, 690–704. doi: 10.1038/s41575-019-0209-208

World Health Organization (2019). *The 2019 WHO AWaRe Classification of Antibiotics for Evaluation and Monitoring of Use*. Geneva: World Health Organization.

Xing, C., Wang, M., Ajibade, A. A., Tan, P., Fu, C., Chen, L., et al. (2021). Microbiota regulate innate immune signaling and protective immunity against cancer. *Cell Host Microbe* 29, 959–974.e7. doi: 10.1016/j.chom.2021.03.016

Yachida, S., Mizutani, S., Shiroma, H., Shiba, S., Nakajima, T., Sakamoto, T., et al. (2019). Metagenomic and metabolomic analyses reveal distinct stage-specific phenotypes of the gut microbiota in colorectal cancer. *Nat. Med.* 25, 968–976. doi: 10.1038/s41591-019-0458-457

Yang, J., McDowell, A., Kim, E. K., Seo, H., Lee, W. H., Moon, C. M., et al. (2019). Development of a colorectal cancer diagnostic model and dietary risk assessment through gut microbiome analysis. *Exp. Mol. Med.* 51, 1–15. doi: 10.1038/s12276-019-0313-314

Yeoh, Y. K., Chen, Z., Wong, M. C. S., Hui, M., Yu, J., Ng, S. C., et al. (2020). Southern Chinese populations harbour non-nucleatum Fusobacteria possessing homologues of the colorectal cancer-associated FadA virulence factor. *Gut* 69, 1998–2007. doi: 10.1136/gutjnl-2019-319635

Yu, G. (2020). Using ggtree to visualize data on tree-like structures. *Curr. Protoc. Bioinformatics* 69, e96. doi: 10.1002/cpbi.96

Yu, J., Feng, Q., Wong, S. H., Zhang, D., Liang, Q. Y., Qin, Y., et al. (2017). Metagenomic analysis of faecal microbiome as a tool towards targeted non-invasive biomarkers for colorectal cancer. *Gut* 66, 70–78. doi: 10.1136/gutjnl-2015-309800

Zeller, G., Tap, J., Voigt, A. Y., Sunagawa, S., Kultima, J. R., Costea, P. I., et al. (2014). Potential of fecal microbiota for early-stage detection of colorectal cancer. *Mol. Syst Biol.* 10:766. doi: 10.15252/msb.20145645

Zhang, J., Haines, C., Watson, A. J. M., Hart, A. R., Platt, M. J., Pardoll, D. M., et al. (2019). Oral antibiotic use and risk of colorectal cancer in the United Kingdom, 1989-2012: a matched case-control study. *Gut* 68, 1971–1978. doi: 10.1136/gutjnl-2019-318593

Zhang, Y., Yu, X., Yu, E., Wang, N., Cai, Q., Shuai, Q., et al. (2018). Changes in gut microbiota and plasma inflammatory factors across the stages of colorectal tumorigenesis: a case-control study. *BMC Microbiol.* 18:92. doi: 10.1186/s12866-018-1232-1236

Zhu, J., Tian, L., Chen, P., Han, M., Song, L., Tong, X., et al. (2019). Over 50000 metagenomically assembled draft genomes for the human oral microbiome reveal new taxa. *bioRxiv* [Preprint]. doi: 10.1101/820365

Zhu, W., Lomsadze, A., and Borodovsky, M. (2010). Ab initio gene identification in metagenomic sequences. *Nucleic Acids Res.* 38:e132. doi: 10.1093/nar/gkq275

**Conflict of Interest:** All authors were employed by company BGI-Shenzhen.

**Publisher's Note:** All claims expressed in this article are solely those of the authors and do not necessarily represent those of their affiliated organizations, or those of the publisher, the editors and the reviewers. Any product that may be evaluated in this article, or claim that may be made by its manufacturer, is not guaranteed or endorsed by the publisher.

frontiers in Microbiology

ORIGINAL RESEARCH
published: 04 January 2022
doi: 10.3389/fmicb.2021.789280

# Whole-Genome Sequencing of Extended-Spectrum Beta-Lactamase-Producing *Escherichia coli* From Human Infections in Finland Revealed Isolates Belonging to Internationally Successful ST131-C1-M27 Subclade but Distinct From Non-human Sources

***Paula Kurittu[1]*, Banafsheh Khakipoor[1], Jari Jalava[2], Jari Karhukorpi[3] and Annamari Heikinheimo[1,4]***

*[1] Department of Food Hygiene and Environmental Health, Faculty of Veterinary Medicine, University of Helsinki, Helsinki, Finland, [2] Finnish Institute for Health and Welfare, Helsinki, Finland, [3] Eastern Finland Laboratory Centre Joint Authority Enterprise (ISLAB), Joensuu, Finland, [4] Finnish Food Authority, Seinäjoki, Finland*

OPEN ACCESS

***Edited by:***
*Jørgen J. Leisner,*
*University of Copenhagen, Denmark*

***Reviewed by:***
*Michael Brouwer,*
*Wageningen University and Research, Netherlands*
*Naouel Klibi,*
*Tunis El Manar University, Tunisia*
*Linda Falgenhauer,*
*University of Giessen, Germany*

***Correspondence:**
*Paula Kurittu*
*paula.kurittu@helsinki.fi*

***Specialty section:***
*This article was submitted to Antimicrobials, Resistance and Chemotherapy, a section of the journal Frontiers in Microbiology*

***Received:*** *04 October 2021*
***Accepted:*** *10 December 2021*
***Published:*** *04 January 2022*

***Citation:***
*Kurittu P, Khakipoor B, Jalava J, Karhukorpi J and Heikinheimo A (2022) Whole-Genome Sequencing of Extended-Spectrum Beta-Lactamase-Producing Escherichia coli From Human Infections in Finland Revealed Isolates Belonging to Internationally Successful ST131-C1-M27 Subclade but Distinct From Non-human Sources. Front. Microbiol. 12:789280. doi: 10.3389/fmicb.2021.789280*

Antimicrobial resistance (AMR) is a growing concern in public health, particularly for the clinically relevant extended-spectrum beta-lactamase (ESBL) and AmpC-producing Enterobacteriaceae. Studies describing ESBL-producing *Escherichia coli* clinical samples from Finland to the genomic level and investigation of possible zoonotic transmission routes are scarce. This study characterizes ESBL-producing *E. coli* from clinical samples in Finland using whole genome sequencing (WGS). Comparison is made between animal, food, and environmental sources in Finland to gain insight into potential zoonotic transmission routes and to recognize successful AMR genes, bacterial sequence types (STs), and plasmids. ESBL-producing *E. coli* isolates ($n$ = 30) obtained from the Eastern Finland healthcare district between 2018 and 2020 underwent WGS and were compared to sequences from non-human and healthy human sources ($n$ = 67) isolated in Finland between 2012 and 2018. A majority of the clinical isolates belonged to ST131 ($n$ = 21; 70%), of which 19 represented O25:H4 and *fimH*30 allele, and 2 O16:H5 and *fimH*41 allele. Multidrug resistance was common, and the most common *bla* gene identified was $bla_{CTX\text{-}M\text{-}27}$ ($n$ = 14; 47%) followed by $bla_{CTX\text{-}M\text{-}15}$ ($n$ = 10; 33%). $bla_{CTX\text{-}M\text{-}27}$ was identified in 13 out of 21 isolates representing ST131, with 12 isolates belonging to a recently discovered international *E. coli* ST131 C1-M27 subclade. Isolates were found to be genetically distinct from non-human sources with core genome multilocus sequence typing based analysis. Most isolates ($n$ = 26; 87%) possessed multiple replicons, with IncF family plasmids appearing in 27 (90%) and IncI1

in 5 (17%) isolates. IncF[F1:A2:B20] replicon was identified in 11, and IncF[F-:A2:B20] in 4 isolates. The results indicate the ST131-C1-M27 clade gaining prevalence in Europe and provide further evidence of the concerning spread of this globally successful pathogenic clonal group. This study is the first to describe ESBL-producing *E. coli* in human infections with WGS in Finland and provides important information on global level of the spread of ESBL-producing *E. coli* belonging to the C1-M27 subclade. The results will help guide public health actions and guide future research.

**Keywords: antimicrobial resistance, whole genome sequencing, extended-spectrum beta-lactamases, multidrug resistance, one health**

## INTRODUCTION

Antimicrobial resistance (AMR) is an increasing public health concern worldwide. Especially extended-spectrum beta-lactamase (ESBL) and AmpC-producing Enterobacteriaceae have spread globally, and infections caused by resistant bacteria are associated with prolonged hospital stays, increased mortality, and healthcare costs (Ray et al., 2018). Clinically relevant *Escherichia coli* and *Klebsiella pneumoniae* have also become common in community-acquired infections in recent years (Devi et al., 2020). The success of these pathogens is highly attributable to epidemic plasmids, which enable AMR spread *via* horizontal gene transfer (Mathers et al., 2015; Rozwandowicz et al., 2018). Transmission of ESBL-producing *E. coli* from animal, food, and environmental sources have previously been found to account for a limited amount of human ESBL-carriage in selected countries (Börjesson et al., 2016; Mughini-Gras et al., 2019), but gaps in knowledge regarding the wider epidemiology of these bacteria and the role in human carriage and infections still exist. Whole genome sequencing (WGS) allows for in-depth analysis of possible genetic links between different sources, and the role of plasmids in the spread of AMR.

Extraintestinal pathogenic *E. coli* (ExPEC) of sequence type (ST) 131 is a globally spread clonal lineage often associated with multidrug resistance (MDR), conferring resistance to ESBLs and fluoroquinolones (Nicolas-Chanoine et al., 2014). A recently recognized subclade within the dominant ST131 clade C, termed C1-M27, has emerged as a common cause of infection globally (Matsumura et al., 2016; Decano and Downing, 2019) but the occurrence of this subclade in Finland remains unknown.

Carbapenemase-producing *E. coli* isolates of human origin have been described using WGS in Finland previously (Räisänen et al., 2020), but to the best of our knowledge, publications covering ESBL-producing *E. coli* isolates from Finland of human clinical origin to a genomic level are scarce. WGS studies on healthy individuals have been conducted in Finland (Verkola et al., 2019; Gröndahl-Yli-Hannuksela et al., 2020) and a national surveillance program routinely implements only phenotypic characterization for ESBL-producers (Räisänen et al., 2019). The proportion of ESBL-producing *E. coli* in blood and urine specimens in patients in Finland has been relatively low, but steadily increasing during recent years (Räisänen et al., 2019). The national surveillance has found 7.3% of all blood specimens and 3.1 and 7.2% of urine specimens in women and men, respectively, positive for ESBL-producing *E. coli* in 2019. A study investigating fecal samples from healthy, adult volunteers in Finland found the prevalence of ESBL-producing *E. coli* or *K. pneumoniae* to be 6.3% (Gröndahl-Yli-Hannuksela et al., 2020). A gap in knowledge regarding *bla* genes and further genomic characterization of ESBL-producing *E. coli* isolates involved in clinical cases in Finland exists.

This study aimed to characterize ESBL-producing *E. coli* isolates obtained from clinical specimens in Finland. This involves genetic comparisons between previously sequenced isolates from healthy human, animal, food, and environmental sources in Finland to evaluate possible genetic overlap and provide genome-level information of the ESBL-producing *E. coli* found in Finland.

## MATERIALS AND METHODS

### Collection of Extended-Spectrum Beta-Lactamase-Producing *Escherichia coli* Isolates From Clinical Samples

Altogether 30 ESBL-producing *E. coli* strains were obtained retrospectively from the Eastern Finland Laboratory Centre Joint Authority Enterprise (ISLAB), covering the healthcare district in Eastern Finland. The samples were part of routine practice collected during 2018–2020 from clinical samples, each originating from a different patient. Stored samples were recultivated in March 2020 and transported to the University of Helsinki for further studies with Copan M40 Transystem sterile transport swabs (Copan Transystem, Copan Diagnostics, Italy).

Briefly, antimicrobial susceptibility testing for specimens other than blood and urine was performed using disk diffusion method according to European Committee on Antimicrobial Susceptibility Testing (EUCAST) standards with third-generation cephalosporins (cefpodoxime, ceftazidime, and ceftriaxone), together with amoxicillin-clavulanic acid (Oxoid, Basingstoke, Hampshire, United Kingdom). Specimens other than blood and urine consisted of samples originating from various body sites and tissue types, including joint, scrotum, maxillary sinus, eye conjunctiva, wound, bile, abscess, bronchoalveolar lavage, and abdominal cavity. Additionally, combination disk method (cefotaxime 30 μg and cefotaxime 30 μg + clavulanic acid 10 μg; ceftazidime 30 μg and ceftazidime 30 μg + clavulanic acid 10 μg) and AmpC disk test (Mast Group

Ltd., Bootle, United Kingdom) were used for presumptive ESBL-producing *E. coli* isolates. Susceptibility testing for urine samples was performed with a Vitek 2 AST-N385 card (bioMeriéux, Marcy-L'Etoile, France), and for blood samples with both Vitek 2 and disk diffusion method according to EUCAST standards, to ensure rapid and accurate diagnosis in possible septicaemia cases.

## DNA Extraction and Sequencing

Bacterial DNA was extracted and purified with a PureLink Genomic DNA Mini Kit (Invitrogen by Thermo Fischer Scientific, Carlsbad, CA, United States) according to manufacturer's instructions. The assessment of DNA quality was carried out using a NanoDrop ND-1000 spectrophotometer (Thermo Fischer Scientific, Wilmington, DE, United States) and DNA quantity was measured using a Qubit 2.0 fluorometer (Invitrogen, Life Technologies, Carlsbad, CA, United States). An optical density of 1.8–2.0 at 260/280 nm and a concentration of $\geq$10 ng/μl with a minimum amount of 0.2 μg were set as thresholds. Library preparation was performed with NEBNext Ultra DNA Library Prep Kit for Illumina (Cat No. E7370L). Sequencing was performed with an Illumina NovaSeq 6000 (Novogene, Cambridge, United Kingdom) with 100 × coverage and 2 × 150 bp read length and a Phred score of Q30 $\geq$ 80%.

Raw reads have been deposited in the European Nucleotide Archive (ENA) at EMBL-EBI under accession number PRJEB47797. Accession numbers are provided in **Supplementary Table 1**.

## Bioinformatic Analyses

Bacterial DNA sequences were analyzed with Ridom SeqSphere+ software v7.0.4 (Ridom GmbH, Germany) (Jünemann et al., 2013) and Center for Genomic Epidemiology (CGE) web-based tools (DTU, Denmark) available at http://www.genomicepidemiology.org. Within Ridom SeqSphere+ pipeline, raw reads were assembled with SKESA v2.3.0 (Souvorov et al., 2018) together with quality control with FastQC v0.11.7 (Babraham Institute, 2021) and adapter trimming with Trimmomatic v0.36 (Bolger et al., 2014), AMR genes were identified with NCBI AMRFinderPlus v3.2.3 (Feldgarden et al., 2019), virulence genes with VFDB (Chen et al., 2016), and ST with *E. coli* MLST Warwick v1.0 (Achtman scheme) based on the PubMLST database (Jolley et al., 2018). Sequences from isolates with novel STs were submitted to the Enterobase database[1] (Zhou et al., 2020) to assign new Achtman scheme STs.

Using default values, PlasmidFinder 2.0 (Carattoli et al., 2014) was employed to detect plasmid replicons and pMLST 2.0 (Carattoli et al., 2014) the plasmid multilocus ST for IncF and IncI1 type replicons. FimTyper 1.0 (Roer et al., 2017) was used to identify the *fimH* allele. ResFinder 4.1 (Camacho et al., 2009; Zankari et al., 2017; Bortolaia et al., 2020), SerotypeFinder 2.0 (Joensen et al., 2015), MLST 2.0 (Larsen et al., 2012), and VirulenceFinder 2.0 (Joensen et al., 2014; Tetzschner et al., 2020) were used to confirm acquired resistance genes, serotype, and ST, respectively.

[1]https://enterobase.warwick.ac.uk/

### Determination of C1-M27 Clade-Specific Prophage-Like Regions

Isolates were compared with BLASTn to strain KUN5781 (GenBank accession: LC209430) (Matsumura et al., 2016) to determine the presence of M27-C1 clade-specific prophage-like regions M27PP1 and M27PP2. Results were visualized with BRIG v0.95 (Alikhan et al., 2011) for isolates with matching regions.

### Core Genome Multilocus Sequence Typing-Based Genetic Comparison

Core genome multilocus sequence typing (cgMLST) targeting 2520 genes was performed using Ridom SeqSphere+ software v7.0.4 (Ridom GmbH, Germany) (Jünemann et al., 2013) to compare all 30 isolates obtained from ISLAB and results were visualized with a minimum spanning tree (MST).

Isolates were also compared to available previously sequenced ESBL/AmpC-producing *E. coli* isolates from Finland (total $n$ = 67) collected between 2012 and 2018 from broiler meat ($n$ = 5) (Päivärinta et al., 2020), broiler caecum ($n$ = 5) (Päivärinta et al., 2020), broiler production including broiler parents ($n$ = 8) (Oikarainen et al., 2019), egg surfaces ($n$ = 4) (Oikarainen et al., 2019) and production environment ($n$ = 1) (Oikarainen et al., 2019), imported food products ($n$ = 16) (Kurittu et al., 2021a), barnacle geese ($n$ = 9) (Kurittu et al., 2021b), wastewater ($n$ = 1) (unpublished), cattle ($n$ = 1) (Päivärinta et al., 2016), veterinarians ($n$ = 9) (Verkola et al., 2019), and healthy adults ($n$ = 8) (Gröndahl-Yli-Hannuksela et al., 2020; **Supplementary Table 2**). cgMLST-based MST and was constructed with Ridom SeqSphere+ software.

# RESULTS

## Extended-Spectrum Beta-Lactamase-Producing *Escherichia coli* From Clinical Samples

Altogether 30 *E. coli* isolates obtained from human clinical samples confirmed as ESBL-producing with phenotypic screening from the Eastern Finland healthcare district between 2018 and 2020 were subjected to WGS. Most isolates ($n$ = 12; 40%) originated from a urine sample, followed by blood samples ($n$ = 8; 27%). A majority of the isolates ($n$ = 21; 70%) belonged to ST131, with the remaining nine isolates representing a different ST each, including ST38, ST1193, ST162, ST537, ST59, and ST405 (**Table 1**). A novel ST was identified in three isolates and the sequences were submitted to the Enterobase database (see text footnote 1) to assign new Achtman scheme STs. The newly assigned STs were as follows: ST12704, ST12703, and ST12705 for isolates D2, D4, and D9, respectively. Sequences from two isolates from previous studies, A41.2-1 and C76.1-2 (Kurittu et al., 2021a), were additionally submitted to Enterobase to assign new Achtman scheme STs. All ST131 isolates from the current study were of serotype O25:H4 and possessed the *fimH*30 allele, except for two isolates, which belonged to serotype O16:H5 and possessed the *fimH*41 allele.

**TABLE 1 |** Genomic characterization of 30 ESBL-producing *Escherichia coli* isolates obtained from human clinical samples in the Eastern Finland healthcare district during 2018–2020.

| Sample | Sample type | Sequence type | Serotype | *fimH* type | *bla* gene(s) | Plasmid replicon(s) | pMLST | Year of isolation |
|---|---|---|---|---|---|---|---|---|
| D1 | Urine | ST131 | O25:H4 | *fimH*30 | $bla_{CTX\text{-}M\text{-}27}$ | IncFIA, IncFIB, IncFIB(H89-PhagePlasmid), IncFII(pRSB107), IncX4 | [F1:A2:B20] | 2020 |
| D2 | Joint | ST12704 | O4:H27 | *fimH*2 | $bla_{CTX\text{-}M\text{-}15}$ | IncFIA, IncFIB, IncFII(pRSB107) | [F1:A1:B10] | 2018 |
| D3 | Scrotum | ST38 | O1:H15 | *fimH*65 | $bla_{CTX\text{-}M\text{-}27}$ | IncFIA, IncFIB, IncFII(pRSB107), Col(BS512), Col156 | [F1:A2:B20] | 2018 |
| D4 | Maxillary sinus | ST12703 | O18:H7* | *fimH*18 | $bla_{CTX\text{-}M\text{-}14}$, $bla_{TEM\text{-}1}$ | IncFIB | [F46:A-:B20] | 2018 |
| D5 | Eye conjunctiva | ST1193 | O75:H5 | *fimH*64 | $bla_{CTX\text{-}M\text{-}55}$ | IncB/O/K/Z, Col(BS512), Col(MG828) | – | 2019 |
| D6 | Wound | ST131 | O25:H4 | *fimH*30 | $bla_{CTX\text{-}M\text{-}15}$, $bla_{TEM\text{-}1}$ | IncFIA, IncFIB, IncFII(pRSB107), Col156 | [F1:A2:B20] | 2019 |
| D7 | Blood | ST131 | O25:H4 | *fimH*30 | $bla_{CTX\text{-}M\text{-}15}$, $bla_{OXA\text{-}1}$ | No plasmid replicons found | – | 2019 |
| D8 | Bile | ST131 | O16:H5 | *fimH*41 | $bla_{CTX\text{-}M\text{-}27}$ | IncFIA, IncFIB, IncFII(pRSB107), IncX3, IncY, Col(BS512), Col156 | [F1:A2:B20] | 2019 |
| D9 | Abscess | ST12705 | O16:H5 | *fimH*41 | $bla_{CTX\text{-}M\text{-}15}$, $bla_{TEM\text{-}1}$ | IncFIB, IncFIB(H89-PhagePlasmid), IncFII(29), IncFII(pCoo) | [F29:A-:B10] | 2019 |
| D10 | Blood | ST131 | O25:H4 | *fimH*30 | $bla_{CTX\text{-}M\text{-}15}$ | IncFIA, IncFIB, Col(BS512) | [F36:A1:B20]** | 2019 |
| D11 | Lung (bronchoalveolar lavage) | ST131 | O25:H4 | *fimH*30 | $bla_{CTX\text{-}M\text{-}27}$ | IncFIA, IncFIB, IncFII(pRSB107), Col156 | [F1:A2:B20] | 2019 |
| D12 | Urine | ST131 | O25:H4 | *fimH*30 | $bla_{CTX\text{-}M\text{-}27}$ | IncFIA, IncFIB, IncFII(pRSB107), IncI1 | [F1:A2:B20] | 2020 |
| D13 | Urine | ST131 | O25:H4 | *fimH*30 | $bla_{CTX\text{-}M\text{-}27}$ | IncB/O/K/Z, IncFIA, IncFIB, IncFII, IncFII(pRSB107), Col156, Col8282 | [F84:A2:B20]** | 2019 |
| D14 | Blood | ST162 | O8:H19 | *fimH*32 | $bla_{SHV\text{-}12}$ | IncFIA, IncFIC(FII), IncI1, IncQ1 | [F18:A6:B-]**/ST26 CC-2 | 2019 |
| D15 | Urine | ST131 | O25:H4 | *fimH*30 | $bla_{CTX\text{-}M\text{-}15}$ | IncFII, IncI1 | [F2:A-:B-]/ST173 | 2019 |
| D16 | Urine | ST131 | O25:H4 | *fimH*30 | $bla_{CTX\text{-}M\text{-}27}$ | IncFIA, IncFIB, IncFII(pRSB107), Col156 | [F1:A2:B20] | 2019 |
| D17 | Abdominal cavity | ST537 | O75:H5 | *fimH*5 | $bla_{TEM\text{-}52}$ | IncI1 | ST36/CC-3** | 2019 |
| D18 | Urine | ST59 | O1:H7 | *fimH*41 | $bla_{CTX\text{-}M\text{-}55}$, $bla_{TEM\text{-}1}$ | IncFII(pCoo) | [F10:A-:B-] | 2019 |
| D19 | Urine | ST405 | O2:H4 | *fimH*56 | $bla_{CTX\text{-}M\text{-}3}$ | IncFIB, IncFII(29), IncI1, Col(BS512), Col156, Col156, Col156 | [F29:A-:B10]/ST57 CC-5 | 2019 |
| D20 | Blood | ST131 | O25:H4 | *fimH*30 | $bla_{CTX\text{-}M\text{-}27}$ | IncFIA, IncFIB, IncFII(pRSB107), Col156 | [F1:A2:B20] | 2020 |
| D21 | Blood | ST131 | O25:H4 | *fimH*30 | $bla_{CTX\text{-}M\text{-}27}$ | IncFIA, IncFIB, IncFII(pRSB107) | [F1:A2:B20]** | 2020 |
| D22 | Urine | ST131 | O25:H4 | *fimH*30 | $bla_{CTX\text{-}M\text{-}27}$ | IncFIA, IncFIB, Col(pHAD28), Col156 | [F-:A2:B20] | 2020 |
| D23 | Wound | ST131 | O25:H4 | *fimH*30 | $bla_{CTX\text{-}M\text{-}15}$ | IncFIA, IncFIB, Col(BS512) | [F-:A1:B20]** | 2020 |
| D24 | Urine | ST131 | O25:H4 | *fimH*30 | $bla_{CTX\text{-}M\text{-}15}$, $bla_{OXA\text{-}1}$ | IncFIA, IncFIB, IncX4, Col156 | [F-:A2:B20] | 2020 |
| D25 | Blood | ST131 | O25:H4 | *fimH*30 | $bla_{CTX\text{-}M\text{-}27}$ | IncFIA, IncFIB | [F-:A2:B20] | 2020 |
| D26 | Urine | ST131 | O25:H4 | *fimH*30 | $bla_{CTX\text{-}M\text{-}27}$ | IncFIA, IncFIB, IncFIB(H89-PhagePlasmid), IncFII(pRSB107), IncI1 | [F1:A2:B20]/IncI1 unknown | 2020 |

*(Continued)*

**TABLE 1 |** (Continued)

| Sample | Sample type | Sequence type | Serotype | *fimH* type | *bla* gene(s) | Plasmid replicon(s) | pMLST | Year of isolation |
|---|---|---|---|---|---|---|---|---|
| D27 | Blood | ST131 | O25:H4 | *fimH*30 | $bla_{CTX\text{-}M\text{-}15}$ | IncFIA, IncFIB, Col(BS512) | [F22:A1:B20]** | 2020 |
| D28 | Blood | ST131 | O16:H5 | *fimH*41 | $bla_{CTX\text{-}M\text{-}15}$, $bla_{TEM\text{-}1}$ | IncFIB, IncFII(29), Col156 | [F29:A-:B10] | 2020 |
| D29 | Urine | ST131 | O25:H4 | *fimH*30 | $bla_{CTX\text{-}M\text{-}27}$ | IncFIA, IncFIB, IncFII(pRSB107), Col156 | [F1:A2:B20] | 2020 |
| D30 | Urine | ST131 | O25:H4 | *fimH*30 | $bla_{CTX\text{-}M\text{-}27}$ | IncFIA, IncFIB, Col(pHAD28), Col156 | [F-:A2:B20] | 2020 |

*SerotypeFinder 2.0 (Center for Genomic Epidemiology) used to verify result.
**Uncertain hit, ST cannot be trusted.

All isolates were found to match their respective phenotype genotypically, as all were genotypically confirmed to carry at least one *bla* gene representing an ESBL phenotype. The most common *bla* gene identified was $bla_{CTX\text{-}M\text{-}27}$ ($n$ = 14; 47%) followed by $bla_{CTX\text{-}M\text{-}15}$ ($n$ = 10; 33%). $bla_{CTX\text{-}M\text{-}27}$ was identified in 13 out of the 21 isolates representing ST131 and additionally from one isolate of ST 38. Eight out of the 10 $bla_{CTX\text{-}M\text{-}15}$ were harbored by ST131, with 7 representing the serotype O25:H4 together with *fimH* allele 30, while 1 was of serotype O16:H5 with *fimH*41 allele. Two isolates of novel STs, ST12704 (isolate D2) and ST12705 (isolate D9), were found to possess $bla_{CTX\text{-}M\text{-}15}$. Regarding other $bla_{CTX-M}$ genes, $bla_{CTX\text{-}M\text{-}55}$ occurred in two isolates (D5 of ST1193 and D18 of ST59), and $bla_{CTX\text{-}M\text{-}14}$ and $bla_{CTX\text{-}M\text{-}3}$ each in one isolate each (D4 of ST12703 and D19 of ST405, respectively). $bla_{SHV\text{-}12}$ was found from one isolate (D14) of ST 162 and $bla_{TEM\text{-}52}$ from one isolate (D17) of ST 537.

All isolates were found to harbor at least one plasmid replicon, except for D7, from which no replicons were identified. Altogether 17 different replicons were detected with IncFIB ($n$ = 24), IncFIA ($n$ = 21), IncFII ($n$ = 13), and Col156 ($n$ = 13) type replicons were most prevalent. The majority of the isolates ($n$ = 26; 87%) possessed multiple replicons, with IncF family plasmids appearing in 27 (90%) isolates. IncI1 plasmids were recovered from five isolates (D14, D15, D17, D19, and D26), all with varying pMLST profiles. Plasmids of pMLST IncF[F1:A2:B20] type were identified in 11 isolates, and pMLST IncF[F-:A2:B20] in 4 isolates.

Multidrug resistance, resistance to at least one agent in three or more antimicrobial categories (Magiorakos et al., 2012), was common among the isolates with multiple acquired resistance genes identified in 21 (70%) isolates, including genes against aminoglycosides, tetracycline, sulfonamides, macrolides, and trimethoprim (**Table 2**). Acquired sulfonamide resistance genes, *sul1* and *sul2*, were found either alone or together in 18 (60%) of the isolates.

Genes conferring trimethoprim resistance, either *dfrA17*, *dfrA12*, *dfrA1*, or *dfrA14*, were detected in 16 (53%) isolates. Of these genes, *dfrA17* was the most prevalent ($n$ = 11; 37%), followed by *dfrA12* ($n$ = 3; 10%). *dfrA1* and *dfrA14* appeared in one isolate each.

Aminoglycoside resistance [*aadA5*, *aadA2*, *aph(3″)-Ib*, *aph(6)-Id*, and/or *aac(6′)-Ib-cr*] was detected in 20 (67%) isolates and tetracycline resistance in 18 (60%) isolates [*tet*(A) in 17 and *tet*(M) in one isolate]. No carbapenemase genes were detected.

Chromosomal quinolone resistance mutations in *gyrA*, *parC*, *parE*, or *marR* were recovered from 27 of the 30 isolates, whereas plasmid-mediated quinolone resistance (PMQR) gene *aac(6′)-Ib-cr* was additionally identified in two isolates (D7 and D24). Chromosomal mutations in *ptsI* and *uhpt* associated with fosfomycin resistance were discovered in 23 (77%) isolates.

All the isolates harbored multiple virulence factors, with extraintestinal pathogenic *E. coli* (ExPEC) associated virulence genes (Johnson et al., 2003) *pap* (P fimbrial adhesin), *kpsMII* (polysialic acid transport protein; group 2 capsule), *iutA* (ferric aerobactin receptor), and *sfa* (S and F1C fimbriae) recovered from 29, 28, 26, and 18 isolates, respectively. Only isolate D2 lacked the previously described threshold of two or more of the five virulence genes (*pap*, *kps*, *iutA*, *sfa*/*foc*, *afa*/*dra*) defined as discriminatory for ExPEC classification (Johnson et al., 2003; Kanamori et al., 2017). No Shiga toxin (*stx*) genes were found. Virulence factors are presented according to their pathogenicity factor groups (Nesta et al., 2012; Pitout, 2012; Chen et al., 2016; Sarowska et al., 2019; Duan et al., 2020; Dekker et al., 2021) in **Table 2** together with resistance genes other than *bla*.

Assembly statistics including the number of bases and contigs, the N50 value and average coverage for each isolate are available in **Supplementary Table 3**.

## Identification of C1-M27 Clade-Specific Prophage-Like Regions

All 12 ST131 *E. coli* isolates with $bla_{CTX\text{-}M\text{-}27}$ and *fimH*30 allele were found to possess the C1-M27 clade-specific prophage-like 11,894-bp region M27PP1 together with the 7 bp direct repeats (Matsumura et al., 2016; **Figure 1**). Four of these 12 samples additionally possessed the 19,352-bp prophage-like region M27PP2.

## Core Genome Multilocus Sequence Typing Comparison of Human Extended-Spectrum Beta-Lactamase-Producing *Escherichia coli* Isolates From the Eastern Finland Healthcare District

All of the 30 human ESBL-producing *E. coli* isolates obtained from the Eastern Finland healthcare district were compared with a cgMLST-based MST (**Figure 2**). Results indicate isolates

**TABLE 2 |** Virulence and antimicrobial resistance genes other than *bla* identified in 30 ESBL-producing *Escherichia coli* isolates obtained from Finnish patients collected in the Eastern Finland healthcare district during 2018–2020.

| | | | | Virulence factors | | | | |
|---|---|---|---|---|---|---|---|---|
| **Sample** | **Acquired resistance genes other than *bla*** | **Fosfomycin resistance mutations** | **Quinolone resistance mutations** | **Adherence** | **Invasion** | **Iron uptake** | **Toxins** | **Effector delivery system** |
| D1 | *aadA5, aph(3″)-Ib, aph(6)-Id, mph*(A), *sul1, sul2, tet*(A), *dfrA17* | *ptsI* (V25I), *uhpT* (E350Q) | *gyrA* (D87N), *gyrA* (S83L), *parC* (E84V), *parC* (S80I), *parE* (I529L) | *fimA, fimC, fimD, fimE, fimF, fimG, fimH, fimI, papB, papI, yagV/ecpE, yagW/ecpD, yagX/ecpC, yagY/ecpB, yagZ/ecpA, ykgK/ecpR* | *aslA, kpsD, kpsM, ompA* | *chuA, chuS, chuT, chuU, chuV, chuW, chuX, chuY, entB, entC, entE, entF, entS, fdeC, fepA, fepB, fepC, fepD, fepG, fes, iucA, iucB, iucC, iutA* | *sat* | |
| D2 | *aph(3″)-Ib, aph(6)-Id, mph*(A), *sul2, dfrA14* | Not found | Not found | *fimA, fimB, fimC, fimD, fimE, fimF, fimG, fimH, fimI, yagV/ecpE, yagW/ecpD, yagX/ecpC, yagY/ecpB, yagZ/ecpA, ykgK/ecpR* | *aslA, ibeA, kpsD, kpsM, ompA* | *chuA, chuS, chuT, chuU, chuV, chuW, chuX, chuY, entB, entC, entD, entE, entS, fdeC, fepA, fepB, fepC, fepD, fepG, fes* | *pic, set1A, set1B, vat* | |
| D3 | *aadA5, aph(3″)-Ib, aph(6)-Id, mph*(A), *sul1, sul2, tet*(A), *dfrA17* | Not found | *gyrA* (D87N), *gyrA* (S83L), *parC* (S80I) | *fdeC, fimA, fimB, fimC, fimD, fimE, fimF, fimG, fimH, fimI, papB, papI, papX, sfaX, yagV/ecpE, yagW/ecpD, yagX/ecpC, yagY/ecpB, yagZ/ecpA, ykgK/ecpR* | *aslA, kpsD, kpsM, ompA* | *chuA, chuS, chuT, chuU, chuV, chuW, chuX, chuY, entB, entC, entD, entE, entS, fepA, fepB, fepC, fepD, fepG, fes, iucA, iucB, iucC, iutA* | *sat* | *espL1, espL4, espR1, espX1, espX4, espX5, espY1, espY2, espY3, espY4* |
| D4 | *tet*(M) | Not found | *marR* (S3N) | *fdeC, fimA, fimB, fimC, fimD, fimE, fimF, fimG, fimH, fimI, focC, focD, focF, focI, papB, papC, papD, papF, papI, papJ, papK, sfaA, sfaB, sfaC, sfaD, sfaE, sfaF, sfaG, sfaH, sfaS, sfaY, yagV/ecpE, yagW/ecpD, yagX/ecpC, yagY/ecpB, yagZ/ecpA, ykgK/ecpR* | *aslA, ibeA, kpsD, kpsM, kpsT, ompA* | *chuA, chuS, chuT, chuU, chuV, chuW, chuX, chuY, entB, entC, entD, entE, entS, fepA, fepB, fepC, fepD, fepG, fes, iroB, iroC, iroD, iroE, iroN* | *cnf1, hlyA, hlyB, hlyC, hlyD, vat* | |
| D5 | Not found | *uhpT* (E350Q) | *gyrA* (D87N), *gyrA* (S83L), *marR* (S3N), *parC* (S80I), *parE* (L416F) | *fdeC, fimA, fimB, fimC, fimD, fimE, fimF, fimG, fimH, fimI, papB, papI, papX, sfaX, yagV/ecpE, yagW/ecpD, yagX/ec, yagY/ecpB, yagZ/ecpA, ykgK/ecpR* | *aslA, kpsD, kpsM, kpsT, ompA* | *chuA, chuS, chuT, chuU, chuV, chuW, chuX, chuY, entB, entC, entE, entS, fepA, fepB, fepC, fepD, fepG, fes, iucA, iucB, iucC, iutA* | *sat, vat* | |
| D6 | *aadA5, aph(3″)-Ib, aph(6)-Id, mph*(A), *sul1, sul2, tet*(A), *dfrA17* | *ptsI* (V25I), *uhpT* (E350Q) | *gyrA* (D87N), *gyrA* (S83L), *parC* (E84V), *parC* (S80I), *parE* (I529L) | *fdeC, fimA, fimB, fimC, fimD, fimE, fimF, fimG, fimH, fimI, papB, papI, papX, sfaX, yagV/ecpE, yagW/ecpD, yagX/ecpC, yagY/ecpB, yagZ/ecpA, ykgK/ecpR* | *aslA, kpsM, ompA* | *chuA, chuS, chuT, chuU, chuV, chuW, chuX, chuY, entB, entC, entE, entF, entS, fepA, fepB, fepC, fepD, fepG, fes, iucA, iucB, iucC, iutA* | *sat* | |
| D7 | *aac(6′)-Ib-cr* | *ptsI* (V25I), *uhpT* (E350Q) | *gyrA* (D87N), *gyrA* (S83L), *parC* (E84V), *parC* (S80I), *parE* (I529L) | *fdeC, fimA, fimC, fimD, fimE, fimF, fimG, fimH, fimI, papC, papD, papF, papG, papJ, papK, yagV/ecpE, yagW/ecpD, yagX/ecpC, yagY/ecpB, yagZ/ecpA, ykgK/ecpR* | *aslA, kpsD, kpsM, ompA* | *chuA, chuS, chuT, chuU, chuV, chuW, chuX, chuY, entB, entC, entE, entF, entS, fepA, fepB, fepC, fepD, fepG, fes, iucA, iucB, iucC, iutA* | *cnf1, hlyA, hlyB, hlyC, hlyD, sat* | |

*(Continued)*

**TABLE 2 |** (Continued)

| Sample | Acquired resistance genes other than *bla* | Fosfomycin resistance mutations | Quinolone resistance mutations | Virulence factors | | | | |
|---|---|---|---|---|---|---|---|---|
| | | | | **Adherence** | **Invasion** | **Iron uptake** | **Toxins** | **Effector delivery system** |
| D8 | *aadA5, aph(3″)-Ib, aph(6)-Id, mph*(A), *sul1, sul2, tet*(A), *dfrA17* | *ptsI* (V25I), *uhpT* (E350Q) | *gyrA* (D87N), *gyrA* (S83L), *parC* (E84V), *parC* (S80I), *parE* (I529L) | *fdec, fimA, fimB, fimC, fimD, fimE, fimF, fimG, fimH, fimI, papB, papI, papX, sfaX, yagV/ecpE, yagW/ecpD, yagX/ecpC, yagY/ecpB, yagZ/ecpA, ykgK/ecpR* | *aslA, kpsD, kpsM, ompA* | *chuA, chuS, chuT, chuU, chuV, chuW, chuX, chuY, entB, entC, entE, entS, fepA, fepB, fepC, fepD, fepG, fes, iucA, iucB, iucC, iutA* | *sat, vat* | |
| D9 | Not found | *ptsI* (V25I), *uhpT* (E350Q) | *gyrA* (S83L), *parE* (I529L) | *fdeC, fimA, fimB, fimC, fimD, fimE, fimF, fimG, fimH, fimI, papB, papI, papX, sfaX, yagV/ecpE, yagW/ecpD, yagX/ecpC, yagY/ecpB, yagZ/ecpA, ykgK/ecpR* | *aslA, kpsD, kpsM, ompA* | *chuA, chuS, chuT, chuU, chuV, chuW, chuX, chuY, entB, entC, entE, entS, fepA, fepB, fepC, fepD, fepG, fes, iucA, iucB, iucC, iutA* | *sat* | |
| D10 | *aadA2, mph*(A), *sul1, tet*(A), *dfrA12* | *ptsI* (V25I), *uhpT* (E350Q) | *gyrA* (D87N), *gyrA* (S83L), *parC* (E84V), *parC* (S80I), *parE* (I529L) | *fdeC, fimA, fimC, fimD, fimE, fimF, fimG, fimH, fimI, papC, papD, papF, papG, papJ, papK, yagV/ecpE, yagW/ecpD, yagX/ecpC, yagY/ecpB, yagZ/ecpA, ykgK/ecpR* | *aslA, kpsD, kpsM, ompA* | *chuA, chuS, chuT, chuU, chuV, chuW, chuX, chuY, entB, entC, entE, entF, entS, fepA, fepB, fepC, fepD, fepG, fes, iucA, iucB, iucC, iutA* | *hlyA, hlyB, hlyC, hlyD, sat* | |
| D11 | *aadA5, aph(3″)-Ib, aph(6)-Id, mph*(A), *sul1, sul2, tet*(A), *dfrA17* | *ptsI* (V25I), *uhpT* (E350Q) | *gyrA* (D87N), *gyrA* (S83L), *parC* (E84V), *parC* (S80I), *parE* (I529L) | *fdeC, fimA, fimC, fimD, fimE, fimF, fimG, fimH, fimI, papB, papI, papX, sfaX, yagV/ecpE, yagW/ecpD, yagX/eC, yagY/ecpB, yagZ/ecpA, ykgK/ecpR* | *aslA, kpsD, kpsM, ompA* | *chuA, chuS, chuT, chuU, chuV, chuW, chuX, chuY, entB, entC, entE, entF, entS, fepA, fepB, fepC, fepD, fepG, fes, iucA, iucB, iucC, iutA* | *sat* | |
| D12 | *aadA5, aph(3″)-Ib, aph(6)-Id, mph*(A), *sul1, sul2, tet*(A) | *ptsI* (V25I), *uhpT* (E350Q) | *gyrA* (D87N), *gyrA* (S83L), *parC* (E84V), *parC* (S80I), *parE* (I529L) | *fimA, fimC, fimD, fimE, fimF, fimG, fimH, fimI, papB, papI, yagV/ecpE, yagW/ecpD, yagX/eC, yagY/ecpB, yagZ/ecpA, ykgK/ecpR* | *aslA, kpsD, kpsM, ompA* | *chuA, chuS, chuT, chuU, chuV, chuW, chuX, chuY, entB, entC, entE, entF, entS, fepA, fepB, fepC, fepD, fepG, fes, iucA, iucB, iucC, iutA* | *sat* | |
| D13 | Not found | Not found | *gyrA* (D87N), *gyrA* (S83L), *parC* (E84V), *parC* (S80I), *parE* (I529L) | *fdeC, fimA, fimC, fimD, fimE, fimF, fimG, fimH, fimI, papB, papX, sfaX, yagV/ecpE, yagW/ecpD, yagX/eC, yagY/ecpB, yagZ/ecpA, ykgK/ecpR* | *aslA, kpsD, kpsM, ompA* | *chuA, chuS, chuT, chuU, chuV, chuW, chuX, chuY, entB, entC, entE, entF, entS, fepA, fepB, fepC, fepD, fepG, fes, iucA, iucB, iucC, iutA* | *sat* | |
| D14 | *aadA2, aph(3″)-Ib, aph(6)-Id, mph*(B), *cmlA1, sul1, sul2, tet*(A), *dfrA1* | Not found | *gyrA* (D87N), *gyrA* (S83L), *parC* (S80I) | *fdeC, fimA, fimB, fimC, fimD, fimE, fimF, fimG, fimH, fimI, papC, yagV/ecpE, yagW/ecpD, yagX/eC, yagY/ecpB, yagZ/ecpA, ykgK/ecpR* | *ompA* | *entB, entC, entD, entE, entS, fepA, febB, fepC, fepD, fepG, fes, iucA, iucB, iucC, iutA* | *astA, east1* | *espX1, espX4, espX5* |
| D15 | Not found | *ptsI* (V25I), *uhpT* (E350Q) | *gyrA* (D87N), *gyrA* (S83L), *parC* (E84V), *parC* (S80I), *parE* (I529L) | *fdeC, fimA, fimC, fimD, fimE, fimF, fimG, fimH, fimI, papB, papI, papX, sfaX, yagV/ecpE, yagW/ecpD, yagX/eC, yagY/ecpB, yagZ/ecpA, ykgK/ecpR* | *aslA, kpsD, kpsM, ompA* | *chuA, chuS, chuT, chuU, chuV, chuW, chuX, chuY, entB, entC, entE, entF, entS, fepA, fepB, fepC, fepD, fepG, fes, iucA, iucB, iucC, iutA* | *sat* | |

*(Continued)*

**TABLE 2 |** (Continued)

| Sample | Acquired resistance genes other than *bla* | Fosfomycin resistance mutations | Quinolone resistance mutations | Virulence factors | | | | |
|---|---|---|---|---|---|---|---|---|
| | | | | Adherence | Invasion | Iron uptake | Toxins | Effector delivery system |
| D16 | *aadA5, aph(3″)-Ib, aph(6)-Id, mph*(A), *sul1, sul2, tet*(A), *dfrA17* | *ptsI* (V25I), *uhpT* (E350Q) | *gyrA* (D87N), *gyrA* (S83L), *parC* (E84V), *parC* (S80I), *parE* (I529L) | *fdeC, fimA, fimC, fimD, fimE, fimF, fimG, fimH, fimI, papB, papI, papX, sfaX, yagV/ecpE, yagW/ecpD, yagX/eC, yagY/ecpB, yagZ/ecpA, ykgK/ecpR* | *aslA, kpsD, kpsM, ompA* | *chuA, chuS, chuT, chuU, chuV, chuW, chuX, chuY, entB, entC, entE, entF, entS, fepA, fepB, fepC, fepD, fepG, fes, iucA, iucB, iucC, iutA* | *sat* | |
| D17 | Not found | Not found | *marR* (S3N) | *fdeC, fimA, fimC, fimD, fimE, fimF, fimG, fimH, fimI, yagV/ecpE, yagW/ecpD, yagX/eC, yagY/ecpB, yagZ/ecpA, ykgK/ecpR* | *aslA, ibeA, kpsD, kpsM, ompA* | *chuA, chuS, chuT, chuU, chuV, chuW, chuX, chuY, entB, entC, entE, entS, fepA, fepB, fepC, fepD, fepG, fes* | *pic, set1A, set1B, vat* | |
| D18 | Not found | *uhpT* (E350Q) | Not found | *fimA, fimB, fimC, fimD, fimE, fimF, fimG, fimH, fimI, papX, sfax* | *aslA, kpsD, kpsM, kpsT, ompA* | *chuA, chuS, chuT, chuU, chuV, chuW, chuX, chuY, entB, entC, entE, entS, fepA, fepB, fepC, fepD, fepG, fes, iucA, iucB, iucC, iucD, iutA* | *sat* | *espL1, espR1, espX1, espX4, espY2, espY4* |
| D19 | Not found | Not found | Not found | *fdeC, fimA, fimB, fimC, fimD, fimE, fimF, fimG, fimH, fimI, papC, papD, papG, papI, papJ, papK, yagV/ecpE, yagW/ecpD, yagX/eC, yagZ/ecpA, ykgK/ecpR* | *aslA, kpsD, kpsM, ompA* | *chuA, chuS, chuT, chuU, chuV, chuW, chuX, chuY, entB, entC, entD, entE, entS, fepA, fepB, fepC, fepD, fepG, fes, iucA, iucB, iucC, iutA* | *hlyA, hlyB, hlyC, hlyD, sat* | *espL1, espL4, espX1, espX4, espX5, espY2, espY3, espY4* |
| D20 | *aph(3″)-Ib, aph(6)-Id, sul2, tet*(A) | *ptsI* (V25I), *uhpT* (E350Q) | *gyrA* (D87N), *gyrA* (S83L), *parC* (E84V), *parC* (S80I), *parE* (I529L) | *fdeC, fimA, fimC, fimD, fimE, fimF, fimG, fimH, fimI, papB, papI, papX, sfax, yagV/ecpE, yagW/ecpD, yagX/ecpC, yagY/ecpB, yagZ/ecpA, ykgK/ecpR* | *aslA, kpsD, kpsM, ompA* | *chuA, chuS, chuT, chuU, chuV, chuW, chuX, chuY, entB, entC, entE, entF, entS, fepA, fepB, fepC, fepD, fepG, fes, iucA, iucB, iucC, iutA* | *sat* | |
| D21 | Not found | *ptsI* (V25I), *uhpT* (E350Q) | *gyrA* (D87N), *gyrA* (S83L), *parC* (E84V), *parC* (S80I), *parE* (I529L) | *fdeC, fimA, fimC, fimD, fimE, fimF, fimG, fimH, fimI, papB, papI, papX, sfax, yagV/ecpE, yagW/ecpD, yagX/ecpC, yagY/ecpB, yagZ/ecpA, ykgK/ecpR* | *aslA, kpsD, kpsM* | *chuA, chuS, chuT, chuU, chuV, chuW, chuX, chuY, entB, entC, entE, entF, entS, fepA, fepB, fepC, fepD, fepG, fes, iucA, iucB, iucC, iutA* | *sat* | |
| D22 | *aadA5, aph(3″)-Ib, aph(6)-Id, mph*(A), *sul1, sul2, tet*(A), *dfrA17* | *ptsI* (V25I), *uhpT* (E350Q) | *gyrA* (D87N), *gyrA* (S83L), *parC* (E84V), *parC* (S80I), *parE* (I529L) | *fdeC, fimA, fimC, fimD, fimE, fimF, fimG, fimH, fimI, papB, papI, yagV/ecpE, yagW/ecpD, yagX/ecpC, yagY/ecpB, yagZ/ecpA, ykgK/ecpR* | *aslA, kpsD, kpsM, ompA* | *chuA, chuS, chuT, chuU, chuV, chuW, chuX, chuY, entB, entC, entE, entF, entS, fepA, fepB, fepC, fepD, fepG, fes, iucA, iucB, iucC, iutA* | *sat* | |
| D23 | *aadA2, mph(A), sul1, tet*(A), *dfrA12* | *ptsI* (V25I), *uhpT* (E350Q) | *gyrA* (D87N), *gyrA* (S83L), *parC* (E84V), *parC* (S80I), *parE* (I529L) | *fdeC, fimA, fimC, fimD, fimE, fimF, fimG, fimH, fimI, papC, papD, papF, papG, papJ, papK, yagV/ecpE, yagW/ecpD, yagX/ecpC, yagY/ecpB, yagZ/ecpA, ykgK/ecpR* | *aslA, kpsD, kpsM, ompA* | *chuA, chuS, chuT, chuU, chuV, chuW, chuX, chuY, entB, entC, entE, entF, entS, fepA, fepB, fepC, fepD, fepG, fes, iucA, iucB, iucC, iutA* | *hlyD, sat* | |

*(Continued)*

**TABLE 2 |** (Continued)

| Sample | Acquired resistance genes other than *bla* | Fosfomycin resistance mutations | Quinolone resistance mutations | Virulence factors | | | | |
|---|---|---|---|---|---|---|---|---|
| | | | | Adherence | Invasion | Iron uptake | Toxins | Effector delivery system |
| D24 | *aac(6′)-Ib-cr* | *ptsI* (V25I), *uhpT* (E350Q) | *gyrA* (D87N), *gyrA* (S83L), *parC* (E84V), *parC* (S80I), *parE* (I529L) | *fdeC, fimA, fimC, fimD, fimE, fimF, fimG, fimH, fimI, papB, papI, papX, sfaX, yagV/ecpE, yagW/ecpD, yagX/ecpC, yagY/ecpB, yagZ/ecpA, ykgK/ecpR* | *aslA, kpsD, kpsM, ompA* | *chuA, chuS, chuT, chuU, chuV, chuW, chuX, chuY, entB, entC, entE, entF, entS, fepA, fepB, fepC, fepD, fepG, fes, iucA, iucB, iucC, iutA* | *sat* | |
| D25 | *aadA5, aph(3″)-Ib, aph(6)-Id, mph*(A), *sul1, sul2, tet*(A), *dfrA17* | *ptsI* (V25I), *uhpT* (E350Q) | *gyrA* (D87N), *gyrA* (S83L), *parC* (E84V), *parC* (S80I), *parE* (I529L) | *fdeC, fimA, fimC, fimD, fimE, fimF, fimG, fimH, fimI, papB, papI, papX, sfax, yagV/ecpE, yagW/ecpD, yagX/ecpC, yagY/ecpB, yagZ/ecpA, ykgK/ecpR* | *aslA, kpsD, kpsM, ompA* | *chuA, chuS, chuT, chuU, chuV, chuW, chuX, chuY, entB, entC, entE, entF, entS, fepA, fepB, fepC, fepD, fepG, fes, iucA, iucB, iucC, iutA* | *sat* | |
| D26 | Not found | *ptsI* (V25I), *uhpT* (E350Q) | *gyrA* (D87N), *gyrA* (S83L), *parC* (E84V), *parC* (S80I), *parE* (I529L) | *fdeC, fimA, fimC, fimD, fimE, fimF, fimG, fimH, fimI, papB, papI, yagV/ecpE, yagW/ecpD, yagX/ecpC, yagY/ecpB, yagZ/ecpA, ykgK/ecpR* | *aslA, kpsD, kpsM, ompA* | *chuA, chuS, chuT, chuU, chuV, chuW, chuX, chuY, entB, entC, entE, entF, entS, fepA, fepB, fepC, fepD, fepG, fes, iucA, iucB, iucC, iutA* | *sat* | |
| D27 | *aadA2, mph*(A), *sul1, tet*(A), *dfrA12* | *ptsI* (V25I), *uhpT* (E350Q) | *gyrA* (D87N), *gyrA* (S83L), *parC* (E84V), *parC* (S80I), *parE* (I529L) | *fdeC, fimA, fimC, fimD, fimE, fimF, fimG, fimH, fimI, papC, papD, papF, papG, papJ, papK, yagV/ecpE, yagW/ecpD, yagX/ecpC, yagY/ecpB, yagZ/ecpA, ykgK/ecpR* | *aslA, kpsD, kpsM, ompA* | *chuA, chuS, chuT, chuU, chuV, chuW, chuX, chuY, entB, entC, entE, entF, entS, fepA, fepB, fepC, fepD, fepG, fes, iucA, iucB, iucC, iutA* | *cnf1, hlyA, hlyB, hlyC, hlyD, sat* | |
| D28 | *aadA5, aph(3″)-Ib, aph(6)-Id, mph*(A), *sul1, sul2, tet*(A), *dfrA17* | *ptsI* (V25I), *uhpT* (E350Q) | *gyrA* (S83L), *parE* (I529L) | *afaA, afaB-I, afaC-I, afaC-III, afaD, daaA, daaC, daaD, daaF, draA, draB, draC, draD, draP, fdeC, fimA, fimB, fimC, fimD, fimE, fimF, fimG, fimH, fimI, papB, papI, papX, sfaX, yagV/ecpE, yagW/ecpD, yagX/ecpC, yagY/ecpB, yagZ/ecpA, ykgK/ecpR* | *aslA, kpsD, kpsM, ompA* | *chuA, chuS, chuT, chuU, chuV, chuW, chuX, chuY, entB, entC, entE, entS, fepA, fepB, fepC, fepD, fepG, fes* | *hlyA, hlyB, hlyC, hlyD* | |
| D29 | *aadA5, aph(3″)-Ib, aph(6)-Id, mph*(A), *sul1, sul2, tet*(A), *dfrA17* | *ptsI* (V25I), *uhpT* (E350Q) | *gyrA* (D87N), *gyrA* (S83L), *parC* (E84V), *parC* (S80I), *parE* (I529L) | *fdeC, fimA, fimC, fimD, fimE, fimF, fimG, fimH, fimI, papB, papI, papX, sfaX, yagV/ecpE, yagW/ecpD, yagX/ecpC, yagY/ecpB, yagZ/ecpA, ykgK/ecpR* | *aslA, kpsD, kpsM, ompA* | *chuA, chuS, chuT, chuU, chuV, chuW, chuX, chuY, entB, entC, entE, entF, entS, fepA, fepB, fepC, fepD, fepG, fes, iucA, iucB, iucC, iutA* | *sat* | |
| D30 | *aadA5, aph(3″)-Ib, aph(6)-Id, mph*(A), *sul1, sul2, tet*(A), *dfrA17* | *ptsI* (V25I), *uhpT* (E350Q) | *gyrA* (D87N), *gyrA* (S83L), *parC* (E84V), *parC* (S80I), *parE* (I529L) | *fdeC, fimA, fimC, fimD, fimE, fimF, fimG, fimH, fimI, papB, papI, papX, sfaX, yagV/ecpE, yagW/ecpD, yagX/ecpC, yagY/ecpB, yagZ/ecpA, ykgK/ecpR* | *aslA, kpsD, kpsM, ompA* | *chuA, chuS, chuT, chuU, chuV, chuW, chuX, chuY, entB, entC, entE, entF, entS, fepA, fepB, fepC, fepD, fepG, fes, iucA, iucB, iucC, iutA* | *sat* | |

within ST131 form clusters, meaning allelic differences were ≤10, whereas isolates of different STs are genetically distant with allelic differences ranging from 640 to over 2000 between two isolates. Three different clusters were observed within isolates belonging to the ST131 C1-M27 clade: D11 and D16, D26 and D12, and D25 together with D30 and D22. Additionally, one cluster between three isolates (D23, D27, and D10) was identified, comprising isolates with the same ST (ST131), serotype (O25:H4), fimH type (*fimH*30), and AMR gene resistance profile [*aadA2*, $bla_{CTX\text{-}M\text{-}15}$, *mph*(A), *sul1*, *tet*(A), *dfrA12*].

## Core Genome Multilocus Sequence Typing Comparison to Previously Sequenced Extended-Spectrum Beta-Lactamase/AmpC-Producing *Escherichia coli* Isolates in Finland

The 30 human ESBL-producing *E. coli* isolates obtained from the Eastern Finland healthcare district were additionally compared to available, previously sequenced ESBL/AmpC-producing *E. coli* isolates obtained from different sources in Finland (**Figure 3**). A cgMLST-based MST included 2520 gene targets.

Isolates obtained in the current study failed to form close clusters with isolates recovered from earlier studies, although the least distance (24 allelic difference) was observed between isolate D30 and EL24E, an isolate from a healthy veterinarian volunteer. Both isolates were of ST 131 and harbored $bla_{CTX\text{-}M\text{-}27}$.

Other relatively close connections were also observed among isolates originating from human samples (18–44 allelic differences), all of ST 131, and positive for $bla_{CTX\text{-}M\text{-}15}$. Two isolates from the current study, D9 and D28, differed by 44 and 40 alleles, respectively, from SRR11638572, an isolate recovered from a healthy Finnish volunteer. Two veterinarian isolates from a previously published study, EL216E and EL256E, differed by 18 and 26 alleles, respectively, from the same Finnish volunteer sample.

In addition to clusters observed within the isolates from the current study, isolates originating from poultry production (Oikarainen et al., 2019) formed two clusters with samples from the same study, and broiler meat (isolates 5 and 33) and broiler caecum (Q11 and A12) (Päivärinta et al., 2020) formed a cluster each. C15, a $bla_{CMY-2}$-carrying ST1594 *E. coli* isolate from broiler caecum (Päivärinta et al., 2020), did not differ at all with cgMLST-based MST analysis from H58, an isolate originating from barnacle goose (Kurittu et al., 2021b).

# DISCUSSION

We used WGS to characterize 30 ESBL-producing *E. coli* isolates obtained from clinical samples in Eastern Finland and performed cgMLST-based genomic comparisons to ESBL/AmpC-producing *E. coli* isolates of human, animal, food, and environmental origins isolated in Finland previously. ESBL-producing *E. coli* isolates from human sources were found to be genetically distinct from non-human sources in Finland. However, most ST131 $bla_{CTX\text{-}M\text{-}27}$-positive *E. coli* isolates from human clinical samples were found to belong to a recently discovered international *E. coli* ST131 C1-M27 subclade, providing important insight to the epidemiology and increasing spread of this globally successful pathogenic clonal group. Strains within the C1-M27 clade carry $bla_{CTX\text{-}M\text{-}27}$, possess *fimH* allele 30 and a prophage-like genomic island termed M27PP1, sometimes together with another prophage-like region, M27PP2 (Matsumura et al., 2016). $bla_{CTX\text{-}M\text{-}27}$ has been noted to rival the globally dominant human-associated $bla_{CTX\text{-}M\text{-}15}$ in many parts of the world, having been isolated from human, animal, food, or environmental sources in multiple countries in Europe, North America, and Asia (Bevan et al., 2017).

ST131 has become the dominant ExPEC lineage causing infections in humans worldwide (Banerjee and Johnson, 2014; Nicolas-Chanoine et al., 2014; Mathers et al., 2015). Subclones of ST131 *E. coli*, mainly H30 and H30Rx, are associated with fluoroquinolone resistance, and $bla_{CTX\text{-}M\text{-}15}$ in the case of H30Rx (Banerjee et al., 2013). Previously $bla_{CTX\text{-}M\text{-}15}$ has been the most prevalent *bla* gene identified from human isolates, but recent studies have noted a rise in the prevalence of $bla_{CTX\text{-}M\text{-}27}$, starting from Japan in the late 2000s (Matsumura et al., 2016), and more recently a rapid increase in fecal carriage was observed in children in France (Birgy et al., 2017), along with human isolates from Germany (Ghosh et al., 2017), as well as from samples from hospitalized patients from four European cities (Berlin, Geneva, Madrid, and Utrecht) (Merino et al., 2018). Worldwide distribution is further demonstrated with the recent finding of ST131 *E. coli* belonging to C1-M27 clade in Brazil from a marine sample (Fernandes et al., 2020). Worryingly, ST131-$bla_{CTX\text{-}M\text{-}27}$-*E. coli* has been noted to have a higher transmission rate compared to ST131-$bla_{CTX\text{-}M\text{-}15}$-*E. coli* in an Israeli hospital setting (Adler et al., 2012). Our findings support the notion of a shift in the most dominant $bla_{CTX-M}$ observed in human samples, and the emergence of $bla_{CTX\text{-}M\text{-}27}$ as a challenger for $bla_{CTX\text{-}M\text{-}15}$. Our findings regarding isolates within C1-M27 clade also are in line with previous studies where a majority of isolates were found to possess only the M27PP1 prophage-like region, instead of possessing both M27PP1 and M27PP2 (Matsumura et al., 2016; Decano and Downing, 2019). Interestingly, M27PP1 was also found with 100% coverage and 99.95% identity with BLASTn from sample D18, which carries $bla_{CTX\text{-}M\text{-}55}$ and $bla_{TEM\text{-}1}$ and is of ST 59 and of *fimH* type H41.

$bla_{CTX\text{-}M\text{-}55}$ was identified in two of our isolates, D5 and D18, with different STs (ST1193 and ST59, respectively). This *bla* gene was additionally identified from two previously sequenced ESBL-producing *E. coli* isolates from Finland, one from an imported food sample (coriander from Malaysia) representing ST155 (Kurittu et al., 2021a) and one from a healthy, human adult fecal sample, representing ST58 (Gröndahl-Yli-Hannuksela et al., 2020). $bla_{CTX\text{-}M\text{-}55}$-harboring *E. coli* has been reported especially in samples from meat and food-producing animals, as well as in humans in Asian countries (Zheng et al., 2012; Zhang et al., 2014; Zeng et al., 2021). Studies conducted in China have noted an increase in the proportion of $bla_{CTX\text{-}M\text{-}55}$ compared to other prevalent $bla_{CTX-M}$ genes, such as $bla_{CTX\text{-}M\text{-}15}$ and $bla_{CTX\text{-}M\text{-}14}$, in human patient material (Zhang et al., 2014; Zeng et al., 2021), depicting the rapidly evolving epidemiology

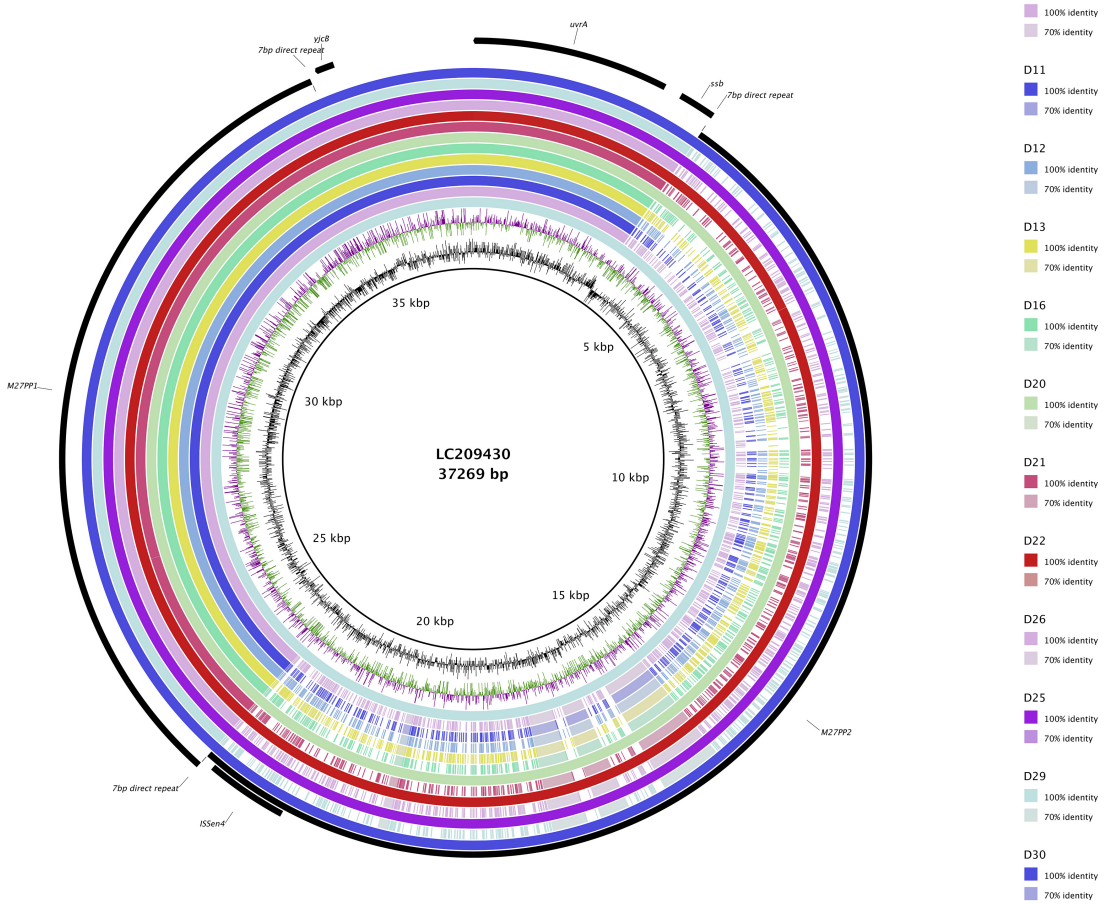


**FIGURE 1 |** ST131 *Escherichia coli* C1-M27 clade-specific regions, prophage-like genomic islands M27PP1 and M27PP2, of KUN5781 (GenBank accession: LC209430) compared to CTX-M-27-producing ST131 *E. coli* with *fimH*30 allele from the current study. GC content and GC skew are depicted on the inner map with distance scale and predicted coding sequences depicted on the outer ring.

of these enzymes. In addition to $bla_{CTX\text{-}M\text{-}55}$, ST1193 *E. coli* was notably recognized as the most prevalent ST among uropathogenic *E. coli* (UPEC) isolates in female patients in China (Zeng et al., 2021). A rapid increase in ST1193 has also been detected in the United States from clinical fluoroquinolone-resistant *E. coli* isolates from urine samples (Tchesnokova et al., 2019). The only ST1193 isolate recovered in our study from an eye conjunctive sample (D5) harbored chromosomal quinolone resistance genes (*gyrA*, *marR*, *parC*, *parE*) in addition to $bla_{CTX\text{-}M\text{-}55}$. Isolates from the previously mentioned study were, however, rarely resistant to beta-lactams, which was not the case in our sample. An Australian study has described fluoroquinolone-resistant ST131 and ST1193 *E. coli* as being less prevalent in animals compared to humans, and considers humans most likely as the source for possible findings of these bacteria in animals (Kidsley et al., 2020). Although not found in the comparative analysis of our study, ST131 *E. coli* isolates belonging to C1-M27 subclade have also been isolated previously from animal sources, more specifically from two pig isolates in the United Kingdom (Duggett et al., 2021) and companion animals in France (Melo et al., 2019).

A recent study in the United States found $bla_{CTX\text{-}M\text{-}27}$ to be the second most common *bla* gene after $bla_{CTX\text{-}M\text{-}15}$ in clinical human isolates, and notably $bla_{CTX\text{-}M\text{-}27}$ was associated with ST38 *E. coli* (Mostafa et al., 2020). The $bla_{CTX\text{-}M\text{-}27}$ gene on ST38 *E. coli* was found to be mostly plasmid-borne, residing in an IncF[F2:A-:B10] or IncF[F1:A2:B20] plasmid (Mostafa et al., 2020). One isolate (D3) in our study was positive for $bla_{CTX\text{-}M\text{-}27}$-carrying ST38 *E. coli*, and this isolate harbored several IncF type replicons [IncFIA, IncFIB, IncFII(pRSB107)] together

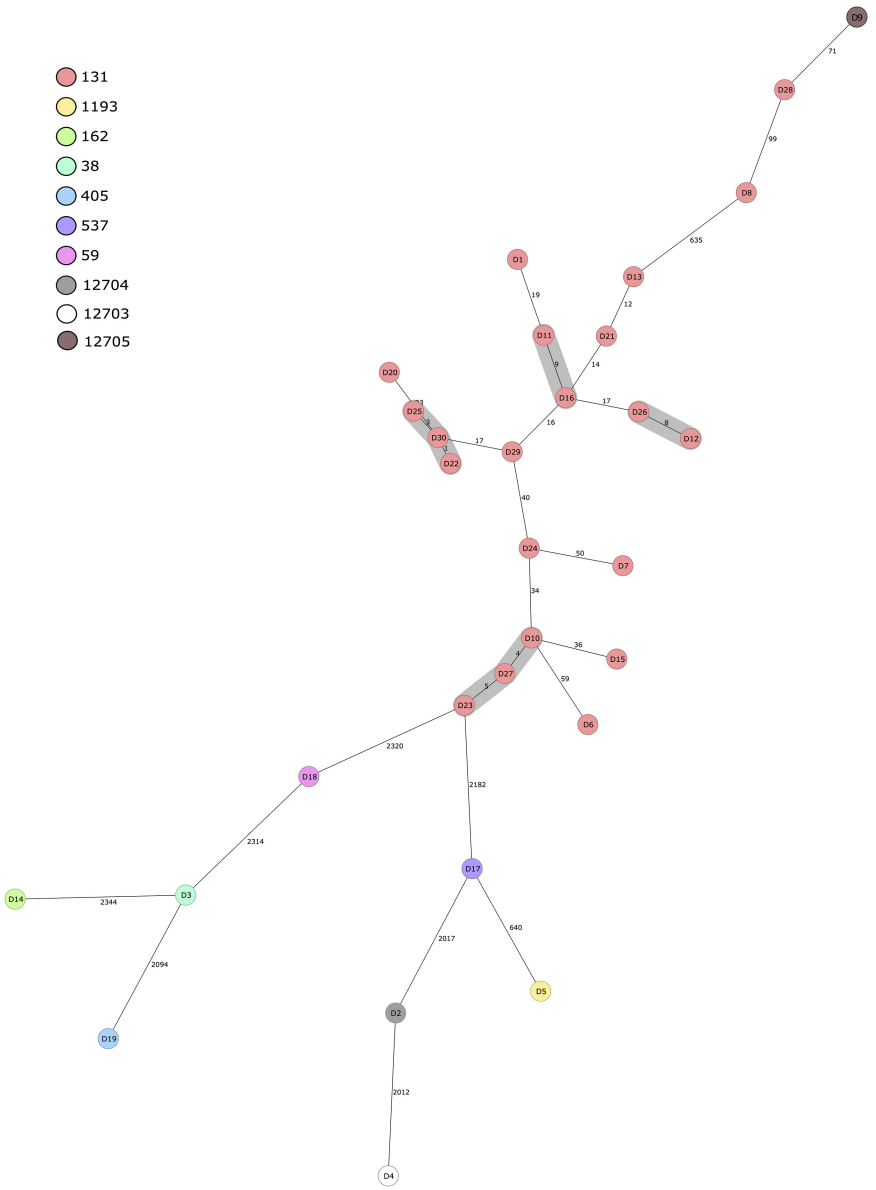


**FIGURE 2 |** Minimum spanning tree of 30 human ESBL-producing *Escherichia coli* isolates obtained from patients in Eastern Finland during 2018–2020. Tree was calculated in Ridom SeqSphere+ with 2513 core genome multilocus sequence typing (cgMLST) targets and 7 *E. coli* MLST Warwick targets (pairwise ignoring missing values, logarithmic scale). Nodes are colored according to sequence type. Number of allelic differences between isolates are indicated on the connecting lines. Clusters are defined as ≤10 allelic difference and shaded in gray.

with Col plasmids [Col(BS512), Col156] and represented the replicon ST [F1:A2:B20].

The majority of our human clinical isolates harbored plasmid replicons belonging to the IncF family, which have been identified as important carriers of globally successful AMR genes, especially those encoding for ESBLs (Villa et al., 2010; Rozwandowicz et al., 2018). Thirteen of our isolates harbored an IncFII replicon together with FIA and FIB replicons, which together form a typical IncF multireplicon (Villa et al., 2010). The most common IncF replicon type identified in our isolates was [F1:A2:B20], which was found from 10 ST131 *E. coli* isolates carrying $bla_{CTX\text{-}M\text{-}27}$ ($n = 9$) and $bla_{CTX\text{-}M\text{-}15}$ ($n = 1$), and from one ST38 carrying $bla_{CTX\text{-}M\text{-}27}$, similar to the findings of a study conducted in the United States (Mostafa et al., 2020). This supports the observation that plasmids belonging to pMLST [F1:A2:B20] are associated with the C1-M27 subclade (Ghosh et al., 2017; Mostafa et al., 2020). IncI1 plasmid replicons belonging to different pMLST profiles were identified in five isolates (D14, D15, D17, D19, and D26), together with $bla_{SHV\text{-}12}$, $bla_{CTX\text{-}M\text{-}15}$, $bla_{TEM\text{-}52}$, $bla_{CTX\text{-}M\text{-}3}$, and $bla_{CTX\text{-}M\text{-}27}$, respectively. IncI type plasmids, especially with $bla_{CTX\text{-}M\text{-}1}$, are frequently found from *E. coli* from poultry sources (Rozwandowicz et al., 2018).

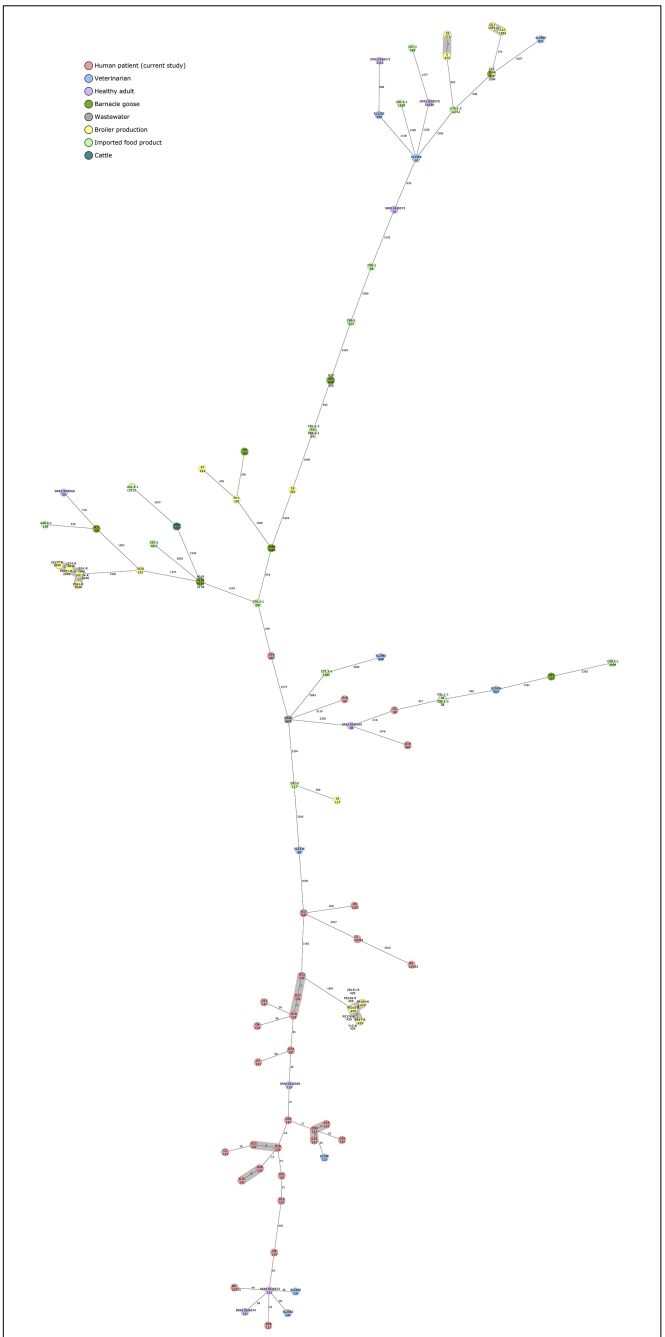


**FIGURE 3 |** Minimum spanning tree of 97 ESBL/AmpC-producing *Escherichia coli* isolates calculated in Ridom SeqSphere+ with 2513 core genome multilocus sequence typing (cgMLST) targets and 7 *E. coli* MLST Warwick targets (pairwise ignoring missing values, logarithmic scale). Nodes are colored according to isolation source. Sequence type is indicated under the isolate name. Number of allelic differences between isolates are indicated on the connecting lines. Clusters are defined as ≤10 allelic difference and shaded in gray.

The pMLST results should, however, be interpreted with care, since long-read sequencing would allow for more robust and accurate identification of plasmid structures and gene locations. As plasmids are important mediators of AMR worldwide (Carattoli, 2013; Rozwandowicz et al., 2018), further plasmid characterization through hybrid sequencing methods is warranted to investigate the epidemiological events in more detail in future studies. Another limitation of our study is the limited number of human clinical isolates analyzed, and the confined geographical origin of the samples. Our results do, however, represent a period of several years and multiple different specimen types, which provide an initial overview of the situation of ESBL-producing *E. coli* in clinical samples in Finland. Furthermore, our results strengthen the finding of $bla_{CTX\text{-}M\text{-}27}$-harboring *E. coli* belonging to C1-M27 subclade gaining prevalence in Europe and describe the first published finding of C1-M27-clade isolates in Finland.

Multidrug resistance was common among the human clinical isolates analyzed in our study. Trimethoprim resistance is often associated with UPEC isolates, and our frequent finding of *dfrA17* and *dfrA12* genes is in line with a previous study conducted in Korea, which observed *dfrA17* and *dfrA12* as the most prevalent trimethoprim resistance genes in urinary tract isolates (Lee et al., 2001). Chromosomal quinolone resistance, as well as acquired tetracycline, aminoglycoside, and sulfonamide resistance genes, was also common in our human isolates.

Our findings are in line with earlier studies investigating the possible origins of ESBL-producing *E. coli* in humans. ESBL-producing *E. coli* isolates from human sources were found to be genetically distant from isolates obtained from food, animal, and environmental sources with a cgMLST-based MST approach. The total sample size, however, was relatively small, and closer genetic connections could possibly have been observed with a larger dataset. The only relatively close connections between human clinical isolates sequenced in this study and previously sequenced ESBL-producing *E. coli* isolates from Finland were observed among human-derived samples from veterinarians and a healthy, adult volunteer. The isolates represented ST131 and carried either $bla_{CTX\text{-}M\text{-}27}$ or $bla_{CTX\text{-}M\text{-}15}$, representing typical results for a human-derived sample. The only close connections among the other previously sequenced isolates from non-human sources in Finland were observed between isolates originating from poultry sources. Interestingly, ST1594 with AmpC type beta-lactamase, $bla_{CMY-2}$, was identified from a broiler caecal sample and a barnacle goose fecal sample and showed no allelic variation in the cgMLST-based MST analysis.

A population-based modeling study with a larger dataset conducted in the Netherlands investigating the community-acquired ESBL-carriage and its attributable sources concluded that human-to-human transmission is the main route for acquiring ESBL *E. coli*, even though food, animals, and environmental sources were found to account for transmission to a lesser extent (Mughini-Gras et al., 2019). Another study conducted in Sweden found no evidence for clonal transmission events between ESBL/AmpC-producing *E. coli* in humans, animals, and the environment, but similarities were discovered in resistance genes and plasmids, indicating possible limited transmission potential (Börjesson et al., 2016).

In conclusion, $bla_{CTX\text{-}M\text{-}27}$ was found to be the most prevalent ESBL gene in human clinical samples, and no clear evidence for animal, food, or environmental genetic overlap was observed in our dataset. Our results prove the spread of *E. coli* belonging to the C1-M27 clade has been successful, and WGS-based methods for surveillance of AMR trends and is effective and warranted for future studies. Surveillance studies are needed to detect the rapid evolution and epidemiology of ESBL genes, and future studies focusing on plasmid-mediated AMR spread are needed to assess the epidemiological links between different bacterial sources further.

## DATA AVAILABILITY STATEMENT

The datasets presented in this study can be found in online repositories. The names of the repository/repositories and accession number(s) can be found in the article/ **Supplementary Material**.

## AUTHOR CONTRIBUTIONS

PK, AH, BK, and JJ contributed to the concept and design of the study. JK performed the sample collection. PK and BK analyzed the whole genome sequence data and performed the subsequent analysis and constructed images of the sequence analysis. PK drafted the manuscript. BK, AH, and JK revised the manuscript. All authors have read and approved the final draft of the manuscript.

## FUNDING

This study received funding from the Finnish Foundation for Veterinary Research and the Doctoral School of Environmental, Food and Biological Sciences in University of Helsinki.

## ACKNOWLEDGMENTS

We would like to thank senior laboratory technician Kirsi Ristkari for valuable help with laboratory work.

## SUPPLEMENTARY MATERIAL

The Supplementary Material for this article can be found online at: https://www.frontiersin.org/articles/10.3389/fmicb.2021.789280/full#supplementary-material

## REFERENCES

Adler, A., Gniadkowski, M., Baraniak, A., Izdebski, R., Fiett, J., Hryniewicz, W., et al. (2012). Transmission dynamics of ESBL-producing *Escherichia coli* clones in rehabilitation wards at a tertiary care centre. *Clin. Microbiol. Infect.* 18, E497–E505. doi: 10.1111/j.1469-0691.2012.03999.x

Alikhan, N. F., Petty, N. K., ben Zakour, N. L., and Beatson, S. A. (2011). BLAST ring image generator (BRIG): simple prokaryote genome comparisons. *BMC Genomics* 12:402. doi: 10.1186/1471-2164-12-402

Babraham Institute (2021). *Babraham Bioinformatics–FastQC A Quality Control Tool for High Throughput Sequence Data*. Available online at: https://www.bioinformatics.babraham.ac.uk/projects/fastqc/ (accessed August 18, 2021)

Banerjee, R., and Johnson, J. R. (2014). A new clone sweeps clean: the enigmatic emergence of *Escherichia coli* sequence type 131. *Antimicrob. Agents Chemother.* 58, 4997–5004. doi: 10.1128/AAC.02824-14

Banerjee, R., Robicsek, A., Kuskowski, M. A., Porter, S., Johnston, B. D., Sokurenko, E., et al. (2013). Molecular epidemiology of *Escherichia coli* sequence type 131 and its H30 and H30-Rx subclones among extended-spectrum-β-lactamase-positive and -negative *E. coli* clinical isolates from the Chicago region, 2007 to 2010. *Antimicrob. Agents Chemother.* 57, 6385–6388. doi: 10.1128/AAC.01604-13

Bevan, E. R., Jones, A. M., and Hawkey, P. M. (2017). Global epidemiology of CTX-M β-lactamases: temporal and geographical shifts in genotype. *J. Antimicrob. Chemother.* 72, 2145–2155. doi: 10.1093/jac/dkx146

Birgy, A., Bidet, P., Levy, C., Sobral, E., Cohen, R., and Bonacorsi, S. (2017). CTX-M-27–producing *Escherichia coli* of sequence type 131 and clade C1-M27, France. *Emerg. Infect. Dis.* 23:885. doi: 10.3201/eid2305.161865

Bolger, A. M., Lohse, M., and Usadel, B. (2014). Trimmomatic: a flexible trimmer for Illumina sequence data. *Bioinformatics* 30, 2114–2120. doi: 10.1093/bioinformatics/btu170

Börjesson, S., Ny, S., Egervärn, M., Bergström, J., Rosengren, Å, Englund, S., et al. (2016). Limited dissemination of extended-spectrum β-lactamase- and plasmid-encoded AmpC-producing *Escherichia coli* from food and farm animals, Sweden. *Emerg. Infect. Dis.* 22, 634–640. doi: 10.3201/eid2204.151142

Bortolaia, V., Kaas, R. S., Ruppe, E., Roberts, M. C., Schwarz, S., Cattoir, V., et al. (2020). ResFinder 4.0 for predictions of phenotypes from genotypes. *J. Antimicrob. Chemother.* 75, 3491–3500. doi: 10.1093/jac/dkaa345

Camacho, C., Coulouris, G., Avagyan, V., Ma, N., Papadopoulos, J., Bealer, K., et al. (2009). BLAST+: architecture and applications. *BMC Bioinformatics* 10:421. doi: 10.1186/1471-2105-10-421

Carattoli, A. (2013). Plasmids and the spread of resistance. *Int. J. Med. Microbiol.* 303, 298–304. doi: 10.1016/j.ijmm.2013.02.001

Carattoli, A., Zankari, E., Garciá-Fernández, A., Larsen, M. V., Lund, O., Villa, L., et al. (2014). In Silico detection and typing of plasmids using plasmidfinder and plasmid multilocus sequence typing. *Antimicrob. Agents Chemother.* 58, 3895–3903. doi: 10.1128/AAC.02412-14

Chen, L., Zheng, D., Liu, B., Yang, J., and Jin, Q. (2016). VFDB 2016: hierarchical and refined dataset for big data analysis–10 years on. *Nucleic Acids Res.* 44, D694–D697. doi: 10.1093/nar/gkv1239

Decano, A. G., and Downing, T. (2019). An *Escherichia coli* ST131 pangenome atlas reveals population structure and evolution across 4,071 isolates. *Sci. Rep.* 9, 1–13. doi: 10.1038/s41598-019-54004-5

Dekker, D., Pankok, F., Thye, T., Taudien, S., Oppong, K., Akenten, C. W., et al. (2021). Clonal clusters, molecular resistance mechanisms and virulence factors of Gram-negative bacteria isolated from chronic wounds in Ghana. *Antibiotics* 10:339. doi: 10.3390/antibiotics10030339

Devi, L. S., Broor, S., Rautela, R. S., Grover, S. S., Chakravarti, A., and Chattopadhya, D. (2020). Increasing prevalence of *Escherichia coli* and *Klebsiella pneumoniae* producing CTX-M-Type extended-spectrum beta-lactamase, carbapenemase, and NDM-1 in patients from a rural community with community acquired infections: a 3-year study. *Int. J. Appl. Basic Med. Res.* 10, 156–163. doi: 10.4103/ijabmr.IJABMR_360_19

Duan, Y., Gao, H., Zheng, L., Liu, S., Cao, Y., Zhu, S., et al. (2020). Antibiotic resistance and virulence of extraintestinal pathogenic *Escherichia coli* (ExPEC) vary according to molecular types. *Front. Microbiol.* 11:2960. doi: 10.3389/fmicb.2020.598305

Duggett, N., Ellington, M. J., Hopkins, K. L., Ellaby, N., Randall, L., Lemma, F., et al. (2021). Detection in livestock of the human pandemic *Escherichia coli* ST131 fimH 30(R) clone carrying bla CTX-M-27. *J. Antimicrob. Chemother.* 76, 263–265. doi: 10.1093/jac/dkaa407

Feldgarden, M., Brover, V., Haft, D. H., Prasad, A. B., Slotta, D. J., Tolstoy, I., et al. (2019). Validating the AMRFINder tool and resistance gene database by using antimicrobial resistance genotype-phenotype correlations in a collection of isolates. *Antimicrob. Agents Chemother.* 63:e00483-19. doi: 10.1128/AAC.00483-19

Fernandes, M. R., Sellera, F. P., Cunha, M. P. V., Lopes, R., Cerdeira, L., and Lincopan, N. (2020). Emergence of CTX-M-27-producing *Escherichia coli* of ST131 and clade C1-M27 in an impacted ecosystem with international maritime traffic in South America. *J. Antimicrob. Chemother.* 75, 1647–1649. doi: 10.1093/jac/dkaa069

Ghosh, H., Doijad, S., Falgenhauer, L., Fritzenwanker, M., Imirzalioglu, C., and Chakraborty, T. (2017). BlaCTX-M-27–encoding *escherichia coli* sequence type 131 lineage c1-m27 clone in clinical Isolates, Germany. *Emerg. Infect. Dis.* 23, 1754–1756. doi: 10.3201/eid2310.170938

Gröndahl-Yli-Hannuksela, K., Lönnqvist, E., Marttila, H., Rintala, E., Rantakokko-Jalava, K., and Vuopio, J. (2020). Performance of the check-direct ESBL screen for BD MAXTM for detection of asymptomatic faecal carriage of extended-spectrum β-lactamase (ESBL)-producing *Escherichia coli* and *Klebsiella pneumoniae*. *J. Glob. Antimicrob. Resist.* 22, 408–413. doi: 10.1016/j.jgar.2020.04.015

Joensen, K. G., Scheutz, F., Lund, O., Hasman, H., Kaas, R. S., Nielsen, E. M., et al. (2014). Real-time whole-genome sequencing for routine typing, surveillance, and outbreak detection of verotoxigenic *Escherichia coli*. *J. Clin. Microbiol.* 52, 1501–1510. doi: 10.1128/JCM.03617-13

Joensen, K. G., Tetzschner, A. M. M., Iguchi, A., Aarestrup, F. M., and Scheutz, F. (2015). Rapid and easy in silico serotyping of *Escherichia coli* isolates by use of whole-genome sequencing data. *J. Clin. Microbiol.* 53, 2410–2426. doi: 10.1128/JCM.00008-15

Johnson, J. R., Murray, A. C., Gajewski, A., Sullivan, M., Snippes, P., Kuskowski, M. A., et al. (2003). Isolation and molecular characterization of nalidixic acid-resistant extraintestinal pathogenic *Escherichia coli* from retail chicken products. *Antimicrob. Agents Chemother.* 47, 2161–2168. doi: 10.1128/AAC.47.7.2161-2168.2003

Jolley, K. A., Bray, J. E., and Maiden, M. C. J. (2018). Open-access bacterial population genomics: BIGSdb software, the PubMLST.org website and their applications [version 1; referees: 2 approved]. *Wellcome Open Res.* 3:124. doi: 10.12688/wellcomeopenres.14826.1

Jünemann, S., Sedlazeck, F. J., Prior, K., Albersmeier, A., John, U., Kalinowski, J., et al. (2013). Updating benchtop sequencing performance comparison. *Nat. Biotechnol.* 31, 294–296. doi: 10.1038/nbt.2522

Kanamori, H., Parobek, C. M., Juliano, J. J., Johnson, J. R., Johnston, B. D., Johnson, T. J., et al. (2017). Genomic analysis of multidrug-resistant *Escherichia coli* from North Carolina community hospitals: ongoing circulation of CTX-M-producing ST131-H30Rx and ST131-H30R1 Strains. *Antimicrob. Agents Chemother.* 61:e00912-17. doi: 10.1128/AAC.00912-17

Kidsley, A. K., White, R. T., Beatson, S. A., Saputra, S., Schembri, M. A., Gordon, D., et al. (2020). Companion animals are spillover hosts of the multidrug-resistant human extraintestinal *Escherichia coli* pandemic clones ST131 and ST1193. *Front. Microbiol.* 11:1968. doi: 10.3389/fmicb.2020.01968

Kurittu, P., Khakipoor, B., Aarnio, M., Nykäsenoja, S., Brouwer, M., Myllyniemi, A.-L., et al. (2021a). Plasmid-borne and chromosomal ESBL/AmpC genes in *Escherichia coli* and *Klebsiella pneumoniae* in global food products. *Front. Microbiol.* 12:125. doi: 10.3389/fmicb.2021.592291

Kurittu, P., Khakipoor, B., Brouwer, M. S. M., and Heikinheimo, A. (2021b). Plasmids conferring resistance to extended-spectrum beta-lactamases including a rare IncN+IncR multireplicon carrying blaCTX-M-1 in *Escherichia coli* recovered from migrating barnacle geese (*Branta leucopsis*). *Open Res. Eur.* 1:46. doi: 10.12688/openreseurope.13529.1

Larsen, M. V., Cosentino, S., Rasmussen, S., Friis, C., Hasman, H., Marvig, R. L., et al. (2012). Multilocus sequence typing of total-genome-sequenced bacteria. *J. Clin. Microbiol.* 50, 1355–1361. doi: 10.1128/JCM.06094-11

Lee, J. C., Oh, J. Y., Cho, J. W., Park, J. C., Kim, J. M., Seol, S. Y., et al. (2001). The prevalence of trimethoprim-resistance-conferring dihydrofolate reductase genes in urinary isolates of *Escherichia coli* in Korea. *J. Antimicrob. Chemother.* 47, 599–604. doi: 10.1093/jac/47.5.599

Magiorakos, A. P., Srinivasan, A., Carey, R. B., Carmeli, Y., Falagas, M. E., Giske, C. G., et al. (2012). Multidrug-resistant, extensively drug-resistant and pandrug-resistant bacteria: an international expert proposal for interim standard definitions for acquired resistance. *Clin. Microbiol. Infect.* 18, 268–281. doi: 10.1111/j.1469-0691.2011.03570.x

Mathers, A. J., Peirano, G., and Pitout, J. D. D. (2015). The role of epidemic resistance plasmids and international high- risk clones in the spread of multidrug-resistant Enterobacteriaceae. *Clin. Microbiol. Rev.* 28, 565–591. doi: 10.1128/CMR.00116-14

Matsumura, Y., Pitout, J. D. D., Gomi, R., Matsuda, T., Noguchi, T., Yamamoto, M., et al. (2016). Global *Escherichia coli* sequence type 131 clade with blaCTX-M-27 gene. *Emerg. Infect. Dis.* 22:1900. doi: 10.3201/EID2211.160519

Melo, L. C., Haenni, M., Saras, E., Duprilot, M., Nicolas-Chanoine, M.-H., and Madec, J.-Y. (2019). Emergence of the C1-M27 cluster in ST131 *Escherichia coli* from companion animals in France. *J. Antimicrob. Chemother.* 74, 3111–3113. doi: 10.1093/jac/dkz304

Merino, I., Hernández-García, M., Turrientes, M.-C., Pérez-Viso, B., López-Fresneña, N., Diaz-Agero, C., et al. (2018). Emergence of ESBL-producing *Escherichia coli* ST131-C1-M27 clade colonizing patients in Europe. *J. Antimicrob. Chemother.* 73, 2973–2980. doi: 10.1093/jac/dky296

Mostafa, H. H., Cameron, A., Taffner, S. M., Wang, J., Malek, A., Dumyati, G., et al. (2020). Genomic surveillance of ceftriaxone-resistant *Escherichia coli* in Western New York suggests the extended-spectrum β-Lactamase blaCTX-M-27 is emerging on distinct plasmids in ST38. *Front. Microbiol.* 11:1747. doi: 10.3389/fmicb.2020.01747

Mughini-Gras, L., Dorado-García, A., van Duijkeren, E., van den Bunt, G., Dierikx, C. M., Bonten, M. J. M., et al. (2019). Attributable sources of community-acquired carriage of *Escherichia coli* containing β-lactam antibiotic resistance genes: a population-based modelling study. *Lancet Planet. Health* 3, e357–e369. doi: 10.1016/S2542-5196(19)30130-5

Nesta, B., Spraggon, G., Alteri, C., Moriel, D. G., Rosini, R., Veggi, D., et al. (2012). FdeC, a novel broadly conserved *Escherichia coli* adhesin eliciting protection against urinary tract infections. *mBio* 3:e00010-12. doi: 10.1128/mBio.00010-12

Nicolas-Chanoine, M. H., Bertrand, X., and Madec, J. Y. (2014). *Escherichia coli* st131, an intriguing clonal group. *Clin. Microbiol. Rev.* 27, 543–574. doi: 10.1128/CMR.00125-13

Oikarainen, P. E., Pohjola, L. K., Pietola, E. S., and Heikinheimo, A. (2019). Direct vertical transmission of ESBL/pAmpC-producing *Escherichia coli* limited in poultry production pyramid. *Vet. Microbiol.* 231, 100–106. doi: 10.1016/j.vetmic.2019.03.001

Päivärinta, M., Latvio, S., Fredriksson-Ahomaa, M., and Heikinheimo, A. (2020). Whole genome sequence analysis of antimicrobial resistance genes, multilocus sequence types and plasmid sequences in ESBL/AmpC *Escherichia coli* isolated from broiler caecum and meat. *Int. J. Food Microbiol.* 315:108361. doi: 10.1016/J.IJFOODMICRO.2019.108361

Päivärinta, M., Pohjola, L., Fredriksson-Ahomaa, M., and Heikinheimo, A. (2016). Low occurrence of extended-spectrum β-lactamase-producing *Escherichia coli* in finnish food-producing animals. *Zoonoses Public Health* 63, 624–631. doi: 10.1111/zph.12277

Pitout, J. D. D. (2012). Extraintestinal pathogenic *Escherichia coli*: a combination of virulence with antibiotic resistance. *Front. Microbiol.* 3:9. doi: 10.3389/fmicb.2012.00009

Räisänen, K., Ilmavirta, H., and Bakteerien Mikrobilääkeresistenssi Suomessa (2019). *Bakteerien mikrobilääkeresistenssi Suomessa - Finres 2019*. Available online at: http://urn.fi/URN:ISBN:978-952-343-588-9 (accessed August 10, 2021).

Räisänen, K., Lyytikäinen, O., Kauranen, J., Tarkka, E., Forsblom-Helander, B., Grönroos, J. O., et al. (2020). Molecular epidemiology of carbapenemase-producing Enterobacterales in Finland, 2012–2018. *Eur. J. Clin. Microbiol. Infect. Dis.* 39, 1651–1656. doi: 10.1007/s10096-020-03885-w

Ray, S., Anand, D., Purwar, S., Samanta, A., Upadhye, K. V., Gupta, P., et al. (2018). Association of high mortality with extended–spectrum β-lactamase (ESBL) positive cultures in community acquired infections. *J. Crit. Care* 44, 255–260. doi: 10.1016/j.jcrc.2017.10.036

Roer, L., Tchesnokova, V., Allesoe, R., Muradova, M., Chattopadhyay, S., Ahrenfeldt, J., et al. (2017). Development of a web tool for *Escherichia coli* subtyping based on fimh alleles. *J. Clin. Microbiol.* 55, 2538–2543. doi: 10.1128/JCM.00737-17

Rozwandowicz, M., Brouwer, M. S. M., Fischer, J., Wagenaar, J. A., Gonzalez-Zorn, B., Guerra, B., et al. (2018). Plasmids carrying antimicrobial resistance

genes in Enterobacteriaceae. *J. Antimicrob. Chemother.* 73, 1121–1137. doi: 10.1093/jac/dkx488

Sarowska, J., Futoma-Koloch, B., Jama-Kmiecik, A., Frej-Madrzak, M., Ksiazczyk, M., Bugla-Ploskonska, G., et al. (2019). Virulence factors, prevalence and potential transmission of extraintestinal pathogenic *Escherichia coli* isolated from different sources: recent reports. *Gut Pathog.* 11:10. doi: 10.1186/s13099-019-0290-0

Souvorov, A., Agarwala, R., and Lipman, D. J. (2018). SKESA: strategic k-mer extension for scrupulous assemblies. *Genome Biol.* 19:153. doi: 10.1186/s13059-018-1540-z

Tchesnokova, V. L., Rechkina, E., Larson, L., Ferrier, K., Weaver, J. L., Schroeder, D. W., et al. (2019). Rapid and extensive expansion in the United States of a new multidrug-resistant *Escherichia coli* clonal group, sequence type 1193. *Clin. Infect. Dis.* 68, 334–337. doi: 10.1093/cid/ciy525

Tetzschner, A. M. M., Johnson, J. R., Johnston, B. D., Lund, O., and Scheutz, F. (2020). In silico genotyping of *Escherichia coli* isolates for extraintestinal virulence genes by use of whole-genome sequencing data. *J. Clin. Microbiol.* 58:e01269-20. doi: 10.1128/JCM.01269-20

Verkola, M., Pietola, E., Järvinen, A., Lindqvist, K., Kinnunen, P. M., and Heikinheimo, A. (2019). Low prevalence of zoonotic multidrug-resistant bacteria in veterinarians in a country with prudent use of antimicrobials in animals. *Zoonoses Public Health* 66, 667–678. doi: 10.1111/zph.12619

Villa, L., García-Fernández, A., Fortini, D., and Carattoli, A. (2010). Replicon sequence typing of IncF plasmids carrying virulence and resistance determinants. *J. Antimicrob. Chemother.* 65, 2518–2529. doi: 10.1093/jac/dkq347

Zankari, E., Allesøe, R., Joensen, K. G., Cavaco, L. M., Lund, O., and Aarestrup, F. M. (2017). PointFinder: a novel web tool for WGS-based detection of antimicrobial resistance associated with chromosomal point mutations in bacterial pathogens. *J. Antimicrob. Chemother.* 72, 2764–2768. doi: 10.1093/jac/dkx217

Zeng, Q., Xiao, S., Gu, F., He, W., Xie, Q., Yu, F., et al. (2021). Antimicrobial resistance and molecular epidemiology of uropathogenic *Escherichia coli* isolated from female patients in Shanghai, China. *Front. Cell. Infect. Microbiol.* 11:751. doi: 10.3389/fcimb.2021.653983

Zhang, J., Zheng, B., Zhao, L., Wei, Z., Ji, J., Li, L., et al. (2014). Nationwide high prevalence of CTX-M and an increase of CTX-M-55 in *Escherichia coli* isolated from patients with community-onset infections in Chinese county hospitals. *BMC Infect. Dis.* 14:659. doi: 10.1186/s12879-014-0659-0

Zheng, H., Zeng, Z., Chen, S., Liu, Y., Yao, Q., Deng, Y., et al. (2012). Prevalence and characterisation of CTX-M β-lactamases amongst *Escherichia coli* isolates from healthy food animals in China. *Int. J. Antimicrob. Agents* 39, 305–310. doi: 10.1016/j.ijantimicag.2011.12.001

Zhou, Z., Alikhan, N. F., Mohamed, K., Fan, Y., and Achtman, M. (2020). The EnteroBase user's guide, with case studies on *Salmonella* transmissions, Yersinia pestis phylogeny, and *Escherichia* core genomic diversity. *Genome Res.* 30, 138–152. doi: 10.1101/gr.251678.119

**Conflict of Interest:** The authors declare that the research was conducted in the absence of any commercial or financial relationships that could be construed as a potential conflict of interest.

The reviewer MB declared a past collaboration with one of the authors, PK, to the handling editor.

**Publisher's Note:** All claims expressed in this article are solely those of the authors and do not necessarily represent those of their affiliated organizations, or those of the publisher, the editors and the reviewers. Any product that may be evaluated in this article, or claim that may be made by its manufacturer, is not guaranteed or endorsed by the publisher.

frontiers in Microbiology

ORIGINAL RESEARCH
published: 25 January 2022
doi: 10.3389/fmicb.2021.770635

# Molecular Characterization of *Candida auris* Isolates at a Major Tertiary Care Center in Lebanon

*Lina Reslan[1], George F. Araj[1,2]*, Marc Finianos[3], Rima El Asmar[2], Jaroslav Hrabak[3], Ghassan Dbaibo[1,4] and Ibrahim Bitar[3]**

[1] American University of Beirut, Center for Infectious Diseases Research (CIDR) and WHO Collaborating Center for Reference and Research on Bacterial Pathogens, Beirut, Lebanon, [2] Department of Pathology and Laboratory Medicine, American University of Beirut Medical Center, Beirut, Lebanon, [3] Department of Microbiology, Faculty of Medicine and University Hospital in Plzen, Charles University, Plzeň, Czechia, [4] Department of Pediatrics and Adolescent Medicine, Faculty of Medicine, American University of Beirut, Beirut, Lebanon

**Background:** The globally emerging *Candida auris* pathogens poses heavy burden to the healthcare system. Their molecular analyses assist in understanding their epidemiology, dissemination, treatment, and control. This study was warranted to describe the genomic features and drug resistance profiles using whole genome sequencing (WGS) among *C. auris* isolates from Lebanon.

**Methods:** A total of 28 *C. auris* clinical isolates, from different hospital units, were phenotypically identified by matrix-assisted laser desorption/ionization time-of-flight (MALDI-TOF) and tested for antifungal resistance using Vitek-2 system and E test. The complete genomes were determined by WGS using long reads sequencing (PacBio) to reveal the clade distribution and antifungal resistance genes.

**Results:** *Candida auris* revealed uniform resistance to fluconazole and amphotericin B, with full susceptibility to echinocandins. Among key resistance genes studied, only two mutations were detected: Y132F in *ERG11* gene and a novel mutation, D709E, found in *CDR1* gene encoding for an ABC efflux pump. Phylogenetically, *C. auris* genomes belonged to South Asian clade I and showed limited genetic diversity, suggesting person to person transmission.

**Conclusion:** This characterization of *C. auris* isolates from Lebanon revealed the exclusivity of clade I lineage together with uniform resistance to fluconazole and amphotericin B. The control of such highly resistant pathogen necessitates an appropriate and rapid recovery and identification to contain spread and outbreaks.

**Keywords:** ***Candida auris*, whole-genome sequencing, antifungal resistance, South Asian clade, Lebanon**

OPEN ACCESS

***Edited by:***
*Annamari Heikinheimo, University of Helsinki, Finland*

***Reviewed by:***
*Kin-Ming (Clement) Tsui, University of British Columbia, Canada*
*João Nobrega De Almeida Júnior, Universidade de São Paulo, Brazil*

***Correspondence:**
*George F. Araj*
*garaj@aub.edu.lb*
*Ibrahim Bitar*
*ibrahimbitar5@gmail.com*

***Specialty section:***
*This article was submitted to Antimicrobials, Resistance and Chemotherapy, a section of the journal Frontiers in Microbiology*

***Received:*** *04 September 2021*
***Accepted:*** *23 November 2021*
***Published:*** *25 January 2022*

***Citation:***
*Reslan L, Araj GF, Finianos M, El Asmar R, Hrabak J, Dbaibo G and Bitar I (2022) Molecular Characterization of Candida auris Isolates at a Major Tertiary Care Center in Lebanon. Front. Microbiol. 12:770635. doi: 10.3389/fmicb.2021.770635*

## INTRODUCTION

*Candida auris* has been an emerging fungal infection, characterized by high transmissibility, multidrug resistance, and poor outcomes. As such, it is posing serious nosocomial health concerns globally (Forsberg et al., 2019). Its potency in colonizing patients' skin enables patient-to-patient spread, causing outbreaks in healthcare settings (Schelenz et al., 2016; Lockhart et al., 2017).

The recognition and identification of *C. auris* is challenging, as the isolates of this yeast can be misidentified using commonly phenotypic laboratory methods. However, its speciation can be determined by automated systems such as the matrix-assisted laser desorption/ionization time-of-flight (MALDI-TOF) and Vitek System (Rychert et al., 2018; Patel, 2019). Molecular methods based on sequencing of the D1–D2 region of the 28s rDNA or internal transcribed spacer region provide reliable confirmation of species identification (Schoch et al., 2012; Cernakova et al., 2021). Moreover, whole-genome sequencing (WGS)-based methods have increasingly been used to detect and characterize phylogeographic types and transmission dynamics for this emerging pathogen (Lockhart et al., 2017). Since its first recognition in Japan in 2009, genetically divergent lineages have been globally identified and stratified geographically into four main clades: clade I (Southern Asia), clade II (Eastern Asia), clade III (Africa), and clade IV (South America) (Chow et al., 2020). A potentially clade V has been identified in an isolate from a patient in Iran showing a difference of >200,000 single-nucleotide polymorphisms from the other clades (Chow et al., 2019).

Several studies have revealed the genetic profiles of recovered *C. auris* isolates from different countries worldwide (Lockhart et al., 2017; Forsberg et al., 2019; Chow et al., 2020), including few reports from different countries in our MENA region (Al Maani et al., 2019; Alfouzan et al., 2019, 2020; Almaghrabi et al., 2020; Salah et al., 2021). In Lebanon, however, only two clinical studies were reported from the American University of Beirut Medical Center (AUBMC): the first addressed the profile of *C. auris* infection among 14 infected cases (Allaw et al., 2021). The second was a case report on *C. duobushaemulonii* associated with coronavirus disease 2019 (COVID-19) disease (Awada et al., 2021). Thus, in the absence of any characterization of *C. auris* isolates in Lebanon, this study was warranted to describe the genomic features, genetic relationships, and drug resistance profiles using WGS among *C. auris* isolates recovered at a major tertiary care center in this country.

# MATERIALS AND METHODS

## *Candida auris* Isolates Collection

*Candida auris* isolates analyzed in this study were those recovered from patient specimens submitted for fungal investigation (prior to commencing patients' therapy) at AUBMC Clinical Microbiology Laboratory (CML), accredited by the College of American Pathologists since 2004.

A total of 28 isolates were retrieved from 21 patients by plating the specimens on Sabouraud dextrose agar (SAB) medium and incubated them at 37°C. The specimen source of these isolates were as follows: 4 isolates from peripheral blood, 1 from central line catheter, 12 from deep tracheal aspirate (DTA), 8 from urine, 2 from skin screen, and 1 from bronchioalveolar lavage (BAL).

In six patients, isolates were simultaneously recovered from different specimen sources of the same patient: blood and central line catheter from 1 patient; DTA and urine from 2 patients; DTA and skin screening from 1 patient; DTA, skin screening, and urine from 1 patient; and DTA and blood from 1 patient.

## Identification and Speciation of *Candida auris* Isolates

The recovered *Candida* species on SAB medium was submitted directly for identification or subcultured on chocolate agar medium prior to identification. The colonies of these isolates were identified by MALDI-TOF system (Bruker Daltonik, GmbH, Bremen, Germany) and by the Vitek 2 system (BioMérieux, Marcy L'Etoile, France). Species identities were confirmed by PCR following by sequencing using ITS1F/ITS4R primers for the variable internal transcribed spacers ITS1 and ITS2 regions, located between universally conserved genes 18S, 5.8S, and 28S and NL1F/NL2R primers used to detect the D1–D2 region located at the 5′ end of the gene 28S encoding for the large nuclear ribosomal subunit (Schoch et al., 2012).

## Antifungal Susceptibility Testing

The Vitek 2 system, employing the antifungal susceptibility cards (AST-YS 08), was used to determine the minimum inhibitory concentrations (MICs) of the following antifungal agents: fluconazole, voriconazole, caspofungin, micafungin, amphotericin B, and flucytosine. The E-test (AB Biodisk, Solna, Sweden) was used to determine the MICs (μg/ml) of itraconazole (strip concentration range, 0.002–32 μg/ml), using Roswell Park Memorial Institute (RPMI) 1640 media (Sigma, St. Louis, MO, United States), according to what was reported earlier from our laboratory (Araj et al., 2015).

The interpretation of the minimum inhibitory concentrations (MICs) susceptibility breakpoints (μg/ml) for *C. auris* were based on CDC[1] (accessed July 7, 2021) and Clinical and Laboratory Standards Institute (CLSI) guidelines, essentially defined based on those established for closely related *Candida* species (*Candida haemuloni*) and on expert opinion. In this context, the designated resistant breakpoints are as follows: fluconazole, ≥32 μg/ml; anidulafungin, ≥4 μg/ml; caspofungin, ≥2 μg/ml; micafungin, ≥4 μg/ml; amphotericin B, ≥2 μg/ml. Voriconazole susceptibility breakpoints are not applicable and recommended to consider using fluconazole susceptibility as a surrogate susceptibility assessment. There is no published guidance about flucytosine's breakpoint susceptibility.

## Quality Control Isolates

The quality of test performance was controlled by including the reference strains *C. albicans* (ATCC 10231), C. *parapsilosis* (ATCC 22019), and *C. kruseii* (ATCC 6258).

## Whole Genome Sequencing

The genomic DNA of 29 isolates (28 *C. auris* isolates and one *C. haemuloni* as outgroup) was extracted using the NucleoSpin microbial DNA kit (Macherey-Nagel, Duren, Germany). Subsequently, the extracted DNA was sheared to obtain 15-kb fragments using Hydropore long on the Megaruptor

[1]https://www.cdc.gov/fungal/candida-auris/c-auris-antifungal.html

2 (Diagnode). Express kit 2.0 (Pacific Biosciences, Menlo Park, CA, United States) was used for library preparation using the microbial multiplexing protocol according to the manufacturer's recommendations. Library size selection was applied using the AMPure PB beads (Pacific Biosciences, Menlo Park, CA, United States) to select for fragments above 3 kb. Using the SMRT Link v9.0, HGAP4 and microbial assembly pipelines were used to assemble the sequences with a minimum seed coverage of 30, 40, and 50 depending on the coverage. The assemblies of CA3LBN and CA7LBN were annotated; gene prediction was achieved using BRAKER2 v2.1.6 pipeline on fungus mode, which combines GeneMarK-ES v4.65 and AUGUSTUS 3.4.0 for fungal gene prediction and identifying gene locations with the corresponding CDS and messenger RNA (mRNA) qualifiers (Altschul et al., 1990; Stanke et al., 2006, 2008; Ter-Hovhannisyan et al., 2008; Camacho et al., 2009; Hoff et al., 2016, 2019; Bruna et al., 2021). Interproscan 5.50-84.0 (Jones et al., 2014) was used on the COG database to create the xml file to further incorporate in the functional annotation pipeline created by the Funannotate 1.8.7 (Blachowicz et al., 2019; Vasquez-Gross et al., 2020; Smith, 2021). The pipeline starts by running HMMscan (HMMer v3.3) (hmmer.org) with default parameters on the PFAM database, then using emapper 2.1.2 based on eggnog orthology data (Huerta-Cepas et al., 2017, 2019). Sequence searches were performed using Diamond Blastp (Buchfink et al., 2015) on UniProt DB version 2021_02 and MEROPS v12.0; the resulting annotations were combined using Gene2Product v1.69, and later, Signalp 5.0 was used to predict secreted proteins (Almagro Armenteros et al., 2019). Furthermore, transfer RNA (tRNA) identification was done using ARAGORN v1.2.41 (Laslett and Canback, 2004); tRNAs identified and found to be overlapping with any CDS sequences were removed. The ribosomal RNA (rRNA) identification was done by downloading *C. auris* rRNA sequences from the National Center for Biotechnology Information (NCBI) and then by using BLAST + v2.11.0 (Camacho et al., 2009). Assemblies and annotations were assessed using BUSCO V5.2.2 (Manni et al., 2021).

## Phylogeny

The corresponding phylogenies of the 29 genomes of this study, along with all of the 80 *C. auris* sequences found in the NCBI assembly database, were performed. Briefly, the alignment of the core genome, detection of recombination events, and single nucleotide polymorphisms (SNPs) detection were performed using Parsnp v1.2, available in the Harvest suite (Treangen et al., 2014) using CA7LBN (index case), a reference genome for clustering and using CA3LBN (identified as *C. haemuloni*) as an outgroup as described elsewhere (Prakash et al., 2016). SNPs identified in local collinear blocks were subsequently used for reconstructing an approximate maximum-likelihood tree using FastTree2 (Price et al., 2010) while including the general time reversible (GTR) model of nucleotide substitution. The Shimodaira–Hasegawa test was used to assess the support for significant clustering in the observed phylogeny. The interactive tree of life or iTOL (Letunic and Bork, 2019) was used to annotate, modify, and edit the resulting phylogeny.

## Single Nucleotide Polymorphisms Detection

In this study, SNPs of the 27 *C. auris* genomes were compared to the SNPs of the first *C. auris* (CA7LBN detected in October 2020) by using snippy multicommand (snippy-base application v4.5.0) (Seemann, 2015) that generates a core genome multiple alignment against a common reference. The CA7LBN was used as a reference, since it was the index case. The pipeline detects the variants and generates single file for each isolate listing the different variations. The results were compared to detect any possible microevolution events among the genomes with respect to the time of detection.

## Molecular Detection of Antifungal Resistance Genes Mutations

The sequences of *CDR1*, *CDR2*, *ERG1*, *ERG2*, *ERG3*, *ERG5*, *ERG6*, *ERG11*, *ERG24*, *MDR1*, *MRR1*, *TAC1*, and *UPC2* were extracted from the genome of *C. auris* B11221 and were used as reference. *C. auris* B11221 was chosen, since it is susceptible against fluconazole and amphotericin B. Then, the reference genes were blasted against the generated assemblies from the study, and the corresponding genes were detected using BLAST + v2.11.0 (Camacho et al., 2009). Protein products were then compared, and the corresponding amino acid substitutions were detected. All mutations have been confirmed by visually inspecting the alignment of the CCS reads to the assembly.

## Data Availability

All genome assemblies have been deposited at GenBank under the following accession numbers: CP077052–CP077058, CP077045–CP077051, CP076661–CP076667, CP077038–CP077044, CP077031–CP077037, CP077024–CP077030, CP076749–CP076755, CP077017–CP077023, CP077010–CP077016, CP077003–CP077009, CP076996–CP077002, CP076989–CP076995, CP076982–CP076988, CP076975–CP076981, CP076968–CP076974, CP076961–CP076967, CP076954–CP076960, CP076947–CP076953, CP076940–CP076946, CP076933–CP076939, CP076926–CP076932, CP076919–CP076925, CP076912–CP076918, CP076905–CP076911, CP076898–CP076904, CP076891–CP076897, CP076884–CP076890, CP076877–CP076883, and CP076870–CP076876. We annotated two isolates (the index and the outgroup) with the following ascension codes CP076661–CP076667 and CP076749–CP076755 corresponding to CA3LBN and CA7LBN, respectively (**Supplementary Table 1**).

# RESULTS

## Patients Demographics

The gender distribution among the 21 patients showed 12 male (57%) and 9 female (43%). The average and range of age for the male and female patients were 71 years (range, 57–80 years) and 63 years (range, 34–82 years), respectively. The distribution of patients based on their clinical hospital location were nine in intensive care unit (ICU), two in respiratory care unit (RCU), four in coronary care unit (CCU), one in neuro

ICU (NICU), one in emergency department (ED), and four in medical floor.

## Antifungal Susceptibility Results of *Candida auris*

The $MIC_{50}/MIC_{90}$ and range of MICs (μg/ml) for each of the tested antifungal agents against the *C. auris* isolates are shown in **Table 1** as follows: itraconazole, 0.25/1 (range, 0.19–1); fluconazole, ≥32/≥32 (16–32); voriconazole, 0.25/0.25 (range, 0.12–4); caspofungin, 0.25/0.25 (range, 0.25–0.25); micafungin 0.12/0.12 (range, 0.064–0.12); amphotericin B, 8/8 (range, 2–16); flucytosine 1/1 (range, 1–1).

Among the triazole class drugs, *C. auris* was considered to be uniformly resistant to fluconazole, although only 54% of the isolates showed clear resistance to fluconazole (MICs ≥ 32 μg/ml), while 46% of these isolates revealed a level close to the resistance values, an MIC of 16 μg/ml. The voriconazole rates of susceptible, intermediate, and resistant *C. auris* were 36, 61, and 3%, respectively, and that against itraconazole (n = 8 isolates tested) were 0, 75, and 25%, respectively.

Concerning the polyene class, the specified breakpoints of resistance (MICs ≥ 2 μg/ml) for amphotericin B was detected in 100% of the tested isolates. Extrapolating the breakpoint susceptibility reported for *C. auris* isolates by CDC, our results indicated uniform susceptibility (100%, MICs ≤ 4 μg/ml) of these isolates against the tested echinocandin class drugs (micafungin and caspofungin) (**Table 1**).

## Mutations of Drug-Resistance-Associated Genes

All strains expressed fluconazole and amphotericin B resistant phenotypes. Corresponding mutations in drug-resistance-associated genes, namely, *CDR1*, *CDR2*, *ERG1*, *ERG2*, *ERG3*, *ERG5*, *ERG6*, *ERG11*, *ERG24*, *MDR1*, *MRR1*, *TAC1*, and *UPC2*, were investigated in comparison with the reference genes in B11221 strain. Two mutations were detected: the first one in the lanosterol 14-α-demethylase-encoding gene *ERG11* (Y132F) particularly in the first "hot-spot" region located between amino-acids (105–165) and another novel mutation D709E, found in *CDR1* encoding for an ABC efflux pump.

**TABLE 1 |** The antifungal susceptibility results against the 28 isolates of *C. auris*.

| Antifungal agent | Susceptibility findings | | | | | |
|---|---|---|---|---|---|---|
| | MIC50 | MIC90 | MIC range | %S | %I | %R |
| Itraconazole | 0.25 | 1 | 0.19–1 | 0 | 75 | 25 |
| Fluconazole | 32 | ≥32 | 16–≥32 | 0 | 0 | 0 |
| Voriconazole | 0.25 | 0.25 | 0.12 to 4 | 36 | 61 | 3 |
| Caspofungin | 0.25 | 0.25 | 0.25–0.25 | 100 | 0 | 0 |
| Micafungin | 0.12 | 0.12 | 0.064–0.12 | 100 | 0 | 0 |
| Amphotericin B | 8 | 8 | 2–16 | 0 | 0 | 0 |
| Flucytosine | 1 | 1 | 1–1 | ND | ND | ND |

## Phylogenetic Studies and Single Nucleotide Polymorphism Analysis

The 29 genomes generated in our study, with CA3LBN (*C. Haemulonii* isolate) being the outgroup, were compared to all *C. auris* genomes available in the NCBI database (80 genomes). The results indicated that our isolates belonged to clade I (South Asian) among the five known global clades and closely clustered with the branch length showing zero differences between our isolates and the ones from United States, Germany, and India and located in close proximity to *C. auris* isolates recovered from Saudi Arabia, United Arab Emirates, and Hong Kong (**Figure 1**).

The genetic variations and microevolution among the 28 *C. auris* isolates were analyzed and compared to the first isolate detected in October 2020 (CA7LBN). Results revealed a range of one to six SNPs with one SNP in three isolates, two SNPs in five isolates, three SNPs in seven, four SNPs in four, five SNPs in six, and six SNPs in two isolates (**Supplementary Table 1**). SNPs were detected in coding and non-coding regions in the studied isolates. All isolates showed a mutation in *THR1*, a gene encoding for trihydroxynaphthalene reductase, with an amino acid substitution L188G. In addition, five other mutations were detected in different isolates as shown in **Supplementary Table 2**. The rest of the mutations were either in genes coding for uncharacterized proteins (hypothetical proteins) or in non-coding regions.

# DISCUSSION

*Candida auris* infection has been tolling the healthcare systems at major hospitals globally due to its serious threatening impact and its resistance to multiple antifungal agents that limit treatment options. In Lebanon, this is the first study addressing the antifungal profile and molecular features of *C. auris* isolates using the long reads sequencing technique that generated complete genome sequences of these pathogens.

Identification of *C. auris* is generally a challenging experience. Interestingly, the first suspected encounter of *C. auris* happened when yeast colonies were recovered from the blood culture of a 34-year-old Lebanese man who works and lives in Africa (Sierra Leone) and was transferred to AUBMC for management of confirmed COVID-19 severe infection. Identification (ID) by Vitek 2 revealed *C. auris* (96% probability, Bionumber 4110145251301771). Repeat identification on Vitek 2 (August 12, 2020) revealed low discrimination organism (*C. auris* and *C. duobushaemuloins*; Bionumber, 4110145255321771). Unfortunately, our MALDI-TOF was affected by severe tremors of the devastating explosion of the port of Beirut (on August 4, 2020) and could not reveal any identification. Thus, discrimination between these species warranted further testing (molecular, MALDI-TOF, WGS), which was kindly extended by colleagues from Lebanon, United States, and Canada (thanked under acknowledgment), whereby all of them revealed the identification as *C. duobushaemulonii* (Awada et al., 2021). This reflected the difficulties in the proper identification of *C. auris* (Iguchi et al., 2019). Subsequently, the recovered *C. auris* under study were identified by the MALDI-TOF and WGS.

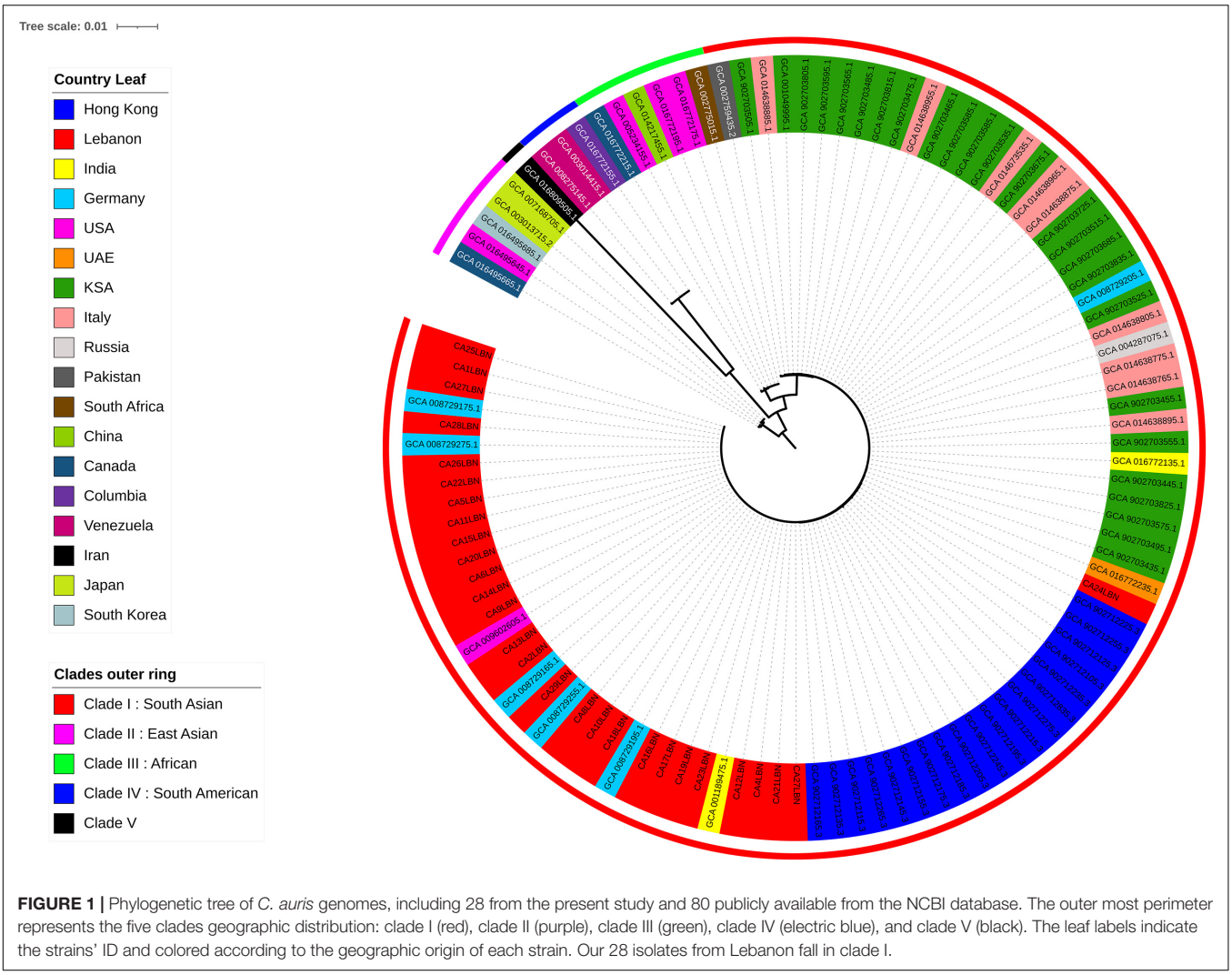


**FIGURE 1 |** Phylogenetic tree of *C. auris* genomes, including 28 from the present study and 80 publicly available from the NCBI database. The outer most perimeter represents the five clades geographic distribution: clade I (red), clade II (purple), clade III (green), clade IV (electric blue), and clade V (black). The leaf labels indicate the strains' ID and colored according to the geographic origin of each strain. Our 28 isolates from Lebanon fall in clade I.

Concerning the phenotypic and genotypic antifungal susceptibility of *C. auris*, it also has its challenges, and it is worth to compare our findings with those reported from different parts of the world. With regard to the antifungal agents mostly used for the treatment of infection due to this pathogen, a couple of agents are relied upon including caspofungin, micafungin, fluconazole, voriconazole, and amphotericin B. Our study generally showed comparable uniform susceptible findings to those reported regionally concerning echinocandins (caspofungin and micafungin) (Emara et al., 2015; Khan et al., 2018; Al Maani et al., 2019; Almaghrabi et al., 2020). However, a sporadic resistance to echinocandins was reported from the United States (1%) (Forsberg et al., 2020), and from India and South Africa (7%) (Lockhart et al., 2017). Moreover, the uniform resistance rates to fluconazole in our study was also comparable to those reported regionally (Emara et al., 2015; Al-Siyabi et al., 2017; Mohsin et al., 2017; Salah et al., 2021) except that of one study in Oman, which reported a lower resistant rate (58%) (Al Maani et al., 2019). Globally, 93% of *C. aris* isolates were resistant to fluconazole (Lockhart et al., 2017). Concerning voriconazole, our results revealed a range of susceptibility against *C. auris*, namely, 36% S, 61% I, and 3% R, while resistant data from our region and other parts of the world showed a range of 8–73.6% (Lockhart et al., 2017; Almaghrabi et al., 2020). Nevertheless, among these triazoles, fluconazole susceptibility has been suggested by CDC to be used as a surrogate marker for second generation triazole (e.g., voriconazole) susceptibility assessment. Still, isolates that are resistant to fluconazole may respond to other triazoles occasionally (see text footnote 1).

As for amphotericin B, the resistance rate against *C. auris* in our study was uniform (100%). This resistant rate is higher than those reported rates (0–62%) from different countries in our region such as Saudi Arabia (62%) (Almaghrabi et al., 2020), Oman (33–50%) (Al-Siyabi et al., 2017; Mohsin et al., 2017; Al Maani et al., 2019), Kuwait (23%) (Emara et al., 2015), United Arab Emirates (0%) (Alatoom et al., 2018), and other countries including Pakistan and India (35%) (Lockhart et al., 2017). In the United States, the reported amphotericin B resistant rate was 33% (Forsberg et al., 2020). Fortunately, the pan- and echinocandin-resistant *C. auris* strains were not detected in Lebanon, as was

recently reported from Texas and District of Columbia (DC) in United States (Lyman et al., 2021).

The molecular characterization of the resistance genes in our study indicated the presence of Y132F mutations in *Erg11* gene in all isolates, reflecting the resistance to azoles. These Y132F substitutions were commonly detected among South Asian isolates particularly Indian and Pakistani strains and considered clade-I-specific markers of resistance against fluconazole (Lockhart et al., 2017). Moreover, Y132F substitution in *ERG11* gene appears to be combined with a novel mutation in the *CDR1* gene, an ATP-binding cassette (ABC)-type efflux pump-encoding gene, which has previously been shown to substantially contribute to azole resistance in *C. auris* (Chowdhary et al., 2018). However, the genetic determinants promoting the increased expression of efflux pump-encoding genes in *C. auris* remain unidentified (Kim et al., 2019; Rybak et al., 2019). Rybak et al. study demonstrates that fluconazole-resistant clinical isolates of *C. auris* exhibit elevated levels of *CDR1* expression and contribute significantly to clinical resistance against the entire class of triazole antifungals. The deletion of *CDR1* in this fluconazole-resistant clinical isolate was sufficient to restore triazole resistance and increase the susceptibility of resistant strains from 64- to 128-fold. Several mechanisms have been proposed for the increased gene expression such as higher levels of mRNA stability, gene amplification, or deregulation because of point mutations in the promoter region.

Unfortunately, there is little or no information about CDR1 hotspot mutations in *C. auris* in the literature.

However, sequence analysis of the *Candida albicans CDR1* gene showed several point mutations located near the promoter of the resistant strains. These point mutations could be distributed within the recognition sequence for the binding of trans-acting transcription factors, and hence, changes to the nucleotide sequence could cause either less efficient binding of transcriptional repressors or increase in the affinity of activators to the promoter region, therefore upregulating CDR1 (Looi et al., 2005).

For amphotericin B, the 100% resistance among our isolates was detected despite the absence of main resistance drivers related to *ERG2*, *ERG3*, and *ERG6* gene mutation (Frias-De-Leon et al., 2020). Such finding indicates that the mechanism of amphotericin resistance remains to be fully elucidated.

All isolates showed a mutation in THR1 (L188G), a gene encoding a homoserine kinase involved in the biosynthesis of threonine. THR1 is considered a potential molecular target for antifungal chemotherapy, since THR1 genes are essential for growth and are required for virulence of *C. albicans* and *C. neoformans* cells (Kingsbury and McCusker, 2008). *C. albicans* cells lacking THR1 accumulate the toxic biosynthetic intermediate homoserine and are attenuated in terms of virulence and die rapidly upon threonine starvation and serum incubation (Kingsbury and McCusker, 2010a,b). Moreover, *C. albicans* THR1-depleted mutants exhibited increased sensitivity to oxidative and osmotic stress (Lee et al., 2018). Regarding the phylogenetic analysis, different findings have been reported globally. In our study, all *C. auris* genomes belonged to clade I showing a limited genetic diversity with SNP difference of $\leq$6, regardless of the recovered source, site of specimen, or time span between isolations, thereby highly reflecting an outbreak due to hospital-associated transmission and confirming what was reported earlier from the same medical center (Allaw et al., 2021). This clade I finding was similar to that reported in Qatar, Saudi Arabia, Oman, Pakistan, and India (Alfouzan et al., 2019). Other studies from different parts of the world reported other clades, for instance, clade III (Africa) among Australian isolates (Biswas et al., 2020), clade IV (South America) among isolates from Chicago (Roberts et al., 2021) and Venzuela (Lockhart et al., 2017), clade II (East Asia) from Japan, and clade V from Iran (Chow et al., 2019).

## CONCLUSION

This first molecular characterization of *C. auris* from Lebanon revealed the exclusivity of clade I lineage among the studied isolates. This clade I together with its uniform resistance to fluconazole and amphotericin B are similar to what was reported from different countries in our region. The control of such highly resistant pathogen necessitates an appropriate and rapid recovery and identification to contain spread and outbreaks.

## DATA AVAILABILITY STATEMENT

The datasets presented in this study can be found in online repositories. The names of the repository/repositories and accession number(s) can be found in the article/**Supplementary Material**.

## AUTHOR CONTRIBUTIONS

GA designed the study. GA and RE collected the *Candida* samples. IB, LR, MF, and RE conducted the experiments. GA, IB, LR, MF, and GD analyzed the data and wrote the manuscript. All authors revised and approved the final draft.

## FUNDING

This study was supported by the Charles University Research Fund PROGRES (project number Q39) and by project CZ.02.1.01/0.0/0.0/16_019/0000787 "Fighting Infectious Diseases," provided by the Ministry of Education Youth and Sports of the Czech Republic.

## ACKNOWLEDGMENTS

Appreciation and thanks are extended to our colleagues and staff noted below for their kind assistance in analyzing the first recovered isolates: Nancy L. Wengenack, Director, Mycology and Mycobacteriology Laboratories, Mayo College of

Medicine, Minnesota, United States; Philippe Dufresne, Director of Laboratoire de Santé Publique du Québec, Canada; Shawn R. Lockhart, Senior Clinical Laboratory Advisor, Mycotic Diseases Branch, Centers for Disease Control and Prevention, Atlanta, GA, United States; and Samia Naccache, Technical Director Microbiology and Molecular Department, LabCorp/Dynacare NW for Swedish Medical Center, Seattle, United States; and to the Clinical Microbiology staff at AUBMC and Fata Akl at CIDR for their technical support.

## SUPPLEMENTARY MATERIAL

The Supplementary Material for this article can be found online at: https://www.frontiersin.org/articles/10.3389/fmicb.2021.770635/full#supplementary-material

**Supplementary Table 1 |** *Candida auris* isolates accession numbers.

**Supplementary Table 2 |** The number and location of SNPs among *Candida auris* isolates.

## REFERENCES

Al Maani, A., Paul, H., Al-Rashdi, A., Wahaibi, A. A., Al-Jardani, A., Al Abri, A. M. A., et al. (2019). Ongoing challenges with healthcare-associated *Candida auris* outbreaks in Oman. *J. Fungi* 5:101. doi: 10.3390/jof5040101

Alatoom, A., Sartawi, M., Lawlor, K., AbdelWareth, L., Thomsen, J., Nusair, A., et al. (2018). Persistent candidemia despite appropriate fungal therapy: first case of *Candida auris* from the United Arab emirates. *Int. J. Infect. Dis.* 70, 36–37. doi: 10.1016/j.ijid.2018.02.005

Alfouzan, W., Ahmad, S., Dhar, R., Asadzadeh, M., Almerdasi, N., Abdo, N. M., et al. (2020). Molecular epidemiology of *Candida auris* outbreak in a major secondary-care hospital in Kuwait. *J. Fungi* 6:307. doi: 10.3390/jof6040307

Alfouzan, W., Dhar, R., Albarrag, A., and Al-Abdely, H. (2019). The emerging pathogen *Candida auris*: a focus on the middle-eastern countries. *J. Infect. Public Health* 12, 451–459. doi: 10.1016/j.jiph.2019.03.009

Allaw, F., Kara Zahreddine, N., Ibrahim, A., Tannous, J., Taleb, H., Bizri, A. R., et al. (2021). First *Candida auris* outbreak during a COVID-19 pandemic in a tertiary-care center in Lebanon. *Pathogens* 10:157. doi: 10.3390/pathogens10020157

Almaghrabi, R. S., Albalawi, R., Mutabagani, M., Atienza, E., Aljumaah, S., Gade, L., et al. (2020). Molecular characterisation and clinical outcomes of *Candida auris* infection: single-centre experience in Saudi Arabia. *Mycoses* 63, 452–460. doi: 10.1111/myc.13065

Almagro Armenteros, J. J., Tsirigos, K. D., Sonderby, C. K., Petersen, T. N., Winther, O., Brunak, S., et al. (2019). SignalP 5.0 improves signal peptide predictions using deep neural networks. *Nat. Biotechnol.* 37, 420–423. doi: 10.1038/s41587-019-0036-z

Al-Siyabi, T., Al Busaidi, I., Balkhair, A., Al-Muharrmi, Z., Al-Salti, M., and Al'Adawi, B. (2017). First report of *Candida auris* in Oman: clinical and microbiological description of five candidemia cases. *J. Infect.* 75, 373–376. doi: 10.1016/j.jinf.2017.05.016

Altschul, S. F., Gish, W., Miller, W., Myers, E. W., and Lipman, D. J. (1990). Basic local alignment search tool. *J. Mol. Biol.* 215, 403–410. doi: 10.1016/S0022-2836(05)80360-2

Araj, G. F., Asmar, R. G., and Avedissian, A. Z. (2015). Candida profiles and antifungal resistance evolution over a decade in Lebanon. *J. Infect. Dev. Ctries* 9, 997–1003. doi: 10.3855/jidc.6550

Awada, B., Alam, W., Chalfoun, M., Araj, G., and Bizri, A. R. (2021). COVID-19 and Candida duobushaemulonii superinfection: a case report. *J. Mycol. Med.* 31:101168. doi: 10.1016/j.mycmed.2021.101168

Biswas, C., Wang, Q., van Hal, S. J., Eyre, D. W., Hudson, B., Halliday, C. L., et al. (2020). Genetic heterogeneity of Australian *Candida auris* isolates: insights from a nonoutbreak setting using whole-genome sequencing. *Open Forum Infect. Dis.* 7:ofaa158. doi: 10.1093/ofid/ofaa158

Blachowicz, A., Chiang, A. J., Elsaesser, A., Kalkum, M., Ehrenfreund, P., Stajich, J. E., et al. (2019). Proteomic and metabolomic characteristics of extremophilic fungi under simulated mars conditions. *Front. Microbiol.* 10:1013. doi: 10.3389/fmicb.2019.01013

Bruna, T., Hoff, K. J., Lomsadze, A., Stanke, M., and Borodovsky, M. (2021). BRAKER2: automatic eukaryotic genome annotation with GeneMark-EP+ and AUGUSTUS supported by a protein database. *NAR Genom. Bioinform.* 3:lqaa108. doi: 10.1093/nargab/lqaa108

Buchfink, B., Xie, C., and Huson, D. H. (2015). Fast and sensitive protein alignment using diamond. *Nat. Methods* 12, 59–60. doi: 10.1038/nmeth.3176

Camacho, C., Coulouris, G., Avagyan, V., Ma, N., Papadopoulos, J., Bealer, K., et al. (2009). BLAST+: architecture and applications. *BMC Bioinform.* 10:421. doi: 10.1186/1471-2105-10-421

Cernakova, L., Roudbary, M., Bras, S., Tafaj, S., and Rodrigues, C. F. (2021). *Candida auris*: a quick review on identification, current treatments, and challenges. *Int. J. Mol. Sci.* 22:4470. doi: 10.3390/ijms22094470

Chow, N. A., de Groot, T., Badali, H., Abastabar, M., Chiller, T. M., and Meis, J. F. (2019). Potential fifth clade of *Candida auris*, Iran, 2018. *Emerg. Infect. Dis.* 25, 1780–1781. doi: 10.3201/eid2509.190686

Chow, N. A., Munoz, J. F., Gade, L., Berkow, E. L., Li, X., Welsh, R. M., et al. (2020). Tracing the evolutionary history and global expansion of *Candida auris* using population genomic analyses. *mBio* 11:e03364-19. doi: 10.1128/mBio.03364-19

Chowdhary, A., Prakash, A., Sharma, C., Kordalewska, M., Kumar, A., Sarma, S., et al. (2018). A multicentre study of antifungal susceptibility patterns among 350 *Candida auris* isolates (2009-17) in India: role of the ERG11 and FKS1 genes in azole and echinocandin resistance. *J. Antimicrob. Chemother.* 73, 891–899. doi: 10.1093/jac/dkx480

Emara, M., Ahmad, S., Khan, Z., Joseph, L., Al-Obaid, I., Purohit, P., et al. (2015). *Candida auris* candidemia in Kuwait, 2014. *Emerg. Infect. Dis.* 21, 1091–1092. doi: 10.3201/eid2106.150270

Forsberg, K., Lyman, M., Chaturvedi, S., and Schneider, E. C. (2020). Public health action-based system for tracking and responding to U.S. Candida drug resistance: AR Lab Network, 2016-2019. *Open Forum Infect. Dis.* 7(Suppl. 1), S206–S207. doi: 10.1093/ofid/ofaa439.465

Forsberg, K., Woodworth, K., Walters, M., Berkow, E. L., Jackson, B., Chiller, T., et al. (2019). *Candida auris*: the recent emergence of a multidrug-resistant fungal pathogen. *Med. Mycol.* 57, 1–12. doi: 10.1093/mmy/myy054

Frias-De-Leon, M. G., Hernandez-Castro, R., Vite-Garin, T., Arenas, R., Bonifaz, A., Castanon-Olivares, L., et al. (2020). Antifungal resistance in *Candida auris*: molecular determinants. *Antibiotics* 9:568. doi: 10.3390/antibiotics9090568

Hoff, K. J., Lange, S., Lomsadze, A., Borodovsky, M., and Stanke, M. (2016). BRAKER1: unsupervised RNA-seq-based genome annotation with GeneMark-ET and AUGUSTUS. *Bioinformatics* 32, 767–769. doi: 10.1093/bioinformatics/btv661

Hoff, K. J., Lomsadze, A., Borodovsky, M., and Stanke, M. (2019). Whole-genome annotation with BRAKER. *Methods Mol. Biol.* 1962, 65–95. doi: 10.1007/978-1-4939-9173-0_5

Huerta-Cepas, J., Forslund, K., Coelho, L. P., Szklarczyk, D., Jensen, L. J., von Mering, C., et al. (2017). Fast genome-wide functional annotation through orthology assignment by eggNOG-mapper. *Mol. Biol. Evol.* 34, 2115–2122. doi: 10.1093/molbev/msx148

Huerta-Cepas, J., Szklarczyk, D., Heller, D., Hernandez-Plaza, A., Forslund, S. K., Cook, H., et al. (2019). eggNOG 5.0: a hierarchical, functionally and phylogenetically annotated orthology resource based on 5090 organisms and 2502 viruses. *Nucleic Acids Res.* 47, D309–D314. doi: 10.1093/nar/gky1085

Iguchi, S., Itakura, Y., Yoshida, A., Kamada, K., Mizushima, R., Arai, Y., et al. (2019). *Candida auris*: a pathogen difficult to identify, treat, and eradicate and its characteristics in Japanese strains. *J. Infect. Chemother.* 25, 743–749. doi: 10.1016/j.jiac.2019.05.034

Jones, P., Binns, D., Chang, H. Y., Fraser, M., Li, W., McAnulla, C., et al. (2014). InterProScan 5: genome-scale protein function classification. *Bioinformatics* 30, 1236–1240. doi: 10.1093/bioinformatics/btu031

Khan, Z., Ahmad, S., Al-Sweih, N., Joseph, L., Alfouzan, W., and Asadzadeh, M. (2018). Increasing prevalence, molecular characterization and antifungal drug

susceptibility of serial *Candida auris* isolates in Kuwait. *PLoS One* 13:e0195743. doi: 10.1371/journal.pone.0195743

Kim, S. H., Iyer, K. R., Pardeshi, L., Munoz, J. F., Robbins, N., Cuomo, C. A., et al. (2019). Erratum for Kim et al., "genetic analysis of *Candida auris* implicates Hsp90 in morphogenesis and azole tolerance and Cdr1 in azole resistance". *mBio* 10:e00346-19. doi: 10.1128/mBio.00346-19

Kingsbury, J. M., and McCusker, J. H. (2008). Threonine biosynthetic genes are essential in *Cryptococcus neoformans*. *Microbiology* 154(Pt. 9), 2767–2775. doi: 10.1099/mic.0.2008/019729-0

Kingsbury, J. M., and McCusker, J. H. (2010a). Cytocidal amino acid starvation of *Saccharomyces cerevisiae* and *Candida albicans* acetolactate synthase (*ilv2*Δ) mutants is influenced by the carbon source and rapamycin. *Microbiology* 156, 929–939. doi: 10.1099/mic.0.034348-0

Kingsbury, J. M., and McCusker, J. H. (2010b). Fungal homoserine kinase (*thr1*Δ) mutants are attenuated in virulence and die rapidly upon threonine starvation and serum incubation. *Eukaryot. cell* 9, 729–737. doi: 10.1128/EC.00045-10

Laslett, D., and Canback, B. (2004). ARAGORN, a program to detect tRNA genes and tmRNA genes in nucleotide sequences. *Nucleic Acids Res.* 32, 11–16. doi: 10.1093/nar/gkh152

Lee, Y. T., Fang, Y. Y., Sun, Y. W., Hsu, H. C., Weng, S. M., Tseng, T. L., et al. (2018). THR1 mediates GCN4 and CDC4 to link morphogenesis with nutrient sensing and the stress response in Candida albicans. *Int. J. Mol. Med.* 42, 3193–3208. doi: 10.3892/ijmm.2018.3930

Letunic, I., and Bork, P. (2019). Interactive Tree Of Life (iTOL) v4: recent updates and new developments. *Nucleic Acids Res.* 47, W256–W259. doi: 10.1093/nar/gkz239

Lockhart, S. R., Etienne, K. A., Vallabhaneni, S., Farooqi, J., Chowdhary, A., Govender, N. P., et al. (2017). Simultaneous emergence of multidrug-resistant *Candida auris* on 3 continents confirmed by whole-genome sequencing and epidemiological analyses. *Clin. Infect. Dis.* 64, 134–140. doi: 10.1093/cid/ciw691

Looi, C. Y., Ec, D. S., Seow, H. F., Rosli, R., Ng, K. P., and Chong, P. P. (2005). Increased expression and hotspot mutations of the multidrug efflux transporter, CDR1 in azole-resistant *Candida albicans* isolates from vaginitis patients. *FEMS Microbiol. Lett.* 249, 283–289. doi: 10.1016/j.femsle.2005.06.036

Lyman, M., Forsberg, K., Reuben, J., Dang, T., Free, R., Seagle, E. E., et al. (2021). Notes from the field: transmission of pan-resistant and echinocandin-resistant *Candida auris* in health care facilities - Texas and the District of Columbia, January-April 2021. *MMWR Morb. Mortal. Wkly Rep.* 70, 1022–1023. doi: 10.15585/mmwr.mm7029a2

Manni, M., Berkeley, M. R., Seppey, M., and Zdobnov, E. M. (2021). BUSCO: assessing genomic data quality and beyond. *Curr. Protoc.* 1:e323. doi: 10.1002/cpz1.323

Mohsin, J., Hagen, F., Al-Balushi, Z. A. M., de Hoog, G. S., Chowdhary, A., Meis, J. F., et al. (2017). The first cases of *Candida auris* candidaemia in Oman. *Mycoses* 60, 569–575. doi: 10.1111/myc.12647

Patel, R. (2019). A moldy application of MALDI: MALDI-ToF Mass Spectrometry for Fungal Identification. *J Fungi* 5:4. doi: 10.3390/jof5010004

Prakash, A., Sharma, C., Singh, A., Kumar Singh, P., Kumar, A., Hagen, F., et al. (2016). Evidence of genotypic diversity among *Candida auris* isolates by multilocus sequence typing, matrix-assisted laser desorption ionization time-of-flight mass spectrometry and amplified fragment length polymorphism. *Clin. Microbiol. Infect.* 22, 277.e1-9. doi: 10.1016/j.cmi.2015.10.022

Price, M. N., Dehal, P. S., and Arkin, A. P. (2010). FastTree 2–approximately maximum-likelihood trees for large alignments. *PLoS One* 5:e9490. doi: 10.1371/journal.pone.0009490

Roberts, S. C., Zembower, T. R., Ozer, E. A., and Qi, C. (2021). Genetic evaluation of nosocomial *Candida auris* transmission. *J. Clin. Microbiol.* 59, e02252-20. doi: 10.1128/JCM.02252-20

Rybak, J. M., Doorley, L. A., Nishimoto, A. T., Barker, K. S., Palmer, G. E., and Rogers, P. D. (2019). Abrogation of triazole resistance upon deletion of CDR1 in a clinical isolate of *Candida auris*. *Antimicrob. Agents Chemother.* 63, e00057-19. doi: 10.1128/AAC.00057-19

Rychert, J., Slechta, E. S., Barker, A. P., Miranda, E., Babady, N. E., Tang, Y. W., et al. (2018). Multicenter evaluation of the Vitek MS v3.0 system for the identification of filamentous fungi. *J. Clin. Microbiol.* 56, e01353-17. doi: 10.1128/JCM.01353-17

Salah, H., Sundararaju, S., Dalil, L., Salameh, S., Al-Wali, W., Tang, P., et al. (2021). Genomic epidemiology of *Candida auris* in qatar reveals hospital transmission dynamics and a South Asian origin. *J. Fungi* 7:240. doi: 10.3390/jof7030240

Schelenz, S., Hagen, F., Rhodes, J. L., Abdolrasouli, A., Chowdhary, A., Hall, A., et al. (2016). First hospital outbreak of the globally emerging *Candida auris* in a European hospital. *Antimicrob. Resist. Infect. Control* 5:35. doi: 10.1186/s13756-016-0132-5

Schoch, C. L., Seifert, K. A., Huhndorf, S., Robert, V., Spouge, J. L., Levesque, C. A., et al. (2012). Nuclear ribosomal internal transcribed spacer (ITS) region as a universal DNA barcode marker for Fungi. *Proc. Natl. Acad. Sci. U.S.A.* 109, 6241–6246. doi: 10.1073/pnas.1117018109

Seemann, T. (2015). *Snippy: Fast Bacterial Variant Calling From NGS Reads [Internet]*. San Francisco, CA: github.

Smith, C. A. (2021). Macrosynteny analysis between lentinula edodes and lentinula novae-zelandiae reveals signals of domestication in lentinula edodes. *Sci. Rep.* 11:9845. doi: 10.1038/s41598-021-89146-y

Stanke, M., Diekhans, M., Baertsch, R., and Haussler, D. (2008). Using native and syntenically mapped cDNA alignments to improve de novo gene finding. *Bioinformatics* 24, 637–644. doi: 10.1093/bioinformatics/btn013

Stanke, M., Schoffmann, O., Morgenstern, B., and Waack, S. (2006). Gene prediction in eukaryotes with a generalized hidden Markov model that uses hints from external sources. *BMC Bioinform.* 7:62. doi: 10.1186/1471-2105-7-62

Ter-Hovhannisyan, V., Lomsadze, A., Chernoff, Y. O., and Borodovsky, M. (2008). Gene prediction in novel fungal genomes using an ab initio algorithm with unsupervised training. *Genome Res.* 18, 1979–1990. doi: 10.1101/gr.081612.108

Treangen, T. J., Ondov, B. D., Koren, S., and Phillippy, A. M. (2014). The Harvest suite for rapid core-genome alignment and visualization of thousands of intraspecific microbial genomes. *Genome Biol.* 15:524. doi: 10.1186/s13059-014-0524-x

Vasquez-Gross, H., Kaur, S., Epstein, L., and Dubcovsky, J. (2020). A haplotype-phased genome of wheat stripe rust pathogen *Puccinia striiformis* f. sp. tritici, race PST-130 from the Western USA. *PLoS One* 15:e0238611. doi: 10.1371/journal.pone.0238611

**Conflict of Interest:** The authors declare that the research was conducted in the absence of any commercial or financial relationships that could be construed as a potential conflict of interest.

**Publisher's Note:** All claims expressed in this article are solely those of the authors and do not necessarily represent those of their affiliated organizations, or those of the publisher, the editors and the reviewers. Any product that may be evaluated in this article, or claim that may be made by its manufacturer, is not guaranteed or endorsed by the publisher.

frontiers | Frontiers in Microbiology

ORIGINAL RESEARCH
published: 23 June 2022
doi: 10.3389/fmicb.2022.866674

# Changes in Fecal Carriage of Extended-Spectrum β-Lactamase Producing Enterobacterales in Dutch Veal Calves by Clonal Spread of *Klebsiella pneumoniae*

*Teresita d.J. Bello Gonzalez[1]*, Arie Kant[1], Quillan Dijkstra[1], Francesca Marcato[2], Kees van Reenen[2], Kees T. Veldman[1] and Michael S. M. Brouwer[1]*

[1]*Department of Bacteriology, Host-Pathogen Interaction, and Diagnostics Development, Wageningen Bioveterinary Research, Lelystad, Netherlands,* [2]*Wageningen Livestock Research, Wageningen University and Research, Wageningen, Netherlands*

OPEN ACCESS

**Edited by:**
*Ravi kant,*
*University of Helsinki, Finland*

**Reviewed by:**
*Lixin Zhang,*
*Michigan State University, United States*
*Raoudha Dziri,*
*Tunis El Manar University, Tunisia*

***Correspondence:**
*Teresita d.J. Bello Gonzalez*
*teresita.bellogonzalez@wur.nl*

**Specialty section:**
*This article was submitted to Antimicrobials, Resistance and Chemotherapy, a section of the journal Frontiers in Microbiology*

**Received:** *31 January 2022*
**Accepted:** *31 May 2022*
**Published:** *23 June 2022*

**Citation:**
*Bello Gonzalez TdJ, Kant A, Dijkstra Q, Marcato F, van Reenen K, Veldman KT and Brouwer MSM (2022) Changes in Fecal Carriage of Extended-Spectrum β-Lactamase Producing Enterobacterales in Dutch Veal Calves by Clonal Spread of Klebsiella pneumoniae. Front. Microbiol. 13:866674. doi: 10.3389/fmicb.2022.866674*

This study aimed to characterize the changes in fecal carriage of Extended-Spectrum β-Lactamase (ESBL) producing Enterobacterales (ESBL-PE) in a single Dutch veal calves. During the rearing period at the Dutch veal farm, a decrease in fecal carriage of cefotaxime-resistant *Escherichia coli* isolates was observed after 2 weeks at the veal farm, while an increase of cefotaxime-resistant *Klebsiella pneumoniae* isolates was demonstrated. *E. coli* and *K. pneumoniae* were isolated from rectal swabs collected from 110 veal calves in week 2, 6, 10, 18, and 24 after their arrival at the farm. ESBL-PE isolates were selectively cultured and identified by MALDI-TOF. ESBL genes were characterized by RT-PCR, PCRs, and amplicon sequencing. A total of 80 *E. coli* and 174 *K. pneumoniae* strains were isolated from 104 out of 110 veal calves. The prevalence of ESBL-*E. coli* decreased from week 2 (61%) to week 6 (7%), while an unexpected increase in ESBL-*K. pneumoniae* colonization was detected in week 6 (80%). The predominant ESBL genes detected in *E. coli* isolates were $bla_{\text{CTX-M-15}}$ and the non-ESBL gene $bla_{\text{TEM-1a}}$, while in *K. pneumoniae* $bla_{\text{CTX-M-14}}$ gene was detected in all isolates. Four cefotaxime-resistant *K. pneumoniae* isolates were randomly selected and characterized in deep by transformation, PCR-based replicon typing, and whole-genome sequencing (WGS). The clonal relatedness of a subgroup of nine animals carrying *K. pneumoniae* ESBL genes was investigated by Multi Locus sequence typing (MLST). In four ESBL-*K. pneumoniae* isolates, $bla_{\text{CTX-M-14}}$ was located on $\text{IncFII}_{\text{K}}$ and $\text{IncFII}_{\text{NK}}$ plasmid replicons and the isolates were multi-drug resistant (MDR). MLST demonstrated a clonal spread of ESBL-*K. pneumoniae* ST107. To the best of our knowledge, this is the first study to report a change in fecal carriage of ESBL-PE over time in the same veal calf during the rearing period.

**Keywords: veal calves, fecal carriage, *Klebsiella pneumoniae*, clonal spread, extended-spectrum β-lactamase producing Enterobacterales**

## INTRODUCTION

Fecal carriage of antibiotic resistant-bacteria represents an important reservoir for the transmission and dissemination of resistance genes within and between commensal bacteria and to pathogens (Munk et al., 2018). Extended-spectrum β-lactamase (ESBLs) producing Enterobacterales (ESBL-PE) constitutes an important group of multidrug-resistant bacteria reported all over the world in humans and animals (Bush and Fisher, 2011). Over the past years, the potential role of food-producing animals as a reservoir of ESBL genes has been described (European Food Safety Authority (EFSA), 2011; Liebana et al., 2013; Schmid et al., 2013). Moreover, food products contaminated by ESBL-PE have also been identified as a source for the dissemination of antibiotic-resistant bacteria to humans through food consumption and/or manipulation (Overdevest et al., 2011). Likewise, plasmid similarities between ESBL-PE isolates obtained from humans and food-producing animals have been described (Kurittu et al., 2021).

The Enterobacterales family inhabit the gastrointestinal tract of humans and several animal species in a symbiotic relationship. Members of this family, particularly *Escherichia coli* and *Klebsiella pneumoniae,* are commonly associated with a variety of severe infections in humans and animals. In dairy cattle and veal calves, these bacteria can cause mastitis as well as respiratory and gastrointestinal infections (Schukken et al., 2012).

In dairy and veal farms, the use of antimicrobials, particularly third- and fourth-generation cephalosporin β-lactam antibiotics, provides a selective pressure for the emergence of resistant bacteria and the increase of antibiotic resistance by the production of ESBLs (Liebana et al., 2013). The usage of these antimicrobials was greatly reduced in the Netherlands which has led to a reduction in the prevalence of ESBLs (NETMAP_MARAN, 2021). The ESBL genes are commonly located on mobile elements including plasmids, facilitating the dissemination of the antibiotic resistance genes between bacteria (Rozwandowicz et al., 2018). Plasmid-encoded ESBL enzymes inactivate a large variety of β-lactam antibiotics including third-generation cephalosporins such as cefotaxime. The CTX-M family is the most predominant ESBL in Enterobacterales isolates from livestock in Europe (Horton et al., 2011; D'Andrea et al., 2013; Waade et al., 2021). In the Netherlands, the CTX-M-1 group (mainly $bla_{\text{CTX-M-1}}$ and $bla_{\text{CTX-M-15}}$) and CTX-M-9 group (mainly $bla_{\text{CTX-M-14}}$) are the most common ESBLs genes identified in *E. coli* isolates obtained from veal calves (NETMAP_MARAN, 2021).

In a previous study, it was reported that usage of antimicrobials, differences in farm management practices, and the environment contribute to the selection and co-selection of antibiotic resistance in veal calves (Hordijk et al., 2013). In the production system in the Netherlands, veal calves are collected from different dairy farms and mixed before they are distributed among veal farms which provides an ideal scenario for the acquisition and transmission of antibiotic-resistant bacteria among the population of calves. During the rearing period at the veal farm, fecal shedding facilitates the dissemination of antibiotic-resistant bacteria including potential pathogens such as *K. pneumoniae* (Genomic Epidemiology Organization Server, n.d.).

The majority of the studies on the occurrence and prevalence of ESBL-*K. pneumoniae* in dairy cattle and veal calves have been confined within raw milk, food products, and bovine mastitis cases (Dahmen et al., 2013; Diab et al., 2017). Nevertheless, CTX-M genes ($bla_{\text{CTX-M-1,}}$ $bla_{\text{CTX-M-15,}}$ and $bla_{\text{CTX-M-14}}$) detected in diseased calves have also been reported in healthy calves (Pubmlst Server, n.d.; Tshitshi et al., 2020). Despite that, limited data are available on the prevalence of fecal carriage of ESBL-*K. pneumoniae* in veal farms during the rearing period.

Between March 2019 and May 2020, we conducted a large longitudinal study on the prevalence of ESBL-*E. coli* in Netherlands. Rectal swabs were collected from calves born in 13 dairy farms and subsequently transported to 8 veal farms across the country where the animals were followed until slaughter. Samples were collected before transportation of the animals from the dairy farm to the veal farm and subsequently at five different time points at the veal farm (2, 6, 10, 18, and 24 weeks; *manuscript submitted*). In one particular veal farm, a decrease in fecal carriage of cefotaxime-resistant *E. coli* isolates was observed 2 weeks after the arrival of calves at the veal farm, while an increase of cefotaxime-resistant *K. pneumoniae* isolates was demonstrated from week 6 until slaughter.

In the present study, we aimed to: (a) identify the resistance genes in 80 cefotaxime-resistant *E. coli* and 174 cefotaxime-resistant *K. pneumoniae* isolates from veal calves obtained during the rearing period in one particular veal farm; (b) follow-up the fecal carriage of ESBL-*K. pneumoniae* isolates from a subgroup of nine animals and one animal carrying ESBL-*E. coli* over time, to identify the clonal relatedness between the isolates recovered, and (c) identify the mobile elements present in four ESBL-*K. pneumoniae* isolates randomly selected by whole-genome sequencing (WGS)-based analyses.

## MATERIALS AND METHODS

### *Escherichia coli* and *Klebsiella pneumoniae* Isolates

A total of 80 *E. coli* and 174 cefotaxime-resistant *K. pneumoniae* isolates were identified from 104 out of 110 calves in week 2, 6, 10, 18, and 24 during the rearing period at the veal farm, see Marcato et al. (2022) for the complete experimental setup. The remaining six animals were culture negative during all time points. In brief, rectal swabs were placed in 3 ml of Buffer Peptone Water (BPW; Becton Dickinson GmbH, Heidelberg, Germany) and incubated overnight at 37°C. After incubation, an aliquot (10 ul) of the enriched solution was plated on MacConkey agar plates with 1 mg/L of cefotaxime and incubated overnight at 44°C (European Reference Laboratory-Antimicrobial Resistance, n.d.).[1] A single random pink colony was streaked onto Heart Infusion Agar (HIS; Becton Dickinson GmbH, Heidelberg, Germany) supplemented with 5% sheep blood and incubated at 37°C for 24 h to obtain a pure culture. Bacterial isolates were subsequently identified by Matrix-Assisted Laser Desorption Ionization-Time of Light mass spectrometry

[1]https://www.eurl-ar.eu/protocols

(MALDI-TOF MS; Bruker Daltonik, Germany). All the isolates were preserved at −80°C for further analysis.

## Molecular Identification of *Escherichia coli* and *Klebsiella pneumoniae* ESBL Encoding Genes

The *E. coli* and cefotaxime-resistant *K. pneumoniae* isolates were further analyzed by a Real-time PCR assay on a light cycler System (Applied Biosystems, 7500 Fast Real-Time PCR System) for the detection of ESBL genes $bla_{\text{CTX-M-1}}$ group, $bla_{\text{CMY}}$, $bla_{\text{TEM}}$, and $bla_{\text{SHV}}$ as previously described, using bacteria cell boiled lysate method as DNA template (Geurts et al., 2017; Veldman et al., 2018). In case of negative results, single PCRs for $bla_{\text{CTX-M-2}}$ group, $bla_{\text{CTX-M-8/25}}$, $bla_{\text{CTX-M-9}}$ group and chromosomal *bla*AmpC were performed (Dierikx et al., 2012; Liakopoulos et al., 2016a). Well-defined strains with known ESBLs genes were included as positive controls in the PCR assays. The identification of the ESBL detected by PCR was confirmed by DNA Sanger sequencing using the PCR product by QIAquick® PCR Purification kit (Qiagen®). Subsequently, the PCR product was purified using Sephadex (Merck) and used for the DNA Sanger sequencing (3130 Genetic Analyzer) as previously described (Liakopoulos et al., 2016a). The sequences were compared with reference sequences obtained from GenBank using the Sequencher 5.4.6 software.

## *Klebsiella pneumoniae* Antimicrobial Susceptibility Testing

Antimicrobial susceptibility tests of four cefotaxime-resistant *K. pneumoniae* isolates randomly selected from the earliest and latest time point possible ($n = 2$ week 6 and $n = 2$ week 24) were tested by broth microdilution using standard European antibiotic panels EUVSEC and EUVSEC2 (Thermo Fisher, "Sensititre™ Gram-Negative MIC Plate" n.d.) (World Health Organization (WHO), n.d.). *E. coli* ATCC 25922 was used as a control reference strain. The results were interpreted using the EUCAST ECOFFs (v7.1),[2] in case epidemiological cut-off values (ECOFFs) for *K. pneumoniae* were lacking, we used *E. coli* ECOFFs for the interpretation. The *K. pneumoniae* isolates, two from week 6 and one from week 24, were obtained from animals that were initially colonized with ESBL-*E. coli* at week 2 carrying $bla_{\text{CTX\_M-15}}$ and non-ESBL $bla_{\text{TEM-1a}}$ gene, while the additional *K. pneumoniae* isolates included from week 24 were colonized with *K. pneumoniae* in week 6 and 10 and negative culture in week 2.

## *Klebsiella pneumoniae* Plasmid and WGS Analysis

The same four ESBL-*K. pneumoniae* isolates used for antimicrobial susceptibility testing were characterized in depth using molecular methods. Plasmids carrying ESBLs genes were extracted from pure culture using a miniprep method and transformed by electroporation into competent DH10B cells (Thermo Scientific, United States) as previously described (Liakopoulos et al., 2016a). The obtained transformants were selected on Luria Bertani (LB) agar plates supplemented with cefotaxime (1 mg/L) and confirmed for the presence of the ESBL gene using PCR. The plasmid typing was performed using the PCR-Based Replicon Typing (PBRT) 2.0 Kit (DIATHEVA, Fano, Italy) as previously described (Carattoli et al., 2005). To confirm the location of the identified genes on the plasmids in the four *K. pneumoniae* selected isolates, WGS was performed. The *K. pneumoniae* DNA was isolated and purified using the Qiagen Blood and tissue DNA isolation kit, and DNA concentration was measured with a CLARIOstar Plus (BMG Labtech). The isolated DNA was used for library preparation using the KAPA HyperPlus Kit (KAPA BIOSYSTEMS). DNA was loaded onto the MiSeq (Illumina) sequencer using the MiSeq Reagent kit v3 (Illumina) with pair-end reads, generating 250–300-bp read length.

In addition, MinION long read sequencing was performed using a single *K. pneumoniae* isolate as representative of the other three isolates randomly selected. DNA extraction was conducted using the Gentra Puregene Blood Kit (Qiagen). The preparation of the DNA for sequencing using 500 ng of purified DNA was performed using the Genomic DNA Ligation kit (SQK-LSK109, Oxford Nanopore Technologies, United Kingdom). The DNA sample was barcoded using the Native barcoding genomic DNA kits (EXP-NBD104 Oxford Nanopore Technologies, United Kingdom). The run of the samples was performed in a Flongle flow cell (FLO-FLG001, Oxford Nanopore Technologies, United Kingdom; Software v19.06.8). Base-calling was set on High-Accuracy base calling, and adapter trimming was performed through Porechop v0.2.3. After demultiplexing and adapter trimming, the Hybrid assemblies of short sequencing reads of the four randomly selected isolates and long-read sequencing reads of the single selected representative isolate were performed using Unicycler v0.4.7. The assembled genome was analyzed using tools from the "Center for genomic Epidemiology" (CGE) website.[3]

## *Klebsiella pneumoniae* and *Escherichia coli* Multi Locus Sequencing Typing

A subgroup of nine animals ($n = 27$ isolates) carrying ESBL-*K. pneumoniae* were followed-up over time to determine whether or not these ESBL-*K. pneumoniae* isolates were clonally related (**Table 1**). Multi Locus Sequencing Typing (MLST) was carried out according to the protocol previously described in the pubmlst web server.[4] The sequence obtained was compared with the sequences available on the Genomic Epidemiology website. In addition, the only animal colonized with ESBL-*E. coli* ($n = 4$ isolates) over time along with the ESBL-*K. pneumoniae* isolates was also included in the MLST analysis. No additional ESBL-*E. coli* isolates were selected for MLST analysis.

## Accession Number

The Illumina (NGS) sequence data sets generated and analyzed in this study have been deposited in the European Nucleotide Archive (ENA) at EMBL-EBI under accession number PRJEB50519.

[2]www.eucast.org

[3]www.genomicepidemiology.org

[4]www.pubmlst.org

**TABLE 1** | Distribution of fecal carriage of ESBL-*Klebsiella pneumoniae* isolates per time point (week 6 until week 24 after arrival of calves at a Dutch veal farm) selected for MLST analysis.

| Animal ID | Week 6 | Week 10 | Week 18 | Week 24 |
|---|---|---|---|---|
| 1 | *K. pneumoniae* | *K. pneumoniae* | | *K. pneumoniae* |
| 2 | *K. pneumoniae* | *K. pneumoniae* | | *K. pneumoniae* |
| 21 | *K. pneumoniae* | *K. pneumoniae* | | *K. pneumoniae* |
| 28 | *K. pneumoniae* | *K. pneumoniae* | *K. pneumoniae* | |
| 37 | *K. pneumoniae* | *K. pneumoniae* | | *K. pneumoniae* |
| 39 | *K. pneumoniae* | | *K. pneumoniae* | *K. pneumoniae* |
| 59 | *K. pneumoniae* | *K. pneumoniae* | *K. pneumoniae* | |
| 70 | *K. pneumoniae* | *K. pneumoniae* | *K. pneumoniae* | |
| 103 | *K. pneumoniae* | *K. pneumoniae* | *K. pneumoniae* | |

## Statistical Analysis

A *t*-test assuming equal variance statistical test was performed to indicate if a significant change was observed over time between animals colonized with cefotaxime-resistant *E. coli* and *K. pneumoniae*.

# RESULTS

Veal calves were followed longitudinally from the dairy farms to the veal farm as previously described. A total of 80 *E. coli* and 174 cefotaxime-resistant *K. pneumoniae* isolates from rectal swabs obtained from 104 out of 110 veal calves located in the same veal farm in the Netherlands were analyzed. In this particular farm, a decrease of fecal carriage of cefotaxime-resistant *E. coli* isolates was observed from week 2 after transportation of calves from the dairy farms to the veal farm (61.3%) to week 6 at the veal farm (7.3%). Instead, an increase of fecal carriage of cefotaxime-resistant *K. pneumoniae* isolates was observed from week 6 until week 24 (**Figure 1**; $p > 0.05$). We did not detect cefotaxime-resistant *K. pneumoniae* isolates previous to week 6. The prevalence of cefotaxime-resistant *K. pneumoniae* isolates fluctuated during the rearing period, where the highest prevalence was detected in week 6 (80%) and the lowest in week 18 (7.3%). Calves were individually treated with antibiotics [β-Lactam (ampicillin, benzylpenicillin), amphenicol (florfenicol) and, aminoglycoside (gentamicin)] in week 2 ($n = 18$), week 6 ($n = 32$), week 10 ($n = 78$), week 18 ($n = 31$) and week 24 ($n = 30$) due to a respiratory disease (unspecified) for at least 8 weeks. In addition, a nonsteroidal anti-inflammatory drug was given in combination with the antibiotics during the same period. Three batch antibiotic treatments at herd level included tetracycline and aminoglycosides which were provided *via* the milk for 10 feedings within the first 6 weeks after arrival to the veal farms. Since the differences in the production system and management were considered minimal between all the veal farms, no data for risk factor analysis were included at this level.

## Molecular Identification of *Escherichia coli* and *Klebsiella pneumoniae* ESBL Encoding Genes

The $bla_{\text{CTX-M-1}}$ group and $bla_{\text{TEM}}$ genes were detected by RT-PCRs in all of the cefotaxime-resistant *E. coli* isolates. The sequencing results showed that $bla_{\text{CTX\_M-15}}$ was present in all the *E. coli* isolates and in combination with the non-ESBL $bla_{\text{TEM-1a}}$ in 74 *E. coli* isolates (**Supplementary Table 1**), the other six *E. coli* isolates contains only the $bla_{\text{CTX-M-15}}$ gene.

Furthermore, the $bla_{\text{SHV}}$ and $bla_{\text{TEM}}$ were detected by RT-PCRs in all the cefotaxime-resistant *K. pneumoniae* isolates. The sequencing results showed that a non-ESBL allelic variant identified as $bla_{\text{TEM-1b}}$ and a novel chromosomal variant sharing 99.5% identity to $bla_{\text{SHV-1-8}}$ and other variants was identified, which results in a synonymous amino acid sequence. We also obtained positive PCR products for $bla_{\text{CTX-M-9}}$ and $bla_{\text{CTX-M-14}}$ genes. The sequencing analysis indicates that the fragment sequence corresponds to $bla_{\text{CTX-M-14}}$. Furthermore, all the cefotaxime-resistant *K. pneumoniae* isolates were tested by PCR and the sequencing results indicates the presence of the $bla_{\text{CTX-M-14}}$ in all the isolates (**Supplementary Table 1**).

The antimicrobial susceptibility test of four randomly selected *K. pneumoniae* isolates showed an identical resistance profile. The isolates were susceptible to colistin, carbapenems (imipenem, meropenem, ertapenem), azithromycin, chloramphenicol, nalidixic acid, tigecycline, and resistant to ciprofloxacin, gentamicin, sulfamethoxazole, trimethoprim, and tetracycline (**Table 2**). The ESBL phenotype was confirmed by showing resistance to cefotaxime and ceftazidime, susceptibility to cefoxitin, and synergy with clavulanic acid in combination with cefotaxime and ceftazidime.

## *Klebsiella pneumoniae* Plasmid and WGS Data Analysis

Transformation experiments were performed using competent *E. coli* to determine if the $bla_{\text{CTX-M-14}}$ gene was present on a transferable plasmid. Using the four ESBL-*K. pneumoniae* isolates showed a successful transferability of the $bla_{\text{CTX-M-14}}$ gene. The plasmid-based replicon typing analysis detected the presence of two replicons in the transformants: $\text{IncFII}_{\text{K}}$ and $\text{IncFIB}_{\text{KN}}$ type. Hybrid analysis of long-short read sequencing showed that the $bla_{\text{CTX-M-14}}$ gene and the plasmids replicons previously identified were located in a 258.971 bp contig in *K. pneumoniae* isolates 2 week 24. The other three isolates were sequenced with short-read sequencing only which resulted in $bla_{\text{CTX-M-14}}$ and the plasmid replicons in separate smaller contigs. Additionally, plasmid-mediated quinolone resistance (PMQR) genes *qnrS1* and *OqxAB* were identified in the four *K. pneumoniae* isolates, along with genes conferring resistance to aminoglycosides, sulfamethoxazole, fosfomycin, tetracycline, trimethoprim and quaternary ammonium compound-resistance protein (**Table 3**).

## ESBL-*Klebsiella pneumoniae* Clonality Screening by MLST

MLST analysis was carried out on a set of 27 ESBL-*K. pneumoniae* isolates from nine veal calves that were colonized at multiple time-points to determine the clonality of the *K. pneumoniae*. All 27 ESBL-*K. pneumoniae* isolates presented an identical sequence type, all belonging to ST 107. Similarly, all the 4 ESBL-*E. coli* isolates obtained from a single animal colonized at the same rearing period as the animals colonized by ESBL-*K. pneumoniae* present an identical sequence type, all belonging to ST 46.

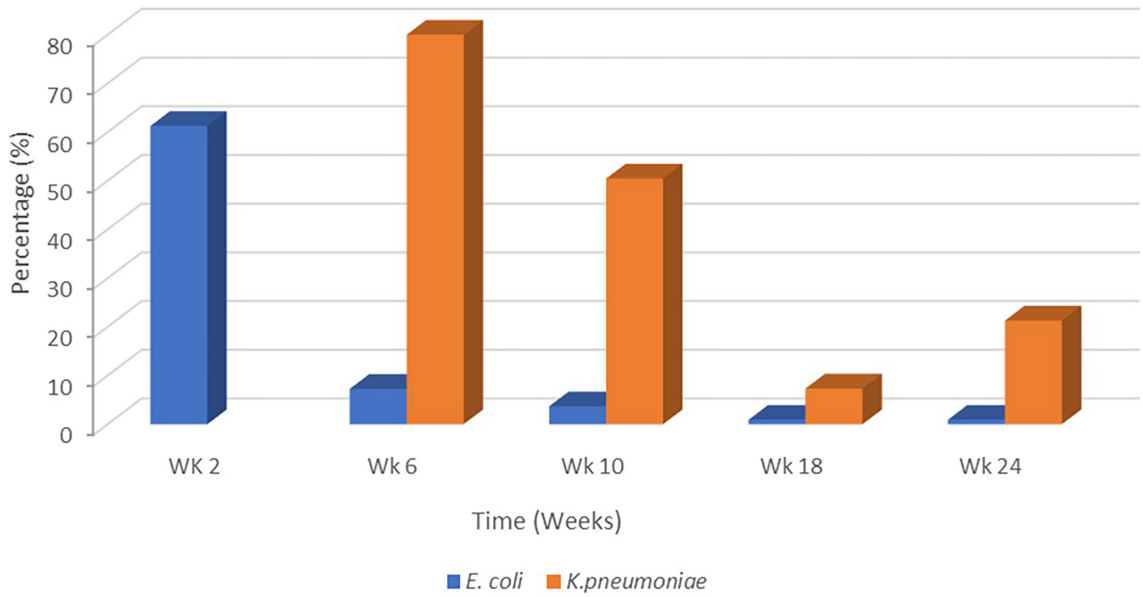


**FIGURE 1 |** Percentage of animals colonized by cefotaxime-resistant *Escherichia coli* and *Klebsiella pneumoniae* isolates recovered over time during the rearing period at the veal farm from week 2 after arrival of calves at the veal farm until week 24.

## DISCUSSION

The World Health Organization (WHO) has included third-generation cephalosporin-resistant *E. coli* and *K. pneumoniae* into the group of "critical pathogens" due to the increasing challenges for infection treatment, highlighting the importance of the monitoring and prevention of infections in humans and animals. In humans, Meijs et al. (2021) have recently reported a high prevalence of fecal carriage of ESBL-*E. coli* and ESBL-*K. pneumoniae* in veterinary healthcare workers in the Netherlands compared to the general Dutch population (9.8% and 5%, respectively) (Meijs et al., 2021). Likewise, in Dutch hospitals, the prevalence of ESBL-*K. pneumoniae* in 2020 increased up to 15% compared to 2019 (12%) (NETMAP_MARAN, 2021). In the longitudinal study reported in the present manuscript, an unexpected increase in fecal carriage of ESBL-*K. pneumoniae* was detected in veal calves. This increase occurred in one single farm, 6 weeks after arrival of the calves to the veal farm and occurred along with a decrease in ESBL-*E. coli* which is typical in many farms at this time point (*submitted manuscript*). A previous study showed a similar low prevalence of ESBL-*E. coli* after 10 weeks at the veal farm (Hordijk et al., 2013). Previously, Adler et al. (2015) showed that the prevalence of ESBL-PE was high in calves (age, < 4 months) compared to adult cows (age > 25 months) (Adler et al., 2015). At the slaughterhouses, a high prevalence of ESBL producers has been reported in France (29.4%) (Haenni et al., 2014) and Switzerland (25%) (Geser et al., 2012), whereas a shift in enteric bacteria species carrying ESBL producers in the same calves has not been reported previously. Therefore, we assessed the characterization of fecal carriage ESBL-*E. coli* and ESBL-*K. pneumoniae* isolates from selected veal calves and the distribution of the ESBL genes present in the calves' population over time.

In our study, the $bla_{\text{CTX-M-15}}$ was the dominant ESBL gene detected in *E. coli*. In the Netherlands, the percentage of ESBL-*E. coli* reported in calves at slaughter age was 47% in 2018 and decreased to 38.1% in 2020, in which the CTX-M-1 group was the most dominant ESBL type detected (NETMAP_MARAN, 2021). The global spread of $bla_{\text{CTX-M-15}}$ has been associated with particular *E. coli* clones such as clonal complex ST131 (Nicolas-Chanoine et al., 2014) and ST46 (Mshana et al., 2011). The *E. coli* clone ST46 harboring $bla_{\text{CTX-M-15}}$ was detected in our study. The ST46 harboring $bla_{\text{CTX-M-15}}$ has been previously identified in healthy chickens and pigs in Nigeria (Chah et al., 2018), in bovine feces in Tunisia (Hassen et al., 2019) and in the aquatic environment in Bangladesh (Rashid et al., 2015), suggesting that ESBL_*E. coli* clonal spread occurs in different environments across the world.

Furthermore, in the *K. pneumoniae*-cefotaxime resistance isolates in our study, the $bla_{\text{CTX-M-14}}$ gene was identified in all the isolates. From those, four isolates were randomly selected to determine their antimicrobial susceptibility phenotype, indicating that those isolates were multidrug-resistant and displayed a typical ESBL phenotype. In addition, the non-ESBL $bla_{\text{TEM-1b}}$ and a novel chromosomal variant of $bla_{\text{SHV}}$ were detected by PCR and amplicon sequencing and confirmed by WGS. Previous studies also reported the presence of non-ESBLs

**TABLE 2 |** Antimicrobial susceptibility testing expressing the Minimal Inhibitory Concentration (MIC) determined in four *Klebsiella pneumoniae* isolates collected from calves in week 6 and week 24 at the veal farm.

| Isolate ID | 63_wk6 | 68_wk6 | 2_wk24 | 37_wk24 |
|---|---|---|---|---|
| EUVSEC* panel | | MIC(mg/L) | | |
| Ampicillin | >64 | >64 | >64 | >64 |
| Azithromycin | 16 | 16 | 16 | 16 |
| Cefotaxime | >4 | >4 | >4 | >4 |
| Ceftazidime | 2 | 1 | 2 | 2 |
| Chloramphenicol | ≤8 | ≤8 | ≤8 | ≤8 |
| Ciprofloxacin | 1 | 1 | 1 | 0.5 |
| Colistin | ≤1 | ≤1 | ≤1 | ≤1 |
| Gentamicin | >32 | >32 | 32 | >32 |
| Meropenem | ≤0.03 | ≤0.03 | ≤0.03 | ≤0.03 |
| Nalidixic acid | 8 | 8 | 8 | 8 |
| Sulfamethoxazole | >1,024 | >1,024 | >1,024 | >1,024 |
| Tetracycline | >64 | >64 | >64 | >64 |
| Tigecycline | 1 | 1 | 0.5 | 1 |
| Trimethoprim | >32 | >32 | >32 | >32 |
| EUVSEC2** panel | | | | |
| Cefepime | 4 | 8 | 4 | 8 |
| Cefotaxime | 64 | 32 | 64 | 64 |
| Cefotaxime/clavulanic acid | ≤0.06/4 | ≤0.06/4 | 0.12/4 | 0.12/4 |
| Cefoxitin | 4 | 4 | 4 | 4 |
| Ceftazidime | 2 | 2 | 2 | 2 |
| Ceftazidime/clavulanic acid | 0.25/4 | 0.25/4 | 0.25/4 | 0.25/4 |
| Ertapenem | ≤0.015 | 0.06 | 0.03 | 0.03 |
| Imipenem | 0.25 | 0.25 | 0.25 | 0.5 |
| Meropenem | ≤0.03 | ≤0.03 | ≤0.03 | 0.06 |
| Temocillin | 4 | 8 | 4 | 16 |

**EUVSEC, EU Surveillance Salmonella/Escherichia coli.*
***EUVSEC2, EU Surveillance ESBL.*

**TABLE 3 |** Molecular profile of fecal carriage of ESBL-*Klebsiella pneumoniae* obtained from calves during the rearing period at a Dutch veal farm.

| Antibiotic family | *Resistance gene* | % Identity | Accession no. | ST | Replicon type |
|---|---|---|---|---|---|
| Beta-lactams | $bla_{\text{CTX-M-14}}$ | 100 | AF252622 | 107 | $\text{IncFIB}_{\text{K}}$, $\text{IncFIB}_{\text{Kn}}$ |
| | $bla_{\text{TEM-1B}}$ | 100 | AY458016 | | |
| | $bla_{\text{SHV-1-8}}$ | 99.5 | GQ407137 | | |
| Aminoglycoside | *aph(6)-Id* | 100 | M28829 | | |
| | *aph(3″)-Ib* | 100 | AF321551 | | |
| | *aac(3)-IId* | 99.8 | EU022314 | | |
| Sulfonamides | *Sul1* | 100 | U12338 | | |
| | *Sul2* | 100 | AY034138 | | |
| Fosfomycin | *Fos*A | 96.4 | ACZD01000244 | | |
| Tetracycline | *tet* (D) | 100 | AF467077 | | |
| | *tet* (A) | 100 | AJ517790 | | |
| Trimethoprim | *dfr*A*1* | 100 | X00926 | | |
| Quinolones | *qnr*S*1* | 100 | AB187515 | | |
| Efflux pump | *Oqx*A | 99.4 | EU370913 | | |
| | *Oqx*B | 99.4 | EU370913 | | |
| QACs | *qac*E | 100 | X68232 | | |

*The molecular profile was identical in the four Klebsiella pneumoniae isolates sequenced.*

$bla_{\text{TEM}}$ and $bla_{\text{SHV}}$ allelic variants in *K. pneumoniae* strains in clinical and non-clinical isolates including water, soil and animals raised for food production (Liakopoulos et al., 2016b; Shahraki-Zahedani et al., 2016). In addition to beta-lactams, it is concerning that resistance genes to other antibiotic classes including fluoroquinolones, tetracycline and aminoglycosides were also detected here, but considering results of a recent study in human *K. pneumoniae* isolates in the Netherlands, our results are not surprising (Hendrickx et al., 2020).

Several studies reported that the dissemination of the $bla_{\text{CTX-M-15}}$ gene among Enterobacterales has been facilitated by the IncFII plasmids (Peirano and Pitout, 2010; Mansour et al., 2015; Stercz et al., 2021). In our study we showed that the $bla_{\text{CTX-M-14}}$ gene dissemination was facilitated by the $\text{IncFII}_{\text{K}}$

and $IncFIB_{KN}$ plasmid replicons in four ESBL-*K. pneumoniae* isolates tested. Previous studies showed the presence of *K. pneumoniae* isolates harboring $bla_{CTX\text{-}M\text{-}14}$ located on $IncFIB_K$ and $IncFII_K$ obtained from healthy red kangaroos (Wang et al., 2020) and from a clinical isolate in China (Zhang et al., 2017). Likewise, the spread of the $bla_{CTX\text{-}M\text{-}14}$ gene in Enterobacterales has been predominantly associated with IncFII and IncK plasmid replicons in humans and animals including cattle in several countries (Hou et al., 2012; Stokes et al., 2012).

Several clonal lineages of *K. pneumoniae* have been reported widely in the United States and Europe such as ST258 and are currently present in several European countries (Woodford et al., 2011; Rodrigues et al., 2014; Ríos et al., 2017), supporting the epidemic potential of these clones. Our results showed that ST107 was the only ST type identified among ESBL-*K. pneumoniae* isolates in a single veal farm. The *K. pneumoniae* ST107 has been previously identified in *K. pneumoniae* isolates harboring $bla_{KPC\text{-}2}$ from a hospital environment (Fu et al., 2018), *K. pneumoniae* producing NDM (NDM-9) from a human clinical isolate in China (Wang et al., 2014), and in *K. pneumoniae* isolates harboring $bla_{SHV\text{-}11}$ from pigs and $bla_{CTX\text{-}M\text{-}1}$ from cattle (Klaper et al., 2021).

We aimed to determine if the isolates were clonally related by calculating the pairwise Single-Nucleotide Polymorphism (SNPs) distances based on the core genome predicted genes. The high number of SNPs detected exclude the possibility to confirm this hypothesis (data not shown). However, it seems that these isolates may have been present at the farm beyond the time of a single production round. To confirm this hypothesis additional sampling of the farm, a bigger sample size and molecular analysis will need to be performed.

The low diversity of ESBL-PE reported in this study and the clonal spread of ESBL-*K. pneumoniae* during the rearing period highlight the importance to reinforce the hygiene and management practices in farms as previously reported (Bokma et al., 2019; Damiaans et al., 2019). Recently, Atterby et al. (2019) showed that direct contact with animal manure and animal slaughter products are potential risk factors for fecal carriage of ESBL-*E. coli* and ESBL-*K. pneumoniae* in humans and animals. Additionally, the authors indicated that daily removal of animal manure could decrease the environmental exposure to antibiotic-resistant bacteria (Atterby et al., 2019). In the current study, the fecal carriage of ESBL-*K. pneumoniae* started to spread rapidly from week 6 after the calves were transferred from the dairy farm to the veal farm, suggesting that the ESBL-*K. pneumoniae* originated from the veal farm environment, although colonization of one of the animals before transport from the dairy to the veal farm or contact with other calves or animals present in the farm cannot be ruled out. While the pathogen that was responsible for clinical respiratory problems on this farm has not been investigated, *K. pneumoniae* could have caused these symptoms while the usage of antimicrobials may have increased transmission. As such, an increase in hygiene measures on farms in which respiratory disease is seen could lead to a decrease in intestinal colonization which in turn could lead to a decrease in environmental contamination. We also hypothesis that the administration of nonsteroidal anti-inflammatory drug (NSAID) for at least 2 weeks continuously in combination with antibiotics to control the respiratory infection, could perhaps contribute to the presence of *K. pneumoniae* in feces because the use of this drug can cause gastrointestinal upset such as irritation, therefore affecting the colonization resistance population present in the gastrointestinal tract. Further research is needed to better understand the relationship between animals, farmworkers, and the environment to further assess and limit the exposure and risk of fecal carriage of antibiotic-resistant bacteria.

## DATA AVAILABILITY STATEMENT

The datasets presented in this study can be found in online repositories. The names of the repository/repositories and accession number(s) can be found at: https://www.ebi.ac.uk/ena, PRJEB50519.

## ETHICS STATEMENT

The animal study was reviewed and approved by The Central Committee on Animal Experiments (the Hague, Netherlands; approval number 2017.D-0029). Written informed consent was obtained from the owners for the participation of their animals in this study.

## AUTHOR CONTRIBUTIONS

MB and KvR designed the study. FM collected the samples and data. TB performed the sample analysis, processed the data, and wrote the manuscript. AK and QD contributed with the laboratory work. MB, KV, FM, and KvR contributed to review and editing the manuscript. All authors contributed to the article and approved the submitted version.

## FUNDING

The collection of isolates that were used for this study was funded by the Dutch Ministry of Agriculture, Nature and Food Quality grant BO-43-111-011. Funding for the analysis of the isolates was received from the European Union's Horizon 2020 research and innovation programme through One Health EJP Project Full-Force [grant agreement number 773830] with co-funding from TKI bureau AgriFood.

## SUPPLEMENTARY MATERIAL

The Supplementary Material for this article can be found online at: https://www.frontiersin.org/articles/10.3389/fmicb.2022.866674/full#supplementary-material

## REFERENCES


Adler, A., Sturlesi, N., Fallach, N., Zilberman-Barzilai, D., Hussein, O., Blum, S. E., et al. (2015). Prevalence, risk factors, and transmission dynamics of extended-spectrum-β-lactamase-producing enterobacteriaceae: a national survey of cattle farms in Israel in 2013. *J. Clin. Microbiol.* 53, 3515–3521. doi: 10.1128/JCM.01915-15

Atterby, C., Osbjer, K., Tepper, V., Rajala, E., Hernandez, J., Seng, S., et al. (2019). Carriage of carbapenemase- and extended-spectrum cephalosporinase-producing *Escherichia coli* and *Klebsiella pneumoniae* in humans and livestock in rural Cambodia; gender and age differences and detection of blaOXA-48in humans. *Zoonoses Public Health* 66, 603–617. doi: 10.1111/zph.12612

Bokma, J., Boone, R., Deprez, P., and Pardon, B. (2019). Risk factors for antimicrobial use in veal calves and the association with mortality. *J. Dairy Sci.* 102, 607–618. doi: 10.3168/jds.2018-15211

Bush, K., and Fisher, J. F. (2011). Epidemiological expansion, structural studies, and clinical challenges of new β-lactamases from gram-negative bacteria. *Annu. Rev. Microbiol.* 65, 455–478. doi: 10.1146/annurev-micro-090110-102911

Carattoli, A., Bertini, A., Villa, L., Falbo, V., Hopkins, K. L., and Threlfall, E. J. (2005). Identification of plasmids by PCR-based replicon typing. *J. Microbiol. Methods* 63, 219–228. doi: 10.1016/j.mimet.2005.03.018

Chah, K. F., Ugwu, I. C., Okpala, A., Adamu, K. Y., Alonso, C. A., Ceballos, S., et al. (2018). Detection and molecular characterisation of extended-spectrum β-lactamase-producing enteric bacteria from pigs and chickens in Nsukka, Nigeria. *J. Glob. Antimicrob. Resist* 15, 36–40. doi: 10.1016/j.jgar.2018.06.002

D'Andrea, M. M., Arena, F., Pallecchi, L., and Rossolini, G. M. (2013). CTX-M-type β-lactamases: a successful story of antibiotic resistance. *Int. J. Med. Microbiol.* 303, 305–317. doi: 10.1016/j.ijmm.2013.02.008

Dahmen, S., Métayer, V., Gay, E., Madec, J. Y., and Haenni, M. (2013). Characterization of extended-spectrum beta-lactamase (ESBL)-carrying plasmids and clones of Enterobacteriaceae causing cattle mastitis in France. *Vet. Microbiol.* 162, 793–799. doi: 10.1016/j.vetmic.2012.10.015

Damiaans, B., Renault, V., Sarrazin, S., Berge, A. C., Pardon, B., Ribbens, S., et al. (2019). Biosecurity practices in Belgian veal calf farming: level of implementation, attitudes, strengths, weaknesses and constraints. *Prev. Vet. Med.* 172:104768. doi: 10.1016/j.prevetmed.2019.104768

Diab, M., Hamze, M., Bonnet, R., Saras, E., Madec, J. Y., and Haenni, M. (2017). OXA-48 and CTX-M-15 extended-spectrum beta-lactamases in raw milk in Lebanon: epidemic spread of dominant *Klebsiella pneumoniae* clones. *J. Med. Microbiol.* 66, 1688–1691. doi: 10.1099/jmm.0.000620

Dierikx, C. M., van Duijkeren, E., Schoormans, A. H. W., van Essen-Zandbergen, A., veldman, K., Kant, A., et al. (2012). Occurrence and characteristics of extended-spectrum-β-lactamase- and AmpC-producing clinical isolates derived from companion animals and horses. *J. Antimicrob. Chemother.* 67, 1368–1374. doi: 10.1093/jac/dks049

European Food Safety Authority (EFSA) (2011). Scientific opinion on the public health risks of bacterial strains producing extended-spectrum β-lactamases and/or AmpC βlactamases in food and food-producing animals. *EFSA J.* 9:2322. doi: 10.2903/j.efsa.2011.2322

European Reference Laboratory-Antimicrobial Resistance (n.d.). Available at: https://www.eurlar.eu/CustomerData/Files/Folders/21-protocols/390_protocol-for-validation-of-macconkey-and-ctx-agar-plates-final03112017.pdf

Fu, L., Huang, M., Zhang, X. Z., Yang, X. Y., Liu, Y., Zhang, L. H., et al. (2018). Frequency of virulence factors in high biofilm formation blaKPC-2 producing *Klebsiella pneumoniae* strains from hospitals. *Microb. Pathog.* 116, 168–172. doi: 10.1016/j.micpath.2018.01.030

Genomic Epidemiology Organization Server (n.d.). Available at: http://genomicepidemiology.org/

Geser, N., Stephan, R., and Hächler, H. (2012). Occurrence and characteristics of extended-spectrum β-lactamase (ESBL) producing Enterobacteriaceae in food producing animals, minced meat and raw milk. *BMC Vet. Res.* 8:21. doi: 10.1186/1746-6148-8-21

Geurts, Y., Brouwer, M., Noorman, K., Kant, A., Ceccarelli, D., Veldman, K., et al. (2017). "Development of sensitive and cost-effective real-time PCR assays for rapid detection of the beta-lactamases genes CTX-M1, SHV, TEM and Amp C gene CMY2 in Enterobacteriaceae." in *Proceeding of the 27th European Congress of Clinical Microbiology and Infectious Diseases 2017*. April 22, 2017. Vienna (European Society for Clinical Microbiology and Infectious Diseases).

Haenni, M., Châtre, P., Métayer, V., Bour, M., Signol, E., Madec, J. Y., et al. (2014). Comparative prevalence and characterization of ESBL-producing Enterobacteriaceae in dominant versus subdominant enteric flora in veal calves at slaughterhouse, France. *Vet. Microbiol.* 171, 321–327. doi: 10.1016/j.vetmic.2014.02.023

Hassen, B., Saloua, B., Abbassi, M. S., Ruiz-Ripa, L., Mama, O. M., Hassen, A., et al. (2019). Mcr-1 encoding colistin resistance in CTX-M-1/CTX-M-15-producing *Escherichia coli* isolates of bovine and caprine origins in Tunisia. First report of CTX-M-15-ST394/D *E. coli* from goats. *Comp. Immunol. Microbiol. Infect. Dis.* 67:101366. doi: 10.1016/j.cimid.2019.101366

Hendrickx, A., Landman, F., de Haan, A., Borst, D., Witteveen, S., van Santen-Verheuvel, M. G., et al. (2020). Plasmid diversity among genetically related *Klebsiella pneumoniae* blaKPC-2 and blaKPC-3 isolates collected in the Dutch national surveillance. *Sci. Rep.* 10:16778. doi: 10.1038/s41598-020-73440-2

Hordijk, J., Mevius, D. J., Kant, A., Bos, M. E. H., Graveland, H., Bosman, A. B., et al. (2013). Within-farm dynamics of ESBL/AmpC-producing *escherichia coli* in veal calves: a longitudinal approach. *J. Antimicrob. Chemother.* 68, 2468–2476. doi: 10.1093/jac/dkt219

Horton, R. A., Randall, L. P., Snary, E. L., Cockrem, H., Lotz, S., Wearing, H., et al. (2011). Fecal carriage and shedding density of CTX-M extended-spectrum β-lactamase-producing *Escherichia coli* in cattle, chickens, and pigs: implications for environmental contamination and food production. *Appl. Environ. Microbiol.* 77, 3715–3719. doi: 10.1128/AEM.02831-10

Hou, J., Huang, X., Deng, Y., He, L., Yang, T., Zeng, Z., et al. (2012). Dissemination of the fosfomycin resistance gene fosA3 with CTX-M β-lactamase genes and rmtB carried on incfII plasmids among *Escherichia coli* isolates from pets in China. *Antimicrob. Agents Chemother.* 56, 2135–2138. doi: 10.1128/AAC.05104-11

Klaper, K., Hammerl, J. A., Rau, J., Pfeifer, Y., and Werner, G. (2021). Genome-based analysis of *klebsiella* spp. Isolates from animals and food products in germany, 2013–2017. *Pathogens* 10:573. doi: 10.3390/pathogens10050573

Kurittu, P., Khakipoor, B., Aarnio, M., Nykäsenoja, S., Brouwer, M., Myllyniemi, A. L., et al. (2021). Plasmid-borne and chromosomal ESBL/AmpC genes in Escherichia coli and *Klebsiella pneumoniae* in global food products. *Front. Microbiol.* 12:592291. doi: 10.3389/fmicb.2021.592291

Liakopoulos, A., Geurts, Y., Dierikx, C. M., Brouwer, M. S. M., Kant, A., Wit, B., et al. (2016a). Extended-spectrum cephalosporin- resistant Salmonella enterica serovar Heidelberg strains, the Netherlands. *Emerg. Infect. Dis.* 22, 1257–1261. doi: 10.3201/eid2207.151377

Liakopoulos, A., Mevius, D., and Ceccarelli, D. (2016b). A review of SHV extended-spectrum β-lactamases: neglected yet ubiquitous. *Front. Microbiol.* 7:1374. doi: 10.3389/fmicb.2016.01374

Liebana, E., Carattoli, A., Coque, T. M., Hasman, H., Magiorakos, A. P., Mevius, D., et al. (2013). Public health risks of enterobacterial isolates producing extended-spectrum β-lactamases or AmpC β-lactamases in food and food-producing animals: an EU perspective of epidemiology, analytical methods, risk factors, and control options. *Clin. Infect. Dis.* 56, 1030–1037. doi: 10.1093/cid/cis1043

Mansour, W., Grami, R., Ben Haj Khalifa, A., Dahmen, S., Châtre, P., Haenni, M., et al. (2015). Dissemination of multidrug-resistant blaCTX-M-15/IncFIIk plasmids in *Klebsiella pneumoniae* isolates from hospital- and community-acquired human infections in Tunisia. *Diagn. Microbiol. Infect. Dis.* 83, 298–304. doi: 10.1016/J.DIAGMICROBIO.2015.07.023

Marcato, F., van den Brand, H., Kemp, B., Engel, B., Schnabel, S. K., Jansen, C. A., et al. (2022). Calf and dam characteristics and calf transport age affect immunoglobulin titers and hematological parameters of veal calves. *J. Dairy Sci.* 105, 1432–1451. doi: 10.3168/jds.2021-20636

Meijs, A. P., Gijsbers, E. F., Hengeveld, P. D., Dierikx, C. M., de Greeff, S. C., and van Duijkeren, E. (2021). ESBL/pAmpC-producing *Escherichia coli* and *Klebsiella pneumoniae* carriage among veterinary healthcare workers in the Netherlands. *Antimicrob. Resist. Infect. Control* 10:147. doi: 10.1186/s13756-021-01012-8

Mshana, S. E., Imirzalioglu, C., Hain, T., Domann, E., Lyamuya, E. F., and Chakraborty, T. (2011). Multiple ST clonal complexes, with a predominance of ST131, of *Escherichia coli* harbouring blaCTX-M-15 in a tertiary hospital in Tanzania. *Clin. Microbiol. Infect.* 17, 1279–1282. doi: 10.1111/j.1469-0691.2011.03518.x

Munk, P., Knudsen, B. E., Lukjacenko, O., Duarte, A. S. R., van Gompel, L., Luiken, R. E. C., et al. (2018). Abundance and diversity of the faecal resistome in slaughter pigs and broilers in nine European countries. *Nat. Microbiol.* 3, 898–908. doi: 10.1038/s41564-018-0192-9

NETMAP_MARAN (2021). Available at: https://www.wur.nl/nl/show/Nethmap-MARAN-2021.htm (Accessed January, 2022).

Nicolas-Chanoine, M. H., Bertrand, X., and Madec, J. Y. (2014). *Escherichia coli* st131, an intriguing clonal group. *Clin. Microbiol. Rev.* 27, 543–574. doi: 10.1128/CMR.00125-13

Overdevest, I., Willemsen, I., Rijnsburger, M., Eustace, A., Xu, L., Hawkey, P., et al. (2011). Extended-spectrum β-lactamase genes of *Escherichia coli* in chicken meat and humans, the Netherlands. *Emerg. Infect. Dis.* 17, 1216–1222. doi: 10.3201/eid1707.110209

Peirano, G., and Pitout, J. D. D. (2010). Molecular epidemiology of *Escherichia coli* producing CTX-M β-lactamases: the worldwide emergence of clone ST131 O25:H4. *Int. J. Antimicrob. Agents* 35, 316–321. doi: 10.1016/j.ijantimicag.2009.11.003

Pubmlst Server (n.d.). Available at: https://pubmlst.org/

Rashid, M., Rakib, M. M., and Hasan, B. (2015). Antimicrobial-resistant and ESBL-producing *Escherichia coli* in different ecological niches in Bangladesh. *Infect. Ecol. Epidemiol.* 5:26712. doi: 10.3402/iee.v5.26712

Ríos, E., López, M. C., Rodríguez-Avial, I., Culebras, E., and Picazo, J. J. (2017). Detection of *Escherichia coli* ST131 clonal complex (ST705) and *Klebsiella pneumoniae* ST15 among faecal carriage of extended-spectrum β-lactamase- and carbapenemase-producing Enterobacteriaceae. *J. Med. Microbiol.* 66, 169–174. doi: 10.1099/jmm.0.000399

Rodrigues, C., Machado, E., Ramos, H., Peixe, L., and Novais, Â. (2014). Expansion of ESBL-producing *Klebsiella pneumoniae* in hospitalized patients: a successful story of international clones (ST15, ST147, ST336) and epidemic plasmids (IncR, IncFIIK). *Int. J. Med. Microbiol.* 304, 1100–1108. doi: 10.1016/j.ijmm.2014.08.003

Rozwandowicz, M., Brouwer, M. S. M., Fischer, J., Wagenaar, J. A., Gonzalez-Zorn, B., Guerra, B., et al. (2018). Plasmids carrying antimicrobial resistance genes in Enterobacteriaceae. *J. Antimicrob. Chemother.* 73, 1121–1137. doi: 10.1093/jac/dkx488

Schmid, A., Hörmansdorfer, S., Messelhäusser, U., Käsbohrer, A., Sauter-Louis, C., and Mansfeld, R. (2013). Prevalence of extended-spectrum β-lactamase-producing *Escherichia coli* on Bavarian dairy and beef cattle farms. *Appl. Environ. Microbiol.* 79, 3027–3032. doi: 10.1128/AEM.00204-13

Schukken, Y., Chuff, M., Moroni, P., Gurjar, A., Santisteban, C., Welcome, F., et al. (2012). The "other" gram-negative Bacteria in mastitis. Klebsiella, Serratia, and more. *Vet. Clin. North Am. Food Anim. Pract.* 28, 239–256. doi: 10.1016/j.cvfa.2012.04.001

Shahraki-Zahedani, S., Rigi, S., Bokaeian, M., Ansari-Moghaddam, A., and Moghadampour, M. (2016). First report of TEM-104-, SHV-99-, SHV-108-, and SHV-110-producing *Klebsiella pneumoniae* from Iran. *Rev. Soc. Bras. Med. Trop.* 49, 441–445. doi: 10.1590/0037-8682-0114-2016

Stercz, B., Farkas, F. B., Tóth, Á., Gajdács, M., Domokos, J., Horváth, V., et al. (2021). The influence of antibiotics on transitory resistome during gut colonization with CTX-M-15 and OXA-162 producing *Klebsiella pneumoniae* ST15. *Sci. Rep.* 11:6335. doi: 10.1038/s41598-021-85766-6

Stokes, M. O., Cottell, J. L., Piddock, L. J. V., Wu, G., Wootton, M., Mevius, D. J., et al. (2012). Detection and characterization of pCT-like plasmid vectors for Bla ctx-M-14 in *Escherichia coli* isolates from humans, turkeys and cattle in England and Wales. *J. Antimicrob. Chemother.* 67, 1639–1644. doi: 10.1093/jac/dks126

Tshitshi, L., Manganyi, M. C., Montso, P. K., Mbewe, M., and Ateba, C. N. (2020). Extended spectrum beta-lactamase-resistant determinants among carbapenem-resistant Enterobacteriaceae from beef cattle in the north West Province, South Africa: a critical assessment of their possible public health implications. *Antibiotics* 9:820. doi: 10.3390/antibiotics9110820

Veldman, K., Swanenburg, M., Ceccarelli, D., and Mevius, D. (2018). *Monitoring of Antimicrobial Resistance and Antibiotic Usage in Animals (MARAN) in the Netherlands in 2017*. Lelystad: Wageningen Bioveterinary Research.

Waade, J., Seibt, U., Honscha, W., Rachidi, F., Starke, A., Speck, S., et al. (2021). Multidrug-resistant enterobacteria in newborn dairy calves in Germany. *PLoS One* 16:e0248291. doi: 10.1371/journal.pone.0248291

Wang, X., Kang, Q., Zhao, J., Liu, Z., Ji, F., Li, J., et al. (2020). Characteristics and epidemiology of extended-Spectrum β-lactamase-producing multidrug-resistant *Klebsiella pneumoniae* from red kangaroo. *China. Front. Microbiol.* 11:560474. doi: 10.3389/fmicb.2020.560474

Wang, X., Li, H., Zhao, C., Chen, H., Liu, J., Wang, Z., et al. (2014). Novel NDM-9 metallo-β-lactamase identified from a ST107 *Klebsiella pneumoniae* strain isolated in China. *Int. J. Antimicrob. Agents* 44, 90–91. doi: 10.1016/j.ijantimicag.2014.04.010

Woodford, N., Turton, J. F., and Livermore, D. M. (2011). Multiresistant gram-negative bacteria: the role of high-risk clones in the dissemination of antibiotic resistance. *FEMS Microbiol. Rev.* 35, 736–755. doi: 10.1111/j.1574-6976.2011.00268.x

World Health Organization (WHO) (n.d.). Available at: https://www.who.int/medicines/publications/WHO-PPL-Short_Summary_25Feb-ET_NM_WHO.pdf

Zhang, D., Yin, Z., Zhao, Y., Feng, J., Jiang, X., Zhan, Z., et al. (2017). P1220-CTXM, a pKP048-related IncFIIK plasmid carrying blaCTX-M-14 and qnrB4. *Future Microbiol.* 12, 1035–1043. doi: 10.2217/fmb-2017-0026

**Conflict of Interest:** The authors declare that the research was conducted in the absence of any commercial or financial relationships that could be construed as a potential conflict of interest.

**Publisher's Note:** All claims expressed in this article are solely those of the authors and do not necessarily represent those of their affiliated organizations, or those of the publisher, the editors and the reviewers. Any product that may be evaluated in this article, or claim that may be made by its manufacturer, is not guaranteed or endorsed by the publisher.

# Advantages of publishing in Frontiers

**OPEN ACCESS**
Articles are free to read for greatest visibility and readership

**FAST PUBLICATION**
Around 90 days from submission to decision

**HIGH QUALITY PEER-REVIEW**
Rigorous, collaborative, and constructive peer-review

**TRANSPARENT PEER-REVIEW**
Editors and reviewers acknowledged by name on published articles

**Frontiers**
Avenue du Tribunal-Fédéral 34
1005 Lausanne | Switzerland

**Visit us:** www.frontiersin.org
**Contact us:** frontiersin.org/about/contact

**REPRODUCIBILITY OF RESEARCH**
Support open data and methods to enhance research reproducibility

**DIGITAL PUBLISHING**
Articles designed for optimal readership across devices

**FOLLOW US**
@frontiersin

**IMPACT METRICS**
Advanced article metrics track visibility across digital media

**EXTENSIVE PROMOTION**
Marketing and promotion of impactful research

**LOOP RESEARCH NETWORK**
Our network increases your article's readership